File 123M/47
Filed 13/10/05
05/04133
Attachment 3
MINERAL RESOURCES
13 OCT 2005
TASMANIA

Acid Mine Drainage at the Comstock Ag-Pb-Zn Mine, Western Tasmania.

Unnikki Meskanen

B.Sc.

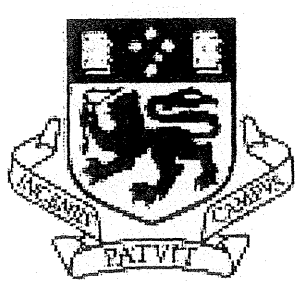

School of Earth Sciences

University of Tasmania

A Research Thesis submitted in partial fulfilment of the requirements of the Degree of Bachelor of Science with Honours.

November 2000

ABSTRACT

The Comstock mine is located within the pyritic alteration zone with host rocks comprising Late Proterozoic clastic and carbonaceous rocks of the Oonah Formation. The mine has been worked periodically since the late 1800's, and between then and the 1950's a system of shafts and adits have been driven along the shallow, ore veins. Oxidation of the sulphidically altered host rocks, and gangue minerals, occurred when the shafts exposed the rocks. Acid mine drainage reactions have occurred to the extent that Comstock Creek is now depauperate of aquatic fauna, and contains large amounts of oxy-hydroxide precipitate.

A water quality sampling regime was conducted in order to determine the background water quality of the site. Water is contaminated both above and below the mine site, with high acidity and concentrations of Al, Fe, Pb, and As commonly exceeding ANZECC recommended guidelines. This contamination appears to be reduced during high-flow conditions, and increases during low-flow conditions. The most contaminated sites sampled with respect to water quality were situated within the current area of mining activity. The least contaminated sites were small, 50m long exploration adits with very low flows.

Geochemical modelling was performed on selected water sample data, and predicted that most zinc is in its' free ionic state in site waters, whereas iron is borderline between its' free ionic Fe^{2+} state and an iron-oxide. Predicted saturation indices suggested precipitates were most likely to comprise pyrite and hematite, with both reactions releasing H^{+} ions.

A selection of acid-base-accounting tests were performed on rock samples from around the mine in order to determine the effects of site geology on the water composition. Tests revealed that samples were net acid producing, and that all will require careful management with regard to potential long-term contamination of Comstock Creek.

Acknowledgements

This thesis would not be what it is without the help of a great number of people, I would like to thank every-one. The following people deserve special mentions for the time and energy they have contributed.

*David Cooke provided support, advice and encouragement throughout the year; you did a good job, thanks Dave.

*Bass Resources were very generous with company resources, time and enthusiasm; thanks to everyone in the office and at the mine.

*A special mention to Paul Heath, Mine Geologist, for all the time he spent chauffeuring, field assisting, tour guiding, advising, rally driving, and laughing; it was aid beyond the call of duty.

*The staff of the geochem. labs., Phil, Nilar, and Katie, were patient and generous with equipment, advice, time and space; sorry about the mud.

* Pete and Simon helped with the technical stuff.

*The Geography Department loaned equipment and books, and the Zoology Department lent me the "Flow Mate".

*Jacob Russell, co-conspirator in all things Comstock, was helpful with maps, references etc.

*Pete Hollings read drafts when Dave was swamped, thanks Pete.

* My long-suffering field assistants were wonderful, thanks to Edith, James, Abe, Greg, Kate and Jasmin, the work-experience girl.

*My family were a great source of support throughout the year.

*My friends helped me stay sane, it was lovely to be in contact with the real world.

* Thanks also to everyone who booted the soccer ball.

*I would also like to thank; the Tasmanian Museum and Art Gallery, Ashley Townsend, David Steele, Marc Norman, and the Shaw's blokes, for help of various types.

Section One: Introduction and Background Information.

Chapter 1: Introduction

Chapter 2: Geology

Section 2: Water Quality Analysis

Chapter 3: Methodology and Site Locations

Chapter 4: Background Water Quality

Section 3: Acid Base Accounting

Chapter 6

Section 4: Conclusions and Recommendations

Chapter 7: Conclusions

Chapter 8: Potential Remediation Strategies

List of Figures

Chapter 1

Chapter 2

Chapter 3

Chapter 4

Chapter 5

Chapter 6

List of Tables

Chapter 3

Chapter 4

Chapter 5

Chapter 6

List of Plates

Chapter 1

Chapter 3

Chapter 5

Section One:

Introduction and Background Information.

Chapter 1
Introduction

1.1 Introduction

1.1.1. Introduction

Acid Mine Drainage (AMD) has been occurring at the Comstock Ag-Pb-Zn Mine since the lease was first worked. The exposure of abundant pyrite, intermixed with the ore, has resulted in the products of pyrite oxidation being washed through prospecting adits, and down Comstock Creek.

The Comstock Ag-Pb-Zn mine occurs within the Zeehan mineral field on the West Coast of Tasmania (figure 1-1). The mineral field extends from the coastal settlement of Remine and runs east of Zeehan. The field comprises a classic zoned hydrothermal ore system (Both & Williams, 1968) (Figure 1-2). Comstock is located within the pyritic alteration zone, and ore consists of argentiferous galena and sphalerite in a predominately quartz and pyrite gangue (Tear 2000).

Historic mining of the lease has concentrated on the shallow, high-grade veins (Blisset, 1962; Twelvetrees 1900). The operations led to establishment of open-cut pits, adits and shafts (Blisset, 1962). A system of tunnels undercuts approximately 500m^2 of the lease and drains into Comstock Creek via the No.1 adit (Figures 1-3 & 1-4).

Currently, most of the surface water flows into the tunnel system (Plate 1-1);

- Comstock Creek is diverted into the tunnels via a large shaft at the north end of the lease,
- shafts capture small amounts of precipitation and surface flow,
- water percolating through the Balstrup Fault is diverted into an old shaft,
- the South Comstock open-cut captures much of the onsite surface flow which then seeps through faults crossing the pit and enters the tunnels.

A.Comstock Creek entering the tunnel system.

B. The Main Adit, where Comstock Creek exits the tunnel system.

C. The South Comstock Open Cut.

D. The shaft that diverts water from the Balstrup fault into the tunnel system (prior to excavation of the decline).

Plate 1-1

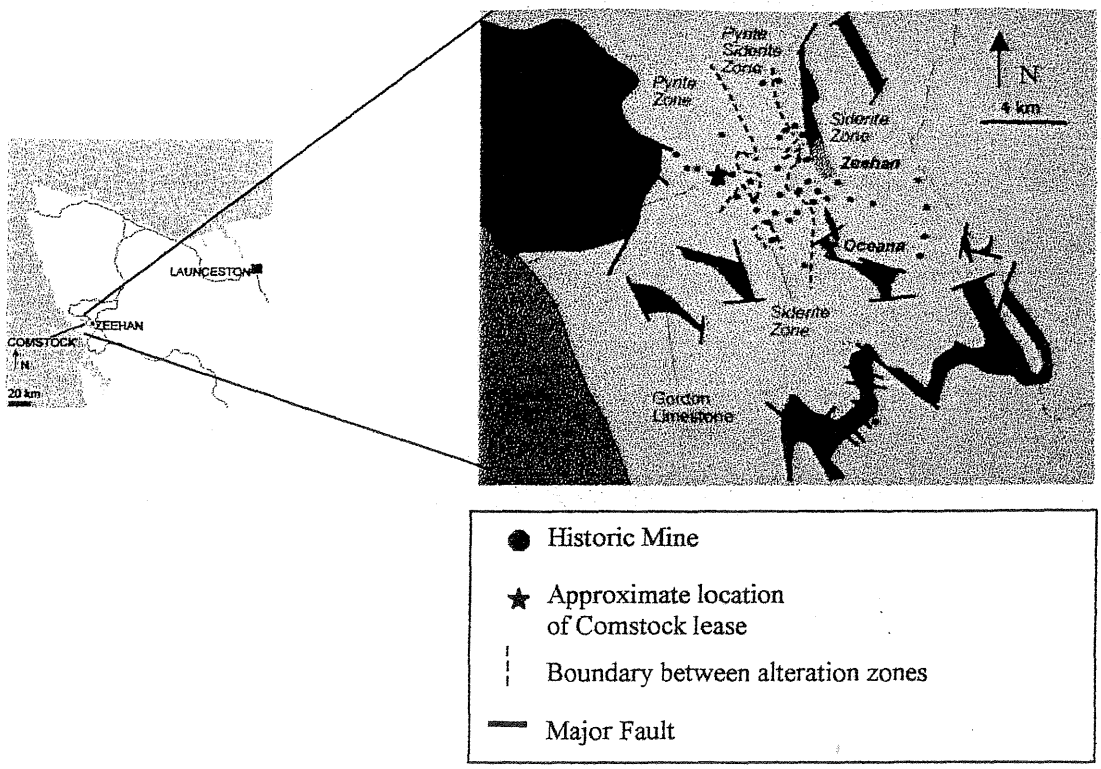

Figure 1-1. Location of Comstock Mine. (altered from unknown source.)

Figure 1-2. The zones of the Zeehan Mineral Field (modified after Both & Williams 1968)

Water flowing through the tunnels exits via the No.1 adit into Comstock Creek. Comstock Creek has been heavily impacted by the drainage water composition, which includes elevated levels of metals (Comstock DPEMP; DPIWE File # 06-23-17). It is probable that no microfauna dwells in Comstock Creek from below the mine lease, to the confluence with the Little Henty River (Comstock DPEMP). Acid mine drainage is occurring on-site because the workings exacerbate acid rock drainage. The disturbances allow oxygen and water to interact with potentially acid producing lithologies to an extent that would not naturally occur. Acid rock drainage (ARD) is thought to be produced by host lithologies, as these contain significant amounts of disseminated pyrite and other sulphides (Parr, 1993), as well as by the sulphide ore.

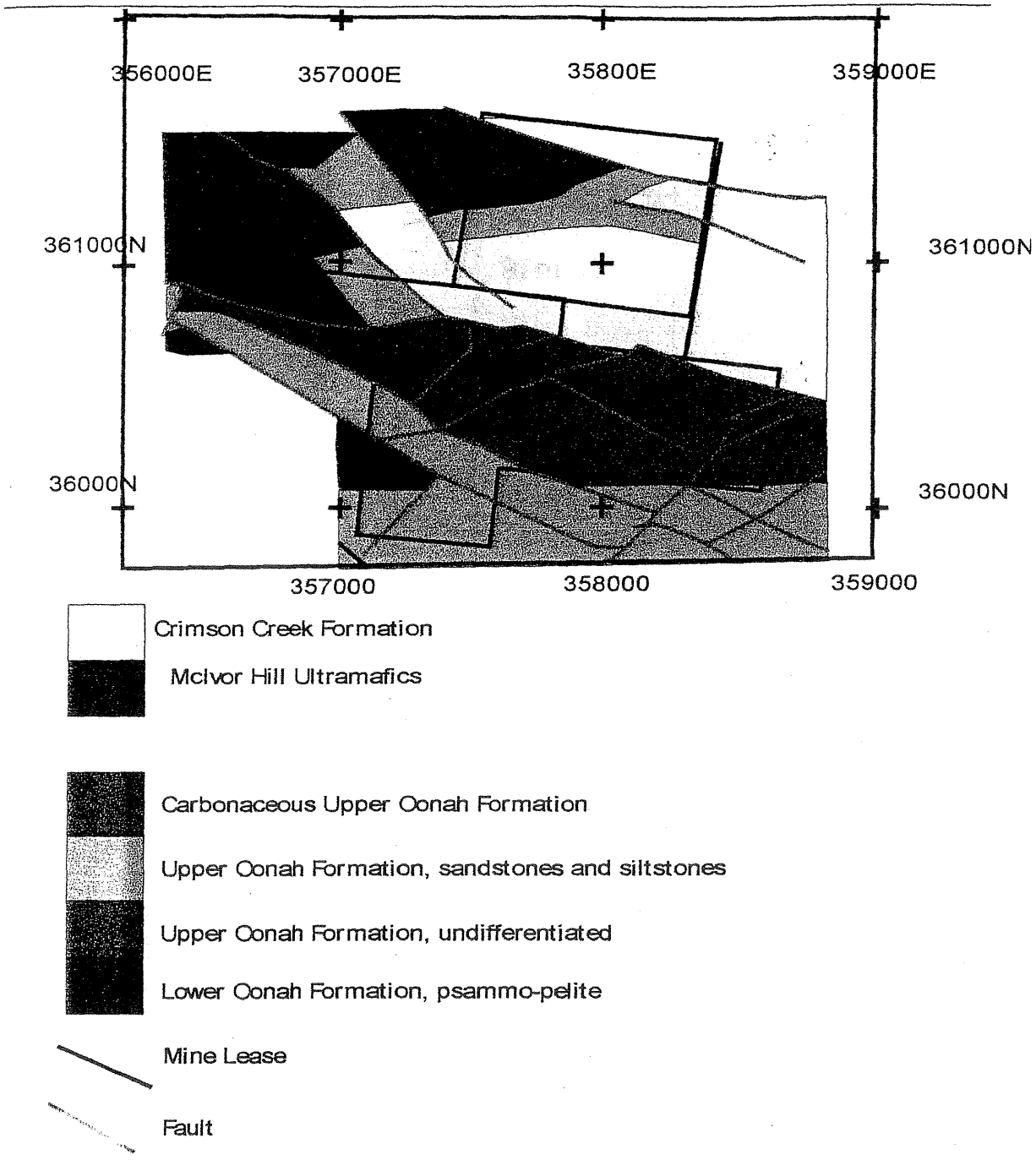

Figure 1-3 Plan View of Mine Site Showing Subsurface Projection of Underground adits

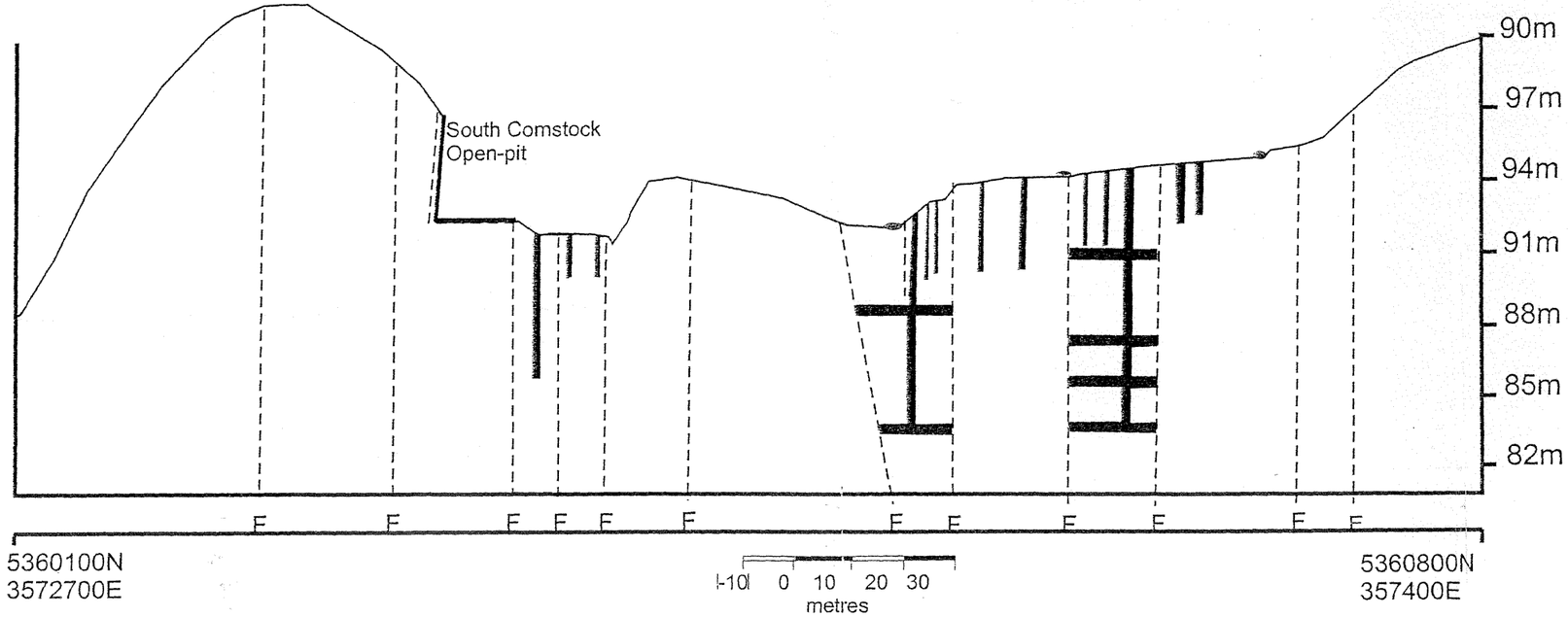

Longitudinal Projection: Main Lode

- Comstock Creek
- Adit cross-section
- Tunnel/ shaft
- Open-cut pit
- Faults

1.8 Aims

This study examines drainage water compositions on the Comstock lease, and identifies point sources of contamination that will require remediation. The local geological materials are investigated from the perspective of potential contaminant sources. Climactic effects on water chemistry are also investigated, as are downstream sediments, to determine primary and secondary precipitation effects. The major aims of this thesis are to;

- Determine the composition of water discharging from historic adits, and calculate mass loadings of contaminants entering and travelling down Comstock Creek, under base flow and storm flow conditions.
- Determine the potential impact of rock types and minerals on water chemistry.

This study deals with the historic mine workings of the Comstock lease, and does not incorporate an investigation of current mining activities, except where water has been diverted into underground workings by the current mine operators.

1.7 Thesis Structure

This thesis consists of three sections, each of which contains several chapters. The first section contains literature review material and provides the background to my study.

The second presents research results from the current studies, focussing on water analysis and rock and mineral analysis.

The final section of this thesis collates and summarises the salient results from each analytical technique and focuses on the major pollution issues highlighted by the study with respect to their possible environmental impacts. The potential for amelioration of AMD on site is also discussed with reference to feasibility and practicality.

1.2. Site Description

1.2.1. Location and Access.

The Comstock Lease is situated on the west coast of Tasmania, 4 km west of Zeehan. The lease is 146 hectares (E.A.R. 2000) and lies between Mt. Zeehan and Mt. Heemskirk, approximately 16 km east of Trial Harbour. Access to the site is via an unsealed public road that provides access to Remine, the settlement at Trial Harbour. Recently, Oceania Tasmania Pty. Ltd. widened and improved the road to allow safer transport of up to 16 loads of material a day.

1.2.2. Geomorphology.

Comstock lies within a fold structure province (Davies, 1967) characterised by steep slopes, high drainage density and trellis drainage patterns (Banks *et al.*, 1977). Comstock is situated in the headwaters of the Little Henty catchment where drainage patterns are only slightly controlled by Cambrian and Precambrian lithologies (Banks *et al.*, 1977). The site has been identified as having high probabilities of water-logging, moderate flooding and low possibilities of sheet erosion (Comstock E.A.R, Permit Conditions 2000).

The humid conditions of the region cause preferential decomposition of aluminous rocks compared with more siliceous types (Banks *et al.*, 1977). Soils produced by such weathering have deep, clay-rich profiles. As a result aluminous rocks crop out poorly compared to the siliceous lithologies (Banks *et al.* 1977). Limestone crops out rarely because it is readily eroded by interaction with acidic groundwater. The soils associated with limestone tend to be thick, dark and clay-rich (Banks *et al.* 1977). Gossaneous outcrops are poorly developed because the relatively cool temperatures associated with the west coast during the Quaternary result in slow reaction rates (Banks *et al.* 1977).

1.2.3. Climate.

Tasmania has a modified marine Mediterranean climate. The close vicinity of the ocean modifies heat absorption and storage, thus tempering seasonal temperature variations (Jackson, 1999). Elevated regions are cooler because temperatures drop by approximately 0.6° per 100m increase in elevation (Jackson, 1999). The Comstock lease lies 280 metres above sea level (Comstock EAR. 2000).

Banks (*et al.* 1977) suggest that the Comstock site is located within a superhumid precipitation province. A strong precipitation gradient lies across Tasmania because orographic effects combine with the strong westerly circulation of climate cells. Precipitation on the west coast has an average yearly variation of less than 10mm with the Heemskirk Ranges exhibiting the most variation (+/-16mm a year) (Banks *et al.*, 1977). Mountainous regions in the west receive up to 3600 mm of rain a year compared with some eastern regions that receive less than 500mm a year (Jackson, 1999; Figure 1-4a). At the same time mean annual evaporation is known to be more than 1000mm north of Trial Harbour, compared with 750mm inland (Banks et al. 1977) (figure 1-4b).

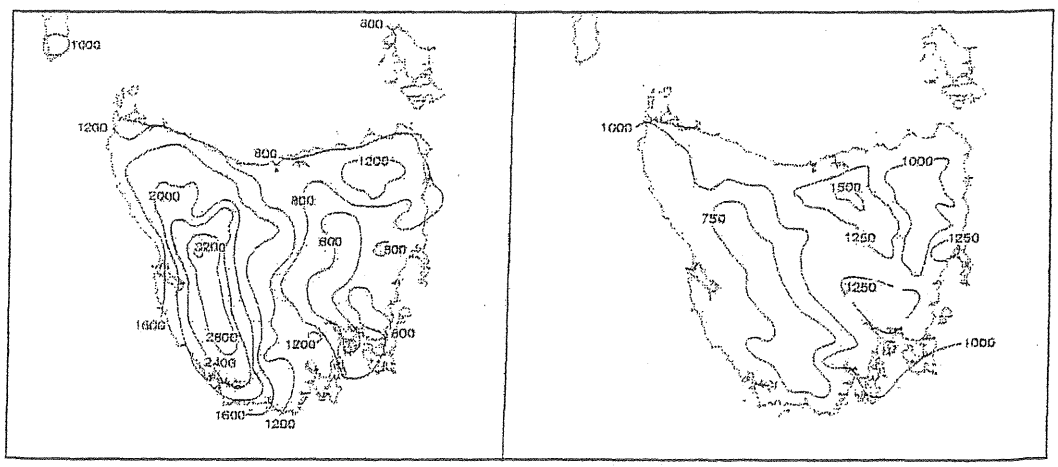

Figure 1-4a. Mean Annual Rainfall (mm) over Tasmania.

Figure 1-4b. Mean Annual Evaporation (mm) over Tasmania.

(Banks et al.1977).

The amount of rainfall at Comstock is similar to Zeehan rainfall (Figure 1-5).

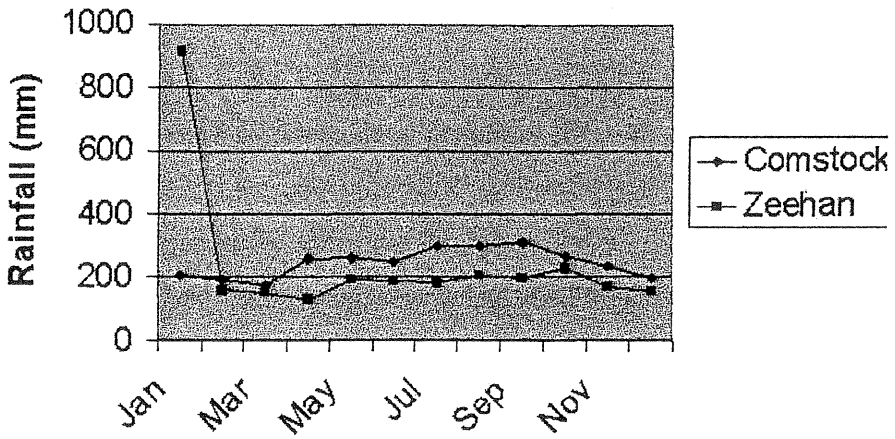

Figure 1-5. Rainfall at Comstock and Zeehan between 1924-1944 (HEC)

1.4.4 Vegetation.

The current distribution of vegetation communities at Comstock is a result of drainage conditions and fire regimes. Fires started by aboriginals and prospectors have created a mosaic of non-climactic vegetation communities. There are four major vegetation communities on the lease (DPEMP 2000);

- Large crowned rainforest with *Nothofagus cunninghamii*,
- Closed scrub,
- *Eucalyptus nitida* open forest,
- Sedgeland and open heath.

1.5 Background

1.5.1 Site History.

The Zeehan mineral field came to the attention of prospectors in 1882 when Frank Long discovered argentiferous galena in Peasoup Creek. The following years saw an

influx of prospectors seeking their fortunes in the harsh, remote wilderness of the West Coast and leases were established wherever signs of ore were found. The Zeehan township was soon established near the discovery site, providing a base for prospectors from where further exploration of the area could be organised (Blainey, 1993).

The area around the Comstock lease has been intermittently explored and worked since the prospecting rush (Figure 1-5). Much work at the mine has historically been hampered by problems with equipment and flooding (RGC Report 1997). Originally Comstock was worked for the high grade, shallow veins of galena and mining was conducted in shallow workings and deep trenches (Blisset, 1962). At the turn of the century, worldwide demand for zinc catalysed exploration for sphalerite. The last decade has seen the mine reopened by Oceania (Knight, 1997). Diamond drilling, mapping, surveying and geophysical exploration are being used to determine the distribution and extent of payable ore (Knight, 1997).

Figure 1-5. Comstock Mine Lease circa 1910. (Tasmanian Museum and Art Gallery)

W. Barlow claimed the Comstock lease (No. 712-87M) in 1888, later that year Comstock Mining Co. N.L took over the 80-acre lease (Blisset, 1962). The extent of the Main (No.1) lode was explored in 1890 when the lower adit was driven NE from the eastern bank of Comstock Creek (Blisset, 1962). By 1891 the adit was 660 feet long and intersected the main lode. At this time problems with water and equipment were encountered and work was ceased.

When Barlow pegged lease no. 712-87M, W.H. Foley claimed 80 acres directly south. This title was then sold to the South Comstock Silver Mining Company N.L. in 1889. Work on the lease was brief, with only one small drive put in (Blisset, 1962). In 1896 F. O'Neill and W. Flaherty took over the lease (renamed 966-93M) and mined the main lode as a deep open-cut operation (Blisset, 1962). Between 1901 and 1903 Zeehan South Comstock Ltd. acquired both leases and proceeded to profitably mine and export zinc and lead (Blisset, 1962). When the shallow ore was exhausted the Broken Hill Proprietary Block 10 Co. Ltd. took out options and in 1912 transferred the titles, but by 1916 the site was again abandoned (Blisset, 1962).

In 1924, parts of the area were held by H. Tompkins and R. Clarke, and by J. A. Cornish. Cornish had 5 acres on the Comstock east lode (9140M) and by 1928 Allison's Comstock Lead Zinc Co. N.L. were working this site (Blisset, 1962). The next year the Lucknow Prospecting Syndicate owned the lease (Blisset, 1962). J. Dunkley and company successfully worked the Main Lode for argentiferous galena for between 1926 and 1927 (Blisset, 1962). Government employees extended the Lower adit to 1 909 feet in 1935 but no payable ore was found (Blisset, 1962). In 1947 M. C. Howard, R. M. Waller and E. Tomkins bought up the entire lease area of 359 acres (123-47 M) (Blisset, 1962).

The Electrolytic Zinc Company of Australasia Ltd. obtained the lease in 1 948 and conducted an intensive investigation of potential ore using surveying and diamond drilling (Blisset, 1962). Small amounts of ore were extracted in 1951-52 (Blisset, 1962). By 1952, 4021 tonnes of galena and 3245 tonnes of zinc were mined. It is estimated that

from this ore, 1625 tonnes of galena, 2100 tonnes of zinc and 165 000 ounces of silver had been recovered (MRT Report #85-2315).

In 1989 Oceania extracted 7334 tonnes of ore from the South Comstock open cut and sent it to Pasminco mill (Rosebery) for concentration (Knight, 1997). For five years, until 1995, Renison actively explored the entire EL 42/87 looking for payable amounts of tin that was possibly present from a cupola style of emplacement similar to that seen at Queen Hill (Knight, 1997).

1.4. Current Operation

1.4.1. The Company.

The Bendall Group have held the Comstock lease for the last 15 years (M. Bendall, pers. comm.). Oceania Tasmania Pty. Ltd. owns the Comstock lease and Zeehan Zinc run the mining operation. Zeehan Zinc is a Tasmanian company with the major share holder being Oceania Tasmania Pty. Ltd (DPEMP 2000).

1.4.2. Style of Operation.

Currently the Comstock mine is approved for level 2 activity, this means 10 000 tonnes of ore can be excavated each year (DPEMP 2000). Allisons lode is currently being mined and drilled. A decline has been excavated to 30m depth in order to open up the lode. The current operation is essentially synchronous exploration and excavation (P. Heath, pers. comm. 2000).

1.5. Relevant Legislation

1.5.1. State.

The Comstock Mine operates as a level 2 activity under the *Land Use Planning and Approvals Act 1993* (LUPAA) (Comstock EAR 2000). Environmental impacts on site

must adhere to guidelines set out in the *Environmental Management and Pollution Control Act 1994* (EMPCA). On site development is also covered by the *State Policies and Projects Act 1993* (SPPA). Comstock is classified as a quarry under LUPAA and as such, needs to follow safety and environmental guidelines described within the *Quarry Code of Practice 1999* (QCP). Within the QCP are requirements to: 1) aid planning authorities with LUPAA and EMPCA assessments; 2) meet the *Workplace Health and Safety Act 1995* (WHSA); and 3) comply with the *Mineral Resource Development Act 1995* (MRDA; Quarry Code of Practise 1999). As a result of acid drainage issues on site, adherence to *Protected Environmental Values* (PEVs) described within the *State Policy on Water Quality Management* (SPWQM) is highly desirable but not legally binding (Comstock EAR 2000).

Other regulations pertaining to the Comstock operation are included under the following acts (Comstock EAR 2000):

- *Environment Protection (Waste Disposal) Regulations 1974,*
- the *Dangerous Goods Act 1998,*
- the *Workplace Health and Safety Act 1995,*
- the *Workplace Health and Safety Regulations 1998,* and
- the *Dangerous Goods (Road and Rail Transport) Regulations 1998.*

1.6. Previous Work

1.6.1. Water Quality.

The Department of Primary Industry, Water and the Environment have sampled water above and below No. 1 adit (Figure 1-?) since 1997. Samples were analysed for total and dissolved contaminants (DPIWE, File #06-23-17). Their results have revealed that the concentrations of some trace metals (Pb, Fe, Mn, Zn), exceeded guidelines for potable water recommended by ANZECC/NWQS (1992).

In a reconnaissance study, Parr (1997) related mine drainage water composition to mineralogical zonation within the Zeehan mineral field. A number of mine sites within the Zeehan field were identified to be discharging contaminated water in the Zeehan catchment. These sites were situated within various lithologies of the Zeehan field thus providing an opportunity to study to effects of lithological controls on acid mine drainage. Drainage waters within the pyritic zone were more found to be more contaminated than waters from sites within the sidero-pyrite or siderite zones (Parr, 1997). Pyritic drainage compositions were classified as being high-acid, high-metal to acid high metal. Siderite drainage compositons were found to be near-neutral, low-metal to acid, high-metal. Drainage waters within sidero-pyrite alteration water compositions were intermediate between the two extremes of alteration (Parr, 1997).

The geology of the immediate area has not been studied in detail but the nearby Zn-Pb-Ag skarn deposit, known as Sylvestor Prospect, has been studied (Taylor, 1993). The study concluded that skarn and sulphide mineralisation in the Sylvestor prospect was occurred when carbonate units were replaced by fluids that originated from the emplacement of the Heemskirk Granite. Later meteoric water circulation catalysed precipitation of late stage skarn assemblages and sulphide minerals in the footwall of the Balstrup fault.

Regional geology and ore distribution have been studied at numerous times (i.e. Blisset, 1962; Both, 1966; Both & Williams, 1968; Findlay & Brown, 1992; Klominsky, 1972; Twelvetrees & Ward, 1910). The Zeehan mineral field is now considered to be a zoned hydrothermal mineral system, created as a result of the emplacement of the Heemskirk granite massif (i.e. Blisset, 1962; Both, 1966; Both & Williams, 1968). (Findlay & Brown, 1992; Klominsky, 1972; Twelvetrees & Ward, 1910). Zonation comprises four main zones, identified on the basis of the gangue mineralogy observed at historic and active mine sites around Zeehan. Zones comprise, a cassiterite rich mineralogy; a pyrite rich mineralogy, a siderite and pyrite rich mineralogy, and; a siderite rich mineralogy. Znation has been related directly to progressive changes in the physical and chemical environment of ore deposition (Both, 1966; Both & Williams, 1968).

Chapter 2
Geology

2.1 Introduction

The Comstock Ag-Pb-Zn mine is situated within the Zeehan mineral field on the west coast of Tasmania (Figure 2-1). The mineral field extends from the coastal settlement of Remine and to the east of Zeehan. Both & Williams (1968), described a mineralogical zonation within the Zeehan field, originating from the emplacement of the Heemskirk Granite. Zonal arrangements comprise a cassiterite zone within the granite, followed by a pyrite zone, a sidero-pyrite zone, and a siderite zone.

This chapter describes the regional setting of the Comstock mine, and details the geology and ore deposits that occur in the lease.

2.2 Regional Setting

2.2.1 Introduction

The Zeehan mineral field is hosted by Upper Proterozoic and Palaeozoic rocks which have been intruded by Devonian igneous rocks which outcrop west of Zeehan (Figure 2.1: Williams *et al.*, 1989).

2.2.2 Geological History

The Oonah Formation contains the oldest rocks exposed in the Zeehan mineral field, being Proterozoic in age (Williams *et al.*, 1989). The Oonah Formation has been interpreted to be a distal turbidite sequence (Brown, 1986), and has been divided into upper and lower successions (Taylor, 1993). The Lower Oonah Formation comprises

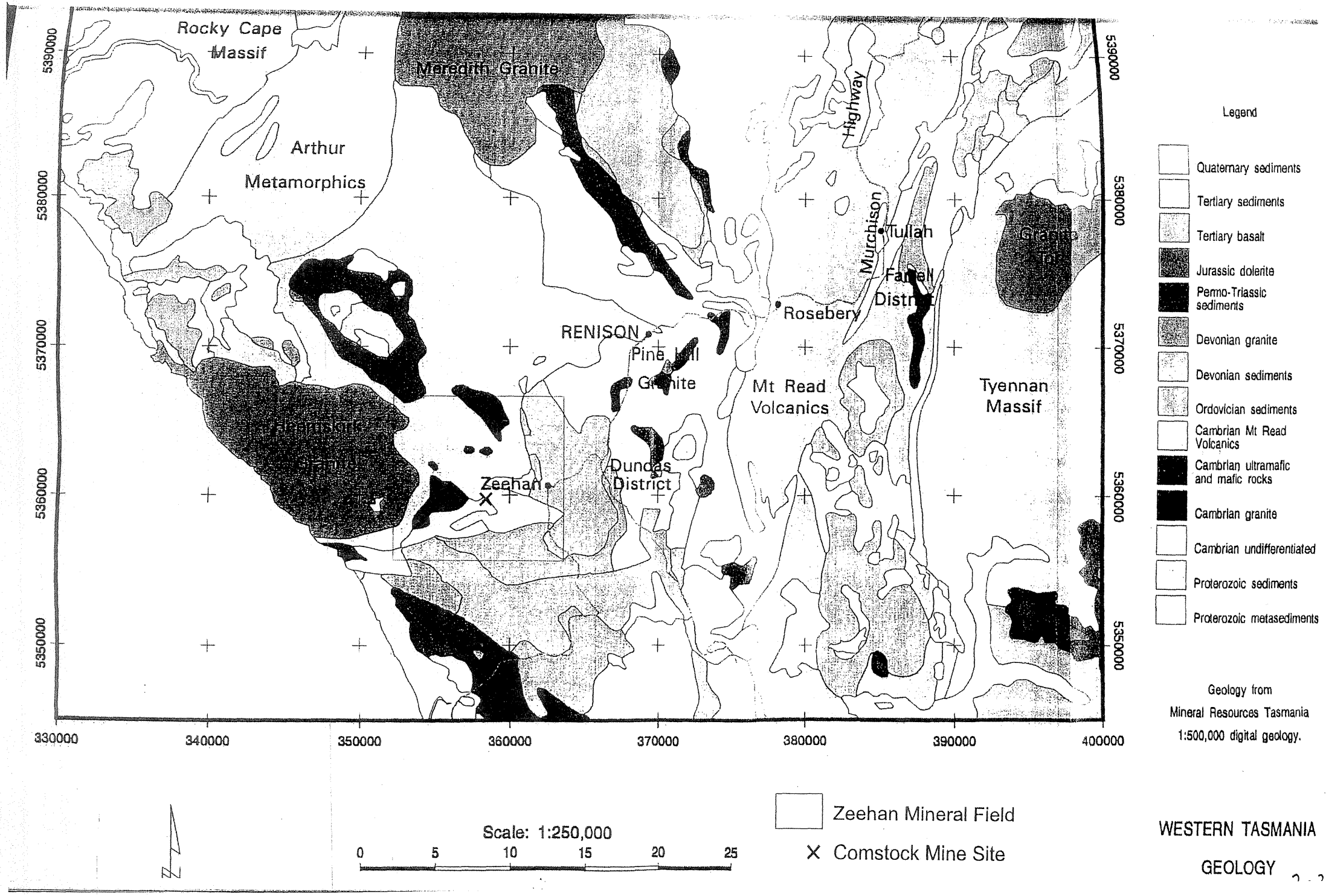
Rocky Cape Massif
Meredith Granite
Arthur Metamorphics
Lyell Highway
Murchison
Tullah
Rosebery
Farrell Distrct
RENISON
Pine Hill Granite
Mt Read Volcanics
Tyennan Massif
Zeehan
Dundas District
5390000
5380000
5370000
5360000
5350000
330000
340000
350000
360000
370000
380000
390000
400000
Legend
Quaternary sediments
Tertiary sediments
Tertiary basalt
Jurassic dolerite
Permo-Triassic sediments
Devonian granite
Devonian sediments
Ordovician sediments
Cambrian Mt Read Volcanics
Cambrian ultramafic and mafic rocks
Cambrian granite
Cambrian undifferentiated
Proterozoic sediments
Proterozoic metasediments
Geology from Mineral Resources Tasmania 1:500,000 digital geology.
Scale: 1:250,000
0 5 10 15 20 25
Zeehan Mineral Field
Comstock Mine Site
WESTERN TASMANIA
GEOLOGY

quartzite, shales and slates, whereas the Upper Oonah Formation contains acid to intermediate volcanics, siltstones, limestone, dolomite, and graphitic shales (Summons, 1983). The Oonah Formation was intensely deformed by the Penguin orogeny, prior to the deposition of Palaeozoic sequences.

The Eo-Cambrian Success Creek Group unconformably overlies the Oonah Formation. The Success Creek Group formed as localised basin infill, in a shallow-marine environment (Brown, 1989). The Cambrian Crimson Creek Formation conformably overlies the Success Creek Group, and consists of a succession of volcaniclastic turbidite units deposited in a shallow-water environment (Brown, 1989).

The Heemskirk Granite massif comprises two calc-alkaline granitoids that intruded the Oonah Formation during the Devonian (Klominsky, 1972). Gravity data indicate an associated granitiod intrusive, extending from the Heemskirk Granite to Zeehan. Cupolas on the subsurface granite outcrop at several locations (Leaman, 1999); the McIvor Hill Ultramafic complex is one of the many Cambrian gabbros and ultramafic dykes that outcrop around the field. The McIvor Hill complex is a fault-bounded body of serpentinite, gabbros and mafic volcanics (Taylor, 1993).

2.2.3 Structure

The Zeehan field has undergone at least four deformation events (Summons, 1983). The first (D1) occurred in the Late Precambrian Penguin Orogeny (Berry *et al.* 1990), intensely deforming the Oonah Formation and producing recumbant isoclinal folding, not present in younger units (Knight, 1997).

Reverse faults and cataclasite formed in the Devonian, during D2. The second deformation was associated with mid-Cambrian thrusting and emplacement of the ultramafic intrusives (Berry *et al.* 1990).

D3 occurred during the mid-Devonian Tabberabberran Orogeny (Taylor, 1993), and produced tight, NW trending folds (e.g. Heemskirk Anticlinorium), and, later north-

plunging, NE trending open folds (Taylor, 1993). The last phase of deformation (D4) produced NNE trending, normal faults that dip steeply to the east (Knight, 1997).

2.2.4 Regional Mineral Distribution

Zonation of the classic hydrothermal ore minerals, associated with emplacement of the Devonian Heemskirk Granite massif (Both & Williams, 1968; Slater 1996). An inner cassiterite zone occurs within the granite. It is enclosed by a pyritic zone adjacent to the granite, followed by a sideropyrite zone and an outer siderite zone (Figure 2-2; Both & Williams, 1968).

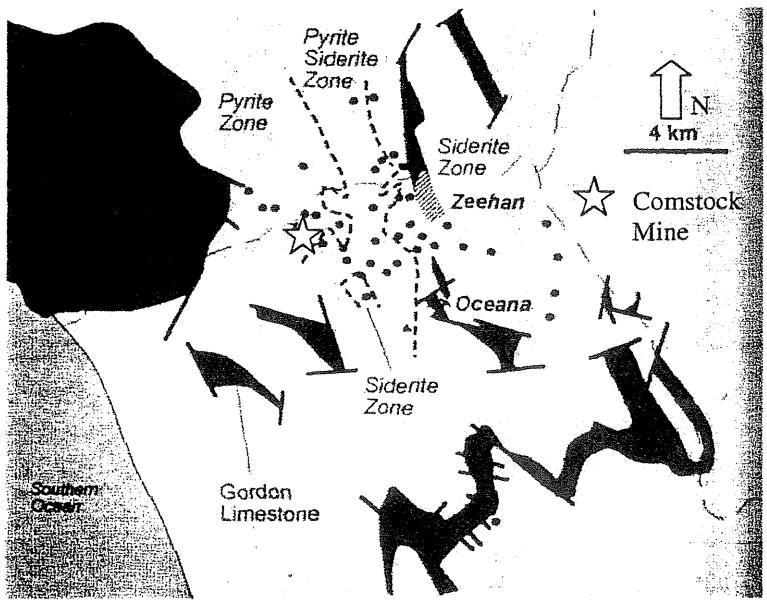

Figure 2-2. The zonation of hydrothermal ore minerals, that surround the Heemskirk Granite.

2.3 Site Geology

2.3.1 Introduction

The Comstock Pb-Zn-Ag mine lies within the pyritic alteration zone of the Zeehan field, 3km east of the Heemskirk Granite (Figure 2-2). Rocks of the Upper Oonah Formation host the deposit (Figure 2-3). Ag-Pb-Zn ore occurs as massive sulphide deposits, veins and in serpentinite-magnetite skarn (Taylor, 1993).

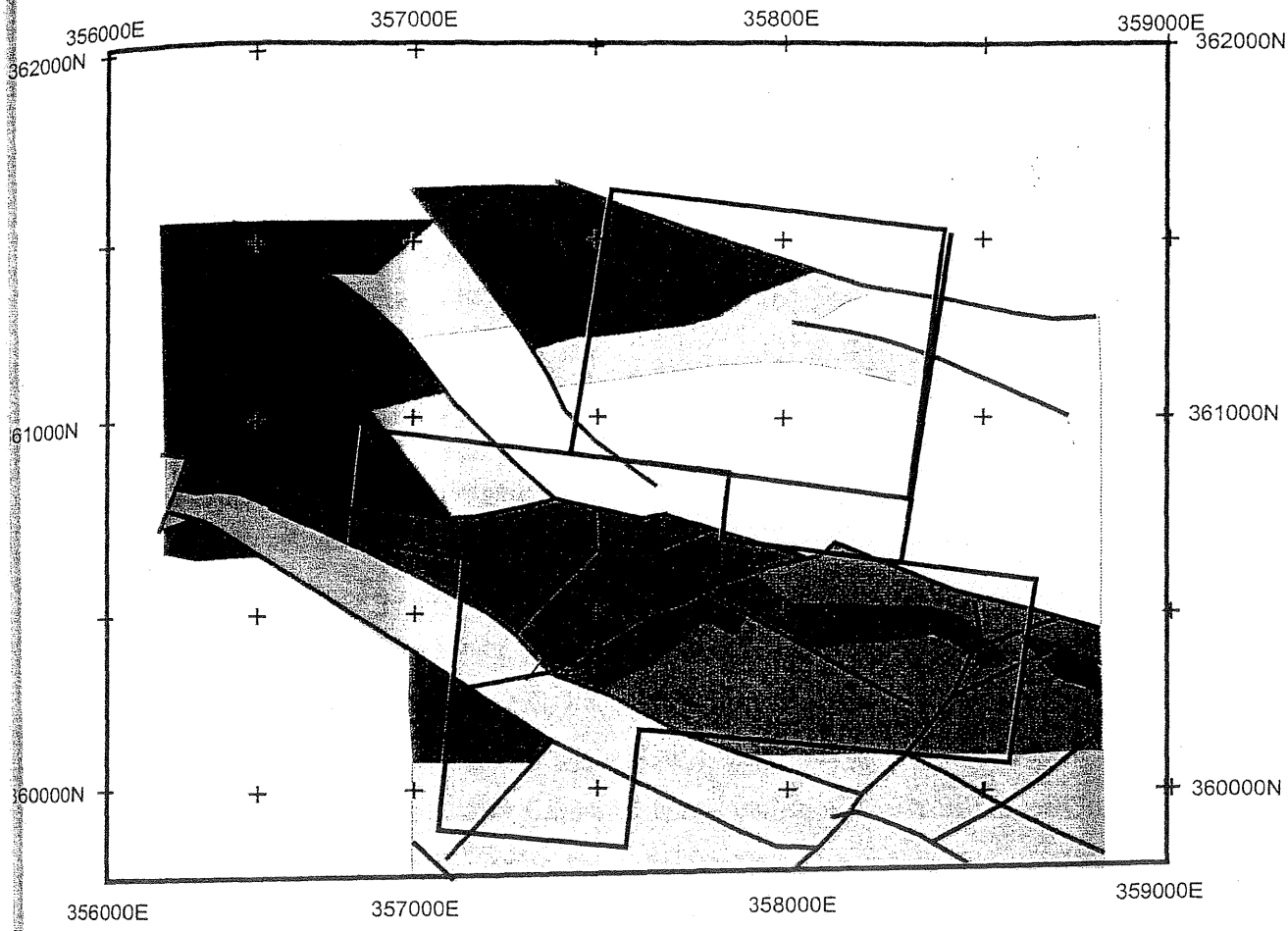

Figure 2--3: Plan View of Mine Geology.

2.3.2 Geology

2.3.2.1 Lower Oonah Formation

The Lower Oonah Formation outcrops in the NW corner of the lease (Figure 2-3). Thinly bedded, fine-grained, micaceous, sandstone and siltstone are intercalated with medium-grained, massive, quartzitic sandstone, interbedded with minor siltstone and mudstone layers (Taylor, 1993). This unit does not host ore and none of the mine workings are positioned within it.

3.3.2.2 Upper Oonah Formation

Rocks of the Upper Oonah Formation outcrop throughout the lease. Lithologies within this unit occur as sub-units. A finely laminated, sandstone-siltstone sequence is very similar to units in the lower Oonah Formation (Taylor, 1993). Grey, dolomitic and calcareous beds are interspersed with carbonaceous shale. Volcanic lithologies comprising vesicular pillow basalts, pyroclastics and breccias are also present within the lease (Taylor, 1993; Figure 2-3). Cataclasite, consisting of clasts of Upper Oonah rocks within a carbonaceous matrix, crops out sporadically. The cataclasite mainly occurs in, but is not restricted to, the major fault zones throughout Upper Oonah lithologies and along the contact between the Upper Oonah and Crimson Creek Formations (Taylor, 1993).

Analysis of a "graphite" within the Upper Oonah shales, determined that only minor graphite is present in the carbonaceous shale (Crossing, 1992).

At Comstock, contact metamorphism, or metasomatism, has variously altered the mineralogy and texture of sandstone and siltstone in the Upper Oonah Formation. Recrystallisation and alteration during mineralisation resulted in assemblages of biotite + sericite + chlorite + ilmenite + pyrrhotite + chalcopyrite + minor carbonate and rutile (Halsall, 1992). Some quartz remains as relic, detrital grains, associated with chlorite in polycrystalline agregates, as feldspar associated with lithic fragments, and filling thin veins (Halsall, 1992). Pyrrhotite is the dominant sulphide; it occurs as irregularly

distributed aggregates, or as coarse aggregates associated with thin, quartz-magnetite veinlets (Halsall, 1992). Faulted sections of this unit are extensively weathered, giving some sections a clay-rich "puggy" texture (Richardson, 2000).

Near mineralised areas, the carbonate have recrystallised and is calcite-talc-silica altered, suggesting the low-temperature development of tremolite-calcite-quartz skarn (Richardson, 2000). The graphitic mudstone contains stockwork veinlets of pyrite (Richardson, 2000).

The volcanic breccia comprises basalt fragments with pervasive, chloritic alteration and interstitial sericite. Trace amounts of calcite occur as fillings in thin veinlets. Pyrite is the dominant sulphide, and specks throughout the rock as porous ~1mm aggregates, or as sparsely disseminated grains (Crossing, 1992).

3.3.2.3 McIvor Hill Complex

The McIvor Hill Ultramafic Complex crops out in a small area on the SW boundary of the mine lease (Figure 2-3). The ultramafics consist of highly-altered gabbros that abut the Upper Oonah beds, south of the Tenth Legion Fault (Taylor, 1993; Tear, 2000).

3.3.3 Structure

The Comstock area comprises isoclinally-folded beds, cut by normal, wrench and reverse faults (Tear, 2000; Knight, 1997). Two major faults (the Tenth Legion Fault and the Balstrup Fault), cut through the lease (Figure 2-3). The central west part of the mine lease contains a broad, open anticlinal fold with a NNW fold axis that plunges shallowly to the north.

Precambrian deformation produced isoclinal folds, crenulation cleavages and variable bedding orientations in the Oonah Formation (Berry *et al.* 1990). The Early

Devonian Tenth Legion Fault strikes WNW and dips shallowly to the north (Tear, 2000), and has thrust Oonah formation rocks over the McIvor Hill Complex.

During the Devonian, the Tabberabberan Orogeny produced a series of folds with N-S trending fold axis and associated N and NW striking faults (Berry, 1994), including the Balstrup Fault and the cataclasite in the Oonah Formation. The NW trending folds from the first compression event, were followed by a set of north trending folds (Knight, 1997).

Late-stage NE to ENE fault trends dipping steeply to the east, are interpreted to have formed during the emplacement of the Heemskirk granite in the Late Devonian (Knight, 1997).

2.3.4.1 Mineralisation

The Comstock deposit contains magnetite-serpentinite skarns, massive sulphide skarns and base-metal veins (Taylor, 1993; Knight, 1997; Tear, 2000). The host rocks are carbonate lithologies of the Upper Oonah Formation and ultramafic rocks of the McIvor Hill Complex (Taylor, 1993). Ore is primarily found at the upper contact of the carbonate beds and where it grades upwards into carbonaceous siltstones and shales (Tear, 2000).

Taylor (1993) identified three stages of skarn formation, at the Sylvestor prospect: 1) contact metamorphism; 2) early metasomatism, and 3) late metasomatism stage. During the contact metamorphic event sandstone, siltstone and carbonate units were hornsfelsed. Early metasomatism created patches of fine-grained pyroxene skarn and minor garnet-pyroxene skarn in the carbonates (Taylor, 1993). The later metsomatic stage formed extensive serpentinite-magnetite skarn and brucite-serpentine-magnetite skarn.

Replacement mineralisation was confined to within 5-10m of the faults that carried fluids. Massive pyrrhotite lenses replace magnetite-serpentinite skarn in the immediate footwall of the Balstrup Fault (Taylor, 1993). Massive pyrite replaced dolomitic carbonate in the Upper Oonah Formation where NE structures cut NW and WNW faults and within anticlinal fold hinges. Pyritic stockwork veins surround the massive sulphide lenses and permeate the Balstrup Fault zone (Taylor, 1993).

2.3.5 Mineralogy

The mineralogy of ore lenses and massive sulphide veins at Comstock consist of argentiferous galena and sphalerite in a predominantely pyrite, quartz and siderite gangue (Both, 1966). A list of minerals that have been documented from Comstock is included in appendix 2. Petrological examination of 15 samples, taken from wallrock and massive suphides associated with the Tenth Legion Fault, allowed identification of four distinct sulphide assemblages (Crossing, 1992).

- Massive pyrrhotite; with sphalerite, galena and chalcopyrite present as irregular patches and as inclusions in pyrrhotite.
- Euhedral pyrite; with sphalerite and galena associated with masses of euhedral pyrite.
- Interstitial pyrrhotite; with sphalerite, galena and chalcopyrite intergrown with pyrrhotite, found interstitial to coarse euhedral pyrite.
- Secondary pyrite; with sphalerite and galena associated with pyrrhotite which has been replaced by fine-grained pyrite-magnetite.

2.3.6 Mechanisms of Mineralisation

The Tenth Legion Fault and the Balstrup Fault are believed to have been conduits for mineralising fluids (Tear, 2000; Tear, 1999; Crossing, 1992). Tear (2000) suggested ore-bearing fluids pooled beneath the Tenth Legion Fault melange, before moving along cross-cutting NNW and NE faults. Fissure-fill veins formed when the bedding planes of fold hinges in quartzite, volcanics or slate were dilated. Fissure-replacement veins formed when extensively fractured, carbonate zones were replaced (Summons, 1983).

Fluids were neutralised rapidly by interaction with the thick, impermeable carbonate horizons (Crossing, 1992). The massive sulphide lens is distal, and genetically related, to a 3.5 km long skarn complex (Crossing, 1992).

2.4 Summary

- The Comstock mine lease is situated within a hydrothermal zoned, mineral field, in the pyritically-altered zone.
- Zonation arose when enriched fluids, associated with the emplacement of a Devonian granitoid, radiated away from the granite along fault structures and subsequently deposited the ore.
- The mine is situated within a meta-turbidite sequence (Upper Oonah Formation), that was deformed in the Late Precambrian.
- The predominant structures within the mine lease are two WNW striking faults.
- Subsidiary fault structures trend N, NW, and NE to ENE.
- The mine contains argentiferous galena and sphalerite within a primarily quartz and pyrite gangue.
- The ore is hosted within the carbonate sequences of the Oonah Formation.
- Ore is proximal to fold and fault structures, with carbonate-replacement mineralisation near to faults, within cross-cutting structures, and in anticlinal fold axis.

Section Two:

Water Quality Analysis.

Chapter 3

Methodology and Site Locations

3.1 Introduction

Water draining from the tunnel system at Comstock is highly acid, contains heavy metal loadings, and has a medium to high conductivity (DPIWE Files, 1997-2000). Iron oxyhydroxide precipitates are extensive around adit entrances, and abundant precipitates have been observed at least a kilometre downstream of the main adit (Plate 3-1). The presence of these precipitates is evidence of AMD; they consist of abundant iron released during the oxidation of pyrite.

Fieldwork over the winter of 2000 was conducted in order to: 1) quantify water composition under different climatic regimes and, 2) identify geochemical processes that affect water composition. The study included measurement of flow characteristics and water sampling in low and high flow conditions to evaluate contaminant concentrations in different flow regimes. The combination of flow and contaminant data allowed estimation of the amount of contaminant present in Comstock Creek in varied climatic conditions. The nature of contaminant transport was modeled using PHREEQC and PHOX software.

3.2 Sample Sites

Nine water-sampling sites were chosen in order to monitor both background and downstream locations (Figure 3-1). Four sites were situated above the mine and tunnel system, to provide data on the quality of waters entering the site. Four sites were chosen downstream of the mine workings, and an additional site, located above the main adit discharge, was selected to provide information on the quality of water before it was mixed with water from the main adit.

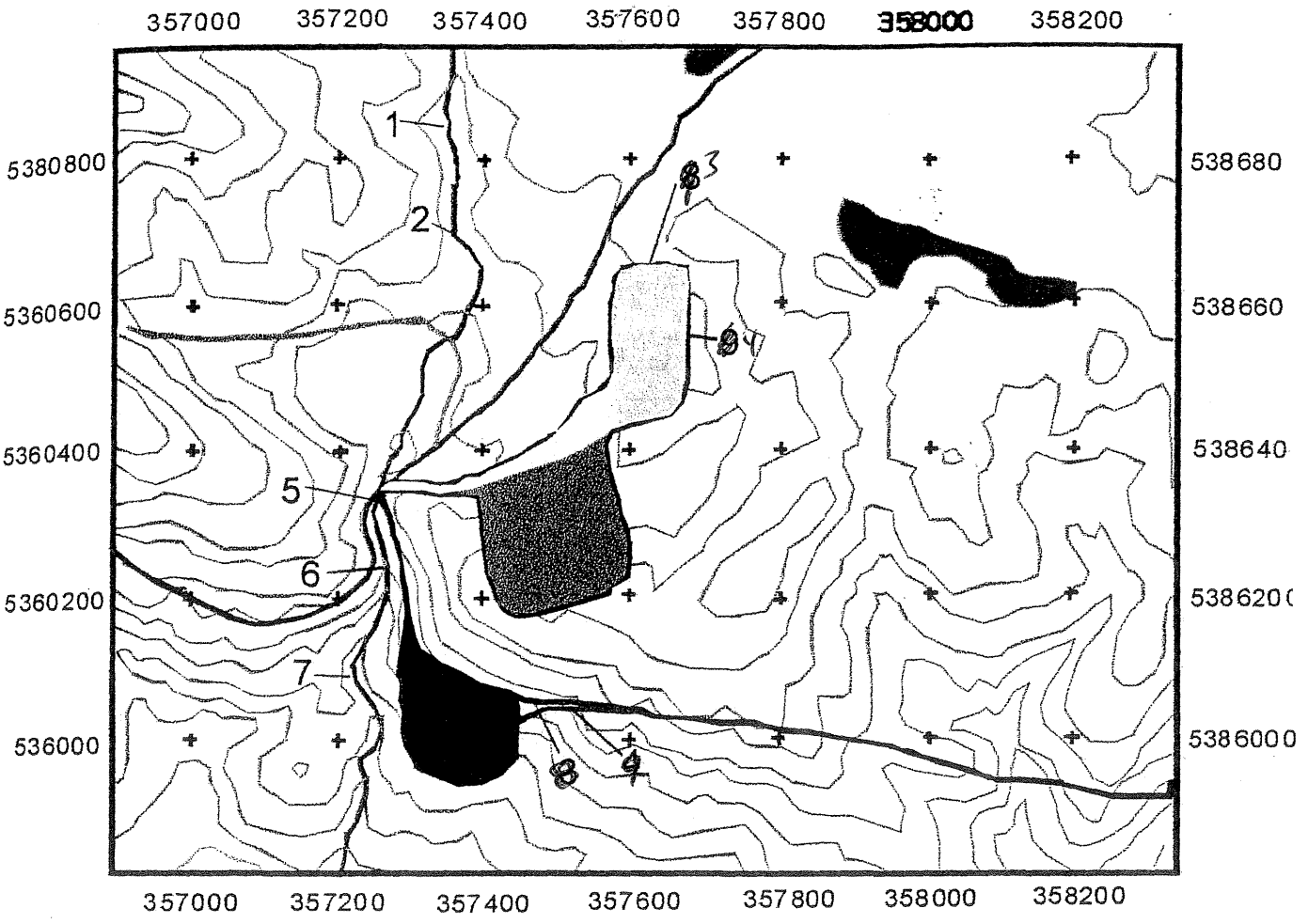

Figure 3-1: Water Sampling Sites at Comstoc

A. Site 1. Background water quality before entering the mine workings.

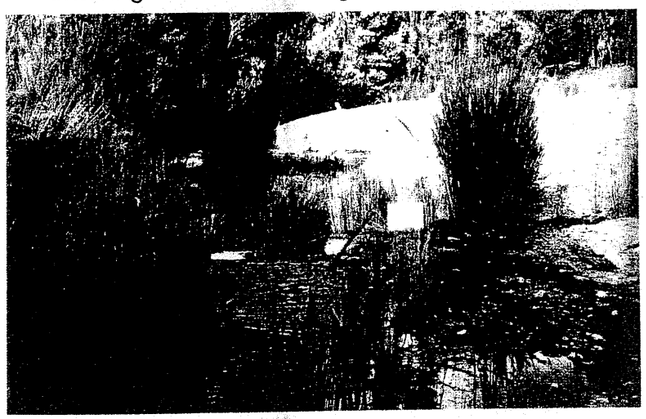

B. Site 2. Water quality before entering the tunnel system..

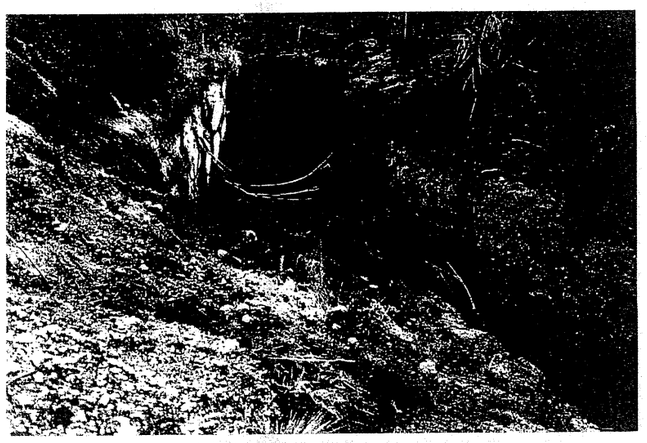

C. Site 3. Water is diverted from the decline, utilising an old shaft (photo prior to decline excavation).

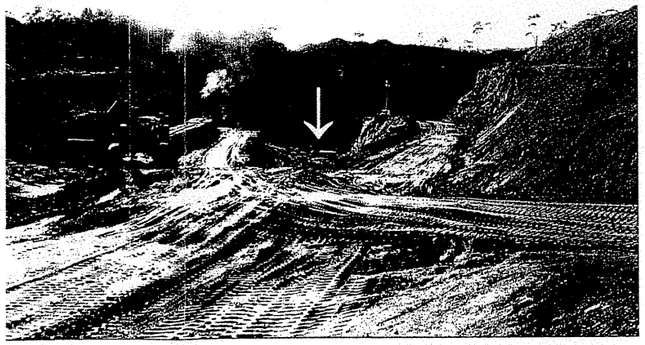

D. Site D. Looking north into the decline,another shaft draining the decline is in the centre of this photograph (under arrow)..

E. Site 5. Water quality downstream of mine, but prior to mixing with main adit (site 6) waters.

Plate 3-1: Water Quality Monitoring Sites.

F. Site 6. Water exiting from the tunnel system (the main adit)..

G. Site 7. Water flowing downstream, out of the mine lease.

Site 1 was chosen to provide an indication of water quality in Comstock Creek above any mine workings (Figure 3-1; Plate 3-1a). Site 2 was situated next to an old crushing site, currently covered in crushed ore and waste rock (Figure 3-1; Plate 3-1b). It was chosen to provide an indication of water quality directly before it entered the tunnel system. Sites 3 and 4 were situated in the decline into Allisons Lode (Figure 3-1; Plate 3-1c); these were chosen to measure the quality of water entering the tunnel system. The mine operators constructed site 3 in order to drain water from the Balstrup Fault, and keep it away from the mining activity (Figure 3-1; Plate 3-1c); it directs flow into a shaft joining the tunnel system. Site 4 was at the sediment-trap (Figure 3-1; Plate 3-1d); the site was constructed to prevent sediment washing into the tunnel system. Surface water from the mine flows through the sediment trap and enters another shaft joining the tunnel system. Both of these sites were ephemeral, such that sampling was opportunistic.

Site 5 was located at a road drain (Figure 3-1; Plate 3-1e); it was chosen to provide information on water parameters downstream of the mine but before mixing with tunnel system drainage waters. Site 6 was situated at the main exit point for all water travelling through the tunnel system (Figure 3-1; Plate 3-1f). Site 7 was approximately 100m downstream of 6 (Figure 3-1; Plate 3-1g), and was chosen in order to determine the effects of mixing and dilution with relatively uncontaminated water, on the quality of water flowing from the tunnel system. Flow measurements were taken at sites 5, 6, and 7, in order to determine mass loads, and therefore quantify contaminant transport. The site would also aid in identification of the effects of mixing on the contaminant loads.

Sites 8 and 9 were at the entrances to two small exploration adits, less than 50m long (Figure 3-1). Flow from these adits was low but they were chosen in order to provide additional information about the effects of geology on water quality.

NUMBERS APPEAR TO BE REVERSED COMPARED TO THE FIG 3-1 TEXT DESCRIPTION HERE

MATCH COLUMN NAMES IN APP 3&4 PHOTOS ON PLATE 3-1

3.3.1 water sampling

Water was analysed to determine pH, redox potential, electrical conductivity and temperature; equipment used and calibration solutions, are listed in Table 3-1. Most testing was conducted in situ but water analysed on the 27 July (high flow) was collected in 2, 1L HDPE bottles that had been rinsed three times with site water before filling. The bottles were immediately transported to the site office for analysis.

Water Parameter	Instrument	Calibration Solution
Electrical Conductivity	WTW Meter	WTW proprietary solution
pH	WTW pH 330 meter & WTW pH electrode	pH 4 and pH 7 buffer solution
Redox Potential (Eh)	Orion Eh Electrode & WTW pH 330 meter	Zobells Solution

Table 3-1: Equipment used for water testing, and solutions used for calibration.

Samples were collected at the same time for anion and cation analysis. Those samples to be analysed for anions were collected in 500ml HDPE bottles. Samples were chilled at approximately 4°C in an Esky and transported to the Department of Primary Industry, Water and the Environment laboratories (DPIWE labs), for analysis by ion-chromatography.

Cation samples were collected in 100ml HDPE bottles. The bottles had been washed with laboratory grade detergent, rinsed three times with tap water, three times with distilled water and soaked in 10% HNO_3 for 24 hours. The bottles were then removed from the solution, rinsed twice with tap water and twice with distilled water, and tops were screwed on firmly. The bottles were not opened again until water samples were added. Each bottle was rinsed three times with site water and the sample was collected upstream of the rinsing area. The water was taken from the middle of the stream, approximately 10cm below the water line (where possible).

Two samples were collected at each site. Total cation samples were collected as described above. Dissolved cation samples were taken with a 0.45μm filter attached to a 10ml syringe; both were in sterile packaging prior to sampling and a new set was used at each site. The bottle were rinsed three times with filtered site water before the 20ml sample was added. For both samples approximately 1ml of 1M HNO_3 was added per 10ml of sample.

Water was collected twice; once when it had been raining for at least a week prior to sampling, and once after 5 days with no significant precipitation.

3.3.2 flow measurement

Water flow in Comstock was measured using the method of Brassington (1992). The stream width was measured, and divided into sections of 20cm. The depth of the stream was measured every 20cm and this was used to determine the area of that section. These values were used to provide an estimate of the area of the stream at that point. Flow velocities were determined using a Flow Mate flow velocity meter. The meter was immersed approximately 10cm below the water surface, at 20cm intervals and three values for water velocity were obtained. If any of the values were anomalous, the velocity measurements were repeated. Values for water velocity at each point were then averaged, and applied to that section. Flow was determined for the entire profile by adding flow values for each section.

3.3.3 mass loads

Mass loads were calculated using a combination of laboratory-determined ion concentrations, and flow measurements. Equation 3-1 was used to determine the loads ;

$$M=Q*C \quad \text{(Equation 3-1)}$$

Where; M = mass load
Q = contaminant concentration
C = flow

3.3.4 modelling

Two geochemical modelling packages were used to predict metal speciation and saturation indices. These programs enabled the nature of the contaminants and potential precipitates, to be determined under both sets of conditions. This allowed the potential bioavailability and toxicity of contaminants to be estimated. Phase changes were compared before and after travelling through the tunnel system, thus providing an indication of the impact tunnel drainage has on the ecological impact of contaminants.

PHREEQC has been designed specifically for modelling aqueous, geochemical reactions, and enables determination of: 1) speciation and saturation indices, 2) reaction paths and advective transport; and 3) inverse modelling of water compositional differences (Parkhurst, 1995). Modelling completed for this thesis was limited to calculations of speciation and saturation indices. The *Wateq4f* database was used to provide thermodynamic data for aqueous species, gas and mineral species, it contains a more comprehensive range of elements than the *PHREEQC* database that is supplied with the program (Parkhurst, 1995).

PHREEQC is limited by a number of assumptions implicit in its calculations. It accounts for non-ideality of solutions using equations that are applicable to low-ionic strength solutions but are less valid in high-ionic stength solutions. The database itself is also internally inconsistent as reaction enthalpies and log K values are derived from a variety of sources (Parkhurst, 1995). As such, results need to be interpreted with reference to the assumptions inherent in the modeling calculations.

PHOX (version 1.3) was used to predict the presence of aqueous species and relative abundances. It was also used to calculate relative mineral stability fields, based on abundance data for each metal. PHOX is also limited by various assumptions built into the model. The most important of these are: 1) only the species listed in the input data table are considered in the predominance diagrams; 2) all activity coefficients are assumed to be 1; 3) only a simple linear model is used to assign phase boundaries; and 4)thermodynamic equilibrium is assumed.

Chapter 4:

Background Water Quality

4.1 Introduction

ARD is affected by climatic, geological, and geographic variation. Mean daily temperatures, precipitation, and evaporation influence Acid Rock Drainage reaction rates. Warm temperatures are associated with increased reaction rates and evaporation, while rain alters water table levels (affecting horizons of oxidation and reduction), and flushes sulphide oxidation products (Kelly, 1988).

During dry periods, secondary metal-salts build-up as oxidation products (Alpers & Zierenberg, 1998), which are consequently flushed during precipitation events. Storm-induced flushing is often associated with a "peak" of acidity, sulphate, and dissolved metals, released into receiving waters (Miller & McHugh, 1994).

4.2 Methodology

Background water quality at Comstock was sampled in two sets of climatic conditions. A wet weather, high flow period was sampled on the 27th of July, 2000, after a prolonged period of rain (Figure 4-1). Dry weather, low-flow samples were obtained on the 22nd of September, 2000, after 5 days of less than 0.5mm of rain (Figure 4-1). A storm event was intensively monitored from the 2nd to the 3rd of September, 2000 (Figure 4-1), after five days of low flow conditions. During the storm event sampling was conducted at one hour intervals, in order to ascertain whether storm events, result in contaminant plumes flushing out of the tunnel system and into Comstock Creek.

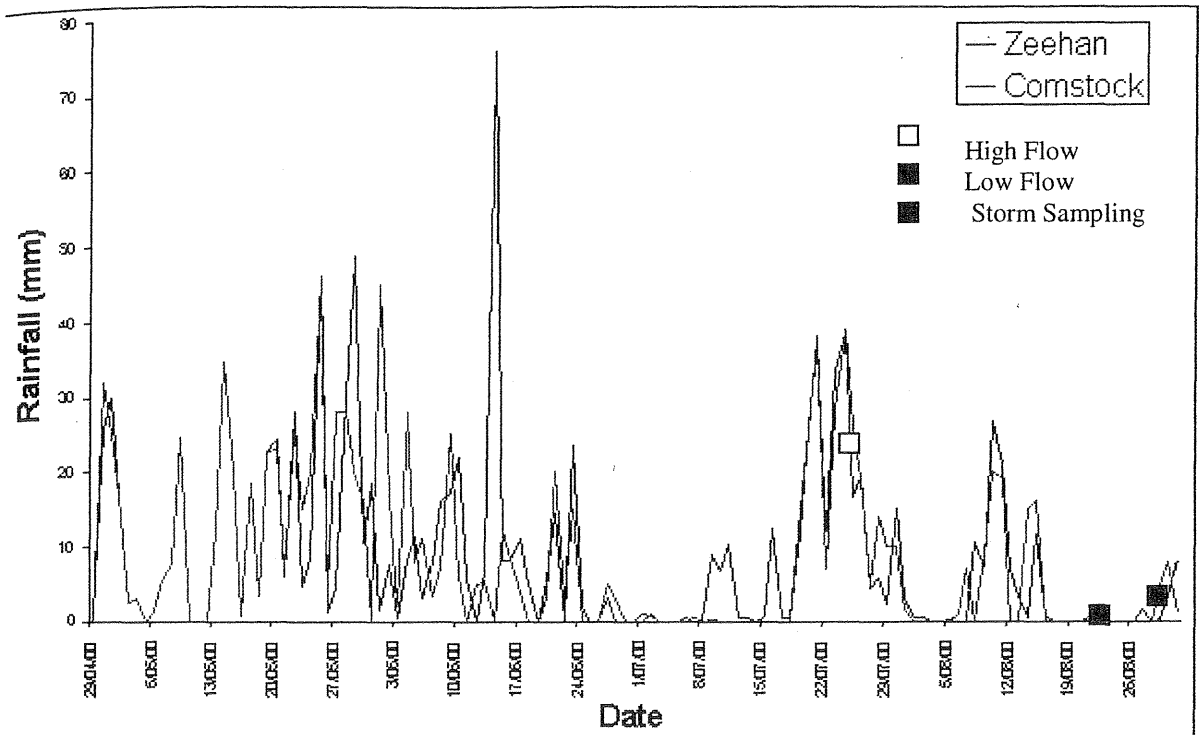

Figure 4-1. Rainfall (mm) at Comstock and Zeehan 29.04.00 – 22.09.00, with respect to sampling times.

4.3 Field Data

4.3.1 Introduction

In situ measurements of pH, Eh, EC and temperature were obtained during each field sampling program. These were used in conjunction with laboratory analysis, to define spatial and temporal contamination patterns in the Comstock drainage system. This allowed the relative contributions of acidity and metal loadings to Comstock Creek to be calculated.

4.3.2 pH

The measured pH increases between background catchment levels (pH 4.58 in high flow and 5.46 in low flow), and downstream of the mine (pH 5.29 in high flow and 5.81 in low flow), during all measured flow conditions (Figure 4-21, 4-31 & 4-41). Catchment waters have

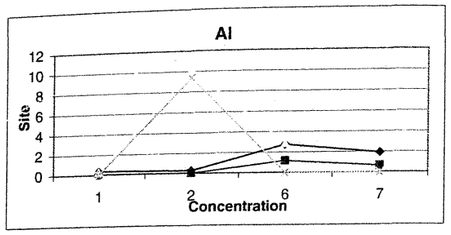

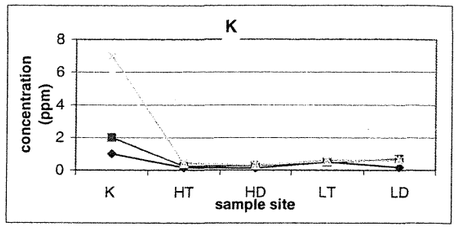

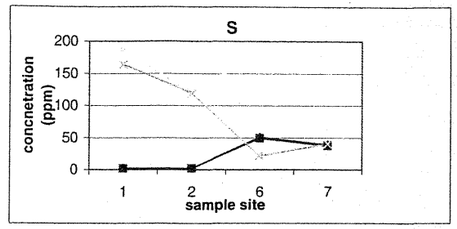

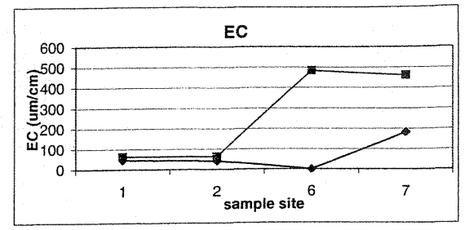

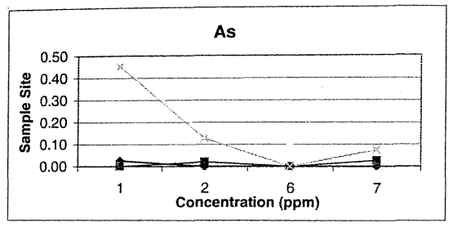

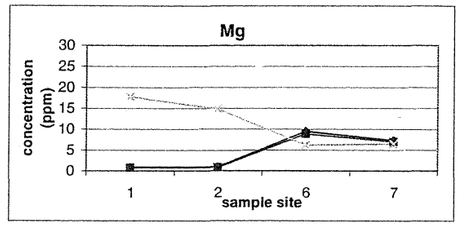

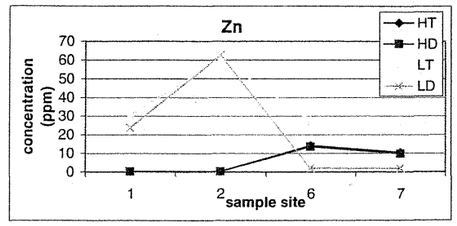

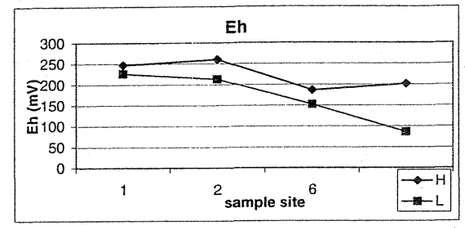

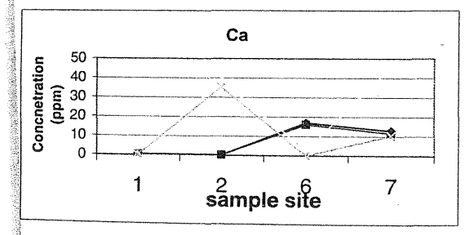

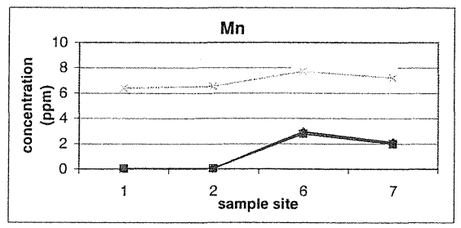

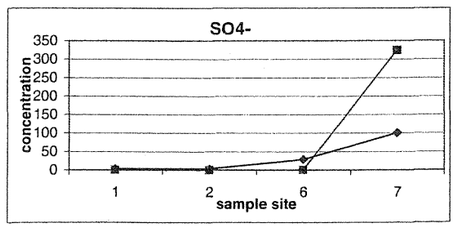

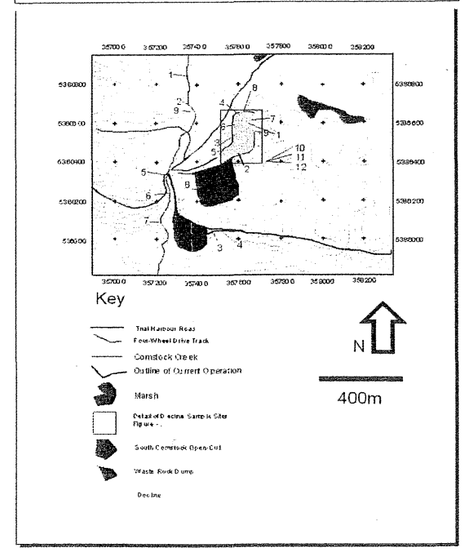

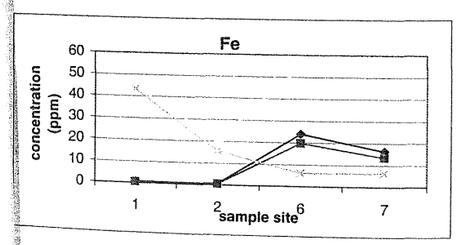

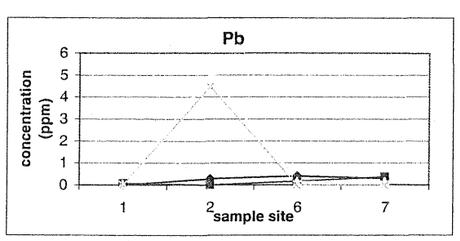

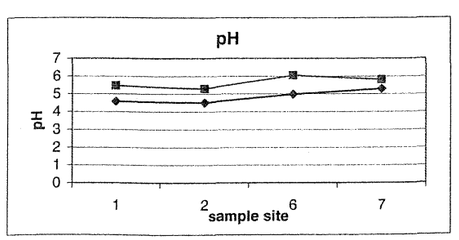

Figure 4-2: water compositions at sites 1, 2, 6 & 7 at comstock

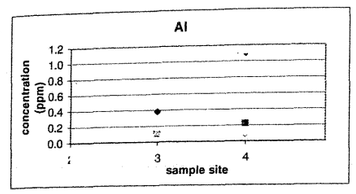

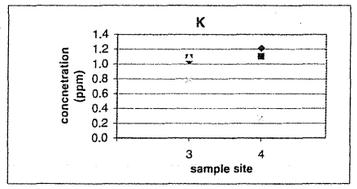

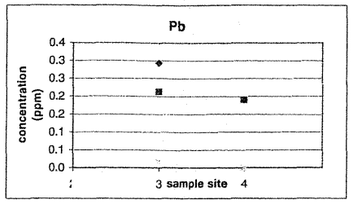

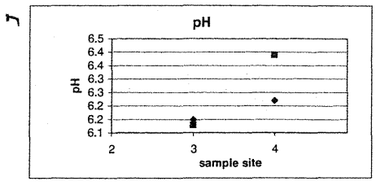

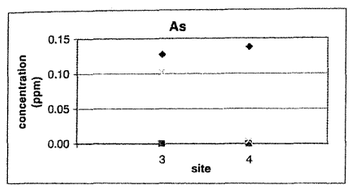

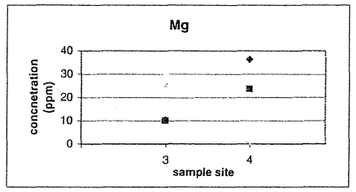

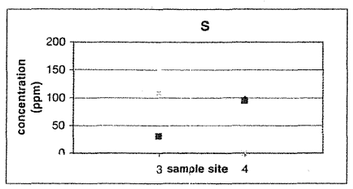

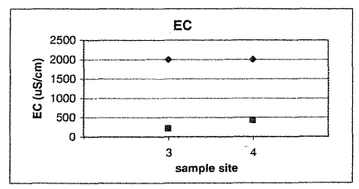

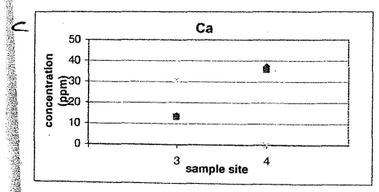

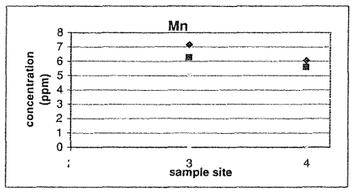

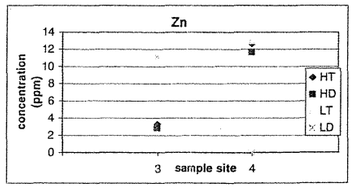

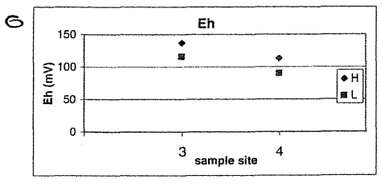

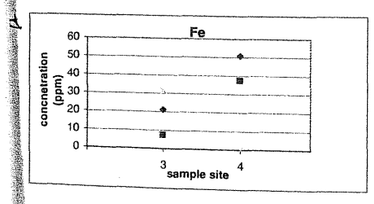

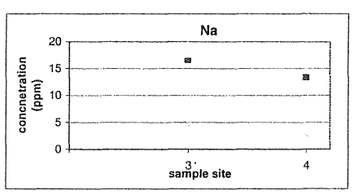

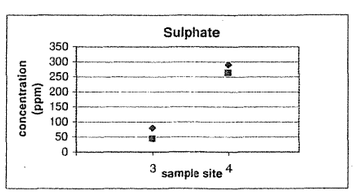

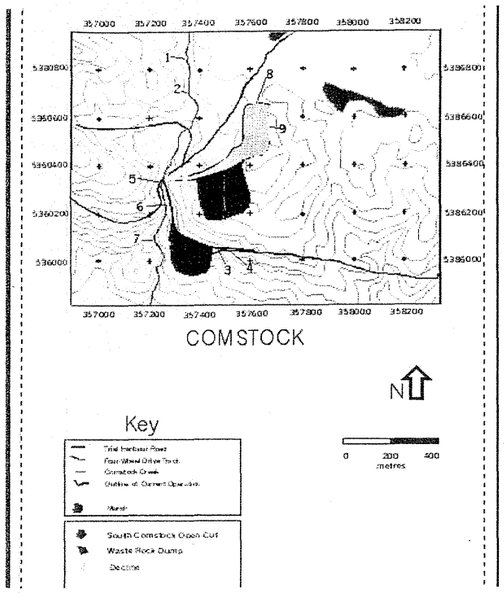

Figure 4-4
Water compositions at sites 3 & 4 at comstock

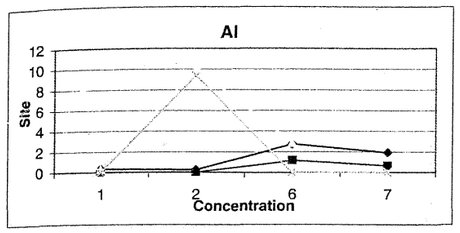

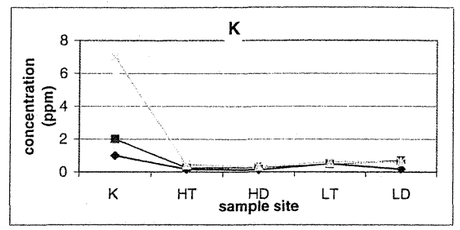

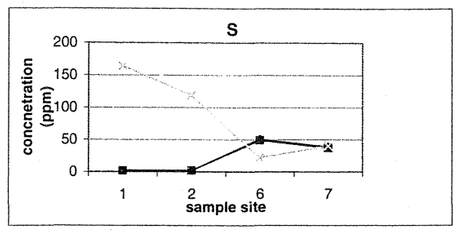

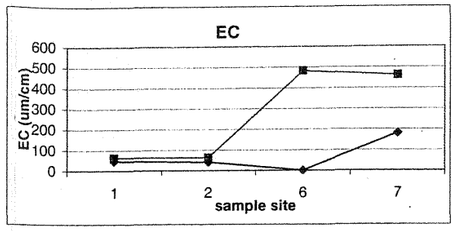

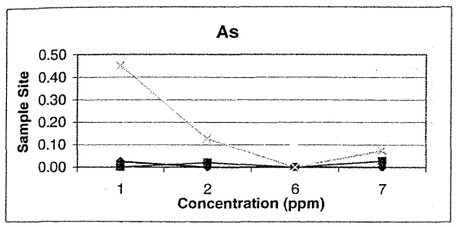

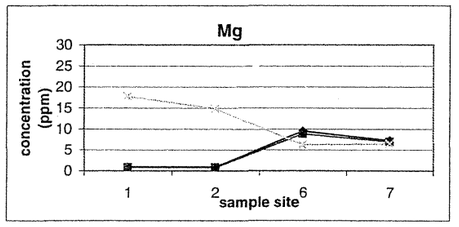

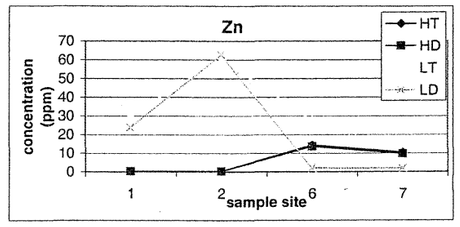

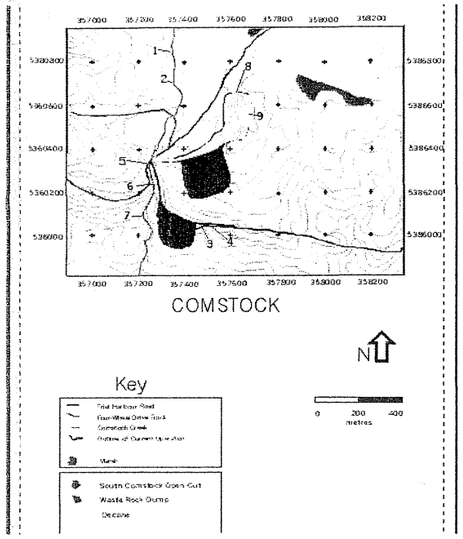

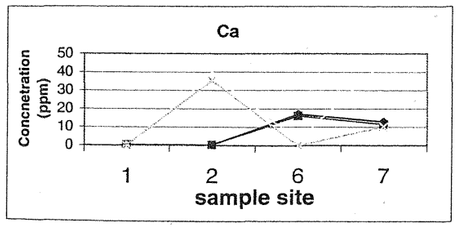

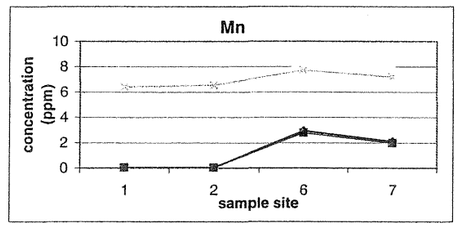

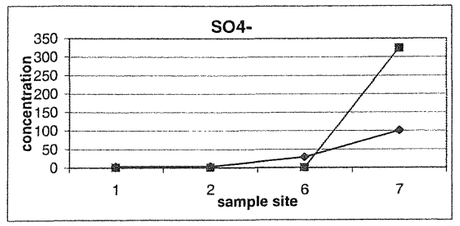

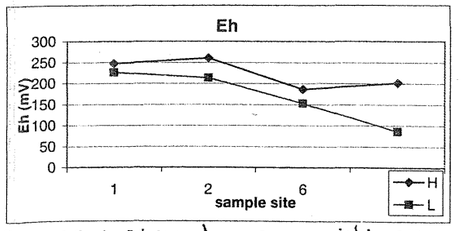

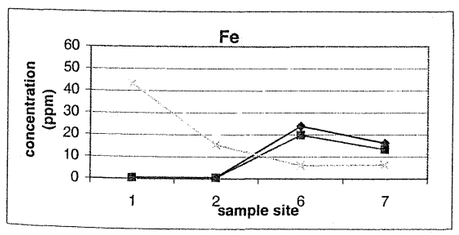

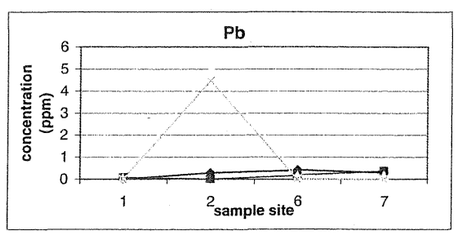

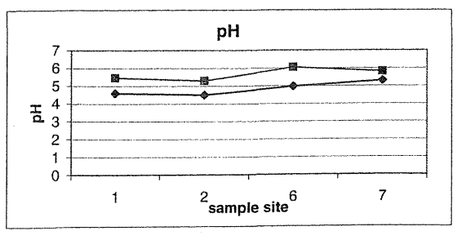

Figure 4-3: Water compositions at sites 1, 2, 6 & 7 at Comstock

a low initial pH, that decreases by about 1 pH unit during high flow conditions. Water sampled at site 2 had pH values that decreased by 0.5 in high flow conditions, compared with low flow values. After flowing through the tunnels, drainage waters are partly neutralised, pH values increase by 0.35 pH units in low flow conditions and 0.71 pH units in high flow conditions.

The largest variation in pH values from high flow to low flow conditions occurs between sites 6 and 7. In high flow conditions, the pH steadily increases from 4.97 pH units to 5.29 pH units downstream (Figure 4-2l). In low flow conditions, there is a drop in pH of about 0.2 pH units (Figure 4-2l).

In high flow weather, the pH of waters in site 8 had a pH value of 6.03, whereas site 9 waters had a pH of 3.29, which was lower than at any other site. Likewise, during low flow conditions the pH of water in site 8 (4.5 pH units), had the lowest pH values measured in those conditions, the sediment trap was not flowing (Figure 4-3l). The pH values of sites 3 (pH 6.15 in high flow, and 6.13 in low flow) and 4 (6.22 in high flow, and 6.39 in low flow) were higher than values obtained at any other site, apart from at site 5, the pH of which was measured as 6.24 in high flow conditions, and 6.42 in low flow conditions (Figure 4-4l).

4.3.3 Redox Potential (Eh)

Eh decreased from 247mV to 201mV between background and downstream sites in high flow conditions (Figure 4-2n). In low flow conditions the decrease was of greater magnitude; background water Eh values measured at 226mV, while downstream waters had an Eh of 86mV (Figure 4-2n). In low flow conditions, Eh decreased by 13 mV, between sites 1 and 2 (226 mV to 213 mV: Figure 4-2n & 4-3o). In high flow conditions there is a slight increase of 13 mV, between the two sites (247 mV to 260 mV: Figure 4-2n & 4-3o). By site 6, water Eh values had decreased by more than 50 mV, compared with the Eh of water immediately prior to entering the tunnel system (site 2), this occurred in both flow regimes (Figure 4-2n). In low flow conditions, Eh values continued to decrease downstream to site 7, in wet weather, Eh has increased in the mixing zone (Figure 4-2n).

The Eh of waters in the decline had the highest values on site during high and low flow conditions, site 8 had Eh values of 298 mV and 344 mV respectively. Site 9 had the highest

Eh value of any sample, measuring 413 mV (Figure 4-3o). At sites 3 and 4, the adits release water with low redox potentials compared with the other sites (116 mV and 90 mV respectively in low flow conditions, and 137 mV and 113 mV in high flow conditions (Figure 4-4o). Only site 7, in low flow conditions, had a lower Eh (86 mV: Figure 4-3o).

4.3.4 Electrical Conductivity

The conductivity of water increased from 63 uS/cm to 461 uS/cm in low flow conditions, and 45.5 uS/cm to 181.7 uS/cm in high flow regimes, between background and downstream sites (Figure 4-2m). Higher conductivities were measured during low flow conditions than high flow conditions. This increase occurs to the greatest extent after waters have passed through the tunnels. Main adit water has vastly increased conductivities compared to inflow sites (Figure 4-3m). Waters in the mixing zone had slightly decreased conductivity compared to main adit samples, but the decrease is slight (Figure 4-3m).

In low flow conditions, sites 3 and 4 had electrical conductivities that were high (216 and 429 uS/cm respectively: Figure 4-4n), although sites 8, 7 and 6 exceeded these values. The electrical conductivity of samples from the two small adits were high in high flow conditions (sites 3 and 4 had ECs that exceeded 2000uS/cm: the conductivities at these sites exceeded the maximum detection limits of the EC meter). This was also the case for waters in the decline and at the main adit.

4.4 Analytical Data

4.4.1 Introduction

Water samples, taken from each sample site in high and low flow conditions were analysed for anion and cation composition. This enabled characterisation of the sample sites in terms of rock and mineralogical influences, degree of contamination, and for modelling. The data obtained is presented in figures 4-2,4-3 & 4-4, and summarised in Table 4-1. All analysis results are presented in Appendix 3.

4.4.2 Results

Water samples were analysed for twenty common elements (Al, As, B, Ba, Ca, Cd, Co, Cr, Cu, Fe, K, Mg, Mn, Mo, Na, Ni, P, Pb, S, Se, Si, Sn, V, and Zn), and nitrate, nitrite,

chloride, sulphate, and carbonate ions using methods described in chapter 3. Figures 4-2, 4-3 and 4-4, spatially and temporally summarise the concentrations of selected elements and parameter values, collected from Comstock during a high and a low flow event. Table 4-1, presents all maximum and minimum values obtained from the sampling.

Low Flow

Parameter	Max. Value	Min. Value	Site of Maximum Value
Al	9.37	0	2
As	0.45	0	2
B	0.13	0	2 & 5
Ba	0.06	0	6 & 7
Ca	35.7	0	5
Cd	0.21	0	2
Co	0.11	0	2
Cr	0	0	N/A
Cu	0.03	0	2
Fe	46.14	0	5
K	0.69	0.16	1
Mg	25.25	0	3
Mn	7.31	0	6
Na	8.55	0.73	8
Pb	4.47	0	2
S	170.12	0	6
Si	5.25	0.76	6
Sn	0.05	0	2
Zn	6.27	0	2
Cl-	27.84	12.84	9
HCO3	6	0	3
SO4-	494	18	9
pH (Lowest)	4.5	6.42	6
Eh	344	62.9	9
EC	OFL	86	9

High Flow

Parameter*	Max. Value	Min. Value	Site
Al	13.06	0	8
As	0.13	0	9
B	0.06	0	8
Ba	0.09	0	3
Ca	35.82	0.24	4
Cd	0.27	0	9
Co	0.33	0	8
Cr	0.05	0	6 & 4
Cu	0.04	0	8
Fe	37.62	0.45	4
K	4.03	0.13	8
Mg	59.35	0.78	8
Mn	6.27	0.04	3
Na	16.62	6.41	3
Pb	5.67	0	8
S	130.42	1.78	8
Si	7.13	0.76	4
Sn	0.07	0	1
Zn	42.39	0.23	9
Cl-	26	9.7	3
HCO3	6	<1	3
SO4-	400	3.7	9
pH (Lowest)	3.29	6.24	8
Eh (mV)	413	113	8
EC (uS/cm)	OFL	38.4	9 & 8

Table 4-1. Maximum values at Comstock water sampling sites, in low and high flow conditions.

*Element concentrations in ppm.

Element concentrations were higher at sites 3 and 4 during low flow conditions, whereas the highest element concentrations in high flow conditions were predominantly found in samples from sites within the decline (sites 8 & 9).

4.5 Comparison with Water Quality Guidelines

4.5.1 Introduction

The Australia New Zealand National Environment Council (ANZECC) have developed water quality guidelines in recognition of the need to protect aquatic ecosystems from the

adverse impacts of trace element and heavy metal contamination (Table 4-2; ANZECC/NWQS 1992). The guidelines recommend acceptable concentrations levels, above which contamination is potentially deleterious to human health, and/or biodiversity. These standards have generally been developed using case studies from places that are climatologically, biologically, geographically and geologically different to the environments of Tasmania's west coast.

Attribute	Recommended Maximum
pH	6.5-9 pH units
Al	0.010
As	0.050
Cu	0.005
Fe	1.00
Pb	0.005
Zn	0.01

Table 4-2. Attributes from ANZECC/NWQS water quality guidelines for protection of aquatic ecosystems, with relevance to this study.

The results of elements and anions that were above detection limits are interpreted with respect to acceptable concentrations (as per ANZECC guidelines) in this section. The ANZECC guidelines concern total contaminant concentrations, as opposed to dissolved contaminant concentrations (generally more bioavailable; Appendix 1).

4.5.2 Aluminium

Aluminium concentrations exceed ANZECC guidelines in most of the samples collected during high flow conditions (Figures 4-2a, 4-3a & 4-4a). This applies to both dissolved and total metal samples, although dissolved metals are less than recommended maximum values in the background sites. Sites 8 and 9 contained the highest concentrations of both dissolved and total aluminium.

During the low-flow sampling regime, aluminium concentrations exceeded recommended concentrations in total samples (Figures 4-2a, 4-3a & 4-4a). Dissolved aluminium concentrations only exceeded recommended maximum concentrations at sites where water does not flow directly into the tunnel system, or Comstock Creek (Figures 4-2a, 4-3a & 4-4a).

4.5.3 Arsenic

Samples collected from sites 3 and 4 during high flow conditions exceeded guidelines for arsenic (0.05ppm; Figures 4-2b, 4-3b & 4-4b). Discrepancies in the concentrations of dissolved vs. total arsenic in samples from sites 8 and 9 suggest sample contamination, possibly from arsenic-rich hydroxide precipitants (Figures 4-2b, 4-3b & 4-4b). Sampling under low flow conditions, revealed that total arsenic concentrations were lower than guidelines in the sample from site 4 (Figures 4-2b, 4-3b & 4-4b). All other sites exceeded recommended limits, with concentrations highest in samples from sites 1 and 2 (0.45 ppm at each).

4.5.4 Cadmium and Copper

Cadmium and copper concentrations were below detection limits in all samples.

4.5.5 Iron

In wet weather, total and dissolved iron concentrations exceeded guidelines at all sites at and below the mine area (Figures 4-2d, 4-3d & 4-4d). During dry weather, dissolved and total iron concentrations exceeded guidelines at almost all sites. Only water from site 4 and site 9 registered no dissolved iron content.

4.5.6 Lead

Total and dissolved lead concentrations in high flow conditions exceeded guidelines at most sites (0.005 ppm); only water from site 2 contained no dissolved lead (Figures 4-2i, 4-3i & 4-4i). The highest concentrations were in water from site 8 (6.19 ppm total, and 5.67 ppm dissolved). In low flow conditions, most site waters contained no dissolved lead, whereas total lead concentrations exceeded recommended limits at almost all of the sites (Figures 4-2i, 4-3i & 4-4i). Only site 4 contained no lead, dissolved or total.

4.5.7 Zinc

Zinc appears to be one of the main contaminants at the mine. In wet weather, every site monitored exceeded guidelines for total and dissolved concentrations (Figures 4-2k, 4-3k &

4-4k). In dry weather, dissolved samples from sites 4 and 9 were free of lead, whereas total and dissolved water samples from all other sites exceeded guidelines (Figures 4-3k & 4-4k).

4.6 Ficklin Plots

4.6.1 Introduction

Ficklin plots are used to categorise mine drainage water quality (Ficklin *et al.*, 1992; Plumlee *et al.*, 1992). Plotting pH against a total concentration of a suite of common, heavy-metal contaminants, drainage waters can be classified in terms of the two major parameters of concern for polluted waterways. Ficklin plots have been generated for the Comstock samples, in order to classify water quality at each site in wet and dry conditions (Figures 4-5 and 4-6).

In his study of drainage water compositions emanating from mines around the Zeehan mineral field, Parr (1997) used Ficklin plots to classify drainage waters at each site, and categorise them in terms of local geological and mineralogical controls. Figures 4-7 and 4-8 illustrate Parr's results for waters emanating from various mines in the Zeehan mineral field.

4.6.2 Results

Figure 4-6 is a Ficklin plot of Comstock water compositions measured during low-flow conditions. It appears that during dry periods, Comstock Creek waters (sites 1 & 2), flowing into the tunnel system are the least contaminated (acid, low metal), whereas waters entering the tunnel system from the Balstrup drain, in the decline, are the most contaminated (site 8), being acid, high-metal. Waters emanating from the main adit at site 6 have near-neutral pH, but metal concentrations were high metal. Similar waters were analysed downstream in site 7 (near-neutral, high-metal). Adits at sites 3 and 4 discharge near-neutral, high-metal in low flow periods.

During high flow conditions, water compositions from individual sites vary markedly from low flow conditions sampling (compare Figures 4-6 and 4-5). Surprisingly, the most contaminated waters were found to be sites 1 and 2 (acid, high-metal). Site 1, upstream of mine workings, which was selected in order to represent the water quality of the catchment, was the found to be the most acidic and metal-rich of any sample taken (Figure 4-5; Appendix 4-1). Waters draining from the main adit (site 6) were found to have acid, high-metal

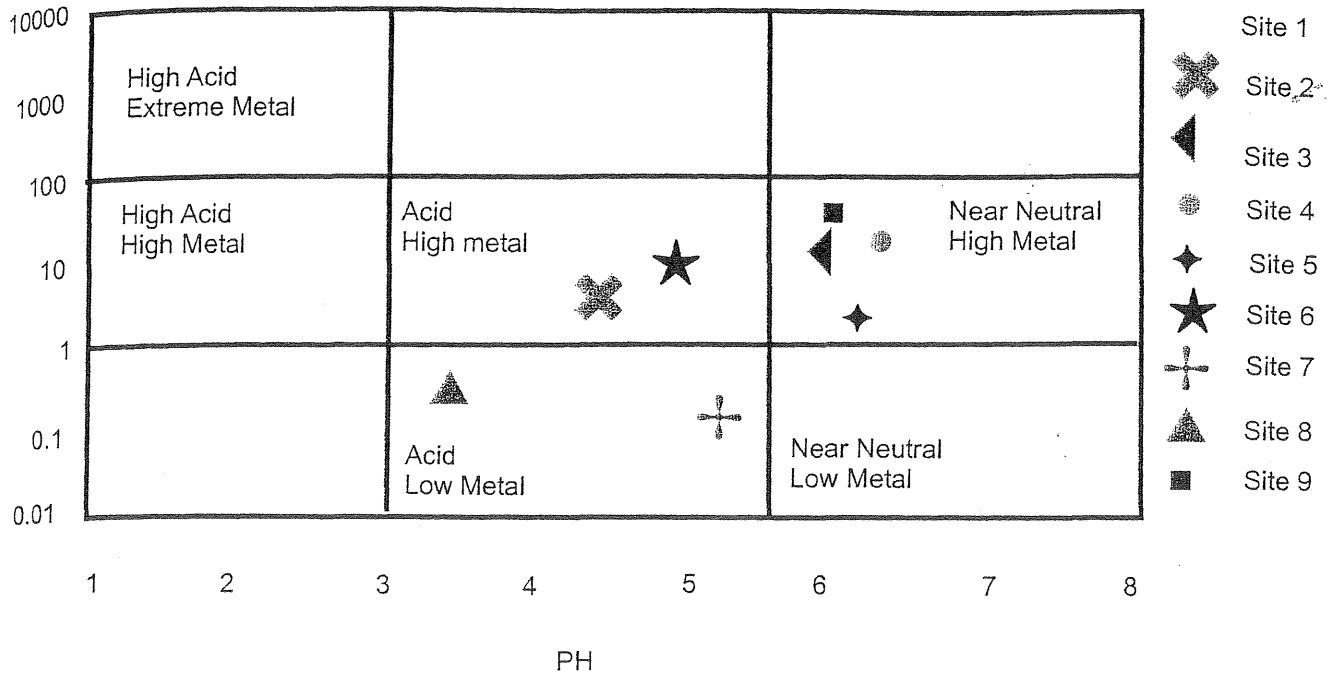

Figure 4-5. Ficklin Plot of Water Compositions from Sites at Comstock, Sampled During High Flow Conditions.

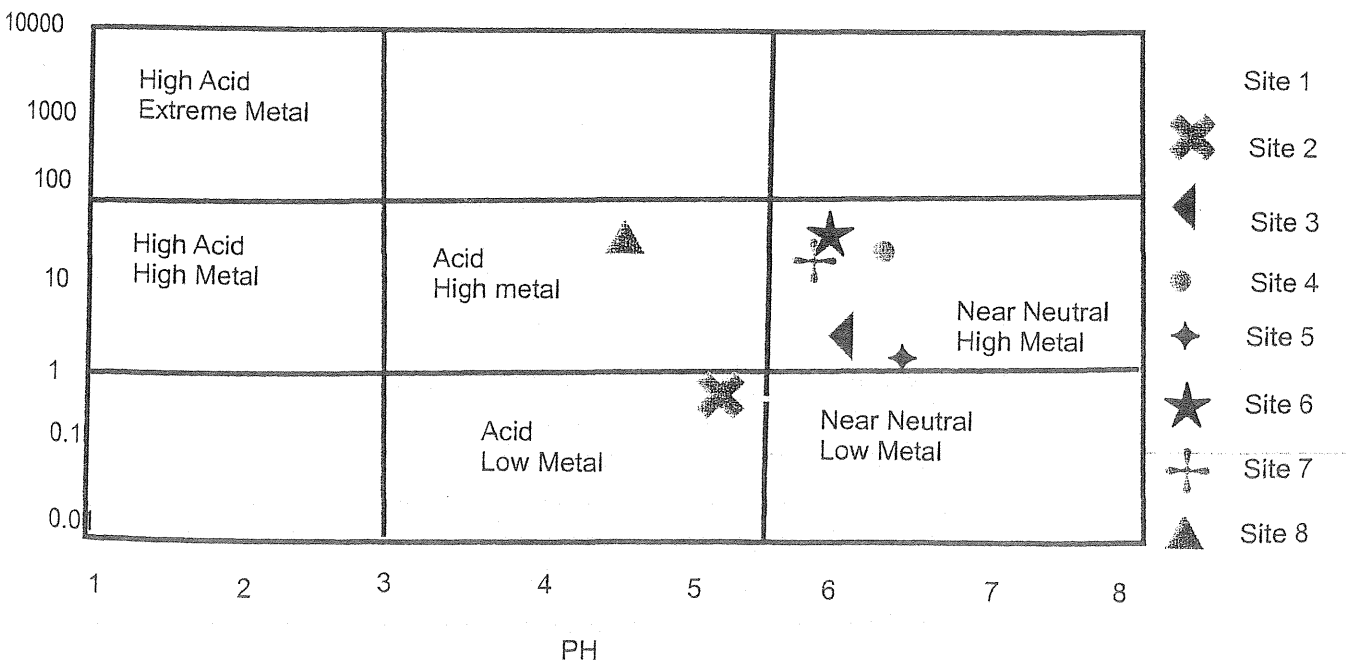

Figure 4-6. Ficklin Plot of Water Compositions from Sites at Comstock Sampled During Low Flow Conditions.

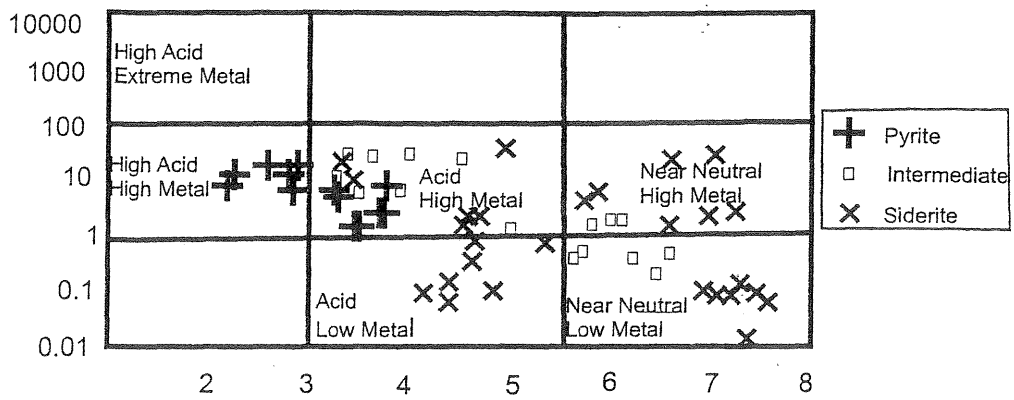

Figure 4-8. Ficklin Plot of Composition of Waters Draining From the Alteration Zones in the Zeehan Mineral Field

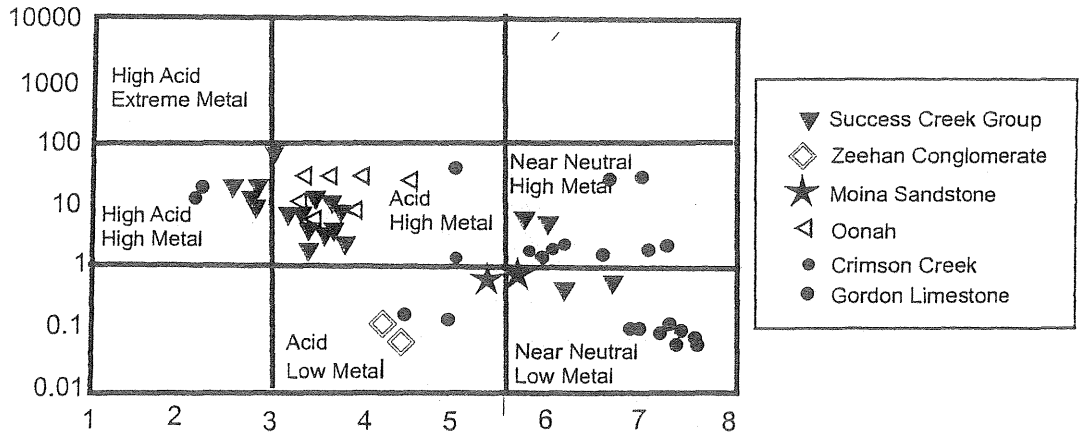

Figure 4-7. Ficklin Plot of Composition of Waters Draining From Selected Rock Types in the Zeehan Mineral Field

compositions, but were less contaminated than the background sites. The least contaminated water was sampled from site 7 (near-neutral, low-metal). Site 8 had the lowest pH, but its metal concentrations were very low (acid, low-metal; Figure 4-5). Site 9 only flowed during the high flow conditions, and had a composition similar to sites 3, 4 and 5 (near-neutral, high metal; Figure 4-5).

4.7 Mass Loads

4.7.1 Introduction

Mass loadings are used to quantify contamination in a stream independent of dilution effects. Element concentrations are multiplied by flow rates, thus providing an absolute value of the amount of contamination moving downstream in a set period (e.g. tonnes/year; kilograms/day).

For this thesis, mass loads were used to determine the degree of metal contamination with respect to flow conditions. Flow rates at sites 5, 6 and 7 were monitored in order to determine the effects of mixing and dilution on the loads of contaminants flowing down Comstock Creek. Full descriptions of the sites at which flow data was recorded, and the methodology used to determine element mass loads, in Comstock Creek is described in Chapter 3. Full data, calculations and results are presented in Appendix 4.

4.7.2 Results

Mass loading values calculated for low and high flow conditions are presented in Tables 4-3 & 4-4, and Figure 4-9, for selected elements.

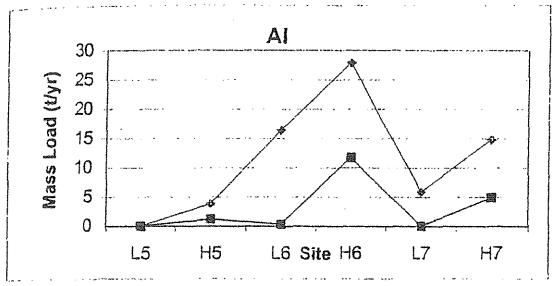

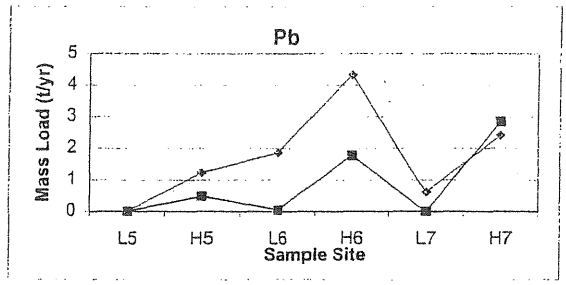

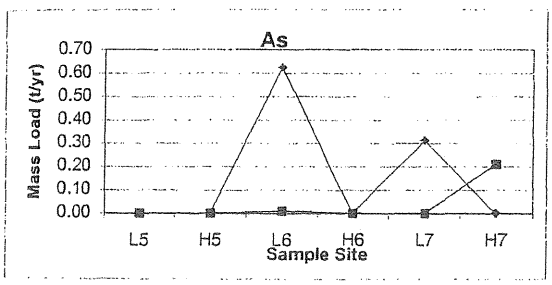

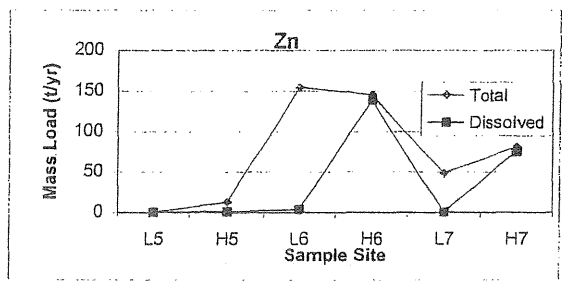

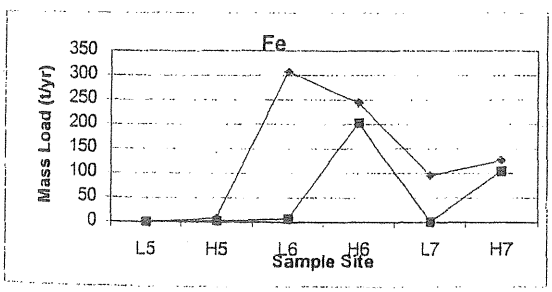

Figure 4-9. Mass loadings of selected elements in high and low flow conditions, at sample sites 5, 6 & 7.

L5: Low flow at site 5
L6: low flow at site 6
L7: Low flow at site 7
H5: High flow at site 5
H6: High flow at site 6
H7: High flow at site 7

	Total Mass Load (t/yr)	Dissolved Mass Load (t/yr)
Al		
Site 5	0.00	0.00
Site 6	16.39	0.33
Site 7	5.80	0.00
As		
Site 5	0.00	0.00
Site 6	0.62	0.01
Site 7	0.31	0.00
Cu		
Site 5	0.00	0.00
Site 6	0.21	0.01
Site 7	0.03	0.00
Fe		
Site 5	0.00	0.00
Site 6	306.32	6.67
Site 7	94.88	0.00
Pb		
Site 5	0.00	0.00
Site 6	1.85	0.04
Site 7	0.61	0.00
Zn		
Site 5	0.00	0.00
Site 6	154.28	3.35
Site 7	48.01	0.00
S		
Site 5	0.00	0
Site 6	1032.04	23
Site 7	318.30	0

Table 4-3. Mass loadings of selected elements at sites 5, 6 and 7 during low flow conditions.

	Total Mass Load (t/yr)	Dissolved Mass Load (t/yr)
Al		
Site 5	3.86	1.19
Site 6	27.86	11.71
Site 7	14.82	4.87
As		
Site 5	0.00	0.00
Site 6	0.00	0.00
Site 7	0.00	0.21
Cu		
Site 5	0.18	0.15
Site 6	0.46	0.55
Site 7	0.27	0.30
Fe		
Site 5	8.17	2.13
Site 6	243.56	201.73
Site 7	125.35	103.19
Pb		
Site 5	1.23	0.48
Site 6	4.32	1.76
Site 7	2.41	2.84
Zn		
Site 5	12.64	0.61
Site 6	145.04	138.32
Site 7	80.57	74.68
S		
Site 5	31.11	7.33
Site 6	515.31	499.44
Site 7	299.42	287.34

Table 4-4. Mass loadings of selected elements at sites 5, 6, and 7 in high flow conditions.

The main adit appeared to be contributing most of the dissolved and total contaminant loads to Comstock Creek. Contaminant input from site 5 was minor compared with contaminant loads emanating from the main adit (site 6), in both flow conditions. In low flows, mass loadings from site 5 were negligible. Mass loads also indicate that, after waters from sites 5 and 6 mixed, there was a decrease in the load of contaminants flowing downstream.

4.7.1 Introduction

Water sampling at Comstock was conducted during the winter, a season typically associated with intense storm events, abundant precipitation and cool temperatures in the Comstock area. During dry periods, sulphides are oxidised prior to the first precipitation event. In such circumstances, a less intense peak of contaminants, associated with water percolation, would be expected.

A storm event, after a period of dry weather was sampled in order to obtain samples of water composition, and flow rates were measured. The first sample was taken 9 hours before the onset of the storm, the second sample was taken approximately 30 minutes after the storm began; sampling was then conducted hourly for 5 hours. Twelve hours after the onset of the storm, and 8 hours after the storm had abated, two water samples were taken an hour apart.

4.7.2 Results

Figure 4-10 illustrates the variation in element concentrations during the intensive monitoring of the storm event (Presented in full in Appendix 5). Total heavy metal concentrations remained fairly steady; although samples taken 12 hours after the storm began, indicated dilution had occurred. With many of the samples, (e.g. silica, sodium, magnesium, calcium and potassium), there was a noticeable decrease in total and dissolved concentrations for the duration of the storm (Figure 4-10). Sulphur and lead concentrations slightly increased, and zinc, manganese and magnesium concentrations remained stable (Figure 4-10).

4.7.3 Comparison with ANZECC/NWQS Guidelines

Dissolved and total aluminium levels exceeded ANZECC/NWQS guidelines before the storm began. Levels remained high throughout, and 12 hours later, concentrations were slightly diluted, but still exceeded guidelines (Figure 4-10).

Total and dissolved iron concentrations exceeded recommended limits throughout the the storm event. Initial, pre-storm levels, and post-storm levels exceeded guidelines (Figure 4-10).

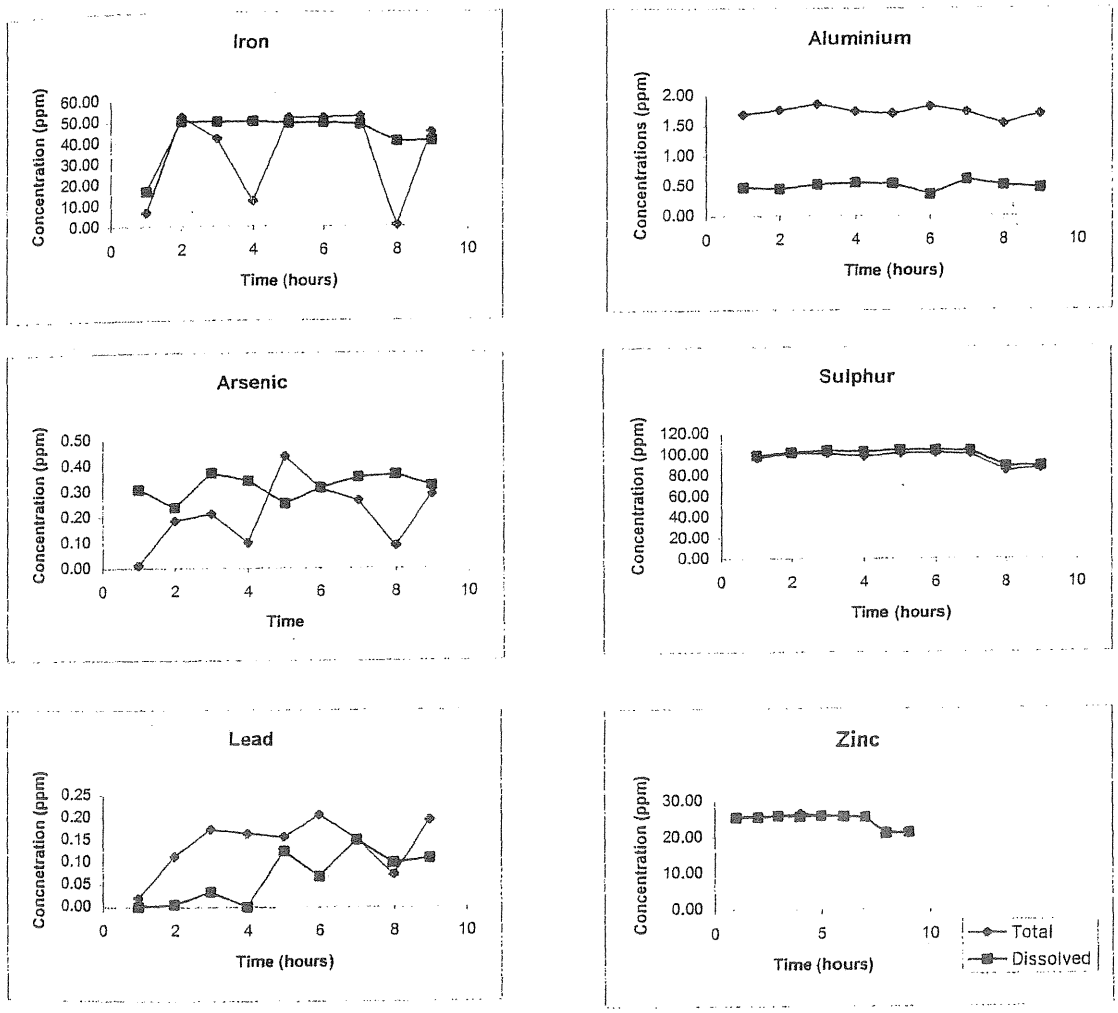

Figure 4-10. Element Concentration Variation During a Storm Event

Total and dissolved zinc concentrations were fairly steady throughout the storm event. The concentrations exceeded recommended levels throughout sampling of the event (Figure 4-10). Even after storm dilution had occurred, the Zn concentrations were still approximately 20 times recommended limits.

4.7.4 Mass Loads

Mass loadings peaked approximately three hours after the onset of rain (Figures 4-11; Appendix 6). Immediately after the rain began, mass loadings rose slightly. This was most obvious in iron, and arsenic samples (figures 4-11b and 4-11 c). For the next two hours, mass loadings rose steadily until peak values were attained approximately three hours after the event began. After this, mass loads dropped steadily and leveled off at values slightly less than pre-storm mass loadings. Samples taken 13 and 14 hours after the storm began demonstrated that post-storm metal loads remained slightly elevated compared with background values (Figure 4-11).

4.8 Discussion

Results of this study suggest that the water quality of Comstock Creek improves with respect to pH as it flows through the tunnel system, however conductivity increases during flow through the underground tunnels. The overall reduction in acidity and redox potential indicates downstream creek water quality is enhanced compared with background water composition.

The increase in pH downstream of the main adit (site 6) in low flow conditions, is most likely to be due to precipitation of iron oxides, involving the release of H^+ ions. The higher Eh values at each site in high flow conditions, compared to low flow regimes, may be due to turbulent flow. It may also be due to the lower acidity of high flow conditions waters.

The slight decrease in EC values observed below the confluence of sites 5 and 6, could be due to precipitation reactions. It may also be due to metal adsorption and ion exchange with the ferrous-oxyhydroxide precipitates that are abundant in Comstock Creek below the main adit.

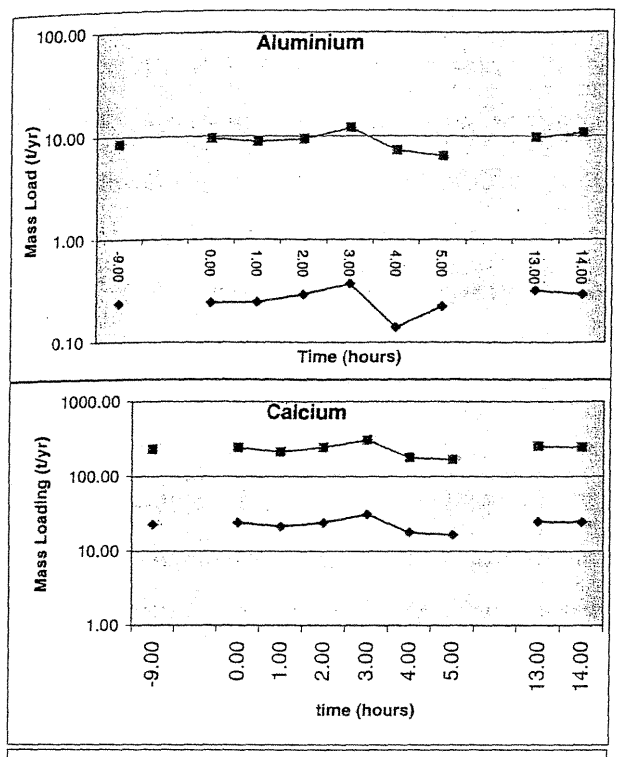

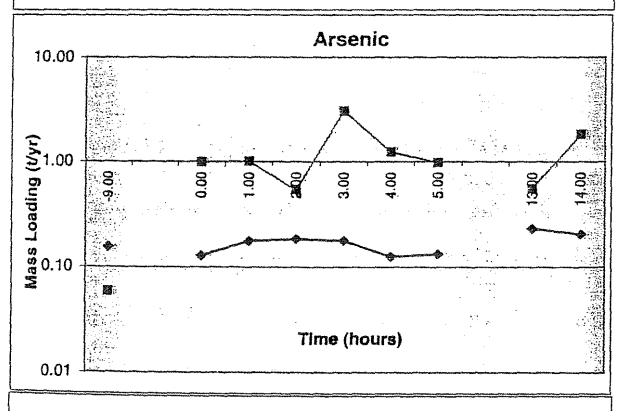

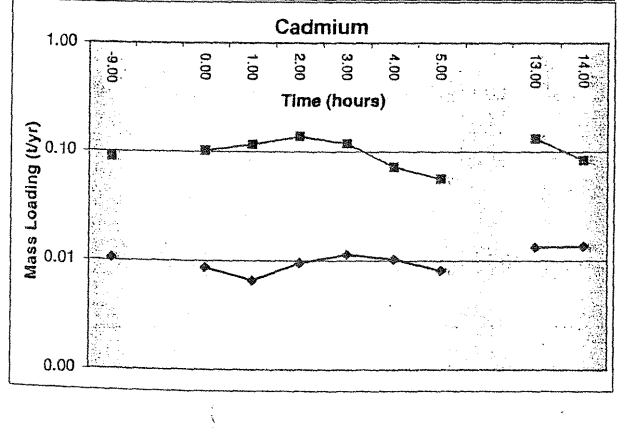

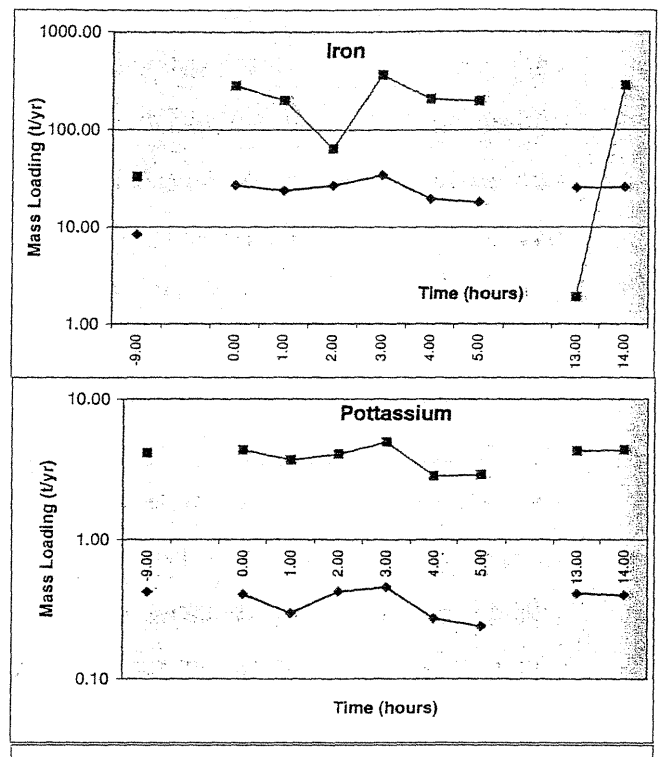

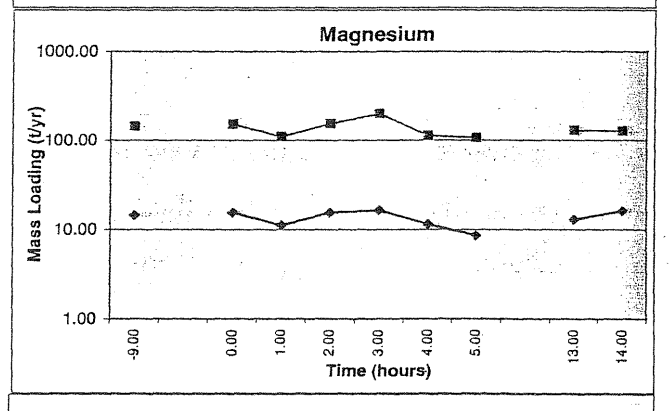

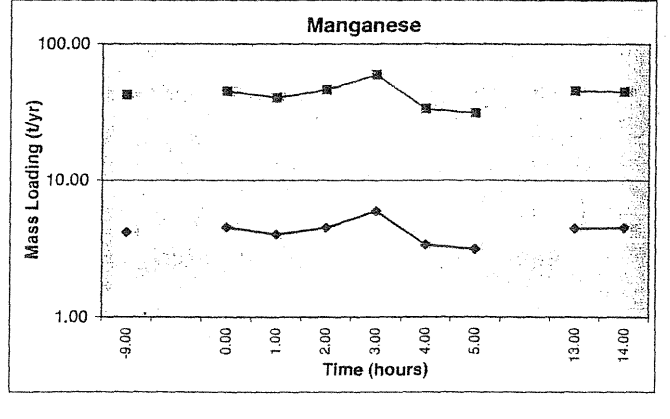

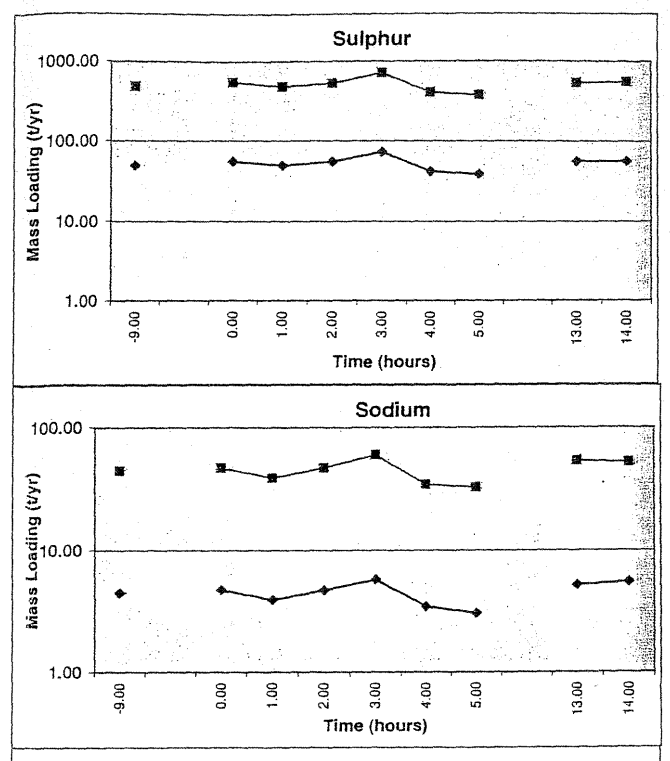

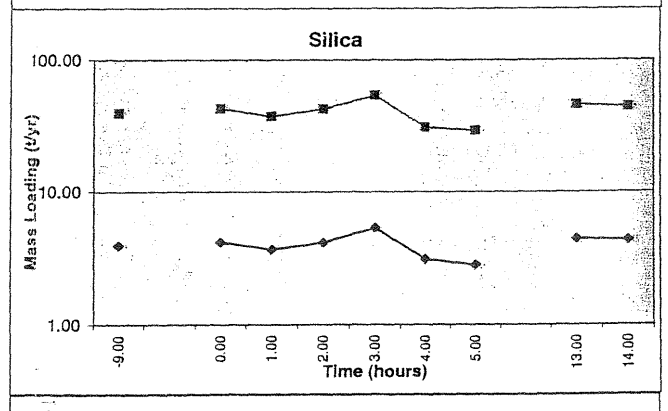

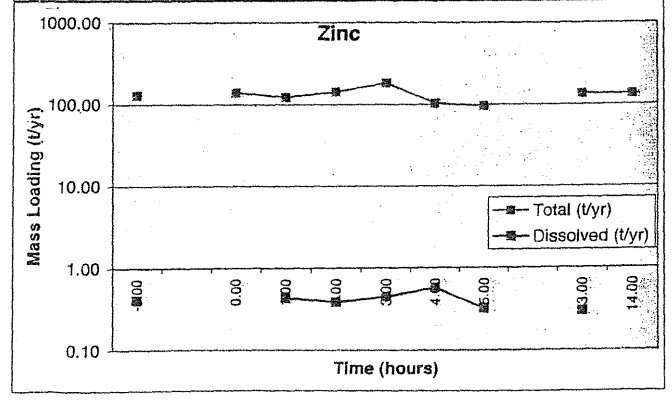

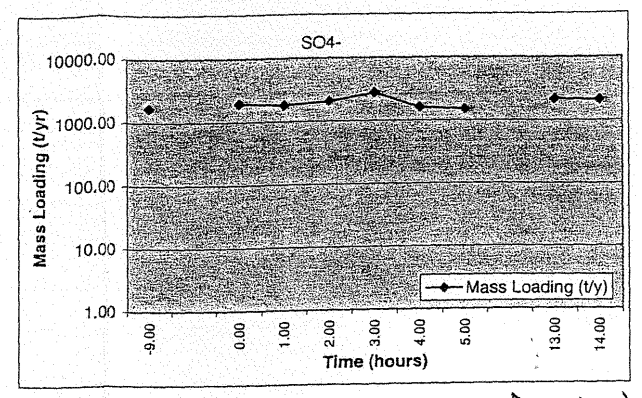

Figure 4-11. Mass loadings of selected elements in water sampled in a storm event.

High pH values and low contaminant concentrations occur upstream of the mine in Comstock Creek, during high flow regimes. This suggests that Comstock Creek waters are fed by an ephemeral water source that has some buffering capacity during rain events.

The main metals of concern appear to be aluminium, cadmium, iron, lead and zinc; their total and dissolved concentrations commonly exceed ANZECC/NWQS water quality recommendations in all high and low flow regimes. During high flow conditions, more sites register total and dissolved contaminant concentrations above recommended levels compared with dry flow conditions. Conversely, arsenic concentrations become problematic only during low-flow conditions.

The influence of the tunnel system on water quality was strong, and related to flow conditions. High flow regimes were associated with remediation in the tunnels, whereas in low flow regimes, the tunnel system was associated with contamination of drainage waters. This suggests that in high flow conditions, contamination is moderated by some mechanism, between the inflow to the tunnel system, downstream of site 2 and the main adit (site 6).

Parr's (1997) research indicated Comstock mine drainage waters, being a mine hosted in pyritically-altered, Oonah formation, should have high acid, high metal, to acid, high metal drainage compositions. Interestingly, it appears that the water entering Comstocks' tunnel system in high flow conditions, in more similar compositions to what may be expected considering Comstocks geology and alteration. This was in contrast to the composition of water emanating from the down stream end. The waters flowing from the main adit (site 6) in high flow conditions, were similar to Parr's results for sites with similar geology to Comstock.

In low flow conditions, main adit (site 6) drainage compositions are more similar to adit drainage compositions within the siderite alteration zone, the Gordon Limestone, or the Success Creek Group. Water entering the tunnels is relatively uncontaminated, and becomes more contaminated as it flows through the tunnels, as may be expected from Parr's Ficklin plots of areas in similar geology.

The intensive hourly sampling program at Comstock demonstrated that storm events are associated with slight changes in heavy metal concentrations and mass loadings. Overall, there appeared to be an small initial increase in concentrations, followed by a leveling out. Post storm concentrations appeared to be diluted. The only exception was observed in iron concentrations, which increased dramatically and were even more elevated in post-storm flows. Dissolution of iron-bearing minerals may explain this phenomenon.

Peaks in the mass loadings data were recorded 3 hours after the onset of rain. This contrasts with the findings of Smith (1998), where a contaminant plume travelled 2km in 30 minutes from the Hercules waste rock dump. The speed at which the "flush" was emitted at Comstock suggests that percolation through rocks, and from the upstream catchment area, may not have been responsible for the main peak shown in the graphs.

It is possible that the peak is associated with surface flows; the decline would be a possible source as its proximity to the main adit, and its small surface area, would encourage "funneling" of surface flows into the drainage shafts. Slower rates of transport compared to surface flow rates indicate that subsurface flow through the tunnel system may be responsible for inhibiting flow rates.

Waters may be moving through areas containing carbonates, or other rocks that could potentially increase the neutralising ability of waters in contact with them, prior to flowing into the mine lease. It is possible that in wet weather, residual carbonates and aluminosilicates further from ore loads are buffering ground waters before they flow through the tunnel system.

High contaminant loads occur upstream of the mine in Comstock Creek, during high flow regimes. This suggests that during rain events, creek waters move through areas not normally flushed or leached. The amount of water, and the velocity at which it moves, would cause extra weathering, abrasion and transport.

Chapter 5

Geochemical Modelling

5.1 Introduction

Geochemical modeling has been undertaken using computer software programs, PHREEQC (Parkhurst, 1995) and PHOX (Polya, 1998) in order to calculate mineral saturation indices, and aqueous speciation of water samples collected during this study. Data used were from the low-flow and high-flow sample sets (Appendix 7). The sites from which data were analysed were; 1) at the two background sites, 1 & 2 (Figure 3-1), which provided information on catchment chemistry, and the chemical composition of water immediately before it enters the tunnels system; 2) the main adit (site 6; Figure 3-1), in order to determine the effects of tunnel flows on water chemistry; and 3) site 7 to determine the species composition of the water flowing down Comstock Creek.

All water analyses used are listed in appendix 5-1. Redox conditions were constrained using measured pe values. Where a value for S(-2) was not entered, because of discrepancies between S and SO^{-}_{4} concentrations, saturation indices for sulphide minerals were not calculated (Parkhurst, 1995).

Data entered into the PHOX program comprised molalities determined from PHREEQC calculations.

5.2 Speciation Calculations

The PHREEQC program can calculate saturation indices (SI) and aqueous speciation. The user enters element concentrations, together with measured pH, redox, and temperature values, and the program calculates distribution of species using selected thermodynamic databases (Wateq4f; Parkhurst *et al.* 1994). WATEQ4F was chosen because it is a more comprehensive database of thermodynamic properties for most minerals than the default PHREEQC database.

Site 1			Site 2		
Ca	Ca^{2+}	99.3%	**Al**	Al^{3+}	68.2%
Cl	Cl^-	100%		$ALOH_2^+$	26.5%
Fe(III)	$Fe(OH)^{2+}$	95.5%		$Al(OH)^{2+}$	5.31%
	$FeOH^+_2$	3.38%	**Cl**	Cl^-	100%
Mn(III)	Mn^{3+}	100%	**Fe(II)**	Fe^{2+}	77.7%
Na	Na^{2+}	100%		$Fe(HS)_2$	22.2%
S(-2)	H_2S	83.4%	**Mn(III)**	Mn^{3+}	100%
	$Zn(HS)_2$	7.49%	**Pb**	$Pb(HS)_2$	100%
	HS^-	1.54%	**S(-2)**	H_2S	46.5%
				$Zn(HS)_2$	25.9%
			Si	H_4SiO_4	100%
			Zn	$Zn(HS)_2$	100%

Table 5-1. Percentage of individual species in water samples at sites 1 and 2 in low flow conditions.

Site 6			Site 5			Site 7		
Ca	Ca^{2+}	97.6%	Al	Al^{3+}	49.8%	Ca	Ca^{2+}	90.4%
	$CaSO_4^-$	2.4%		$AlOH^+_2$	26.4%		$CaSO_4$	9.54%
Cl	Cl^-	100%		$AlSO_4^+$	15.4%	Cl	Cl^-	100%
Fe(II)	Fe^{2+}	98.1%		$Al(OH)^{2+}$	8.15%	Fe(III)	$Fe(OH)^{2+}$	94.1%
	$FeSO_4$	1.87%	Ca	Ca^{2+}	97%		$FeOH_2^+$	5.09%
Mg	Mg^{2+}	97.8%		$CaSO_4$	2.95%	Mg	Mg^{2+}	91.2%
	$MnSO_4^{-2}$	1.85%	Cl	Cl^-	100%		$MgSO_4$	8.78%
Mn(III)	Mn^{3+}	100%	Fe(III)	$Fe(OH)^{2+}$	95.8%	Mn(III)	Mn^{3+}	100%
S	SO_4^{2-}	1.85%		$FeOH^-_2$	2.85%	Na	Na^+	99.6%
	$CaSO_4$	2.52%	Mg	Mg^{2+}	97.4%	S(VI)	SO_4^{2-}	94.4%
	$MgSO_4$	2.52%		$MgSO_4$	2.61%		$CaSO_4$	2.29%
Zn	Zn^{2+}	97.1%	Mn(III)	$Mn3^+$	100%		$MgSO_4$	2.2%
	$ZnSO_4$	2.87%	Na	Na^+	100%	Zn	Zn^{2+}	88.6%
			S(VI)	SO_4^{2-}	88.5%		$ZnSO_4$	11.2%
				$CaSO_4$	5.82%			
				$MgSO_4$	5.42%			
			Si	H_2SiO_4	100%			
			Zn	$Zn(HS)_2$	100%			

Table 5-2. Percentage of individual species in water samples at sites 5, 6, and 7 in low flow conditions.

Site 1			Site 2		
Cl	Cl^-	100%	**Ca**	Ca^{2+}	100%
Fe(II)	Fe^{2+}	99.8%	**Cl**	Cl^-	100%
Mg	Mg^{2+}	99.8%	**Mg**	$Mg2^+$	100%
S(VI)	SO_4^{2-}	99.1%	**S(-2)**	H_2S	100%
Si	H_4SIO_4	100%			

Table 5-3. Percentage of individual species in water samples at sites 1 and 2 in high flow conditions.

Site 6			Site 5			Site 7		
Al	Al^{3+}	72.9%	**Ca**	Ca^{2+}	95.5%	**Al**	Al^{3+}	48.3%
	$AlOH^{2+}$	19.1%		$CaSO_4$	4.5%		$AlOH^{+2}$	24.9%
	$AlSO_4^+$	5%	**Cl**	Cl^-	100%		$AlSO_4^+$	19.3%
	$Al(OH)^{2+}$	3%	**Fe(II)**	Fe^{2+}	96.4%		$Al(OH)^{2+}$	7.3%
Fe(II)	Fe^{2+}	97.2%		$FeSO_4$	3.5%	**Ca**	Ca^{2+}	96.7%
	$Fe(HS)_2$	6.4%	**Mg**	Mg^{2+}	96%		$CaSO_4$	3.3
S(VI)	SO_4^{2-}	86.5%	**Na**	Na^{2+}	100%	**Cl**	Cl^-	100%
	$CaSO_4$	3.8%	**S(VI)**	SO_4^{2-}	98.8%	**Fe(II)**	Fe^{2+}	97.4%
	$AlSO_4$	3.5%	**Si**	H_4SiO_4	99.9%		$FeSO_4$	2.5%
	$MgSO_4$	3.1%				**Mn(III)**	Mn^{3+}	100%
	$FeSO_4$	2.5%				**Na**	Na^+	100%
Si	H_4SiO_4	100%				**S**	SO^{2-}	89.8%
Zn	$Zn(HS)_2$	100%					$CaSO_4$	2.7%
							$MgSO_4$	2.4%
							$FeSO_4$	2.4%
							$ZnSO_4$	1.7
						Si	H_4SiO_4	100%
						Zn	Zn^{2+}	96%
							$ZnSO_4$	3.9%

Table 5-4. Percentage of individual species in water samples at sites 1 and 2 in high flow conditions.

Speciation of elements at the background sites in high and low flow conditions was fairly similar, except for iron and sulphur species. In low flow conditions at site 1, it was predicted that Fe^{3+} would occur as $Fe(OH)^{2+}$, whereas the predicted Fe species in high flow conditions was Fe^{2+}. Site 2 contained iron as Fe^{2+}. Sulphur was predicted to occur as sulphate in high flow conditions at site 1, whereas site 2 in high flow conditions and both sites in low flow conditions were predicted to contain H_2S.

Downstream of the mine, at site #5, #6 and #7, in both sets of conditions, sulphur was present in its oxidised state as sulphate. Iron occurred as Fe^{2+} at all sites in high flow conditions. In

low flows, iron was present in its Fe^{2+} state at the exit from the tunnel system, but by site 7, it had oxidised to $Fe(OH)^{2+}$.

5.3 Saturation Indices

Saturation indices provide information on which chemical phases in a water sample should be supersaturated, assuming that equilibrium is acheived. A saturation index (SI) is derived from the ratio of an elements ion activity product (IAP) to its' equilibrium solubility constant (Ksp; Nordstrom *et al.*, 1979; Equation 5-1).

$$SI = Log_{10}(AP/K) \qquad (5\text{-}1)$$

Where;

AP is activity product

K is solubility product constant

Where this ratio is less than 0, the phase is undersaturated with respect to the solution, and dissolution of those mineral phases is expected. When the SI is 0, the phase is supersaturated and precipitation is likely, provided that reaction kinetics do not impede precipitation. If an element is highly supersaturated, several mineral phases could potentially precipitate. In general, it will be the most saturated phase that will precipitate for a given element. Practice suggests the best approach to modeling potential precipitation and dissolution reactions, is to designate an "equilibrium zone" around zero SI. This caters for the range of uncertainty surrounding SI estimates (Nordstrom *et al.*, 1979).

Saturation indices for the waters listed in Appendix 5-1, were calculated using PHREEQC software.

Site 1				SI	Site 2			SI
High flow	Fe	Haematite	$[Fe_2O_3]$	44.07	Fe	Pyrite	$[FeS_2]$	44.07
Low flow	Fe	Pyrite	$[FeS_2]$	45.78	Mn	Nsutite	$[MnO_2]$	10
Low Flow	Mn	Nsutite	$[MnO_2]$	11.07	K	K-mica	$[KAl_3Si_3O_{10}(OH)_2]$	8.51
					Zn	Sphalerite	$[ZnS]$	4.04
					Pb	Galena	$[PbS]$	3.75
					Si	Quartz	$[SiO_2]$	0.16

Table 5-5. Saturated Indices for the most supersaturated cation phases, calculated using PHREEQC (Parkhurst, 1995).

Site 5			SI	Site 6		SI	Site 7		SI
Low Flow	Fe	Pyrite $[FeS_2]$	42	Fe	Hematite $[Fe_2O_3]$	44.45	Fe	Hematite $[Fe_2O_3]$	20.01
Low Flow	Ca	Leonhardite $[Ca_2Al_4Si_8O_{24}:H_2O]$	16.56	Mn	Nsutite $[MnO_2]$	11.11	Mn	Nsutite $[MnO_2]$	10.74
Low Flow	Al	Pyrophyllite $[Al_2Si_4O_{10}(OH)_2]$	13.66	Si	Quartz $[SiO_2]$	2.04	Si	Quartz $[SiO_2]$	1.51
Low Flow	Mn	Nsutite $[MnO_2]$	10.96	Zn	$ZnSi0_3$	0.7			
Low Flow	Zn	Sphalerite [ZnS]	4.18	Fe	Pyrite $[FeS_2]$	21.44	Fe	Hematite $[Fe_2O_3]$	7.4
High Flow	Fe	Hematite $[Fe_2O_3]$	9.66	Al	Basaluminite $[Al_4(OH)_{10}SO_4]$	3.69	Al	Basaluminite $[Al_4(OH)_{10}SO_4]$	5.9
High Flow				Zn	Sphalerite $[ZnS]$			Quartz $[SiO_2]$	
High Flow									

Table 5-5. Saturated Indices for the most supersaturated cation phases, calculated using PHREEQC (Parkhurst, 1995).

More oxidised samples (those from high flow conditions), are predicted to precipitate out Fe, S, Al, and Zn minerals, with hematite the most common potential mineral precipitate. Low flow conditions were predicted to precipitate pyrite, at sites 1 and 2. Sites 6 and 7, downstream of the tunnel system, were predicted to precipitate hematite reflecting the higher redox potential of the waters. The predicted precipitation of pyrite suggests that the redox values may not be correct.

5.3.2 Potential Precipitation Reactions

Table 5-6 contains the reactions expected to occur as a result of mineral supersaturation. Element speciation dictates reaction byproducts, and determines the amount of acid produced or used during precipitation.

Supersaturated Mineral	Precipitation Equation
Hematite [Fe_2O_3]	$2Fe(HS)_2 + 7O_2 \rightarrow Fe_2O_3 + SO_4^{2-} + 2\mathbf{H^+}$
Pyrite [FeS_2]	$Fe^{2+} + 2SO_4^{2-} \rightarrow FeS_2 + 8O_2$
Nsutite [Mn^{2+}]	$Mn^{2+} + H_2O + 0.5\ O_2 \rightarrow MnO_2 + \mathbf{2H^+}$
Muscovite [$KAl_3Si_3O_{10}(OH)_2$]	$K^+ + 3H_4SiO_4 + 3Al^{3+} \rightarrow KAl_3Si_3O_{10}(OH)_2 + \mathbf{10H^+}$
Sphalerite [ZnS]	$Zn(HS)_2 + 4O_2 \rightarrow ZnS + SO_4^{2-} + 2\mathbf{H^+}$
Galena [PbS]	$Pb(HS)_2 + 4O_2 \rightarrow PbS + SO_4^{2-} + 2\mathbf{H^+}$
Quartz [SiO_2]	$H_4SiO_4 \rightarrow SiO_2 + 2H_2O$
Leonhardite [$Ca_2Al_4Si_8O_{24}.H_2O$]	$2Ca^{2+} + 4Al^{3+} + 8H_4SiO_4 + 21O_2 \rightarrow Ca_2\ Al_4Si_8O_{24}.H_2O + \mathbf{16H^+}$
Pryophyllite [$Al_2Si_4)_{10}(OH)_2$}	$2Al^{3+} + 4H_4SiO_4 + 4O_2 \rightarrow Al_2Si_4O_{10}(OH)_2 + \mathbf{6H^+}$
Basaluminite [$Al_4(OH)_{10}SO_4$]	$4Al^{3+} + SO_4^- + 20H_2O \rightarrow Al_4(OH)_{10}SO_4 + 10O_2 + \mathbf{10H^+}$
$ZnSiO_4$	$Zn^{2+} + H_4SiO_4 + 0.5O_2 \rightarrow ZnSiO_4 + H_2O + \mathbf{2H^+}$

Table 5-6. Precipitation reactions for supersaturated minerals using predominant species.

Almost all the precipitation reactions will produce acid, except for the precipitation of quartz which does not produce, or use, acid.

Nsutite (MnO_2) was predicted to form at all sites in low-flow conditions, whereas in high-flows, it is not predicted to form at any site. The pyrite precipitation from Fe (II) is only expected to occur at the two background sites and the road drain, in low-flow conditions. During periods of high flow, the main adit is the only site where pyrite was predicted to precipitate. This suggests that there was an error in redox measurement during this sampling period.

In low-flow conditions, the background sites are, approximately, producing and neutralising acid in similar proportions. Downstream, the road drain site has the potential to acidify water markedly, a lot of acid will be released by precipitation of leonhardite. The main adit waters will be acidified by precipitation of saturated phases. The downstream mixing area may also be being acidified, but to a lesser degree than the main adit.

In high-flow conditions, upstream sites are predicted to produce some acid, but few phases are present in saturated concentrations. The road drain site will produce some acid, via precipitation of hematite. At the main adit, it has been predicted that acid will be produced predominately through precipitation of basaluminite. Downstream, precipitating mineral phases would be releasing abundant acid, with no buffering reactions predicted.

Section Three:

Acid-Base Accounting.

Chapter 6

Acid-Base Accounting

6.1 Introduction

Acid-base accounting (ABA) is used to assess the potential of rocks to generate or consume acid. It is conducted using a variety of static and kinetic geochemical tests. ABA is formulated around the assumption that acid mine drainage potential can be defined by quantifying the total producible acidity and alkalinity of a given set of lithologies. Static ABA test results are written in calcite units (kg $CaCO_3$/t) in order to provide a constant term of reference for "account balancing". This chapter details the application and results of static and kinetic experiments, conducted on rocks from the Comstock mine lease.

6.2 Rock Samples

6.2.1 Introduction

Grab samples of rocks were taken from a number of sites around the Comstock M.L in order to sample both weathered and unweathered material. The samples were chosen to provide an indication of how the ore mineralogy was affected by a decade of atmospheric exposure; weathering rates, patterns and products were wanted. Acid production and buffering potentials of weathered rocks could be determined and compared with fresh samples. Descriptions of the samples, with respect to hand specimens, thin sections, and XRD analysis results are presented in Table 6-1 (Appendix 6-1 contains full XRF results).

6.2.2 Sampling Regime

Approximately 2 kilograms of altered host rock were sampled from the south Comstock open-cut (Sample #9; Figure 6-1). The samples were taken from a fault zone (Plate 6-1a & b), interpreted to have been a conduit for fluid movement. Sulphides (predominantely pyrite) were present both in the fault zone and the adjacent wall-rock. This location was chosen to represent host rock and ore mineralogy after approximately ten years of atmospheric exposure.

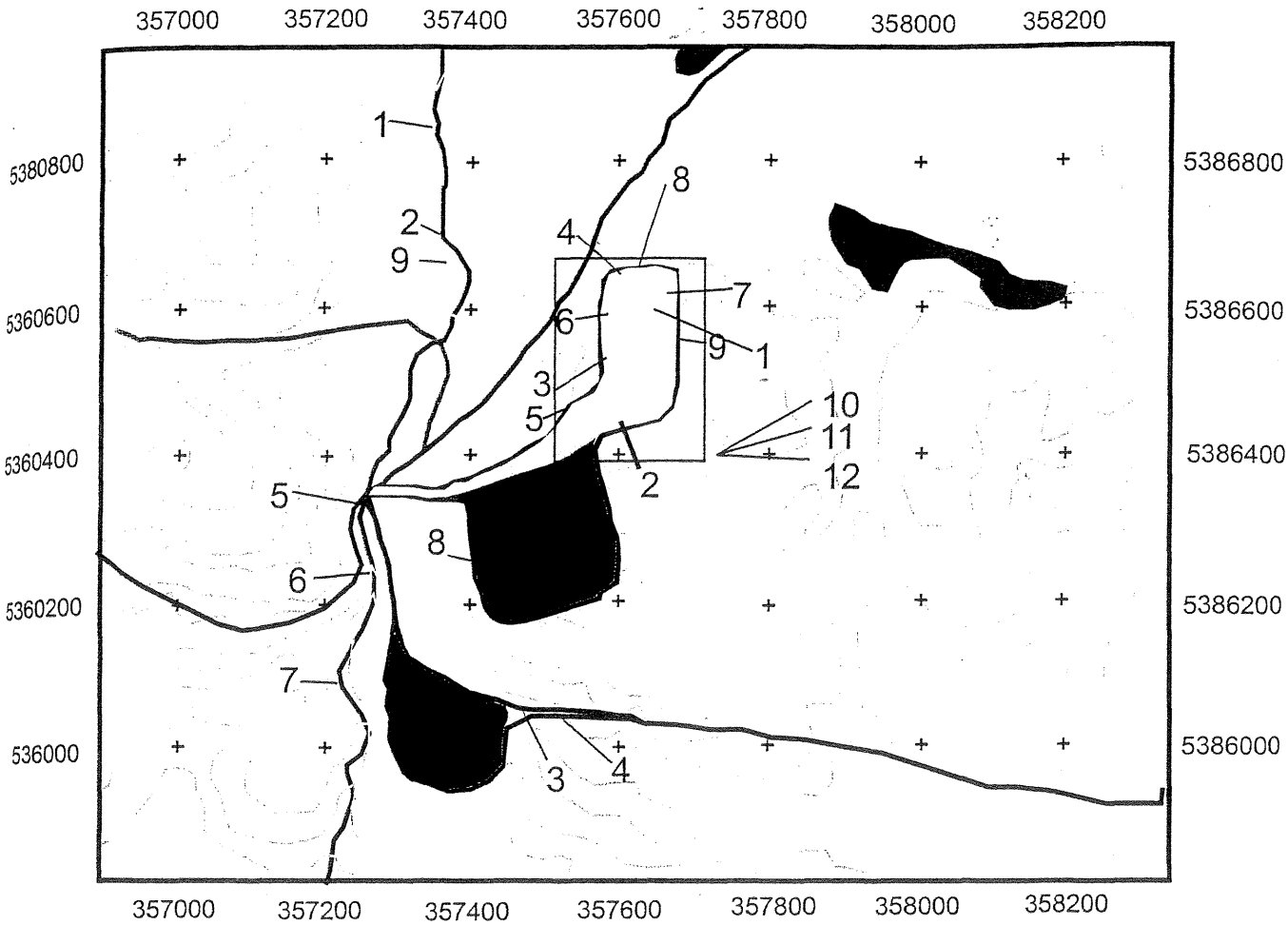

Key

Trial Harbour Road

Four-Wheel Drive Track

Comstock Creek

Outline of Current Operation

Marsh

Detail of Decline Sample Sites
Figure - .

South Comstock Open-Cut

Waste Rock Dump

Decline

N

400m

Figure 6-1: Location of Rock Sample Sites

A; Site 8. South Comstock Open Cut, showing the fault, and pyritically altered host rock.

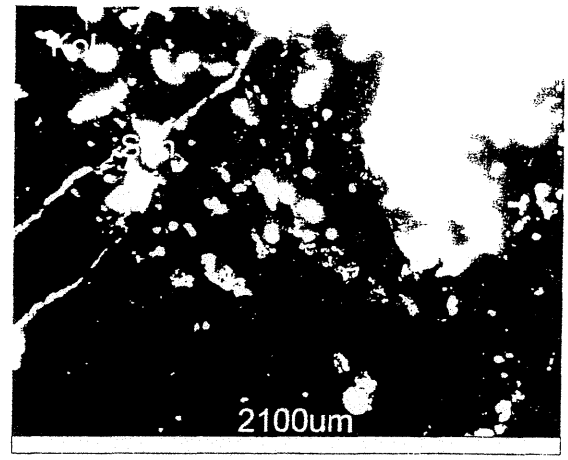

B. Photomicrograph of sample from site 8. With kaolinite (kol), pyrite (pyr) grains, and sphalerite (sph). X5.

: Site 9.

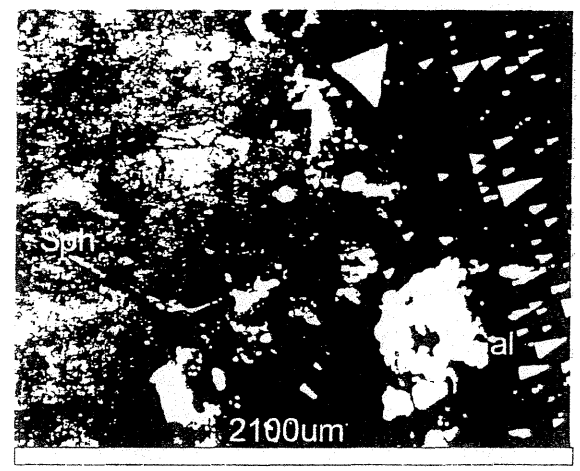

D. Photomicrograph of variably weathered spahlerite (sph), adjacent to pitted galena (gal),from Site 9. X5.

E. The Comstock decline, where samples 1-7 were collected.

Plate 5-1.

The second sample site (sample #8) was in the northwest of the lease, this site was an ore crushing mill in the north-west of the lease (Figures 6-1 & Plate 6-1c & d). Approximately one kilogram of rocks were randomly sampled from where they had been dumped and left.

Seven rock samples were taken from the decline into Allisons Lode (Samples #1-#7; Figure 6-1; Plate 6-1e). Samples were inferred to be representative of fresh, unweathered, material exposed underground. Testing of these samples would measure total acid production and buffering potential of unweathered samples. Finally, the sample mineralogy would be unaffected by atmospheric conditions; thus, any secondary minerals would be due to metasomatism associated with ore fluids, or groundwater percolation.

The samples from the decline were Upper Oonah lithologies, the location of these samples is illustrated on figure 6-1 (plate 6-2a,b,c,d,e & f). A total of 1kg was collected over $1m^2$ at each site. Sample #1 was taken from the northeastern end of the decline on the bottom level. The second sample (#2) came from the southeast end of the decline, on the bottom level near the entrance. The third sample (#3) was from the bottom level, midway along the western wall. Sample #4 was from the northern end, on the second berm. The fifth sample (#5) was from the bottom level of the western wall. Sample #6 was on the second berm at the northwest, and #7 was also from the second berm but came from the north eastern end.

Samples of the main sulphide minerals; pyrite (#10), galena (#11), and sphalerite (#12), were also taken. The minerals were sampled from the on-site ore-stockpile, which comprises ore extracted from Allisons Lode. Approximately one kilogram of randomly selected pieces of each mineral was taken. The sulphides were sampled in order to ascertain the mineralogy, morphology, and structures of the main sulphide minerals. This was required to help define the mechanics and chemistry of acid production at Comstock.

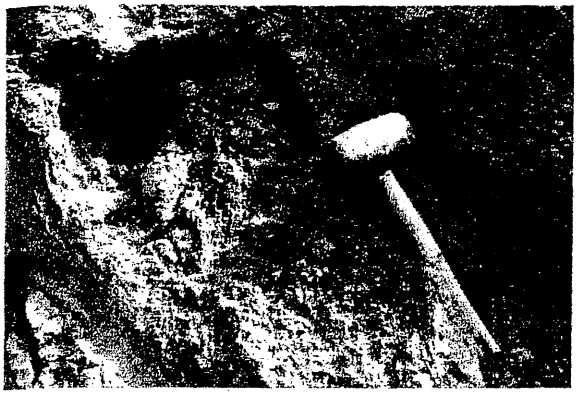

A. Site 7,talc sample.

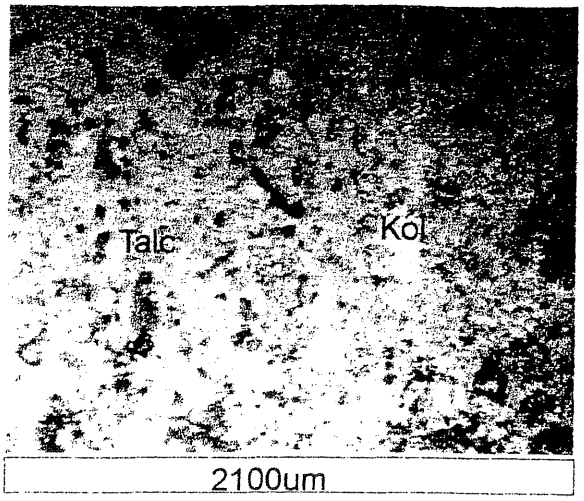

B. Sample 7, talc and kaolinite (kol).

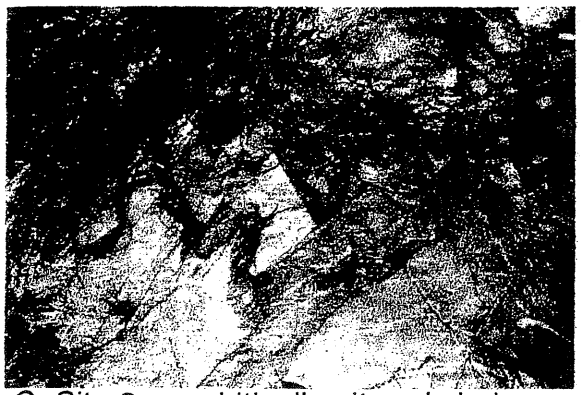

C. Site 2, graphitically altered shale sample.

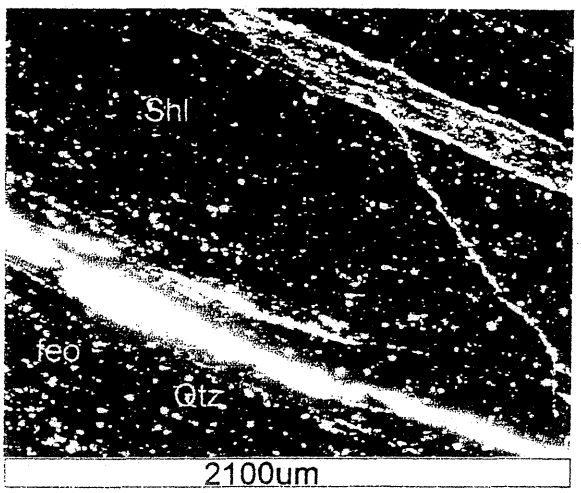

D. Sample #2, shale (shl) with quartz (qtz) vein and iron oxide stain (feo).

E. Site 6, siliceous cap rock sample.

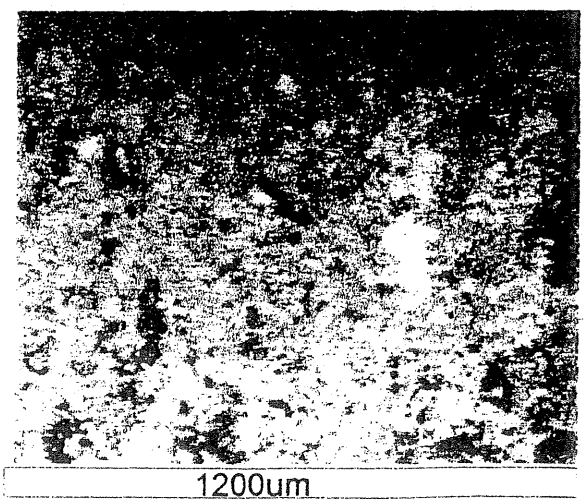

F. Sample #6, siliceous cap rock.

Plate 2.

Sample	Hand Sample Description	Thin Section Description	XRD Results
1	Talc: Grey, very fine grained, 5-10 cm thick beds.	Massive talc with anhedral quartz grains. Some pits, minor microfractures associated with brown iron oxide staining.	>80% Talc 10-15% Quartz <2% Rutile <2% Kaolinite
2	Shale: Black, very fine grained, strongly-bedded; 1-5cm thick. Fissile. Graphitically-altered bedding planes.	Strongly lineated carbonaceous material with interstitial quartz fragments. Extensive micro-faulting, fractures and faults infilled with quartz, some associated with iron oxide staining. Biotite and muscovite present. Euhedral pyrite occurs in cavities and quartz veins.	25-40% Quartz 25-40% Mica 15-25% Amorphous 5-10% Pyrite 2-5% Tourmaline 2-5% Rutile 2-5% Chlorite 2-5% Talc
3	Shale: Dark grey, very fine grained, strongly bedded; 2-5cm thick. Fissile, sparsely disseminated pyrite (approximately 0.1mm grains).	Talc rich layers are subsidiary to the main carbonaceous layers. Some microfaulting. Wide quartz veins, crosscut the section, associated with interstitial muscovite. Abundant pits. Talc laths and hydroxide stains.	25-40% Quartz 15-25% Mica 15-25% Amophous 15-25% Pyrite <2% Talc <2% Chlorite
4	Siliceous Cap Rock: Off-white, very fine grained, very soft, friable. No observable bedding. Abundant sub-cubic pits (0.5mm). Yellow iron oxide staining.	Angular to subrounded quartz abundant in a fine talc matrix. Amphibole is found at the edges of quartz grains.	40-60% Amphibole 25-40% Talc 15-25% Quartz
5	Talc: Light brown with patches of dark brown (carbonaceous?) material. Very fine grained, no observable bedding, very soft, friable.	Abundant talc. Large veins and "patches" of quartz. Iron oxide stained talc patches, some areas with a kaolinite matrix.	>80% Talc 5-10% Quartz 2-5% Pyrite <2% Kaolinite
6	Talc: Light brown, very fine grained, very soft, friable. Iron oxide staining.	Very quartz rich. Abundant iron oxide stained patches. Microfaulted.	60-80% Talc 25-40% Quartz <2% Rutile <2% Kaolinite
7	Talc: Light brown, very fine grained, very soft, friable. Iron oxide staining.	Iron oxide staining of talc. Large quartz grains throughout. Talc and chlorite equally abundant. Very massive, no pits or fractures.	40-60% Quartz 40-60% Talc <2% Pyrite <2% Chlorite

8	Interbedded galena, sphalerite and pyrite: Galena and sphalerite in massive beds. Pyrite as euhedral crystals (approximately 1mm), associated with quartz, very porous. Abundant iron oxide staining. Some sphalerite associated with a white precipitate (?anglesite).	Sphalerite variably stained with red to yellow secondary hydroxides. High fracture density, all filled with iron oxide. Abundant euhedral pyrite. Fractured quartz associated with ?anglesite. Galena with highly etched dissolution pits.	25-40% Pyrite 15-25% Galena 15-25% Sphalerite 15-25% Quartz 2-5% Anglesite 2-5% Talc <2% Kaolinite
9	Pyrite in a talcose host rock: Large, subhedral, pyrite crystals (2cm-1mm). Abundant iron oxide staining. Brown precipitate (?siderite). Host rock partly silicified, variably pitted and stained with iron oxides.	Abundant sphalerite, all stained with iron oxides. Framboidal pyrite.	60-80% Sphalerite 10-15% Pyrite 5-10% Galena 2-5% Quartz <2% Talc
10	Pyrite: Massive, subhedral to euhedral crystals, to 2cm.		>80% Pyrite 2-5% Quartz <2% Galena <2 %Talc <2% Chlorite
11	Galena: Massive to subhedral.		>80% Sphalerite 5-10% Quartz 2-5% Pyrite 2-5% Galena <2% Talc <2% Chlorite
12	Sphalerite: Massive, interspersed with galena, pyrite and quartz.		>80% Galena 5-10% Sphalerite <2% Pyrite <2% Quartz <2% Talc

Table 6-1: Hand, petrographic and XRD descriptions of rock samples.

6.3 Static Tests

6.3.1 Introduction

Static tests are used to determine the potential of a rock to produce AMD. Net Acid Producing Potential (NAPP) is determined from the total sulphur in a sample and, from acid

neutralising capacity (ANC) (Williams & Miller, 1989). Net acid generation (NAG) reinforces results obtained from NAPP tests and allows further, more reliable prediction of AMD. It measures the net acidity generated by oxidation of all available sulphur in the sample, minus neutralisation reactions. Combining laboratory test results with whole rock mineralogy and kinetic leachate assessments, increases confidence in the accuracy of acid drainage predictions (Miller, 1998). The limitations and inherent assumptions of the ABA methods used in this thesis are discussed in Appendix 8.

6.3.2 Methods

6.3.2.1 Total Sulphur:

Total sulphur was determined by X-Ray Fluorescence (XRF; Appendix 9). Approximately 500 grams of each sample were crushed to a gravel size. 100 grams of the sample was then placed in a chrome–tungsten mill and pulverised to a fine powder. This powder was used to create either pressed-powder pills or fusion disks (depending on rock type) before being analysed using the ore2 program on all samples apart from samples #1 and #6, which were analysed using the normal silicates program (Phil Robinson, pers. comm.).

6.3.2.2 Acid Neutralising Capacity:

ANC was tested on powdered samples. Samples were assessed for "fizz" by placing 0.5 grams on a watch glass and adding two drops of 1:3 HCl (10.67%). Any bubbling or audible "fizz" was assessed according to Table 6-2. This assessment is used to determine the amount and concentration of acid used in the second part of the experiment.

Reaction	Fizz Rating	HCl Molarity	Volume of NaOH to be Added (ml)	NaOH Molarity
No Reaction	0	0.5	4	0.1
Slight Reaction	1	0.5	8	0.1
Moderate Reaction	2	0.5	20	0.5
Strong Reaction	3	0.5	40	0.5
Very Strong Reaction	4	1	40	0.5

Table 6-2: Fizz ratings and NaOH characteristics required for the 2nd part of ANC determination (Miller, 1994).

Two grams of each sample were placed in sterilised beakers. The amount of acid corresponding to the "fizz" rating was added to each beaker and mixed with 20ml of distilled

water. A blank solution was also prepared for each "fizz" rating. The beakers were covered with watchglasses and put in a water bath at 80°C for 2 hours, then left overnight to cool to room temperature. Distilled water was added to make a 125ml solution. A titration was then performed, with the designated concentration of NaOH (Table 6-2) slowly added to the samples using a burette. The pH of the sample was monitored using a WTW 330 pH metre, calibrated against pH 7 and 4 buffers prior to the experiment. When the pH of the sample stabilised at pH 7, the amount of NaOH used was recorded.

The ANC value is determined using equation 6-1:

ANC $\%CaCO_3$ =

[(molarity of HCl * mls of HCl) – (Molarity NaOH * mls of NaOH)] * 5.0/2gms

(Equation 6-1)

6.2.3.2 Net Acid Generation Test

NAG tests measure the amount of acid produced when all of the sulphur in a sample has been oxidised and all neutralisation has taken place. NAG tests can be static, sequential or kinetic (Miller, 1998). A static NAG test was used in this assessment following the methodology of Miller *et al.* (1997).

The test was conducted on powdered samples. 100 ml of H_2O_2 was added to 1g of powder in a beaker and covered with a watch glass. The beaker was placed in a fume-hood and left at room temperature overnight and then gently boiled on a hot plate for two hours. The solution was left to cool to room temperature and the final pH was recorded (NAG pH). Deionised water was added to the sample to make up 100 ml. A titration was performed using NaOH, the concentration of which was determined from Table 6-3;

NAG Solution pH	Reagent
>2	0.10 M NaOH
<2	0.50 M NaOH

Table 6-3; NaOH concentrations required from NAG solution pH (Mills, 1999).

NAG is determined using equation 6-2:

$$NAG = 49 * V * 8 * M/W$$

(Equation 6-2)

Where;

NAG = net acid generation potential (kgH_2SO_4/tonne)

V = volume of NaOH titrated (ml)

M = molarity of NaOH (moles/l)

W = weight of sample reacted (g)

6.3.3 Results

The results of NAPP tests are provided, with values stated as $\%CaCO_3$ and $\%H_2SO_4$. Different interpretation methods require NAPP values to be stated as one or the other in order to facilitate comparisons. B.C. AMD Taskforce (1989), proposed that NAPP values lower than –20ppt $CaCO_3$/t will be acid producing. All but two samples tested fall below this value (Table 6-4) and, therefore, are likely to be acid producing.

Sample	Total Sulphur	Maximum Potential Acidity*	Fizz Rating	Paste pH	Acid Neutralising Potential	Net Acid Producing Potential	Net Acid Producing Potential
	%S	kg $CaCO_3$/t			(kg $CaCO_3$/t)	(kg $CaCO_3$/t)	(kg $H2SO_3$/t)
1	NA	N/A	0, no fizz	7.25	-0.75	N/A	N/A
2	0.55	17.19	0, no fizz	6.50	-4.38	-21.56	0.69
3	5.27	164.69	0, no fizz	6.00	-1.55	-166.24	5.32
4	0.52	16.25	0, no fizz	6.50	-1.63	-17.88	0.57
5	1.78	55.63	0, no fizz	4.50	0.25	-55.38	1.77
6	0.04	1.25	0, no fizz	6.00	-7.25	-8.50	0.27
7	N/A	N/A	0, no fizz	6.25	-6.60	N/A	N/A
8	26.37	824.06	0, no fizz	6.00	-8.25	-832.31	26.63
9	28.86	901.88	0, no fizz	5.25	-8.75	-910.63	29.14
10	49.32	1541.25	0, no fizz	3.75	-8.50	-1549.75	49.59
11	33.10	1034.38	0, no fizz	8.25	-16.60	-1050.98	33.63
12	17.61	550.31	0, no fizz	9.50	-18.88	-569.19	18.21

Table 6-4; Results of NAPP Tests.

Other ABA methods are also in use internationally. Net Acid Generation tests are one such example, used because of the rapid, net estimate of acid production that is achieved. Results indicate immediate acid production (NAG pH), and the amount of acid left after neutralisation potential is exhausted (NAG) (Table 6-5). All of this is determined using a single experiment with immediately interpretable results. It does not require a theoretical balancing of acid production against acid neutralisation to be determined, as both mechanisms run to full potential in the course of the experiment.

Sample	NAG pH	M (NaOH)	V (NaOH)	NAG (kg H_2SO_4/ton)	NAG (kg $CaCO_3$/ton)
1	3.38	0.1	0.28	1.37	42.81
2	2.40	0.1	5.51	27.00	843.75
3	2.35	0.1	6.98	34.20	1068.75
4	2.87	0.1	0.91	4.50	140.63
5	3.03	0.1	1.54	7.55	235.94
6	4.01	0.1	0.09	0.44	13.75
7	2.82	0.1	1.41	6.91	215.94
8	5.81	N/A	N/A	N/A	N/A
9	5.94	N/A	N/A	N/A	N/A
10	2.51	0.1	4.84	23.72	741.25
11	5.94	N/A	N/A	N/A	N/A
12	6.11	N/A	N/A	N/A	N/A
Control	4.02	0.1	0.08	0.40	12.5

Table 6-5; Results of NAG Tests.

Miller (1998), has proposed a scheme for assessing a rock's propensity to generate AMD. He designed a classification table that uses NAG pH, static NAG values and NAPP to categorise a rock as potentially acid forming, potentially acid forming–low capacity, non-acid forming, acid consuming or uncertain (Table 6-6):

Primary Geochemical Waste Type	**Final NAG pH**	**Static NAG Value (kg H_2SO_4/t)**	**NAPP (kg H_2SO_4/t)**
Potentially Acid Forming	<4.5	>5	Positive
Potentially Acid Forming - Low Capacity	<4.5	≤5	Positive
Non Acid Forming	≥4.5	0	Negative
Acid Consuming	≥4.5	0	Less than –100
Uncertain	≥4.5	0	Positive
	>4.5	>0	Negative

Table 6-6; Classification scheme of the potential for acid production (Miller, 1998).

According to Millers (1998) classification, the status of all rocks analysed is uncertain and further testing is required. Miller suggested further analysis should include petrological analysis of sample mineralogy, and sequential and kinetic NAG tests.

AMD potential of rocks can be assessed from the ratio between neutralising potential (NAPP) and maximum potential acidity (MPA; Perry, 1999; Soregali & Lawrence, 1997). Patterson & Fergusson (1994) suggested that a Neutralisation Potential to Maximum Potential Acidity ratio (NP/MPA) of less than one indicates acid drainage would form. Soregoli & Lawrence (1997), suggested that where massive sulphides are hosted in fractured rocks, with minimal carbonate buffering, a ratio of less than 4:1 (e.g. 4 %$CaCO_3$: 1%H_2SO_4) suggests AMD will occur. Table 6-7 shows the ratio values for samples from Comstock.

Sample	NP:MPA	AMD Producing Potential
1	N/A	N/A
2	-0.25	Likely
3	-0.001	Likely
4	-0.1	Likely
5	0.004	Likely
6	-5.8	Likely
7	N/A	N/A
8	-0.01	Likely
9	-0.001	Likely
10	-0.006	Likely
11	-0.016	Likely
12	-0.034	Likely

Table 6-7; The NP:MPA ratios and interpretations of the AMD producing potential of Comstock rock samples.

The results indicate that when ratios are used to interpret the data, some of the samples have the potential to produce AMD. All the rocks tested can produce acid drainage, to various degrees, according to the classifications of both Perry (1999), and Soregali & Lawrence, (1997). Sample 5 has some buffering capacity compared to the other samples, but the potentially producible acid exceeds any buffering capacity present as $CaCO_3$. This is indicated by the results of NAG tests and by analysis of AMD propensity using the ratios method.

Analysis using ratios (Patterson & Fergusson, 1994; Soregoli & Lawrence, 1997), suggests that all the Comstock samples are likely to form AMD. There is some discrepancy between the results for samples 4 and 6 between when they are classified using NP:MPA ratios or the NAPP results, and again between Millers (1998) table and the latter methods. The Miller (1998), scheme for classifying rock ABA concludes that all the samples require further testing. As the static, ABA classifications are inconclusive and contain inherently conflicting results, it would be useful to further analyse the samples.

6.3 Kinetic Tests

6.3.1 Introduction

Leach columns were constructed in order to ascertain the AMD potentials of rock samples in a kinetic context, whereas static tests provide a single value. Often kinetic tests will provide more information on the reactivity and long term weathering chemistry of samples.

6.3.2 Methods

The leach columns were constructed from 26 1l HDPE bottles that had their tops cut off. A small hole was drilled through each bottle, approximately 2cm from the base and an approximately 5cm of flexible plastic tubing was fed through the hole. 26 perspex disks were cut and 10, 1mm holes were punched through each disk for drainage (Figure 5-2).

In order to minimise contamination, the disks and bottles were rinsed in distilled water, soaked for 24 hours in 10% HNO_3 solution and rinsed 3 times in distilled water. Quartz gravel was rinsed in distilled water and soaked in 10% HNO_3 for 24 hours, then rinsed 3 times in distilled water. 23 lots of 200g of quartz gravel were weighed out and placed in the bottles; the perspex disks were then placed on top. To prevent drainage, the plastic tube was bent and held with a small piece of plastic tube, approximately 0.5cm in diameter. The plastic ring could easily be removed and refitted during water sampling.

Rocks were prepared for the leach columns by crushing 1kg of each sample in a steel jaw crusher. The gravel sized samples were then put through a 4mm sieve. Two leach columns were filled with 150g of each sample, to provide duplicates. Two leach columns were left as blanks, containing only quartz gravel and water treatment, in order to determine the background effects of the materials used in the leach columns.

The leach columns were left for 7 days at room temperature. On the seventh day, 200ml of distilled water was added to one set of columns whereas the duplicate set were treated with 200 ml of water collected from Comstock Creek, above the mine lease (Figure 6-3). Columns were left for 7 days, and then water samples were collected. A seven day dry period followed by seven days of saturation was designed to approximate precipitation regimes at Comstock in April - June 2000. This cycle was continued for six weeks, such that insitu water parameters were measured 3 times.

pH, electrical conductivity, temperature and redox were measured immediately after collection. PH was measured using a WTW pH 330 meter with a WTW pH electrode, Eh was measured using the same meter and an Orion Eh probe. Conductivity samples were measured using a WTW meter. Samples were also collected for anion and cation analysis. Anion samples were placed in HDPE bottles, provided by the laboratory and immediately transported to the Department of Primary Industry, Water and Environment (DPIWE) analytical laboratory at the University of Tasmania, Sandy Bay campus. Anion analysis was conducted, within 24 hours, on an ion chromatography machine.

Cation samples were filtered into 100ml HDPE bottles that had been rinsed with distilled water, and soaked in 10% HNO_3 for 24 hours. 20 mls of water were collected using a 10 ml syringe fitted with a 0.45µm filter (a fresh syringe and filter was used for each sample), 2mls of 1M HNO_3 was added to each sample. These samples were taken to the Central Science Laboratory (CSL) at the Tasmania University, Sandy Bay campus for analysis on the Inductively Coupled Plasma-Optical Emission Spectrometer (ICP-OES; Table 6-8 describes equipment, and detection limits).

Leach columns were subject to wetting and drying periods of 7 days, such that water quality was measured once every 14 days. The latter samples were only analysed for in situ pH, electrical conductivity, temperature and redox, after the first sampling episode.

PARAMETER	ANALYSIS	ELEMENTS/SPECIES	DETECTION LIMIT
Cations	Inductively-Coupled Optical Emission Spectrometer	Al; As; B; Ba; Ca; Cd; Co; Cr; Cu; Fe; K; Mg; Mn; Na; Pb; S; Si; Sn; Zn.	0. 5ppm
Anions	Ion Chromatography	SO_4^-; NO_2^-; NO_3^-; Cl^-; HCO_3; CO_3.	0.03 ppm

Table 6-8: Ion Analysis; equipment used, ions analysed for and detection limits.

6.3.3 Results

The changes in pH, Eh, and EC are presented in graphical form in Figures 6-3, 6-4, and 6-5, full data is provided in Appendix 10. Test numbers refer to the insitu measurement of water characteristics conducted once a fortnight.

6.3.3.1 pH

Temporal variation in sample pH followed similar patterns in general (Figure 6-3). The first water quality tests had pH below four for all. Most of the samples increased in pH for the second insitu testing, suggesting that acid neutralisation had occurred to some extent. The third testing revealed a general "leveling" of results.

6.3.3.2 Redox

The Eh of leach samples showed a range of levels (Figure 6-4). The majority of samples recorded redox potentials of around 400v. Eh increased in most samples in the second test. By the third test, samples had either, "leveled" off, or increased Eh slightly (generally by less than 100v).

6.3.3.3 Electrical Conductivity

Conductivity decreased in most samples between tests (Figure 6-5). Samples 1N, 1D, 3D, 4N, 4D, 6N, and 6D had initial conductivities greater than 2ms. The lowest initial values were around 0.5ms. The second tests had generally lower conductivities, although samples 2D, 9D and 12 N had higher conductivities. The third tests were, again, generally lower than previous tests. The only exception to this trend was 11N, which recorded a higher conductivity than either of the previous readings. All of the final conductivities were below 1ms, in most instances conductivity was below 0.5ms.

6.3.3.4 Ion Analysis

The concentration of dissolved ions in each of the leach columns was analysed (Figure 6-6). Generally, the majority of ions were common mineral forming elements such as sodium, calcium, magnesium, silica, aluminium, and potassium (Appendix 11). Table 6-9, summarises the leachability of the main heavy metals and sulphate. Samples are labelled as per rock sample sites, the water treatments are distinguished with N for water from Comstock Creek, and D for distilled water.

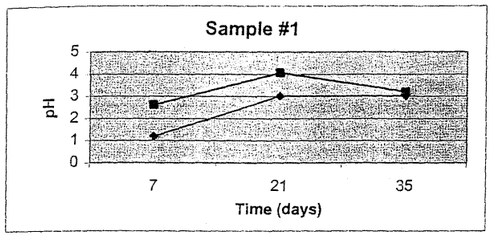

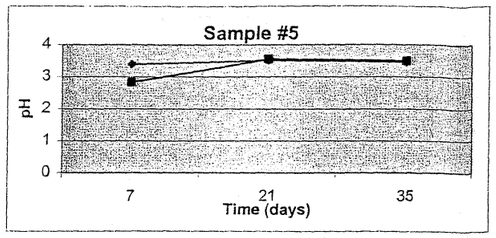

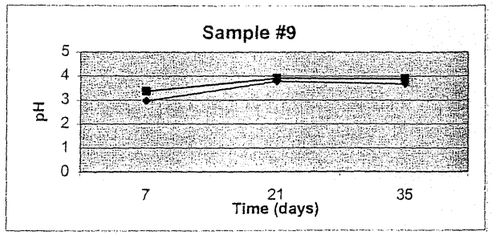

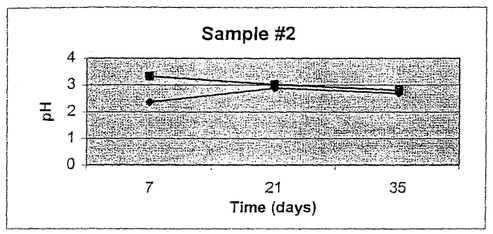

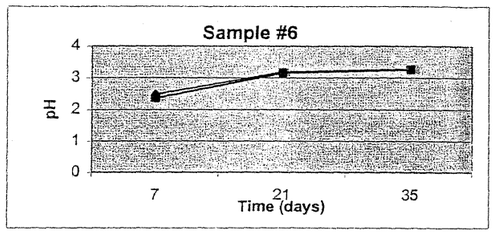

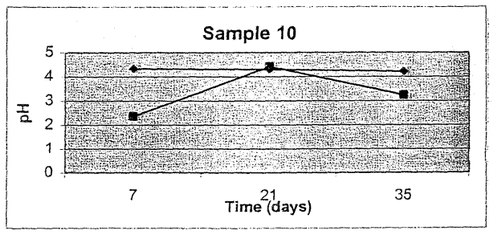

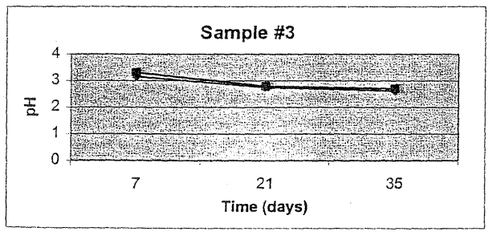

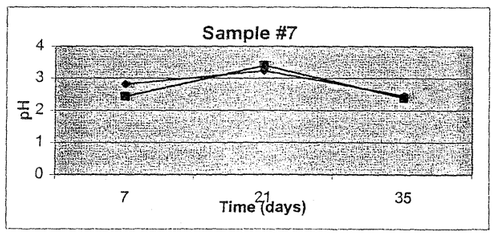

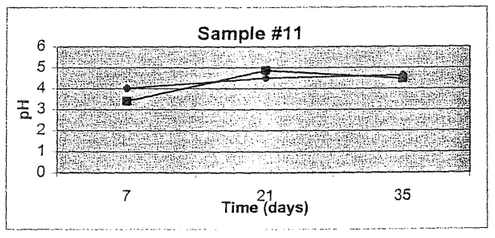

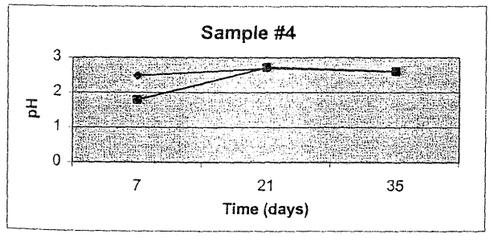

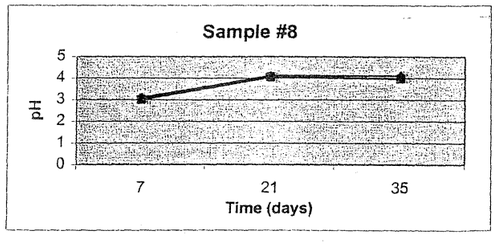

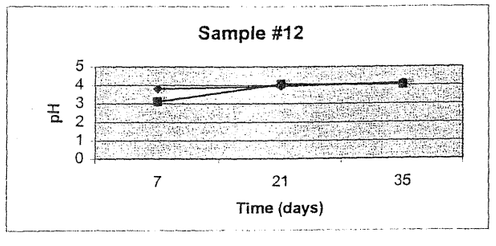

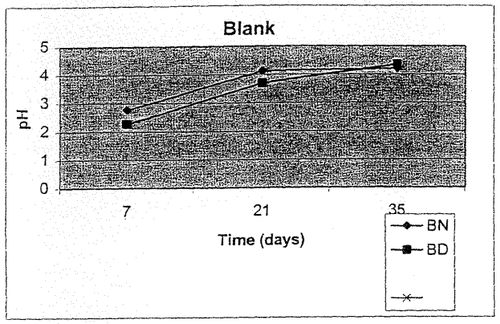

Figure 6-3. Temporal Variation in pH of Leach Columns Treated with Natural and Distilled Water.

BN: Natural Water
BD: Distilled Water

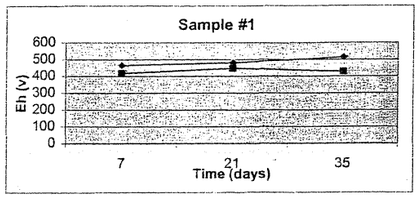

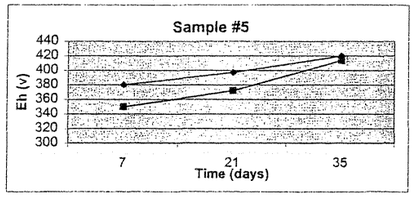

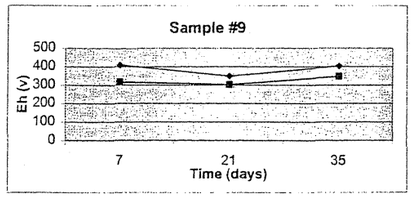

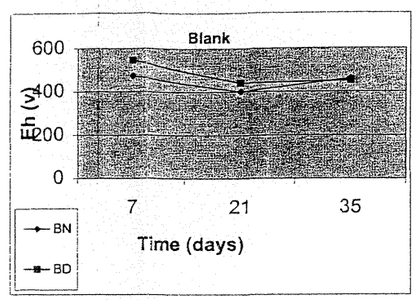

Figure 6-4. Temporal Variation in Eh of Leach Columns Treated with Natural and Distilled Water.

BN: Natural Water
BD: Distilled Water

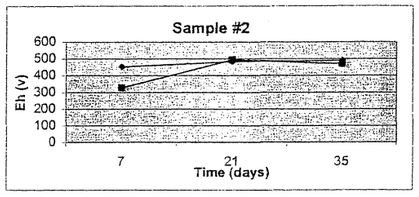

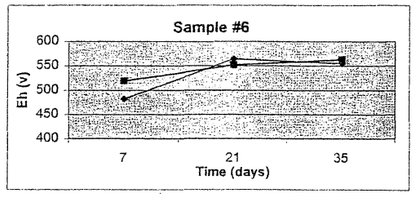

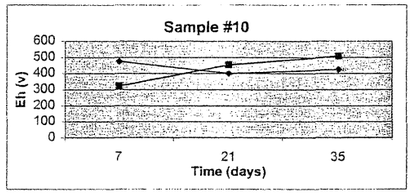

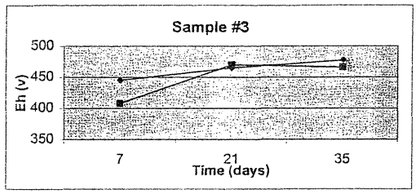

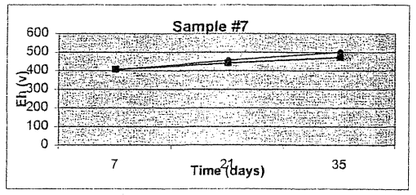

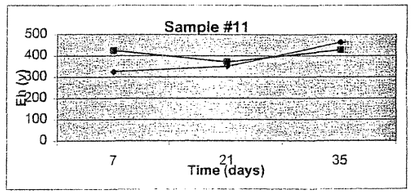

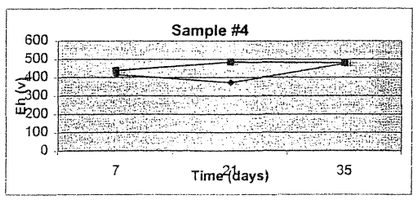

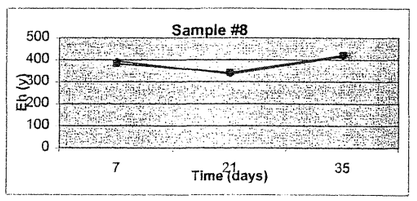

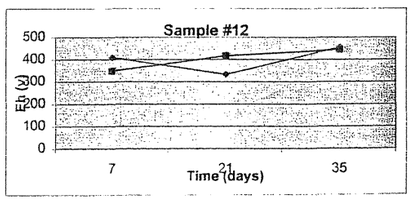

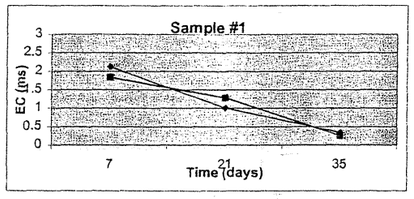

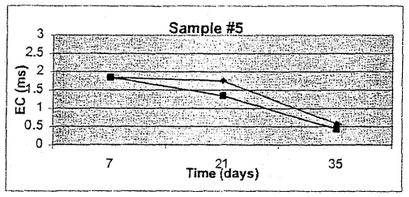

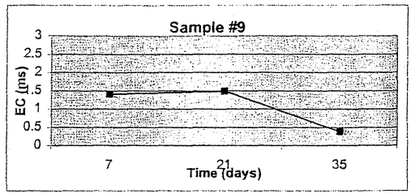

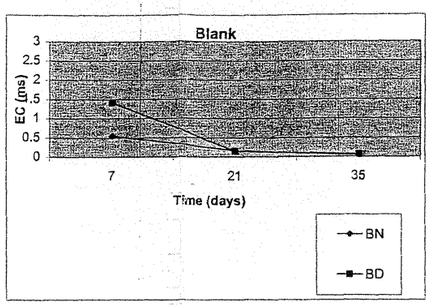

Figure 6-5. Temporal Variation in EC of Leach Columns Treated with Natural and Distilled Water.

BN: Natural Water
BD: Distilled Water

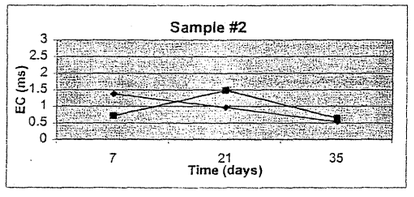

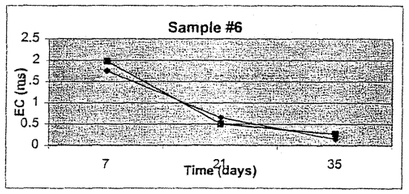

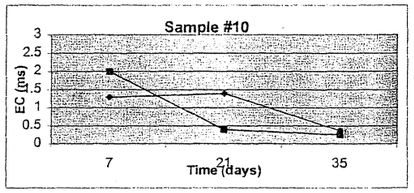

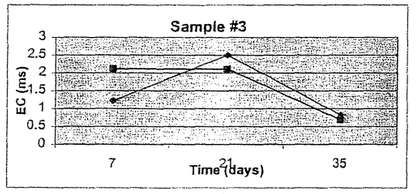

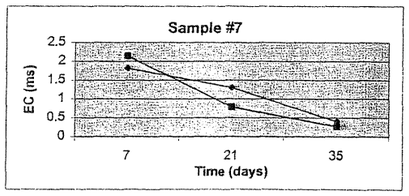

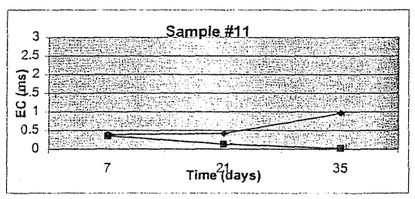

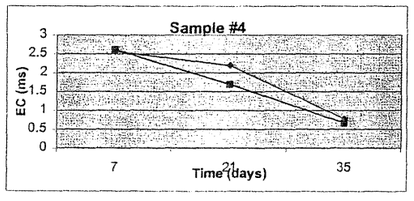

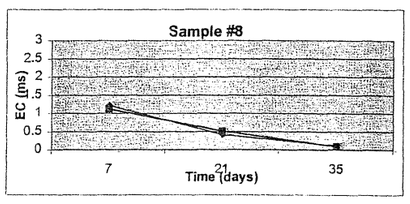

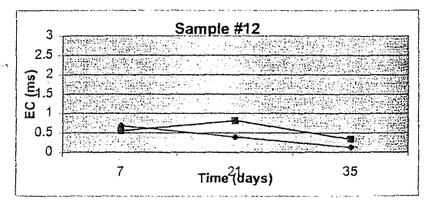

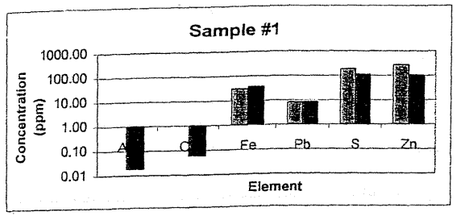

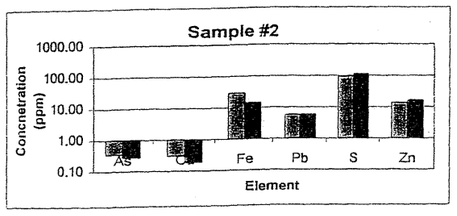

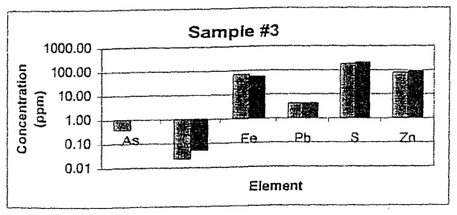

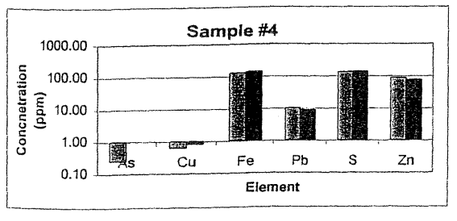

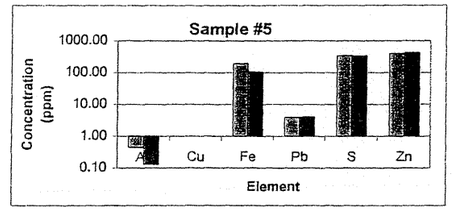

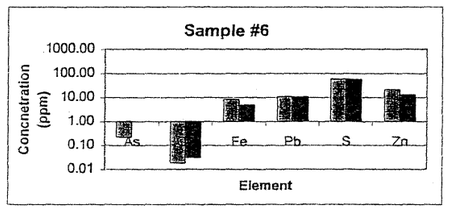

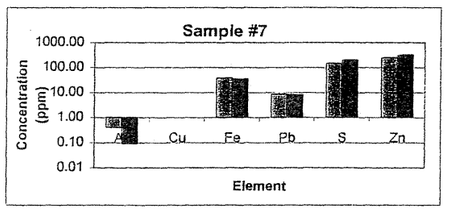

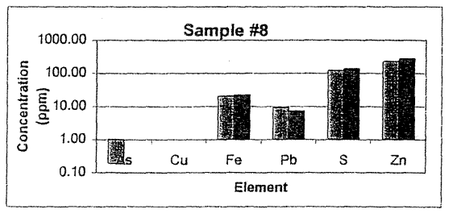

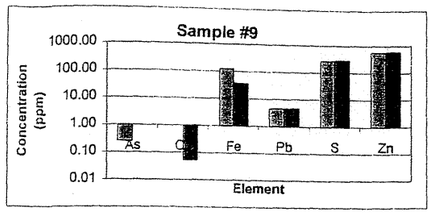

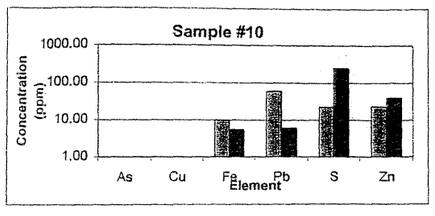

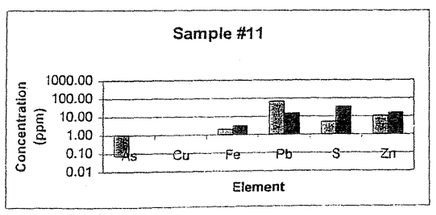

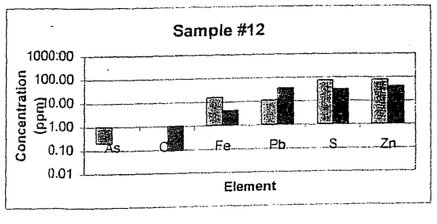

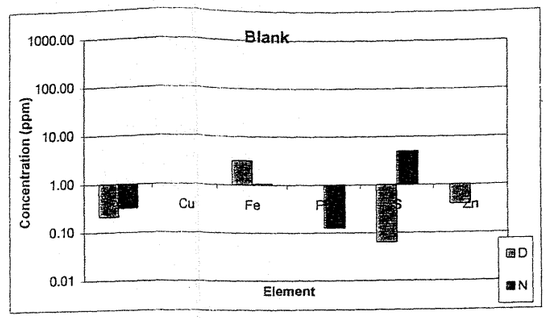

Figure 6-6. Concentrations of Elements in Leachate, for each Leach Column, Treated with Natural and Distilled Water.

D: Distilled Water
N: Natural Water

As

Sample	Whole Rock Composition (%)	Amount Leached (Distilled;%)	Amount Leached (Natural; %)
2	<0.02	<0.175	<0.14
3	<0.02	<0.19	0
4	<0.02	<0.19	0
5	<0.02	<0.22	<0.065
6	<0.02	<0.11	0
7	0	0	0
8	0	0	0
9	0	0	0
10	0	0	0
11	<0.02	<0.035	0
12	0	0	0

S

Sample	Whole Rock Composition (%)	Amount Leached (Distilled;%)	Amount Leached (Natural; %)
2	1	17	21
3	5	3	4
4	1	35	40
5	2	19	19
6	0	144	142
7	0	367	495
8	26	0	1
9	33	0	0
10	49	0	1
11	18	0	0
12	29	1	1

Fe

Sample	Whole Rock Composition (%)	Amount Leached (Distilled;%)	Amount Leached (Natural; %)
2	1	2	1
3	7	1	1
4	4	3	3
5	2	8	4
6	2	0	0
7	1	2	1
8	22	0	0
9	16	0	0
10	58	0	0
11	3	0	0
12	13	1	0

Cu

Sample	Whole Rock Composition (%)	Amount Leached (Distilled; %)	Amount Leached (Natural; %)
2	<0.01	<0.3	<0.19
3	<0.01	<0.02	<0.05
4	<0.01	<0.02	0
5	<0.01	<0.01	0
6	0	0	0
7	0	0	0
8	0	0	0
9	<0.01	0	0
10	<0.01	0	0
11	0	0	0
12	0	0	0

Zn

Sample	Whole Rock Composition (%)	Amount Leached (Distilled;%)	Amount Leached (Natural; %)
2	0	1	1
3	0	13	14
4	0	7	8
5	2	2	2
6	12	0	0
7	0	124	159
8	46	0	0
9	1	0	0
10	<0.01	<20.09	<13.04
11	8	0	0
12	47	0	0

Pb

Sample	Whole Rock Composition (%)	Amount Leached (Distilled;%)	Amount Leached (Natural; %)
2	0	1	1
3	0	2	2
4	0	0	0
5	0	0	0
6	0	1	1
7	0	4	4
8	2	0	0
9	16	0	0
10	1	1	0
11	70	0	0
12	1	0	0

Copper concentrations in the rock samples were very low, and leachate concentrations were below detection limits. Copper appears to be relatively immobile in the leach column conditions, both when distilled and natural waters are the leaching medium (Table 6-9, Figure 6-6).

Zinc concentrations in rock samples were low except for samples 6, 8 11 and 12. Both water treatments leached similar concentrations of zinc. Overall, amounts leached were highest from samples 5, 6, 7, and 12 (Figure 6-6). The results suggest that the total amount of zinc in the rock samples did not control the amounts leached (Table 6-9).

Lead concentrations were highest in rock samples 8, 9, and 11. Distilled water samples with the highest total concentrations of lead were 10 (59.27 ppm) and 11 (65.86 ppm; Table 6-9, Figure 6-6). The natural water treatment released the most lead from 8 (35.15 ppm) and 11. Relative proportions released were highest for samples 3 (N and D), 6 (N and D), 7 (N and D), and 10 (only D).

Arsenic concentrations were low in the rock samples and the leachate. Total concentrations in leachate were highest for samples treated with distilled water (Table 6-9, Figure 6-6). Those samples recorded concentrations of 0.07 ppm to 0.44 ppm, whereas only three samples treated with natural water recorded any measurable arsenic. Percentages leached were low, distilled leachates registered percentages of 0.1-0.2ppm. Natural water treated leachate had only one sample (2) with a concentration above 0.1ppm.

Whole rock sulphur compositions were highest in samples 8, 9, 10, 11 and 12. Percentages leached were highest in samples 7 (N had 14.35% leached, D had 14.1575% leached), and 8 (N had 36.73% leached, D had 49.525% leached; Table 6-9, Figure 6-6).

Iron occurred in the highest concentrations in samples 8, 9, 10 and 12. Leachate with the highest amounts of iron were samples 4 (D and N), 5 (D and N), and 12 (N; Table 6-9, Figure 6-6). The percent of iron leached from the samples was very low, none of the samples had more than 0.8% of there iron leached into solution.

The highest amounts of sulphate were released from sample 8 (N & D) and 5 (N and D). Sample 7 (N and D), 3 (N and D), and 10 (N; Table 6-9, Figure 6-6). The lowest concentrations of sulphate were found in samples 12 (N and D), 11 (N and D), and 10 (D). There was a discrepancy between sulphate and sulphur concentrations in anion and cation

samples. Some samples were determined to have levels of sulphate that exceeded the sulphur concentrations. This may be due to differences in analytical techniques, with different accuracy in calculating S content.

The blank leachate compositions are included to illustrate the level of element contamination possible due to the leach column itself. The leach column was sterilised as per the sample leach columns; however it still contained most of the contaminants sampled for, occasionally at concentrations higher than found in sample leachates. Some of the contamination may have been due to contaminated acids used for sterilisation. The natural waters, in particular contained relatively high concentrations of sulphur, lead and iron.

6.4 Discussion

All samples from the Comstock mine lease appear to have some ability to produce acid, although the method used to interpret the data affects final conclusions about the AMD potential of the sample. The amount of acid potentially produced varies with the experimental methodology used, but the most commonly used method in industry, MPA from total sulphur, suggests that acid will be produced from each of the rocks assessed.

The ANP suggested that almost all of the rocks (excluding sample 5) have no ability to buffer acid. Sample 5 has some ability to buffer acid but the amount of acid produced exceeds any buffering capacity of its constituent minerals. The overall acid-base account is summarised by the NAPP results, which demonstrate that all samples have the potential to produce net acid. Samples 4 and 6 had low net acid production to the degree that under the B.C. AMD taskforce (1989), classification schemes, the samples would be non-acid producing.

Maximum potential acidity calculations were highest in samples with the greatest abundance of pyrite. Following this, other samples with any sulphide mineral in relatively high abundance had a high MPA value; consequently, the highest MPA results were from ore samples. The highest potential acidity value for non-ore samples in the decline, was from a shale containing disseminated pyrite. The sample contained a relatively high abundance of pyrite compared with other host rock samples. Samples with undetectable amounts of sulphide minerals (using X-Ray Diffraction; XRD), constantly had the lowest potential acidity values. The results of MPA tests should correlate with NAPP tests because of the paucity of carbonates in the samples, and this is the case.

A problem with MPA tests conducted on Comstock samples is the amount of organic sulphur in the shales. This may have caused overestimation of potential acid production. In the case of Comstock, it may be advisable to use a pyritic, or sulphide mineral, sulphur method that differentiates between potential acid production and inert sulphur.

Neutralising potential (ANC) reactions are very similar to relative values obtained from MPA data; samples with highest levels of sulphate are least likely to neutralise acid. This could be because the experimental procedure is based around the assumption of all neutralising ability being present as carbonate, thus buffering would occur rapidly. Potential buffering reactions, in the samples, are slow because aluminosilicate dissolution is relatively slow (Sherlock *et al.*, 1995). Therefore, while all the potential acid is produced during the sulphide oxidation stage of the experiment, the amount of time available for buffering to take place may not be long enough for significant aluminosilicate reaction.

The results of NAG tests indicate that there is minimal propensity for buffering in Comstock samples. These tests may be more predictive of acid production at Comstock, because the net result of acid production is weighed against net buffering. Because acid production was tested for, instead of estimated, problems with the type of sulphur were eliminated.

The results of pH analysis show that there was no lag period between water addition and acid production. The first results all had pH below 4.5. This indicates that by the end of the first week of leaching, any carbonate buffering potential had been exhausted. Any immediate buffering capacity in the treatment waters was insufficient to stem acid production. The pH increases in the second tests suggest acidification, from oxidation products on the surface of the samples. A slowed release rate may also have affected later acid production. The products of oxidation may have covered fresh surfaces. The last tests suggest acid production rates (relatively high) leveled out. Overall, the leach columns exhibited net acid production, and little to no buffering capacity.

The main heavy metal contaminants seen in the leachate are zinc and, to a lesser extent, lead. Lead and zinc contamination is predominantely from the talc, carbonaceous shale and pyrite samples.

Sulphate release was greatest in the graphitic shale, and two of the talc samples. The siliceous cap rock also released relatively large amounts of sulphate. Free sulphate indicates acid drainage because it is released during pyrite oxidation. This suggests the graphitic shale, talc and siliceous cap rock are the biggest contributors of acid, apart from the sulphide samples. The Comstock samples, again, prove problematic in such assumptions because of the amount of organic sulphate in the shales. Therefore it is probably best to disregard sulphate production as an indicator of acid drainage in the shale samples.

The fresh sulphides are capable of producing large amounts of acid. This, was observed in both static and kinetic results. They did not release much sulphate, compared with other samples, which may be due to their lower solubilities. In comparison, the weathered sulphide samples are capable of producing a lot of acid which does not appear to be neutralised. This was reinforced in the static data where net acid production was almost as high in weathered sulphide minerals, as it was for the fresh minerals. Kinetically, the weathered samples produced higher amounts of sulphate, and pH was similar to the fresh samples. Possibly, acid production was occurring at a constant level because buffering from host mineralogy has almost expired.

Overall, any relationship between leachate compositions in natural and distilled water treatments is difficult to define. Iron concentrations were less in natural samples, possibly an indication of organic sorption processes. It would be expected that organic matter in the Comstock Creek water would provide additional adsorption sites for free ions. Copper, in particular, strongly associates with organic complexes (Kelly, 1988). This did not occur; in fact, copper was only detected in samples treated with natural water. The common ion effect should be evident, with the solubility of samples decreased because of the presence of the same ions already in the water (Domenico & Schwartz 1998). This may explain some of the variability observed in the ore samples.

From the results of the leach tests, zinc is the primary heavy metal of concern; it is a relatively mobile element and, while it readily adsorbs to iron hydroxides, it is easily re-released when water parameters, such as pH or redox, change. Lead appears to be relatively stable in leach column conditions. Iron is released by sulphide oxidation; the low proportion present in leachate samples, compared with rock compositions, is probably due to

precipitation of iron oxides within the leach column. This may explain the relatively low concentrations of lead seen in some leachates.

6.4 Conclusions

- Rock samples taken from the decline at Comstock had a net capacity to produce acid.
- There is no lag period to acid production.
- The talc samples had some neutralising potential that was exceeded by their acid producing potential.
- Fresh and weathered sulphide samples had similar propensities to produce acid.
- The main potentially toxic elements released in leach columns were zinc, iron, lead and arsenic.
- All samples produced abundant sulphur and sulphate.

Section Four:

Conclusions and Recommendations.

Chapter 7

Conclusions

- A study of the background water quality of sites around the Comstock mine determined that water, in Comstock Creek, flowing onto the lease contained; 0.25ppm total Al, 0.01ppm total Pb, and 0.23ppm total Zn. All concentrations exceed ANZECC recommendations for maximum allowable concentrations for the protection of aquatic ecosystems.
- Concentrations of Pb, Zn, Fe, Al, and As, were above ANZECC recommended levels at some sites, and these were the main contaminants detected in water samples analysed during the study.
- Contaminant concentrations were higher in "baseline samples", collected during high-flow conditions above the mine site, and within active workings, and lower below the tunnel system.
- Contaminant concentrations during low-flow conditions were higher below the mine.
- Site waters ranged in pH from 3.29 at site 8 (within the decline), to 6.24 at site 4.
- Inflow of water into the tunnel system during high flow conditions, resulted in a net reduction in contaminant concentrations.
- Conversely, in low flow conditions, contaminant concentrations in Comstock Creek increase after water entered the tunnel system.
- The sites situated within the decline had the highest concentration of contaminants in high flow, and low flow conditions.
- Rocks sampled from the decline were net acid producing under experimental conditions, during leachate experiments.

- All rocks sampled contributed metals to leachate waters during leachate experiments.

Future Work Recommendations:

- A survey of Comstock Creek, upstream of the mine may be able to find a point source for the elevated contaminant concentrations, found at sites above the mine.
- A more extensive acid-base accounting program, conducted regularly on samples collected from the decline would be useful for determining the future impacts of waste rock piles, as new rock types are exposed.
- A water-sampling program should be set up, so that the effects of current operations can be monitored. For this, it would be good to sample sites above and below, as well as in, the mine lease, and in the decline. The program should include mass loading determinations, contaminant concentration analysis, and in situ, field measurement of pH, Eh, and EC.
- Monitoring for the effects of anthropogenic contamination, for example machinery, within the mine, should begin. A hydrocarbon sampling program should be incorporated.

Chapter 8

Potential Remediation Strategies

8.1 Introduction

From analysis of background water quality in the Comstock catchment, it is apparent that water within any part of Comstock Creek has seldom met guidelines recommended by ANZECC. The ecology of the creek would have been adapted to this, as at other sites around the west coast. Unfortunately, a legacy of historic mining activity has exacerbated acidity, heavy metal loading and oxyhydroxide precipitation to a degree that has relieved the creek of any biological activity beneath the water surface (DELM File 06-23-17).

Reducing the amount of oxyhydroxide precipitate, and the level of trace element and heavy metal contamination within the water would be instrumental in returning the creek to its pre-mining activity composition. The remediation of water quality may enhance biological activity in Comstock Creek.

In order to prevent further degradation of Comstock Creek, it is important that the current mining activity is designed to manage waste rock in an environmentally responsible manner. Such planning could prevent further impacts, and may even alleviate some aspects of the historic drainage problem.

8.2 Remediation

A brief pretreatment of the water before it enters the two drainage shafts in the decline, may help minimise the amount of contamination entering the tunnels from current

activity. As the amount of water involved is minimal this step could be relatively easily employed. The most practical treatment strategy would comprise addition of limestone, lime, caustic soda or bio-fix beads, both to the sediment trap and the Balstrup drain. Given that west coast waters are naturally acid, excessive neutralisation may affect the ecology of ecosystems adapted to these conditions. For this reason, I would suggest that treatment of the waters might best be conducted using a metal removal system instead of increasing alkalinity. Bio-fix beads may be the most appropriate solution for treatment of water before it enters the tunnels. This would prevent the problem of heavy-metal contaminated decline waters entering the tunnel system and maintain water at naturally occurring levels.

Water draining from the main adit should be treated, in order to alleviate contamination of Comstock Creek. A number of options are possible but consideration of topography, rainfall, economic feasibility and practicality indicates only a few options are viable. The first option would comprise addition of biofix beads to the exit point of the main adit. These beads will "fix" heavy metals whilst not affecting acid levels, which are normal for a west coast creek. Biofix beads are a relatively low-cost, practical and easily employed solution to high metal concentrations, particularly where acidity is not necessarily a problem (Jeffers & Corwin, 1991).

The second solution would be to construct artificial wetlands; these could filter heavy metals, whilst maintaining other water parameters (particularly pH), in a relatively natural state. Widening Comstock creek below the main adit (site 6) would not be a major task as small, anastomosed sections form naturally wider, low-flow area. These areas are associated with large ferrous-oxyhydroxide deposits and marsh, replete with *Restionacaea* sedges. Part of this area was dammed previously, so the natural area has already been

disturbed. Vegetation of the wetland could be conducted using seeds propagated from the preexisting wetland situated below the tailings dumpsite.

Alternatively, extension of the existing wetland area to encompass a recontoured Comstock Creek flow path, may be an adequate solution. For this to work the creek would require considerable widening; damming the current flow channel, and re-directing the channnel north by at least 100m would also be required. The topography of the creek allows such a solution, this option would be more expensive and have greater impact on the creek.

8.3 Waste Rock Dump

All rocks from the decline, analysed using ABA methods, have a proven propensity to release acid and metals when exposed to oxidising conditions. This suggests that a waste rock dump is capable of producing AMD. Because of this, it is going to be important that the mine sets up an effective plan for containment of the waste rock. There are two main options available; 1) wet cell containment, or 2) dry cell containment.

8.3.1 Wet Cell Containment

Wet cell containment would comprise ponded waters maintained behind a water-retention dam. Construction of a dam would be designed for containment of waste in a reducing zone, such that sulphides and metals are inert.

The dam should be positioned in an area where minimal disruption to natural areas is likely to occur. At Comstock, the most obvious area for a dam would be in the South Comstock Open-Cut. The site is already disturbed and the close proximity to current operations would minimise costs and risks associated with transport of waste rock. The

dam would require an impermeable lining to prevent seepage along faults and into the tunnels. Regular addition of organic carbon to dam waters would aid sulphate reduction, and precipitation of sulphide minerals (Blowes *et al.* SU).

A spillway for excess waters would be required in order to maintain the dam's ability to retain the waste rock. The amount of rainfall at Comstock suggests dams would fill rapidly. The spillway should lead to a secondary treatment location where water can be further remediated before flowing downstream. A suitable treatment for such waters would comprise a wetland through-flow system, as suggested for tunnel remediation. Dam water could be piped to the pre-existing wetland area allowing water to filter through, thus decontaminating before entering Comstock Creek. This method would require a detailed study in order to determine the amount of water involved in such a scheme.

8.4.3 Dry Cell Containment

Currently, waste rock is dumped over a previously disturbed site. Previous disturbance, in combination with the size of the site, suggests that the area may be suitable for a waste rock pile, although the location of the waste rock on a slope, where that run-off flows into Comstock Creek implies that planning as to the segregation of materials, infiltration by rain and surface flows, and, potential contaminant run-off paths is required.

As none of the waste rock was identified in the ABA study as having any buffering potential, there are going to be problems with AMD unless buffering material is added to the rock piles. Identification of a suitable source of material with abundant buffering potential is recommended. Once this is done, mixing this material with waste rock may limit acid production if water does infiltrate the piles. I would also suggest that

material with the highest propensity to form acid and release heavy metals, is placed in the middle of waste rock piles, where oxidation is least likely to take place.

Without planning, the waste rock piles will be highly permeable and, easily infiltrated by precipitation given the disaggregated nature of the waste material. A number of strategies could be useful for dealing with potential infiltration:

1) Design the piles such that slope angles deflect run-off and minimise seepage of meteoric water into the piles.
2) Covering the piles with low permeability clays will reduce infiltration by water and oxygen.

Construction of infiltration controls downslope and along the base of the tailings piles will reduce the likelihood of contaminated waters entering underlying aquifers, or contaminated surface flows seeping from the base of the pile. In order to achieve this, a sealable sheet-pile barrier should be entrenched downslope of the piles Blowes et al (DU). A permeable sulphate-reduction wall that could treat any contaminated waters that continue to flow down slope may be constructed below the sheet-pile barrier. On the up-side of the sheet-pile barrier, a drain should be constructed to capture seepage. This drain should be diverted to flow to a second treatment area. This may also be the wetlands previously suggested. The wetlands occur almost immediately below the present waste rock piles, and it would not be difficult to divert the drainage slightly.

In order to ensure a large enough capacity to deal with future metal loading over the length of time that AMD will potentially occur, the wetland would require planning. This is likely to be a considerable time as AMD has occurred on-site for over 100 years without abatement. It would require a stringent monitoring and maintenance regime. The monitoring would require water quality tests of all water around the waste rock

piles/dams, wetlands, decline drainage, tunnels, upstream in unaffected catchment areas, and downstream. This would allow evaluation of the effectiveness of the proposed remediation.

Literature Cited

Alpers, C.N. & Zierenberg, R.A. 1998. Geoenvironmental Model of Volcanogenic Massive Sulphide Deposits; in *Metallogeny of Volcanic Arcs,* B.C. Geological Survey, Short Course Notes, Open File 1998-5. pp 0_1 - 0_2.

Australian & New Zealand Environment and Conservation Council; National Water Quality Management Strategy (ANZECC/NWQS),1992. *Australian Water Quality Guidelines for Fresh and Marine Waters*, 141 pp.

Banks, M.R. & Kirkpatrick, K.B. 1977. *Landscape and Man: The Interaction Between Man and Environment in Western Tasmania.* The Proceedings of a Symposium Organised by the Royal Society of Tasmania.

B.C. Acid Mine Drainage Taskforce, 1989. *Draft Acid Rock Technical Guide: Volume 1 Technical Guide*. B.C. Ministry of Energy Mines, Petroleum Resources. Victoria B.C.

Berry, R.F., Elliott, C.G., & Grey, D.R. 1990, *Excursion Guide E3: Structure and Tectonics of Western and Northern Tasmania,* 10th Australian Geological Convention, Hobart.

Blainey,G. 1993. *The Peaks of Lyell.* St Davids Park Publishing.

Blisset, A.H. 1962. *Geological Survey Explanatory Report*, One Mile Geological Map Series, K'55-5-50 Zeehan.

Blowes, D.W., Ptacek, C.J, & Jambor, J.L. Date Unknown. *Remediation and Prevention of Low-quality Drainage from Tailings Impoundments.*

Both,R.A. 1966, *The Zoned Ore Deposits of the Zeehan Mineral Field.* Unpublished PhD thesis, University of Tasmania, 343 pp.

Both, R.A., Williams, K.L. 1968a. *Mineralogical Zoning in the Lead Zinc Ores of the Zeehan Mineral Field, Tasmania. Part 1: Introduction and Review.* Journal of the Geological Society of Australia, 15, pp121-137.

Cartwright, AJ. Komyshan, P. Roberts, P.A. 1976. *E.L. 11/76 Trial Harbour Area. Annual Report for 1983/84.* Mineral Resources of Tasmania (MRT), 85_2385. 1976. Unpublished Report.

Comstock Development Proposal and Environmental Management Plan (DPEMP), 2000. Unpublished, Open File, Great Southern Land Minerals, 42pp.

Comstock Environmental Assessment Report: Permit Conditions- Environmental, 2000. Unpublished, Closed file. Board of Environmental Management and Pollution Control.14pp.

Crossing, D.J.F. 1992. RGC Report no. T/92/17. *El142/87 Zeehan, Summary Review*, Oct 91-Sept 92.

Department of Primary Industry, Water, and the Environment. File no. 06-23-17. Unpublished Open File.

Domenico, P.A. & Scwartz, F.W. 1990. *Physical and Chemical Hydrogeology.* John Wilby & Sons.

Ficklin, W.H. Plumlee, G.S. Smith, K.S. & McHugh, J.B. 1992. Geochemical Classification of Mine Drainages and Natural Drainages in Mineralised Areas, in Kharaka, Y.K. & Maest, A.S. (eds). *Water-Rock Interaction 7-1*, pp 381-384.

Findlay, R.H. & Brown, A.V. 1992. *The Tenth Legion Thrust, Zeehan District: Distribution, Interpretation andRregional and Economic Significance.* Tasmanian Department of Resources and Energy, Division of Mines and Mineral Resources, Report 1992/02.8pp.

Halsall, M. 2000. Mineralogy of Selected Core Samples, appendices in Richardson, S (ed), *Comstock (Zeehan) Project: ML123m/47, ML43m/85, & ML19m95, Final Report.* Report no. Tas0038-01/00, Western metals Resources, Townsville.

Jackson, W.D., 1999. The Tasmanian Environment, in Reid, J.B., Hill, R.S., Brown, M.J., & Hovendon, M.J. (eds) *The Flora of Australia,* Supplementary Series no.8, Australian Biological Resources Study. pp1-38.

Jeffers, T.H. & Corwin, R.R. (1991). *Wastewater Remediation using Immobilised Biological Extractants,* U.S. Bureau of mines, Salt Lakr City, pp31.

Kelly, M. 1988. *Mining and the Freshwater Environment.* Elsevier Science Publishing Co. New York. 231 pp.

Klominsky, J. 1972. *The Heemskirk Granite Massif.* Unpublished PhD Thesis , University of Tasmania 285 pp.

Knight, J.M. 1997. *Comstock Silver-Lead-Zinc Prospect: Information Memorandum.* Unpublished Report.

Leaman, D.E. 1999, *Review and Implications of Geophysical Data, Comstock Prospect.* Leaman Geophysics, 5pp.

Miller, R.W. & McHugh, J.B. 1994. *Natural Acid Drainage from Altered Areas Within and Adjacent to the Upper Alamosa River Basin, Colorado.* U.S Geological Survey, Open File Report 94-144. 47 pp.

Miller, S. 1994. Predicting Acid Drainage in *Groundwork.* 1:2. 1998 pp.8-9

Miller, S. Robertson, A. & Donahoe, T. 1997. *Advances in Acid Drainage Prediction Using the Net Acid Generation (NAG) Test.* Proceedings of the 4th International Conference on Acid Rock Drainage. Vancouver B.C. pp533-549.

Nordstrom, D.K., Jenne, J.A. & Ball, J.W. 1979. Redox Equilibria in Acid Mine Waters, in Jenne, E.A. (ed), *Chemical Modelling in Aqueous Systems.* ACS Symposium Series, 93. 913pp.

Parkhurst, D.L. 1995. Users Guide to PHREEQC- a computor program for speciation, reaction-path, advective transport and inverse geochemical calculations. U.S. Geological Survey, Colorado, 127pp.

Parr, T.E. 1997, *Acid Mine Drainage in the Zeehan District.* Honours Thesis (unpublished). University of Tasmania, 90pp.

Perry, E.F. 1999. *Interpretation of Acid Base Accounting.* Online reference. Http://ww.dep.state.pa.us/dep/deutate/minres/districts/cmdp/chap11.html

Plumlee, G.S. Smith, K.S. Ficklin, W.H. & Briggs, P.H. Geological and Geochemical Controls on the Composition of Mine Drainages and Natural Drainages in Mineralised Areas, in Kharaka, Y.K. & Maest, A.S. (eds). *Water-Rock Interaction 7-1*, pp 419-422.

Polya, D.A. 1998. PHOX: Automoted calculation of mineral stability and aqueous species predominance fields in Eh (or log$f(O_2)$ or pe)-pH space, in Arehart, G.B. and Hulston, J.R. (eds), *Water-Rock Interaction*, 9, pp897-900.

Richardson, S (ed), *Comstock (Zeehan) Project: ML123m/47, ML43m/85, & ML19m95, Final Report.* Report no. Tas0038-01/00, Western metals Resources, Townsville.

Sherlock, E.J. Lawrence, R.W. & Poulin, R. 1995. *On The Neutralisation of Acid Rock Drainage by Carbonates and Silicate Minerals. Environmental Geology,* 25 . Pp 43-54.

Slater, M.J. 1996. *Geology and Geochemistry of the Zeehan Mineral Field.* Honours thesis, University of Tasmania.

Smith, S.E. 1998, *Acid Mine Drainage in the Bakers Creek Waste Rock Dump*, Hercules, Western Tasmania. Honours Thesis (Unpublished), University of Tasmania, 95pp.

Soregali, B.A. & Lawrence R.W. 1997. *Waste Rock Characterisation at Dublin Gulch: A Case Study.* 4th International conference on Acid Rock Drainage. Vancouver, BC. Pp. 631-645.

Summons, T.G. 1983 Ag-Pb-Zn Mineralisation, The Comstock Group of Veins, The Minstock Tribute Area (within consol. ML123M/47), Zeehan District, Western Tasmania. Unpublished Report, Summons Geoservices, 17pp.

Taylor, M.I. 1993. *Skarn and Sulphide Mineralisation of the Sylvestor Prospect, Zeehan Western Tasmania.* Unpublished Honours Thesis, University of Tasmania, 113pp.

Tear, S.J. 1999, *Interim Geological Report on the Comstock Prospect, Zeehan, West Tasmania.* Unpublished Report for Oceania Tasmania, Pty. Limited.
Tear, S.J 2000, *Geological Report on the Comstock prospect, Zeehan, West Tasmania*, Unpublished Report for Oceania Tasmania Pty. Ltd

Twelvetrees, W.H. & Ward, L.K. 1909. Geological Examination of the Zeehan Mineral Field. Geological Survey Bulletin of Tasmania, 7.

Williams, E., McClenaghan, M.P., & Collins, P.L.F. 1989, Mid-Palaeozoic Deformation, Granitoids and Ore Deposits, in Burrett, C.F. & Martin, E.L. (eds) *Geology and Mineral Resources of Tasmania.* Geological Society of Australia, Special Publication no. 15, pp238-292.

Bioavailability and Toxicity:

Controls on the Biological Impact of Elements in Aquatic Environments.

Unnikki Meskanen

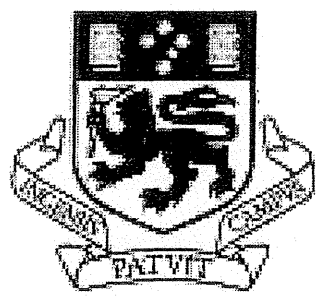

University of Tasmania,

School of Earth Sciences.

Submitted in partial fulfillment of requirements

for the degree of Bachelor of Science with Honours.

Abstract

The biological impact of elements in the aquatic environment is controlled by chemical, physical and biological interactions. Bioavailability is determined by the dynamic interaction of physical and chemical factors. These factors control the distribution of species assemblies which, in turn, determine the partitioning of elements between pore water, sediments and the water column.

Organism exposure to toxins is a function of geochemical partitioning and organism behaviour. Equilibrium partitioning models attempt to compare actual with theoretical bioaccumulation. Once exposure has occurred, physiological processes determine the magnitude of absorption across biological membranes and concentration within organism tissues and resultant toxic effects.

Calculating elemental toxicicity effects is difficult because of biochemical interactions. Differences in physiology between biological species and individual organisms also make prediction of toxicity effects difficult.

Contents

Figures

Tables

Chapter 1

Introduction

1.1 Background

Variations in bioavailability depend on the form in which an element occurs and the organism involved. The chemical conditions of the environment influence speciation while biological activity and physical changes inhibit equilibrium between phases and chemical species concentrations. Therefore any sample contains a number of species of an element (Borg 1995, Fergusson 1991).

Element speciation is a major determinant of bioavailability. This is because animal behaviour and physiology, and the physiology and biochemical processes of plants, cause preferential uptake and internal absorption of certain element species. The partitioning of an element is important because this controls the exposure of organisms to toxins.

Water quality quidelines set standards for the chemical composition of water so that it remains potable and able sustain generations of aquatic life. Physico-chemical, biological or chemical criteria for water quality (Johnston, 1991; ANZECC 1992) provide targets for regulating authorities that oversee the management, protection and treatment of water.

Various assumptions and omissions limit the relevance of current water quality guidelines. Criteria are usually derived from limited studies of a few organisms. As such, they assume that key biological species are as susceptible to toxicity at designated element concentrations as any other species in that environment (ANZECC 1992). There are also limitations in applicability of guidelines to different types of environments, e.g. Roux *et al* (1996) have attempted to derive water quality criteria directly relevant to South African water ways. Variations in the specific environmnet also alter plausible and appropriate standards e.g. west Tasmanian

waters have high background metal concentrations (Hince 1993). Criteria are also based on assumptions of steady-state conditions; consideration of rates and quantities of cycling in reservoirs, residence times, and the speciation of various elements is lacking (Craig 1980). Most management guidelines for protection of aquatic ecosystems are limited to describing desirable limits for total element concentrations within the water column; while chemical species assembly is occasionally analysed, analysis of sediment composition is rare (Roux et al 1996; Wepener et al 2000).

Uptake of toxins from the water column is generally thought to cause biotic impacts. Little assessment of the bioavailability and resultant impact of contaminants within sediments has been done in case studies. Studies that have compared bioavailability and element concentrations in sediments have identified sediments and interstitial waters as an important source of biocontamination (Bindra & Hall d.u.[1]; Campbell & Tessier 1991; Elsokkary 1991; Hugget et al. 1999; Jackson 1991; Lee et al 2000; Sijm et al. 2000; Van der Kooij et al. 1991; Wepener et al. 2000).

1.2 Definitions

A number of terms used in this review have multiple definitions that vary with the context in which they are used. Appendix 1 contains definitions for selected terms relevant to this review.

1.3 Aims

This review will describe the physical, chemical and biological factors that influence bioavailability and toxicity. The effects of element partitioning on bioavailability will be discussed. Controls on biological uptake are related to physico-chemical partitioning, geobiochemical interactions, and biological controls. Toxicity effects are related to element interactions and biochemical controls.

---

[1] d.u. = Date Unknown.

Chapter 2

Controls on Element Bioavailability and Toxicity.

2.1 Introduction

The bioavailability and toxicity of elements depend on how an element exists within the environment. Speciation and resultant partitioning will affect an individual organism's exposure to specific elements. Certain species are easily transported across external biological membranes, while other species of the same element may be more likely to be ingested or inhaled. Some chemical components have a very low bioavailability, often because of minimal exposure to organisms, or because strong chemical bonds prevent dissolution, thus preventing passage through biological membranes.

Biogeochemical cycles exist for 1) element concentration and distribution, 2) rates of chemical modification within reservoirs, and 3) rates of transfer between reservoirs (Craig 1980). Element speciation depends on the biological, physical and chemical characteristics of the environment. In turn, speciation determines partitioning of elements between the water column, the sediments and pore water.

Physical influences on element bioavailability include 1) temperature, 2) phase association, 3) physical adsorption, 4) occlusion within a solid phase, and 5) depositional regime. Chemical influences affect 1) speciation at thermodynamic equilibrium, 2) complexation, 3) compound solubility, 4) phase transitions (associated with precipitation, coprecipitation and chemical adsorption/desorption), 5) redox and 6) pH conditions of the environment, and 7) biochemical processes (Allard 1995; Fergusson 1990; Newman & Jagoe 1994).

2.2 Phase Association

Elements occur in sediments, in pore water or within the water column. Elements within the water column are typically differentiated by size. Contaminants

may exist as dissolved aqueous species or as suspended matter (Fergusson 1990). Evidence suggests a considerable amount of elements are present in a third, colloidal, form (1-500 nm; Benes & Steinnes 1995) where a major contaminant transport system exists (Allard 1995) (Appendix 2). Aquatic sediments can also contain dissolved or colloidal metals within pore waters, or elements that adhere to particle surfaces by adsorption or ion exchange.

The water column and pore waters are pathways for metal flux, deposition and accumulation (Elsokkary 1991). Partitioning of elements between dissolved and solid phases is determined by the following (Amiard 1991, Fergusson 1990);

- speciation (the chemical form of the heavy metal; influenced by pH, redox and presence of other species i.e. inorganic ligands),
- uptake by biota via ingestion or absorption and release during decay,
- redox conditions (e.g. reducing conditions cause oxy-hydroxide species to release Fe (III) and Mn (IV) oxy-hydroxide species)
- precipitation as insoluble species (particularly if heavy metal concentrations are high) and,
- surface chemistry

Solid phases include physical weathering products and chemical precipitates. Metals can occur in secondary forms such as: adsorbed in the lattice of secondary minerals; occluded in Fe-, Al or Mn- hydroxides; or complexed/flocculated with organic matter (Campbell & Tessier 1991; Keller *et al* 1991).

Geochemical phase associations determine the potential bioavailability of any element held within the aquatic environment. Elements within sediments are partitioned into geochemical phases. These include interstitial water, exchangeable, easily reducible, organic sulphur, easily acid extractable, and residual (Bindra & Hall

d.u.). The bioavailability of each phase depends on geochemical mobility, complex stability and biological interactions. Interstitial water holds dissolved heavy metals (Hince 1993). Organic sulphur sorbs or complexes metals. Easily acid extractable elements are the dissolved and particulate metals released from a solution within 24 hours of contact with dilute acid (Ross & Vermet 1995). Residual metals are held in inert lattice positions within detrital minerals. These are often very stable. Exchangeable elements are held by cation exchange and chemical adsorption. Easily reducible phases include ions that are adsorped onto or co-precipitated Al, Fe, and Mn oxides (Hince 1993). Appendix 3 contains a list of the common species assemblages of selected elements, and the resulting effects on bioavailability and toxicity to plants and animals.

2.3 Physical Controls

2.3.1 Temperature

Temperature is an important control of bioavailability and toxicity. Organism viability is affected by thermal tolerance stresses. High temperatures increase metabolic activity. Greater element exposure occurs as a result of increased diffusion rates, active uptake and movement across biological membranes (Mayer et al. 1994). Thus, increased temperatures are responsible for toxin uptake to acute exposure levels.

2.3.2 Depositional regime

Gravitational settling, or diffusion, of metal fluxes creates a marked increase in metal concentrations in the upper layers of sediments compared with the overlying water column (Campbell & Tessier 1991). Turbidity influences mixing, oxygenation and settling rates. Changes to aquatic conditions alter the dynamics of geochemical reactions moving towards equilibrium (Elsokkary 1991).

2.3.3 Physical adsorption

Physical adsorption occurs when dispersion or Van der Waals forces create weak attractions between an ion and a solid particle surface. It requires a large

surface area to volume ratio to generate enough electrostatic force. The process results in the concentration of elements from aqueous phases to the surfaces of particulate matter (Benes & Steinnes 1995). The reverse process is known as desorption.

2.3.4 Occlusion within the solid phase

Occlusion of an element within the solid phase is a form of coprecipitation. The element is held within an inert lattice and irregular distribution within the lattice depend on the rates and conditions of precipitation (Benes & Steinnes 1995).

2.4 Chemical Controls

2.4.1 Phase Transitions

Chemical adsorption involves the concentration of an element (orginally in aqueous phase) on the surface of a solid particle. Chemisorption occurs when a chemical bond forms between a trace element and a site on a solid surface. Electrostatic adsorption occurs when coulomb forces attract ions or colloid particles to an oppositely charged site (Benes & Steinnes 1995). Desorbtion involves the release of the chemically or electrostatically held elements.

Movement to chemical equilibrium facilitates adsorption processes and the amount of an element adsorped depends on free ion concentrations (Hince 1993). Adsorption primarily depends on pH conditions because pH determines whether exchanges are anionic or cationic (low or high pH exchanges respectively; Hince 1993). Soluble complexing ligands tend to form non-adsorbable complexes in the aqueous phase, although Benes and Steinnes (1995) have also noted some opposite effects.

Sorption coefficients are used to describe the distribution of an element between solid phases and solution (Smith *et al* 1994), e.g.

$$K_d = C_{(solid)} / C_{(solution)} \quad (1)$$

Where;

K_d = sorption coefficient

$C_{(solid)}$ = concentration of element on solid surface

$C_{(solution)}$ = concentration of ion in solution

Kd values are only applicable if aquatic conditions (pH, Eh, temperature) are measured when calculations are made and only applies to steady state conditions (Smith *et al* 1994). Domenico & Schwartz (1998) state that metal sorption using K_d is too simplistic for describing metal to mineral surface interactions. They describe K_d as a function of properties of exchanger and solution. Ion values are determined as a function of solution concentrations. Selectivity coefficients are required when aqueous solutions are rich in clay or where solid surface charges alter with changing water chemistry e.g. oxides and hydroxides (Domenico & Schwartz 1998).

Low pH: $XOH + H^+ = XOH^{+2}$ (2)

High pH: $H^+ = H^+ + XO^-$ (3)

Where:

XO- = ionised surface site

XOH = hydroxylated surface

Thus: $M^{2+} + XO^- = XOM^+$ (4)

Where:

M^{2+} = metal ion

XO^- = ionised surface site

XOM = concentration of metal on surface

Precipitation and co-precipitation are responsible or partially (via adsorption) responsible for determining the composition of natural waters. Major elements precipitate when their solubility product is exceeded (Hince 1993). The pH, redox state, available mineral phases, and aqueous species concentrations control precipitation reactions. Commonly trace elements are incorporated within the precipitants lattice. It is uncommon for trace elements to precipitate but in some conditions a sparingly soluble trace element will precipitate to colloidal size (Benes & Steinnes 1995). Co-precipitation occurs when a trace element isomorphously replaces ions of a macrocomponent of the solid. Anomalous mixed crystals form when nonisomorphous concentration takes place (Benes & Steinnes 1995).

2.4.2 Complexation

Complexation involves bonding between metals and ligands, and is an important determinant of trace element phase associations. Diversity complexation processes exist because of the variety of ligands and elements present in natural waters (Benes & Steinnes 1995). Complexation reactions occur rapidly (unlike many redox reactions), thus most natural waters are in complexation equilibrium (Domenico & Schwartz 1998; Hince 1993).

Westall & Stumm (1980) distinguish two types of bonds in aqueous solutions: ion pairs, and coordination complexes. Ion pairs form when metals and ligands retain hydration spheres, thus bonds are primarily held electrostatically via water molecules. Coordination complexes form when electron exchange bonds the metal and ligand together. When certain organic ligands contain multiple coordination-complex forming groups, complexes known as chelates are formed; these chelation complexes are more stable than most other complexes or ion pairs.

Stability constants for a reaction allow calculation of complex strength. Calculations of complex strength are conducted by substituting mass – law equations into mass balance equations (Domenico & Schwartz 1998), e.g:

$$M + xL + yH = MlxHy \quad (5)$$

Thus: $$\beta 1 = [MlxHy] / [M]\,[L]x\,[H]y \quad (6)$$

Where:

L = ligand

M = metal

H = hydrogen ion

$\beta 1$ = stability constant

These equations are related to equilibrium constants for a series of element reactions. When metal concentrations are high enough to effect pH or major element chemistry, the calculations are more complex because many ions react with many ligands (Domenico & Schwartz 1998).

Turner *et al* (1981 cited in Newmann & Jagoe 1994) determined that bond strength depends on cation polarising power and readiness to form covalent bonds. The resultant diagram (Figure 1) shows a complexation pattern where stability constants for hard ligands increase from top to bottom. Hard ligands bind primarily by electrostatic forces and include SO_4^{2-} and F^-. Soft ligands are more likely to form covalent bonds and include Cl^-, HS^-, and S^{2-}, these complexes increase in stability from left to right and slightly increase from top to bottom. Complexes formed by intermediate ligands increase diagonally across the diagram from top left to bottom right, this includes OH^- and CO_3^{2-} (Newmann & Jagoe 1994).

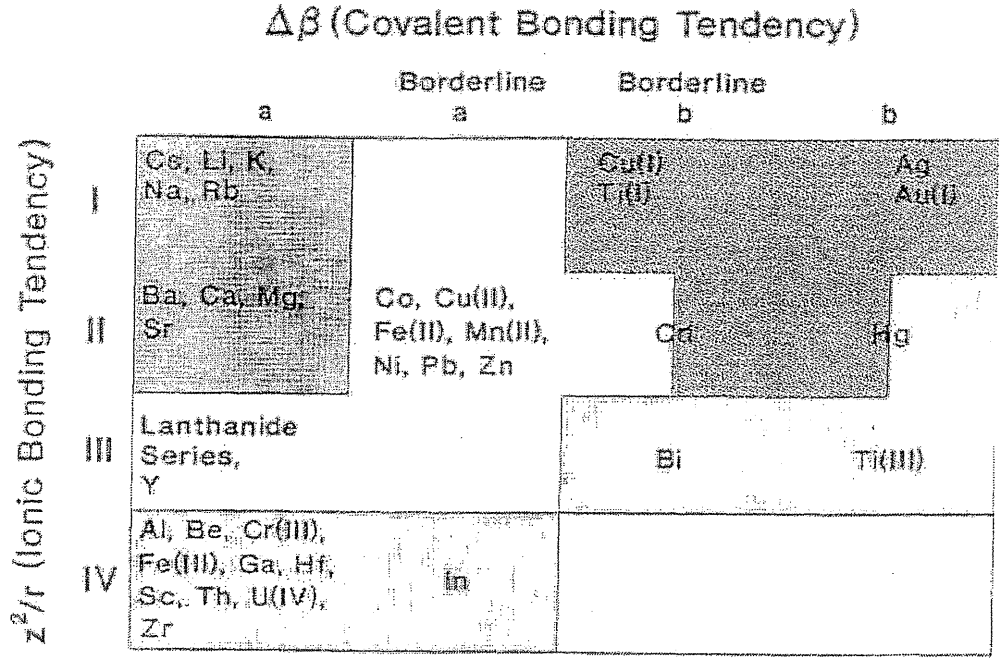

Figure1. Complexation Fields for Ligand Metal Complexes (from Newman & Jagoe 1994)

2.4.3 *pH*

pH is one of the most dominant factors effecting element mobility in natural waters. The acidity of porewater and sediments is often determined by redoxreactions (Newman & Jagoe 1994). The most common of these reactions include (Domenico & Schwartz 1998):

$$FeS + 9/4\ O_2 + 3/2\ H_2O = FeOOH + 2\ SO^{2-}{}_4 + 4H^+ \qquad (7)$$

The above reaction illustrates how the release of H^+ ions increases porewater pH. The mobility of elements is affected by acidification. Hong *et al* (1995) suggest that the mobility of Mn, Zn, Cd, Co and Ni increases in acidic conditions, while neutral to alkaline conditions increase the solubility of S, As, Se, Cr and Mo.

2.4.4 Redox

Natural waters and sediments move towards redox equilibrium, but redox reactions are slow (Hince 1993). Relatively rapid changes to redox conditions prevent attainment of equilibrium. Redox potential and pH are interlinked, with both affecting the mobility and form of elements. Oxidation reactions can increase the acidity of free- and pore-waters by producing hydrogen ions (Hong *et al* 1994).

Oxidation state determines potential chemical reactions and bioavailability. Redox potential tends to depend on the depth of sediment. Deeply buried compounds of manganese or iron are in reducing conditions, thus the stability of adsorbed elements is lowered. Such changes cause remobilisation of free ions, thus reduced porewaters are rich in free ions, although occasionally sulphide complexation occurs. Organic chelators release ions (Hince 1993). Daum & Newland (1982) suggest organic matter inhibits the kinetics of Fe^{2+} oxidation and alters expected oxidation states. Hong *et al* (1995) suggest that when oxidising conditions predominate "chalcophilic" metals such as Hg, Zn, Pb, Cu, and Cd become more mobile, while in reducing conditions Mn and Fe are more mobile.

2.4.5 *Reaction Kinetics*

The rate at which chemical reactions occur within fresh water and sediment determines, to some extent, the rate of transport of elements and energy in and out of the aquatic system. Residence of specific elements may depend entirely on hydraulic movement or is determined by reaction rates. Reactions that occur faster than hydraulic transport can be described using thermodynamic equilibrium theory (Westall & Stumm 1980), while reactions occurring at rates slower than transport rates require kinetic descriptions (Domenico & Schwartz 1998).

2.4.6 Compound Solubility

Free ion concentrations primarily depend on solution equilibria (Daum & Newland 1982). Important environmental influences on solubility include pH, complexing agents, salt concentrations, redox conditions and decomposition of

organic matter (Hong *et al* 1995). Increased temperatures can cause increased dissolution. The reverse situation applies to some compounds (e.g. $CaCO_3$ or $CaSO_4$), where increased temperatures result in lower solubilities. Initially formed solid phases are metastable (Westall & Stumm 1980).

2.4.7 Thermodynamics:

Thermodynamics determine the overall energetics of a chemical system. Concepts of reaction thermodynamics are used to estimate equilibrium which occurs when free energy is at a minimum (Domenico & Schwartz 1998). Equilibrium thermodynamics can be used to theoreticise about approximate chemical speciation (Newman & Jagoe 1994).

2.5 Methylation:

In metalliferous sediments, methylation can allow the formation of organo-metal compounds, i.e. methyl derivatives $(CH_3)_nM$ and their salts $(CH_3)_{n-z}MX_z$. Methylation occurs in any conditions but is more common in reducing environments. Methylmercury is most commonly formed at pH 0-4 (Jackson 1991).

Abiotic methylation of mercury (Fergusson 1991) ;

$$CH_3CoB_{12} + Hg^{2+} \rightarrow H_2OCoB_{12}+ + CH_3Hg^{+} \qquad (8)$$

Hg, As, Se, Ge and Te are most commonly affected possibly followed by Pb, Sn, Tl, In, Sb, Bi and Cd (Borg 1995; Fergusson 1990). Methyl mercury (reaction 1) is known to be the most freely bioavailable, toxic and bioaccumulated form of mecury (Jackson 1991). Methylation of other elements does not always increase toxicity, for example, arsenite becomes the less toxic methylarsonic acid and dimethylarsenic acid (Borg 1995).

2.5 Summary

Physical and chemical conditions control the bioavailability of elements in natural waters. Biogeochemical processes control physico-chemical and geochemical phases. Element bioavailability is constantly altered and adjusted by environmental conditions, which maintains biogeochemical cycling.

Partitioning of elements between water, sediments and porewater controls organism exposure to toxins. Organism behaviour is important in determining which phases are encountered, and a feedback mechanism exists because biotic behaviour partially controls partitioning. The internal physiology of an organism will also affect partitioning, but only after uptake, therefore external environmental conditions are the first control on element bioavailability. The bioavailability of each phase depends on species mobility and complex strength.

Chemical and physical conditions determine the strength of complexes and affect element mobility. Each phase has different potential to release ions and requires different conditions for element uptake and release. Therefore physical and chemical influences greatly control the potential for toxins to be taken up and absorbed by organisms.

Chapter 3

Bioavailability

3.1 Introduction

Geochemical bioavailability refers to the availability of an element to organism uptake (Newman & Jagoe 1994). Bioavailability is calculated from the amount of an active toxin present in a circulatory system compared with the amount present within sediments, porewater or the water column (Hrudrey 1996; Sijm et al. 2000). The pharmacological bioavailability of a substance is determined from absolute or relative bioavailability. Absolute bioavailability is the amount of an element reaching the circulatory system. Relative bioavailability is calculated from: the extent of absorption of a number of doses of the same element; a number of forms of the same element; or different modes of intake of the same element on the same subject (Hrudrey 1996).

The bioavailability of a toxin depends primarily on its speciation and resultant partitioning. An element that exists in its free ionic form is likely to be associated with sediments, particulate matter or colloids and is generally highly bioavailable. An element complexed with natural organic sediments remains bound within sediments and is less bioavailable (Allard 1995). A number of elements are most bioavailable and toxic when they are methylated. Biological modification of bioavailability occurs via trophic interactions, biochemical or physiological adaptation, microhabitat utilisation, animal size and age and particular species characteristics (Craig 1980; Newman & Jagoe 1994; Wepener 2000).

General opinion holds that metal bioavailability in sediments relates to the association of metals with reactive sulphides, as this controls free aquo-ion concentration in pore water (M^{z+}) (Hince 1993, Hugget *et al* 1998, Lee *et al* 2000, Meyer et al 1994). The bioavailability of most metals in interstitial water relates to the pore water M^{z+} (Campbell & Tessier 1991). Toxin levels in pore water have also

been found to have little correlation with tissue contamination (Hugget *et al* 1998, Lee *et al* 2000). Heavy metal concentrations in organism tissues may be a better indicator of sediment contamination levels (Lee *et al* 2000).

3.2 Toxin Exposure to Aquatic Biota

Controlled laboratory feeding studies indicate metal bioavailability differs up to 1000-fold among different sediment types, therefore it is important to determine element partitioning within sediment before estimating bioavailability (Campbell & Tessier 1991). Because of the partitioning problems it is often easiest to divide aquatic biota into two groups (Campbell & Tessier 1991):

- Type A: Benthic algae & rooted aquatic plants are in very close proximity but do not ingest the sediments.
- Type B: Benthic invertebrates ingest sediments and take in toxins from particulate phases.

Type A organisms aquire toxins from interstitial water and solid phases where metals are bound in equilibrium with the free water. Type B organisms are exposed to the same sediments except they also ingest the sediments, thus absorbing toxins within the gut (Campbell & Tessier 1991). The type of water the organism lives in determines its exposure to element species.

3.3 Fauna

3.3.1 *Introduction*

When discussing the effects of toxins on fauna the complexities of physiology that exist between different species are immense. Differences in physiological processes within an individual organism are also complex. The interaction of substances with the aqueous environment dictates element form and species, while synergism and antagonism effect biotic uptake. Physiological processes effect the toxicity of the substance and its metabolites and internal reactions effect absorption

(Alabaster *et al* 1991). The degree of toxicity of any element in any form depends on the behaviour and physiology of the organism it is effecting (Tornbene *d.u.*).

3.3.2 *Entry*

Contaminant uptake occurs via inhalation, ingestion and absorption (Zakrewski 1991). Organisms can intake toxins in aqueous phases, as sedimentary particles or living prey. Filter feeding invertebrates ingest and filter particles in the water column while deposit feeders ingest nutrients at the sediment surface. Both types of organisms ingest living and inert organic and inorganic particles (Amiard 1991). Fish are also known to ingest significant amounts of sediment whilst feeding (Amiard 1991). Aqueous toxin intake occurs in numerous ways (i.e. diffusion across or adsorption to biological membranes), while sediment or food bound toxins only enter an organism by ingestion.

3.3.3 *Ingestion*:

Predicting the bioavailability of a toxin in sediment requires an understanding of sediment ingestion. Toxin ingestion is a function of feeding behaviour and diet (Lee *et al* 2000). Benthic organisms ingest sediments while feeding; filter feeders are directly contaminated by both the free water and by sediments. Deposit feeders are most likely to ingest toxins from sediments and occasionally from the aqueous phase (pore and free water) (Amiard 1991). Thus environmental factors effect element bioavailability.

Particle selection by an organism involves both size considerations (Campbell & Tessier 1991) and nutrition (*i.e.* organic content) (Amiard 1991). Water turbidity affects the amount of time sediment is held in the digestive system (if too many particles enter a filter feeder, particles bypass digestion and form pseudo-faeces; Amiard 1991). The level of exposure also depends on contaminant concentrations.

3.3.4 *Digestion*

The dissolution of soil-bound elements during digestion increases bioavailability. During digestion the gastric contents travel through a number of organs; geochemical phases most likely to be absorbed are those released and formed in response to digestion (Campbell & Tessier 1991). An acid phase takes place in the stomach (or equivalent) (pH 1-3) and a neutralizing phase follows in the intestines (pH 7-8; Hrudrey *et al* 1996). Digestive juice consists of HCl (hydrochloric acid), while intestinal digestion is often associated with $NaHCO_3$ (sodium carbonate) (Amiard 1991).

An example of the digestion process is as follows; a benthic organism ingests a sedimentary particle. Part of the associated organic matter is digested and any associated toxin is released either freely or bonded to a small molecule (Amiard 1991). Dissolved heavy metal concentrations may be lowered in the small intestine as a result of adsorption with soil and food surfaces or by precipitation (Ruby *et al* 1992). The digestive juices dissociate molecules into small, usually soluble molecules (Amiard 1991). After this the toxin is absorbed through membranes or excreted. Absorbed and concentrated elements are then available to the organism with either beneficial or toxic effects.

The bioavailability of digested heavy metals is controlled by geochemical and biological factors. These include rinding by secondary precipitation products, dissolution kinetics and encapsulation by alteration products and inert matrices (Tornbene *d.u.*). Dissolution within the digestive system is directly related to mineralogy, surface area and particle size distribution (Ruby *et al* 1992). High Fe-hydroxide concentrations reduce toxin bioavailability by chelating metals (Amiard 1991). Soil within the digestive tract is likely to form alteration rinds, inert phases and precipitation products (Ruby *et al* 1992).

3.4 Flora

3.4.1 *Introduction*

Plants consist of two main structural components, the root system and the shoot system (stem and leaves). Uptake of soil through plant roots is the primary mode of element uptake, although minor absorption occurs through leaves (Fergusson 1990). Intake is affected by many factors including; soil conditions (pH, Eh, O2, H2O, temperature and nutrients), competition, plant species, root system, (Fergusson 1990), and the speciation, form, availability and solubility of the element (Friedland 1991).

3.4.2 *Entry*

Uptake of trace metals depends on the element and plant species (Friedland 1991) and element mobility is the most important determinant of bioavailability to plants. Soluble and exchangeable metals are easily available to plants (Keller *et al* 1991). Soil pH and Eh influence the chemistry of soils thus the potential for plants to uptake various elements (Appendix 5; Fergusson 1990).

Toxin concentrations within soil influence the rate of uptake of toxins by a plant. In some situations, the concentration of a heavy element in a plant decreases with a corresponding increase in soil contaminant levels (Fergusson 1990). It has been suggested this is due to limitations on the quantity of an element a plant can absorb, also, toxicity symptoms can affect plant ability to uptake any element (Fergusson 1990).

The intake of toxins by aquatic plants can occur in high concentrations. Campbell & Tessier (1991) studied prediction of possible uptake and found that some species provide good correlations between free ion concentrations in interstitial waters and metal concentrations in plant roots. They suggested that for plants without a correlation between aqueous ion concentrations and metal levels in roots, foliar intake might be an important absorption mechanism.

3.4.3 *Internal Transport*;

The transport of metal species inside a plant depends on the metal involved (for example. cadmium can be mobile, whereas lead remains fixed in the root system; Fergusson 1990). Element mobility depends on whether the metal exists as free ions or as a complex (e.g. citrate or oxalate). Metal species can enter both the xylem and the phloem (comprising the vascular system; see appendix 6) and the rate of transport will be a function of water relations (Fergusson 1990).

3.4.4 *Bioaccumulation*

Plant species may be regarded as accumulators, indicators or excluders depending on the metal species being discussed (Kebing in Friedland 1991). Accumulators concentrate large amounts of a toxin without suffering toxicity symptoms. Indicators absorb an amount of metal directly related to the amount of that contaminant in the environment. Excluders avoid taking in toxin. At very high concentrations, the exclusion mechanism does not operate resulting in toxicity (Fergusson 1990).

4.5 Equilibrium Partitioning Theory

Geochemical bioavailability is usually determined using equilibrium partioning theory (EPT). The theory suggests that elements sorbed to soil or sediment are in equilibrium with element concentrations in porewater or the water column. The theory relies on an assumption of sorption equilibrium where elements in water and sediment are in a state of thermodynamic equilibrium (Van der Kooij *et al* 1991; Wepener *et al* 2000). Bioaccumulation factors for exposure to elements in various forms are distinguished although equilibrium partitioning does not consider controls on speciation and phase change considerations are limited (Wepener *et al* 2000).

Water –to-organism accumulation is described by the bioconcentration factor (BCF). A biomagnefication factor (BMF) exists for food sources. Biota-to-sediment accumulation factors (BSAF) describe biological concentration of elements from

sediments. Equilibrium of concentration between porewater and sediment is described by the sorption coefficient (K_d), while equilibrium between porewater and organisms is described by the bioconcentration factor (BCF) (Sijm *et al* 2000). The resulting relationship between sediment and organism is described using the biota-to-sediment accumulation factor (BSAF) (Figure 2).

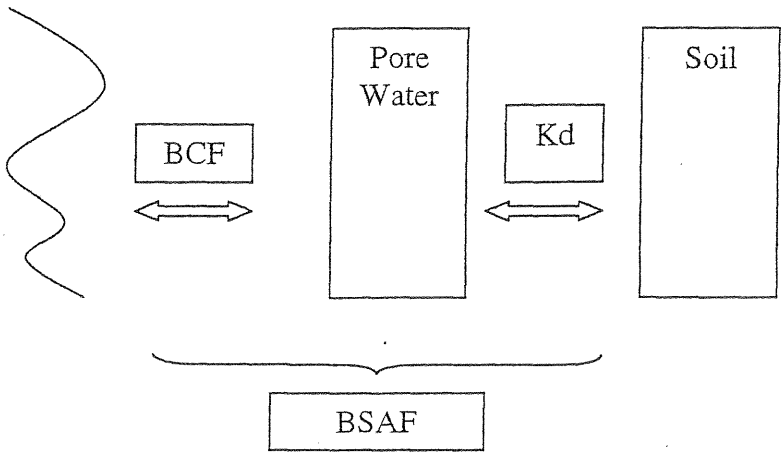

Figure 2. Biota-to-Soil Accumulation Factor (Sijm et al 2000).

Suggestions for deviations from predicted BSAF values include; biotransformation (where the contaminant is transformed), excretion, food chain accumulation, or reduced bioavailability of the element within the sediments (Sijm *et al* 2000). Sijm *et al* (2000) also suggest BSAF theory relies on diffusion processes, whereas active uptake and depuration also effect bioaccumulation and concentration.

A major problem with the application of equilibrium partitioning theory is that speciation relies heavily on environmental variables, thus sorption reactions etc are difficult to predict (Van der Kooij *et al* 1991). Sijm *et al* (2000) suggest a more reliable method of predicting bioavailability is using a biometric approach in conjunction with sediment availability ratios. Biometric methods estimate bioavailability by replicating element partitioning between pore water and organisms;

assuming that only freely dissolved elements are bioavailable. Measurements of element concentration in tissues are indicative of pore water concentration and are known as sediment availability ratios. The two approaches can be combined and used to compare theoretical and actual bioavailability ratios for elements within sediments (Sijm *et al* 2000).

3.6 Summary

Element speciation and resultant partitioning is an important determinant of bioavailability. Mobile species (e.g. free ions) and unstable complexes are more likely to be taken up via ingestion or absorption. They are also more likely to be able to cross biological membranes. This is because internal digestion processes can easily dissolve unstable complexes via pH changes; free ions are able to cross many biological membranes via diffusion and active transport. Feeding behaviour will also affect bioavailability because some ingested particles, in combination with digestion chemistry, will form secondary complexes. This increases the likelihood that the elements will be excreted without being incorporated into organism tissues.

Equilibrium partitioning theory has attempted to model and predict the bioavailability of sediment held species assemblies by comparing theoretical and actual ratios between element concentration in organism tissues and the concentration of an element in sediments. Combinations of biometric replication of porewater-to-organism partitioning and concentration of the element within the organism have been found to provide effective comparisons between theoretical and actual bioavailability.

Chapter 4

Toxicity Predictions

4.1 Introduction

Toxic effects depend on physiological and environmental interactions. Synergistic, antagonistic and additive effects determine some of the toxin impact; the level and duration of exposure are important as well. Bioavailability is fundamental to determining the toxicity of an element; transformational processes change the form or species in which an element occurs internally (Roux *et al* 1996).

Toxic effects can be acute (short-term expression) or chronic (expressed in the long-term). Acute toxicity is determined using an objective, well defined, end-response (usually mortality). Chronic toxicity is harder to define, often chronic toxicity is defined as unacceptable biological effects occurring in an aquatic ecosystem (Roux *et al* 1996). The toxicity of an element is determined by the quantity of species acting on a target site (where active species are delivered) (Hrudrey *et al* 1996).

4.2 Dose-Response Relationships:

Dose-response curves are used to determine the lethality of a compound (Figure3; Zakrewski 1991). LD50s are defined from dose-response experiments, where an LD50 describes the dose required for 50% of testing organisms to be dead within an allocated period (usually 24 or 48 hours). The slopes of semilog dose-response graphs are often used to define safety margins. The slope indicates the increase in toxicity brought about by a change in dose (i.e. a steep slope indicates a greater change to toxicity than a shallow slope) (Zakrewski 1991).

Some trace elements are needed at small dosages and are toxic at high doses; these have a biphasic dose-response relationship (Figure 3). This category includes niacin, selenium, copper and cobalt (Zakrewski 1991). The toxicity effects of a

substance are reversible in some cases. If major damage to organs has not occurred, toxin removal can allow recovery (Zakrewski 1991).

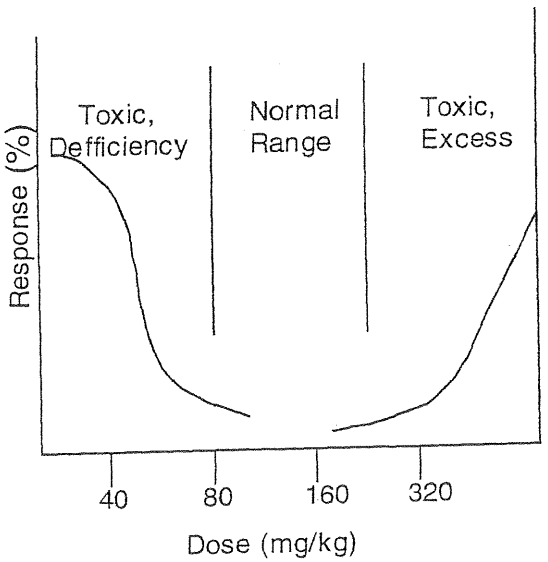

Figure 3. Biphasic Dose-Response Curve of an Element Required for Normal Functioning of an Organism (Zakrewski 1991).

4.2 Synergism and Antagonism

4.2.1 *Introduction*

Assessment of element toxicity is difficult for pure, single substances and very complex for blends of compounds (Johnston 1991). Addition of toxicant effects can lead to effects being greater or less than expected (Alabaster 1987; Fergusson 1990; Roux *et al* 1996). Mechanistic similarities between elements can cause the uptake of one element to positively or negatively affect the rate of uptake of another element.

Synergistic and antagonistic effects depend on(Alabaster 1987) :

- type of toxin and its proportional contribution of toxicity to the mix,
- water characteristics, and effects on toxin speciation,
- organism species and stage in life cycle,
- the type of response, and
- the amount of responses

4.2.2 *Predicting Element Interactions*

Determining the joint effects of two or more toxicants requires an estimation of how much of a response is due to additive effects, and how much is due to the range of concentrations and proportions producing the effects. Plackett & Hewlett (1952 from Alabaster 1987) defined four types of joint actions on a biological response (Table 1).

	Similar Joint Action	Dissimilar Joint Action
Interaction Absent	*Simple similar action*	*Independent action*
Interaction Present	*Complex similar action*	*Dependent action*

Table 1; Joint Actions and Biological Response (Alabaster 1987) .

A joint action is similar if the site of primary action for two chemicals is the same; otherwise the action is dissimilar. A joint action is interactive if a toxin influences the action of the other. Such tables cannot be used if pairings fall into different classes of joint action, or if other joint actions are possible between different pairs. Mixes of two or more chemicals are described using more complex models (Alabaster 1987).

If an organism is exposed to two independently acting toxins, independent or combined toxin action will kill. Anderson and Weber (1975a from Alabaster 1987) described a 'concentration – addition' model that evaluates the joint effects of toxic mixes. An additive joint effect occurs when the action of each toxin is qualitatively identical, even if the effect is produced by different concentrations of each toxin. When each chemical acts on a different physiological or biochemical system and contributes to a common response, a 'response-addition' or 'independent-joint action' model can be used (Alabaster 1987).

Antagonistic interactions are the more common than synergism (Table 2). Where an element has both synergistic and antagonistic effects, the net effects depend on biochemical processes (Fergusson 1990).

Element	Antagonistic to;	Synergistic to;
Cadmium	Ca, P, K, Zn, Al, Se, Mn	Pb, Mn, Fe, Ni, Cu*, Zn*, Fe, Ni, Mg, Cu, Cd
Lead	Ca, P, S, Zn	Cd
Arsenic	P, Mn, Zn, Mn*	
Mercury	P, K	
Selenium	P, S, Mn, Cu, Zn, Cd, W*, Hg	V
Thallium	K	
Copper	Zn	
Zinc	Hg	

* Outside plant and close to roots

Table 2; Common Interactions of Selected Toxins on Flora

(From Fergusson 1990, Alabaster 1987, Jackson 1991)

4.4 Summary

Predicting the toxicity of an element requires knowledge of individual acute and chronic toxic effects. Only relative relationships between dose and response can be determined. Combined element interactions result in synergism, antagonism and adition of toxicity effects. Predicting interactive effects has been attempted using models that take into account interactions and the similarities of actions. Organism biochemistry is the ultimate determinant of toxin effects, therefore any toxicity predictions need to be applied on an individual basis because the characteristics of the organism greatly effect the impacts of a toxin.

Chapter 5

Conclusions

The bioavailability and toxicity of elements in natural aquatic environments depend on chemical physical and biological interactions. The chemical and physical attributes of an aquatic environment determine how and where elements occur. This movement of elements between geochemical phases effects the mobility of elements via bond strength as well as via rates and magnitudes of response to change in environmental conditions.

The partitioning of an element between pore water, sediments and the water column controls the exposure of organisms to toxins. Equilibrium partitioning theory attempts to compare actual bioconcentrations with element bioavailability within sediments. The partitioning is partially effected by the behaviour of organisms because this effects other physico-chemical conditions. Therefore a feedback mechanism exists between geochemical phases and biological activity.

Internal physiology determines the rate and magnitude of absorption of elements across biological membranes. Digestion chemistry can alter the geochemical phases that were originally ingested and dissolution, precipitation, adsorption etc. processes control the absorption and accumulation of elements.

References

Alabaster, J.S. 1991. Water Quality Criteria for European Freshwater Fish in Rose, J. (ed.) 1991. *Water and the Environment.* Gordon and Breach Science Publishers, U.S.A. pp.117-207.

Allard, B. 1995. Ground Water in: Salbu, B. & Steinnes, E. 1995. *Trace Elements in Natural Waters.* CRC Press. U.S.A. pp. 151-176.

Amiard, J.C. 1991. Bioavailability of Sediment Bound Metals for Benthic Aquatic Organisms in Vernet, J.P. (ed.) 1991. *Heavy Metals in the Environment; Trace Metals in the Environment 1.* Elsevier, Switzterland. pp.183-203.

ANZECC, Australian and New Zealand Environment and Conservation Council 1992. *Australian Water Quality Guidelines for Fresh and Marine Waters. National Water Quality Management Strategy.* Australia, pp. 1-1 – 4-19.

Benet, B. & Steinnes, E. 1995. Trace Chemistry Processes in: Salbu, B. & Steinnes, E. 1995. *Trace Elements in Natural Waters.* CRC Press. U.S.A. pp. 21-40.

Bindra, K.S. & Hall, K.J. (date unknown). *Geochemical Partitioning of Trace metals in Sediments and Factors Affecting Bioaccumulation in Benthic Organisms.* Unpublished Report for the National Research Council of Canada. 43 pages.

Borg, H. 1995. Trace Elements in Lakes in Salbu, B & Steinnes, E. (eds.) 1995. *Trace Elements in Natural Waters.* CRC Press, Norway, pp. 177-201.

Campbell, P.G.C. & Tessier, A. 1991. Biological Availability of Metals in Sediments: Analytical Approaches, in Vernet, J.P. (ed.) 1991. *Heavy Metals in the Environment: Trace Metals in the Environment 1.* Elsevier, Amsterdam, pp.161-173.

Campbell, P.G.C. & Stokes, P.M. 1985. *Acidification and Toxicity of Metals to Aquatic Biota.* Canadian Journal of Fisheries and Aquatic Science. 42, pp.2034-2049.

Craig, P.J. 1980. Metal Cycles and Biological Methylation, in Hutzinger, O. 1980 (ed.). *The Handbook of Environmental Chemistry, Volume 1, Part A; The Natural Environment and Biogeochemical Cycles.* Springer-Verlag, Berlin, pp.169-221.

Daum, K.A. & Newland, L.W. 1982. Complexing Effects on Behaviour of Some Metals in: Hutzinger, O. (ed) 1982. *The Handbook of Environmental Chemistry. Volume 2, Part B. Reactions and Processes.* Springer-Verlag, Amsterdam. pp. 129-140.

Dellar, M 1998. Acid Mine Drainage in the Zeehan Mineral District Unpublished honours thesis. School of Earth Science, University of Tasmania. 117 pages.

Deforest, D.K. Brix, K.V. & Adams, W.J. 1999. *Critical Review of Proposed Residue-Based Selenium Toxicity Thresholds for Freshwater Fish.* Human and Ecological Risk Assessment. 5(6) pp.1187-1228.

Domenica, P.A. & Schwartz, F.W. 1998. *Physical and Chemical Hydrogeology.* John Wiley and Sons Inc. U.S.A. 494 pages.

Elinder, C.G. Gehardsson, L. & Oberdoester, G. 1988. Biological Monitoring of Toxic Metals: Overview, in Clarkson, T.W. Nordberg, G.F. & Sager, P.R. (eds.) 1988. *Biological Monitoring of Toxic Metals.* Plenum Press, New York, pp.1-71.

Elsokkary, I.H. 1991. Trace metals in Sediments and Water: A Case Study from Egypt, in Vernet, J.P. (ed.) 1991. *Heavy Metals in the Environment: Trace Metals in the Environment 2.* Elsevier, Amsterdam, pp.355-379.

Fergusson, J.E. 1990. *The Heavy Elements: Chemistry, Environmental Impact and Health Effects.* Pergamon Press, England, 614 pages.

Friedland, A.J. 1991. Trace Metal Dynamics in Forest Soil Organic Horizons in the Eastern and Central United States of America, in Vernet, J.P. (ed.) 1991. *Heavy Metals in the Environment; Trace metals in the Environment 1.* Elsevier, Amsterdam, pp.287-297.

Gupta, A.K. 1999. *Short-term Toxicity of Copper to Channa punctus (Bloch.).* Journal of Environmental Biology, 20(3) pp.227-229.

Gupta, S.K. 1991. Mobilisable Metal in Contaminated Soils and its Ecological Significance, in Vernet, J.P. (ed) 1991. *Heavy Metals in the Environment; Trace Metals in the Environment 2.* Elsevier, Amsterdam. pp. 299-310.

Hince, G.J. 1993. *Heavy Metal Speciation and Transport in the King River.* Unpublished Honours Thesis. Chemistry Department, University of Tasmania at Hobart. 75 Pages.

Hong, J. Forstner, U. & Calmano, W. 1994. Effects of Redox Processes on Acid Producing Potential and Metal Mobility in Sediments in: Hamelink, J.L. Landrum, P.F. Bergman, H.L. & Benson, W.H. (eds.) 1994 *Bioavailability: Physical, Chemical and Biological Interactions.* Lewis Publishers, U.S.A. pp. 155-170

Hong, J. Calamano, W. & Forstner. 1995. Interstitial Waters in: Salbu, B. & Steinnes, E. (eds.) 1995. *Trace Elements in Natural Waters.* CRC Press, U.S.A. pp.117-150.

Hrudey, S.E., Chen, W. & Rousseaux, C.G. 1996. *Bioavailability in Environmental Risk Assessment.* Lewis Publishers, U.S.A. 1294 pages.

Hugget, D.B. Gillespie, W.B. (jr.) & Rodgers, J.H. (jr.) 1999. *Copper Bioavailability in Steilacoom Lake Sediments.* Archives of Environmental Contamination and Toxicology. 36. pp. 120-123.

Jackson, T.A. 1991. Effects of Heavy Metals and Selenium on Mercury Methylation and other Microbial Activities in Fresh Water Sediments, in Rose, J. (ed.) 1991 *Water and the Environment.* Gordon & Breach Science Publishers, U.S.A. pp.191-217.

Johnston, R. 1991. Aquatic Chemistry and the Human Environment, in Rose, J. (ed.) 1991. *Water and the Environment.* Gordon and Breach Science Publishers, U.S.A. pp.71-115.

Kaiser, K.L.E. 1980. *Correlation and Prediction of Metal Toxicity to Aquatic Biota.* Canadian Journal of Fisheries and Aquatic Science, 37, pp.211-218.

Keller, C. Domergue, F.L. & Vedy, J-C. 1991. Biogeochemistry of Copper and Cadmium in unpolluted Forests, in Vernet, J.P. (ed.) 1991. *Heavy Metals in the Environment: Trace Metals in the Environment 1.* Elsevier, Amsterdam, pp.247-271.

Lee, B-G, Griscom, S.B. Lee, J-S. Heesun, J.C. Chul-Hwan, K. Luoma, S.N. & Fisher, N.S. 2000. *Influences of Dietary Uptake and Reactive Sulphides on Metal Bioavailability from Aquatic Sediments.* Science, Jan. 287, pp.283-285.

Lemly, A.D. 1999. *Selenium Impacts on Fish: An Insidious Time Bomb.* Human and Ecological Risk Assessment, 5(6) pp.1139-1151.

Lowson, R.T. 1989. Measurement of Pollutant Transport in Soils, in Australian Mining Industry Council, *Workshop Proceedings, Volume 1.* Ballarat, pp.53-67.

Luckey, 1975. *Environmental Quality and Safety: Supplement Volume 1.* George Thieme Publishers, Stuttgart, pp.1-7.

Mason, R.P. Laporte, J-M. & Andres, S. 2000. *Factors Controlling the Bioaccumulation of Mercury, Methylmercury, Arsenic, Selenium and Cadmium by Freshwater Invertebrates and Fish.* Archives of Environmental Contamination and Toxicology. Springer-Verlag, New York.

Mayer, F.L. (jr.), Marking, L.L. Bills, T.D. & Howe, G.E. 1994. Physicochemical Factors affecting Toxicity in Fresh-Water; Hardness, pH and Temperature in: Hamelink, J.L. Landrum, P.F. Bergman, H.L. & Benson, W.H. (eds.) 1994. *Bioavailability: Physical, Chemical and Biological Interactions.* Lewis Publishers, U.S.A. pp.5-22.

Meyer, J.S. Davison, W.D. Sudby, B. Oris, J.T. Lauren, P.J. Forstner, U. Hong, J & Grosby, D.G. 1994 The Effects of Variable Redox Potentials, pH and Light on Bioavailability in Dynamic Water and Sediment Environments in: Hamelink, J.L. Landrum, P.F. Bergman, H.L. & Benson, W.H. (eds.) 1994. *Bioavailability: Physical, Chemical and Biological Interactions.* Lewis Publishers, U.S.A. pp.155-170.

Newman, M.C. & Jagoe, C.H. 1994. Ligands and Bioavailability of Metals in Aquatic Environments in: Hamelink, J.L. Landrum, P.F. Bergman, H.L. & Benson, W.H. (eds.) 1994. *Bioavailability: Physical, Chemical and Biological Interactions.* Lewis Publishers, U.S.A. pp.39-62.

Oberdoerster & Cherian 1988. Manganese, in Clarkson, T.W. Friberg, L. Norberg, G.F. & Sager, P.R. (eds.) 1988. *Biological Monitoring of Toxic Metals.* Plenum Press, New York, pp. 283-301.

Plenet, S. 1999. *Metal Accumulation in an Epigean and a Hypogean Freshwater Amphipod: Considerations for Water Quality Assessment.* Water Environment Research. 71(7) pp.1298-1309.

Raven,P.H. Evert, R.F. & Eichorn, S.E. 1999. Biology of Plants. 6th ed. W.H. Freeman and Company Worth Publishers, New York, 944 pages.

Ross, H.B. & Vermette, S.J. 1995. Precipitation in: Salbu, B. & Steinnes, E. (eds.) 1995. *Trace Elements in Natural Waters.* CRC Press. U.S.A. pp. 99-116.

Roux, D.J. Jooste, S.H.J. & MacKay, H.M. 1996. *Substance Specific Quality Criteria for the Protection of South African Freshwater Ecosystems: Methods for Derivation and Initial Results for some Inorganic Toxic Substances.* South African Journal of Science. 92. pp.198-206.

Ruby, M.V. Davis, A. Houston-Kempton, J. Drexler, J.W. & Bergstrom, P.D. 1992. *Lead Bioavailability: Dissolution Kinetics under Simulated Gastric Conditions.* Environmental Science and Technology. 26(6). pp.1242-1248.

Sijm, D. Kraaij, R & Belfroid, A. 2000. *Bioavailability in Soils or Sediments: Exposure of Different Organisms and Approaches to Study It.* Environmental Pollution. 108. pp.113-119.

Smith, K.S. Plumlee, G.S. & Ficklin, W.H. 1994. *Predicting Water Contamination from Metal Mines and Mining Wastes.* Workshop 2. International Land Reclamation and Mine Drainage Conference & the Third International Confernce on the Abatement of Acidic Drainage. U.S. Geological Survey. 112 pages.

Tornabene, T.G. Gale, N.L. Koeppe, D.E. Zimdahl, R.L. & Forbes, R.M. (date unknown). Lead Effects on Microorganisms, Plants and Animals, in Boggess, W.R.

(ed.) (date unknown). *Lead in the Environment.* Report for the National Science Foundation, pp.181-193.

Van der Kooij, L.A. Van der Meent, D. Van Leeuwen, C.J. & Bruggerman, W.A. 1991. *Deriving Quality Criteria for Water and Sediments from the Results of Aquatic Toxicicty Tests and Product Standards: Application of the Equilibrium Partitioning Method.* Water Resources, 25(6), pp. 697-705.

Wepener, V. van Vuren, J.H.J. & du Preez, H.H. 2000. *Application of the Equilibrium Partitioning Method to Derive Copper and Zinc Quality Criteria for Water and Sediment: A South African Perspective.* Water S.A. 26(1), pp.97-104.

Westall, J. & Stumm, W. 1980. The Hydrosphere in : Hutzinger, O. (ed.) 1980. *The Handbook of Environmental Chemistry. Volume 1, Part A. The Natural Environment and the Biogeochemical Cycles.* Springer-Verlag, Amsterdam. pp.17-50.

Zakrewski, S.F. 1991. *Principles of Environmental Toxicology.* ACS Professional Reference Book. Washington D.C. 270 pages.

Zimdahl, R.L. & Hasset, J.J. (date unknown). Lead in Soil, in Beggess, W.R. (ed.) (date unknown). *Lead in the Environment.* Report for the National Science Foundation. pp.93-98.

APPENDICES

APPENDIX 1: Glossary

- Bioavailability: describes the extent and rate of absorption of a toxin entering the circulatory system.

- Toxicity: refers to the adverse action of a toxin on an organism. A "trace element" is required by an organism for normal health, though it is only necessary in minute amounts.

- Speciation: concerns variation in element phases.

- Partitioning: describes the distribution of an element between sediments, pore water and the overlying water column.

APPENDIX 2: Species in Water with Respect to Size

Species	Lead & Cadmium (as examples)	Size
Free metal ion	Pb^{2+}, Cd^{2+}	Soluble (<0.0001μm) True solution
Ion pairs, Metal chelates	$PbCO_3$ $PbHCO_3^+$ PbNTA $PbCl^+$ $CdCO_3$ $CdCl^+$ $CdCl_2$	Soluble (<0.0001μm) True solution
Organic complexes	Pb, Cd-fulvic acid complexes	Soluble (>0.0001μm & <0.01μm) True solution
Metal species attatched to high molecular weight organics	Pb, Cd-humic acid complexes	Colloidal (≈0.01μm)
Metal species sorped to colloids	Pb, Cd-$Fe(OH)_3$ Pb, Cd-MnO_2	Colloidal (>0.01μm & <0.1μm)
Metal species in organic material	Pb, Cd-amino acids Pb, Cd-organic acids	Particulate (>0.1μm & <1μm) Solids
Inorganic solids, sorption, precipitation	Pb, Cd-clays $PbCO_{3(s)}$ $CdCO_{3(s)}$ $Pb_3(OH)_2^-$ $(CO_3)_2$ CdS	Particulate (>1μm) Solids

(Altered from Fergusson 1990 p.289)

APPENDIX 3: Speciation of Selected Elements and Resultant Bioavailability and Toxicity.

Aluminium

If waters are either highly acidic or alkaline, or if abundant complexing ligands exist, dissolved Al can occur in elevated concentrations (Borg 1995). Aluminium has a similar mobility in soils, acidic conditions cause complexation of Al with H_2O, OH^-, F^-, SO_4^{2-}, HCO_3^- and positively charged OH^-complexes (Borg 1995).

Aluminium is insoluble in most natural waters, due to their near neutral pH. Higher temperatures can increase the rate of precipitaion of $AlOH_3$ and promote formation of more complex aluminium minerals and more advanced polymerization (Borg 1995).

Aluminium generally has a low toxicity, Al^{3+} is poorly absorbed by biota because colloidal $Al(OH)_3$ is insoluble (Lockey 1975). Al is more toxic when it occurs as a free ion than when it occurs adsorbed onto organics or with tertiary phosphates (Lockey 1975).

Arsenic

Arsenic can occur in sediments as minerals such as FeAsS, FeAsS and As_2S_3, the exact mineralogy depends on local environment and geology (Fergusson 1991). Aqueous arsenic can be sorbed by hydrous iron oxides during oxidation of iron while organic associations are not common (Fergusson 1991). A posistive correlation between elevated iron and arsenic levels exists. Arsenic is present in elevated levels within Fe/Mn precipitants (Fergusson 1991).

Arsenic occurs in four oxidation states, +5, +3, 0 and –3. Oxygenated environments contain As^{5+}, as arsenate ($HAsO_4^{2-}$). Mildly reducing conditions and low redox potentials cause formation of As^{3+}, which is the most mobile arsenic species (Fergusson 1990).

An increase in the oxidizing potential of the environment increases the uptake of the element. As^{3+} is generally the most toxic of the arsenic species (Kaiser 1980). Apte (1989 cited in Dellar 1998) found relative arsenic toxicities to decrease in the order: arsines (R_3As; where R is Cl, H or a metal), As^{3+} (arsenites; $H_nAsO_3^{n3}$), As^{5+}; arsenitates; $H_nAsO_4^{n-3}$), Mma ($MeAsO(OH)_2$; M is a metal), DMA ($Me_2AsOCOH$; Me is a metal), arsenocholine, arsenobetaine and arsenosugars. Arsenic in plants is quite restricted; concentrations are generally higher in roots than in other tissues (Fergusson 1990).

Cadmium

C

admium is commonly sorbed with organics in oxidized sediments (Keller 1991). Colloidal absorption is not common (Fergusson 1991). Reducing conditions cause Cadmium to be less available by tending to adsorb onto carbonates, sulphides or absorption within organics. Alkaline conditions will also limit Cadmium mobility.

C

admium has similar speciation patterns to lead, except that cadmium can occur as a bare ion (Cd^{2+}) exists to pH values of 7-8 (Keller et al 1991). Cadmium carbonates are scarce (to 21%) in oxidizing aquatic environments. Soluble cadmium occurs in reducing conditions as $CdHS^-$. Organic complexes only form if the organic content of the water is high (Fergusson 1990).

A

n increase in the oxidizing potential of the environment increases the uptake cadmium by fauna. Cadmium appears to have a high inherent toxicity, particularly when it occurs as Cd^{2+} (Campbell & Stokes 1985). In plants cadmium appears to be held on cell walls through interactions with sulphur (Fergusson 1990). Cadmium is most commonly found as Cd^{2+}. No deposits of compounds have been found in plants (Tornbene *et al d.u.*).

Lead

Lead speciation within sediments is affected by redox conditions. Galena can form in preference tp lead oxides or carbonates under reducing conditions where H_2S is available (Fergusson 1991). $Pb(OH)_2$ may precipitate at pH <6 when H_2S concentrations are low (Santillan-Medrano & Jurinak 1975 in Zimdahl & Hasset *d.u.*). $PbCO_3$ can occur in oxidized sediments under neutral to alkaline pH conditions (Fergusson 1991). Lead orthophosphate, lead hydroxypyromorphite and tetraplumbite phosphate are also possible above pH 6 (Zimdahl & Hasset *d.u.*).

Lead is more strongly sorbed by Fe/Mn oxides than organic material, and iron- and Manganese oxides can compete for lead (Fergusson 1991). Sorption processes are rapid (Zimdahl & Hasset *d.u.*) and depend on pH. Lead uptake by clays is less dependant on pH if the clay is saturated with cations (Fergusson 1991).

In water lead is most commonly found as $PbCO_{3(aq)}$, $Pb(CO_3)_2^{2-}$, $PbCl^+$, $PbCl_{2(aq)}$, $PbOH^+$, and $Pb(OH)_2$ in fresh waters. Pb^{2+} is only likely to be found in acid conditions or where water has low chloride concentrations (Fergusson 1990).

Lead contamination in organisms is related to how lead occurs in solid phases. Minerals that encapsulate Pb (e.g. SiO_2 , FeS_2) or that precipitate from solution and can absorb lead (e.g. K-jarosite) reduce bioavailability (Ruby *et al* 1992). Lead salts (e.g. $Pb(OAc)_{2)}$ are more bioavailable than $PbSO_4$ (anglesite) because dissolution of $Pb(OAc)_2$ is immediate. Both solid phases are more available than Pb held in soil (Tornabene *et al d.u.*). $PbCl^+$ forms when lead minerals dissolve in the digestive system (Tornabene *et al d.u.*).

Finer lead-rich sediments and increased organic matter will also increase bioavailability (Bindra & Hall *d.u.*). Particle size is thought to affect bioavailability as a result of smaller surface areas and fewer adsorption sites.

Lead generally does not accumulate in vegetation to any large degree (Smith & Siccama 1981 cited in Friedland 1991), but under certain conditions it can be taken up (Tornbene *d.u.*). Lead intake requires a reducing environment because of the insolubility of Pb^{2+} salts that are formed when lead is oxidised (Fergusson 1990). The solubilities of most lead salts increase with decreasing pH. It has been found that lead movement in plants is limited with evidence of lead compounds (e.g. lead pyrophosphate and lead orthophosphate) in cell walls (Craig and Wood 1981 cited in Fergusson 1990).

Mercury

Sediments rapidly sorb mercury ions and metal (Fergusson 1991). Inorganic mercury commonly exists as $Hg(OH)_2$ in normal pH conditions, whereas $HgOH^+$ predominates at lower pH values. Organic complexation depends on the abundance of organic material (Fergusson 1990), with methylated mercury is the most toxic and bioavailable form (Elinder 1988). Humic bonded mercury the main form of Hg in freshwater (Fergusson 1991).

Monovalent mercury is thought to be non-toxic because of the low solubility of its salts, while $Hg^{2+}$is highly toxic because of the ease with which it is methylated (Luckey 1975). Mercury transport in plants also appears to be affected by the plant species it is held within. The translocation of mercury also appears to be greatest when entry occurs via stems or leaves. Similarly to cadmium, formation of Hg-S bonds drastically reduces metal mobility (Fergusson 1990).

Copper

Copper is commonly found in organics and, less commonly, within iron-oxides (Keller 1991). Copper in pore water is usually bound to organics (Keller 1991).

Copper speciation is strongly pH dependent, low pH conditions cause release of abundant Cu^{2+} ions (Luckey 1975).

Copper in reducing conditions has a decreased bioavailability due to sorbtion processes(Campbell & Stokes 1985). Copper can accumulate in living tissues, especially at higher pH conditions. Bindra & Hall *(d.u.)* observed that copper bioavailability increases when copper ions are partitioned into exchangeable or easily reducible phases. Total copper concentrations within sediments were significantly less bioavailable. Cu toxicity is affected by competition between H^+ and Cu^{2+} (Campbell & Stokes 1985). Similar results have been determined for flora; Cu toxicity is higher at higher pH (Campbell & Stokes 1985).

Iron

Fe often occurs within sediments in colloidal humic complexes, and as colloidal hydrous iron-oxides, often associated with organic substances (Borg 1995). Iron is generally found as Fe^{3+} if the water is oxygenated, Fe^{2+} is only stable in acidic and anaerobic environments. Dissolved organic matter influences the oxidation rate of iron and can cause Fe^{2+} to occur in concentrations higher than would otherwise be expected (Borg 1995).

Manganese

Manganese does not occur naturally as a metal; it exists in both anionic and cationic form and occurs in 11 oxidation states (Oberdoerster & Cherian 1988; Elinder *et al* 1988). Divalent cationic salts and hexavalent manganates and permanganates are stable and water-soluble (Luckey 1975). $Mn^{(7)}$ is toxic as $MnCl_2$ and $KMnO_4$, while the most stable form of manganese is MnO2 (Kaiser 1980). Mn is most often found in dissolved forms (partly as Mn^{2+}) in acidic lakes. When water has a higher pH, Mn is more common as colloidal oxyhydroxides (Borg 1995).

$Mn^{(7)}$ is thought to be the most toxic of the Mn species (Kaiser 1980). Salts and oxides of manganese are poorly absorbed due to their poor solubility in the gut.

Selenium

Elemental selenium is non-toxic because it has low solubility. Selenium commonly occurs as compounds of anionic salts such as selenite and selenate (Luckey 1975).

Selenium occurs as Se^{4+} and Se^{6+} species. Se^{4+} can occur as SeO_3^{2-} or $HSeO_3^-$,depending on pH, and is the most common valence state of selenium in fresh waters (Fergusson 1990). Selenium di and tri- oxides dissolve in water to produce selenous and selenic acids (Luckey 1975). A reducing environment causes immobilization of inorganic selenium, while oxidation and biotransformation (plant and invertebrate uptake from sediments) act to increase the bioavailability of selenium (DeForest *et al* 1999).

Plant selenium concentrations are dictated by the state it is within soil. Soluble forms are readily taken up. It can also partially replace sulphur thus forming up to eight organoselenium compounds that have been isolated and identified. Selenium tends to be concentrated in plant roots, active growth points and in seeds (Fergusson 1990).

APPENDIX 4:

Relative Toxicity Estimates

The general assumption of element toxicity is that free metal ions are more toxic than ions bound to large organic molecules. Potential toxicity is also affected by the type and abundance of ligands present (Kaiser 1980), as this determines the form in which an element occurs. The proportion of particulate metal in fresh water decreases with pH because acidity increases the solubility of metal species (Fergusson 1991). The amount of mobile metal in sediments depends on pH, total metals, amount and type of humus and type and content of clay (Gupta 1991).

Response to metal species depends on the organism species and individual characteristics (age, stage in reproductive cycle etc.) Cu has generally been found to be more toxic than Zn (Plenet 1999), while lead is usually less toxic than either Cu or Zn (Tornabene *d.u.*). Shaw (1954 from Kaiser 1980) used principles of co-ordination chemistry to determine that relative toxicity can be predicted as $Mn^{(2+)}<Fe^{(2+)}<Co^{(2+)}<Ni^{(2+)}<Cu^{(2+)}>Zn^{(2+)}$. Relative toxicity values are only relevant to specific species and forms; they usually apply only to certain plant or animal species.

Some generalisations about element toxicity have been made. Kaiser (1980) found ions with higher oxidation numbers have higher potential toxicity, except for Fe ($^{2+)/(3+)}$ and $Mn^{(2+)/(4+)}$ ions. A strong correlation was found for Cr, Mn, Sn, and Se ions with less strong but still significant correlations existing for Pt, Tl, As, Au, and Pb ions. The study found elements in normal oxygenated aquatic environments are more toxic to biota when they occur in less common valent states.

Johnston (1991) suggested toxicity to micro-organisms varies with the strength and stability of covalent metal-ligand bonds. He suggests high strength covalent bonds are more toxic when microbial enzymes are involved. Decreased toxicity occurs when external ligands form the metal bonds. The relative toxicity of

microbial enzyme complexes was found to be Zn<<Cu≈Cd, while relative toxicity of normal metal-ligand bonds was found to be Cu<Zn<Cd (Johnston 1991).

Appendix 5:

Soil Factors that Influence the Availability of Heavy Metals to Plants.

Soil Factor	Change in factor	Effect on Element Availability
Clay Content	Increase	Decrease, due to more binding sites in soil.
Organic Matter	Increase	Decrease, due to more binding sites in soil.
Fe/Mn Oxides	Increase	Decrease, due to more binding sites in soil.
Cation Exchange Capacity (CEC)*	Increase	Decrease, due to more binding sites in soil.
Temperature	Increase	Increase, due to improved kinetics,
Water Stress	Increase	Decrease, due to reduced uptake of water.
Other Elements	Increase	Decrease, due to competition.
Added Phosphate	Increase	Decrease, due to increased vegetation growth.

*CEC is related to the three factors above it.

(Fergusson 1990 p.396)

Appendix 6: The Plant Vascular System.

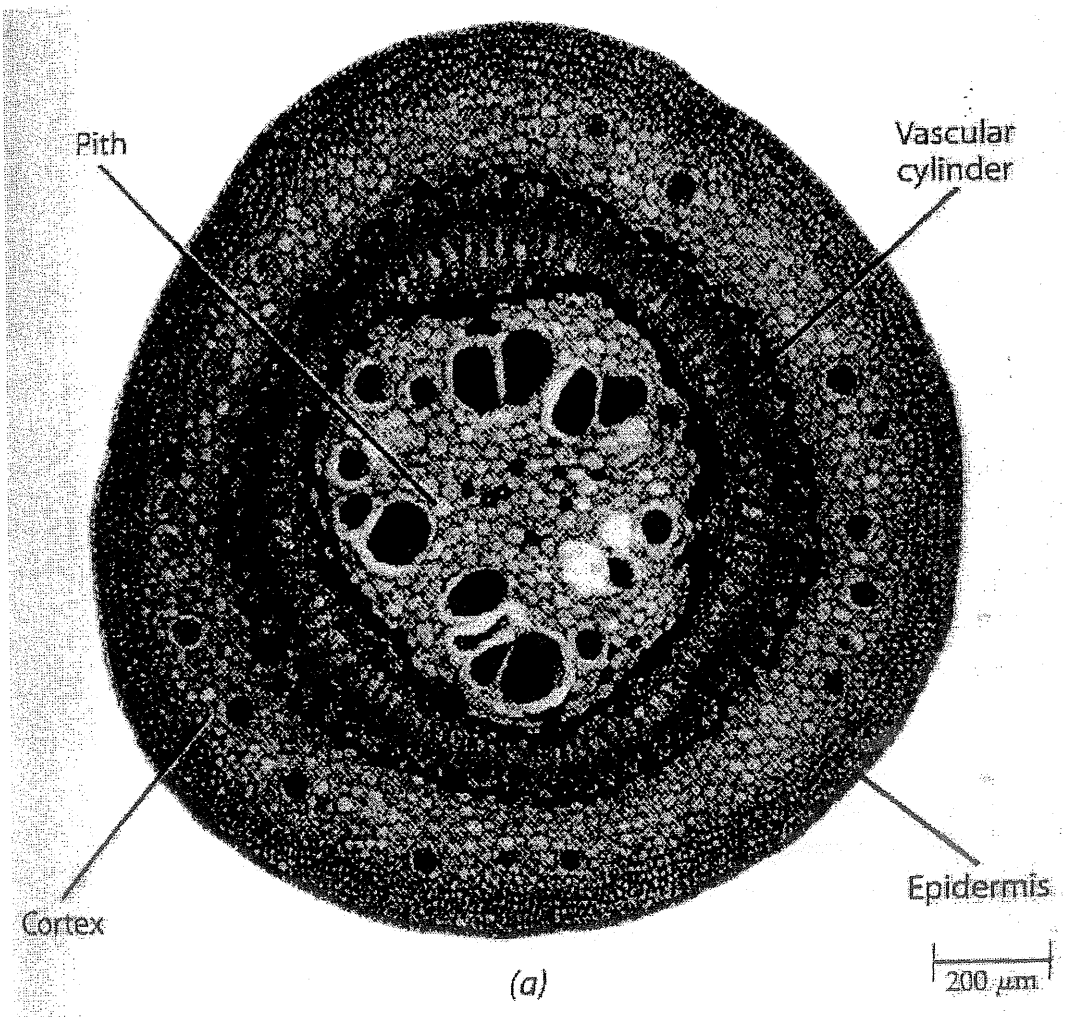

A.
Transverse section through a basswood (*Tilia americana*) stem. Shows where vascular bundles occur in relation to epideris and core (pith). (from Raven *et al* 1999)

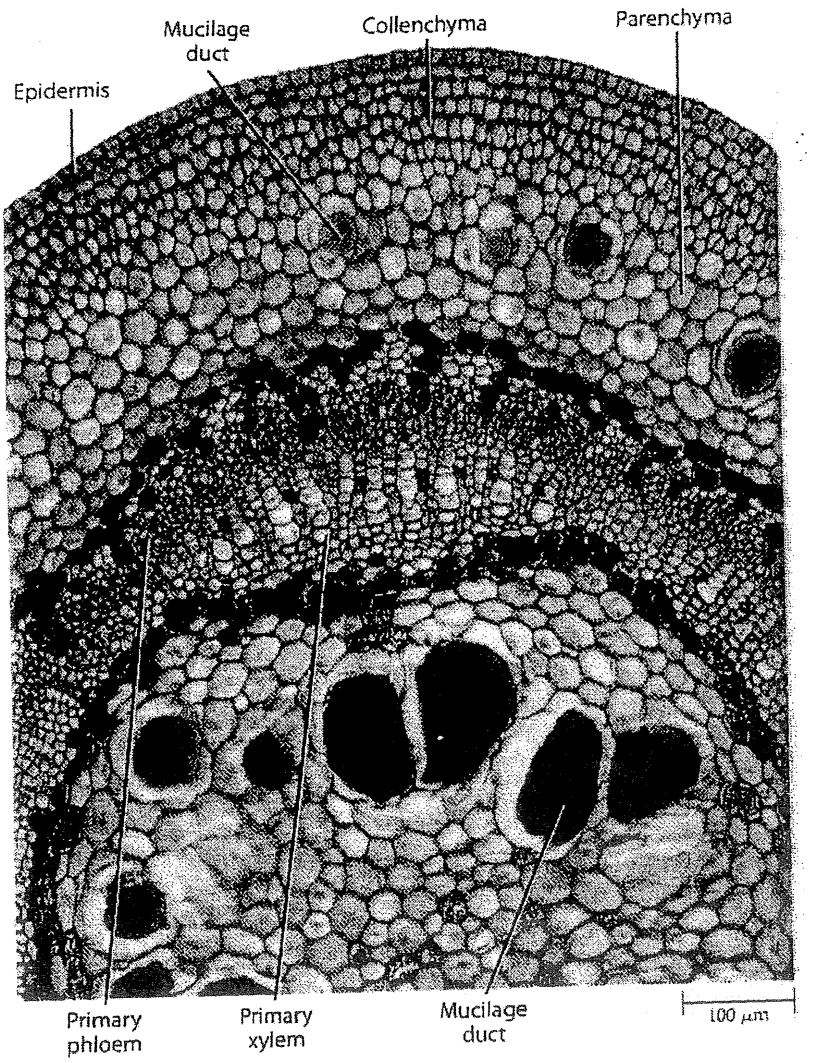

B.
Detail of A.
Shows distribution of phloem and xylem tissues within a plant vascular system.
(from Raven *et al* 1999)

Appendix 2:

Minerals Recorded from Comstock.

Appendices 2. Minerals Recorded from Comstock

Mineral	Frequency (if recorded)
Actinolite ***	
Albite***	
Andradite***	
Anthophyllite***	
Apatite***	
Arsenopyrite*	Rare
Biotite***	
Boulangerite*/***	Rare
Brucite***	
Calcite***	
Carbonate***	
Chalcopyrite*	Rare
Chalcopyrite***	
Chlorite***	
Cordierite***	
Diopside***	
Epidote***	
Exinite***	
Feldspar***	
Galena*	Common
Galena***	
Garnet***	
Goslarite**	Rare
Grossularite***	
Haematite***	
Hastingsite***	
Hisingerite**	Rare
Hydromagnesite**	Rare
Ilmanite***	

Ilvaite***	
Leucoxene***	
Magnesite	
Magnetite***	
Marcasite*	Rare
Marcasite***	
Muscovite***	
Phlogopite***	
Plagioclase***	
Prehnite***	
Pyrite*	Common
Pyrite***	
Pyrrhotite***	
Pyrrohotite*	Rare
Quartz*	Common
Quartz***	
Serpentinite***	
Sphalerit*e	Common
Sphalerite***	
Sphene***	
Talc***	
Tetrahedrite*	Rare
Tourmaline***	
Tremolite***	
Vesuvianite***	
Zoisite***	

*Both, 1962

**Petterd, 1910 in Both, 1962

***Crossing, 1992

Appendix 3:

Water Composition Data for High and Low Flow Conditions.

27/6/00 UNITS ARE PPM

Appendix 3. Water Composition Data for High and Low Flow Conditions.

WET										
	Upstream		Background		Adit 2		Adit 3		Road drain	
Al										
T	0.33	0.33	0.25	0.25	0.38	0.38	1.10	1.10	1.09	1.09
Dissolved	<.0000	0.00	<.0000	0.00	0.11	0.11	0.22	0.22	0.34	0.34
As										
T	0.03	0.03	<.0000	0.00	0.13	0.13	0.14	0.14	<.0000	0.00
Dissolved	<.0000	0.00	0.02	0.02	<.0000	0.00	<.0000	0.00	<.0000	0.00
B										
T	<.0000	0.00	0.10	0.03	<.0000	0.00	<.0000	0.00	<.0000	0.00
Dissolved	0.08	0.04	0.08	0.04	<.0000	0.00	<.0000	0.00	0.01	0.03
Ba										
Total	0.00	0.00	0.00	0.00	0.11	0.11	0.04	0.04	0.02	0.01
Dissolved	0.00	0.00	0.00	0.00	0.09	0.09	0.03	0.03	0.02	0.02
Ca										
Total	0.27	0.27	0.26	0.26	13.80	13.80	37.24	37.24	2.14	2.14
Dissolved	0.24	0.24	0.25	0.25	13.33	13.33	35.82	35.82	1.20	1.20
Cd										
Total	<.0000	0.00	0.00	0.00	0.02	0.02	0.01	0.01	0.03	0.03
Dissolved	<.0000	0.00	<.0000	0.00	0.02	0.02	0.01	0.01	0.00	0.00
Co										
Total	0.01	-0.01	0.02	0.00	0.06	0.04	0.10	0.09	0.03	0.01
Dissolved	0.01	-0.01	0.02	-0.01	0.06	0.03	0.09	0.07	0.03	0.00
Cr										
Total	0.02	0.00	0.03	0.01	0.05	0.03	0.08	0.06	0.01	-0.01
Dissolved	<.0000	0.00	0.01	0.01	0.03	0.02	0.05	0.05	0.02	0.01
Cu						0.00				
Total	0.01	-0.01	0.01	-0.02	0.04	0.01	0.01	-0.01	0.05	0.02
Dissolved	0.03	0.00	0.03	0.00	0.04	0.00	0.00	-0.03	0.04	0.01
Fe										
Total	0.60	0.58	0.60	0.58	21.21	21.19	50.78	50.76	2.31	2.30
Dissolved	0.47	0.45	0.47	0.45	7.44	7.42	37.64	37.62	0.60	0.58
K										
Total	0.16	0.16	0.24	0.24	1.04	1.04	1.21	1.21	0.46	0.46
Dissolved	0.13	0.13	0.28	0.28	1.09	1.09	1.10	1.10	0.24	0.24
Mg										
Total	0.90	0.90	0.92	0.92	10.40	10.40	36.29	36.29	2.36	2.35
Dissolved	0.78	0.78	0.83	0.82	10.11	10.11	23.69	23.69	1.38	1.37
Mn										
Total	0.05	0.05	0.05	0.05	7.15	7.15	6.03	6.03	0.32	0.32
Dissolved	0.04	0.04	0.04	0.04	6.27	6.27	5.58	5.58	0.07	0.07
Mo										
Total	<.0000	0.00	0.00	0.00	0.01	0.01	0.02	0.02	0.00	0.00
Dissolved	<.0000	0.00	0.00	0.00	0.01	0.01	0.01	0.01	<.0000	0.00
Na										
Total	7.39	7.18	7.46	7.25	17.36	17.15	14.31	14.10	7.30	7.09
Dissolved	6.57	6.41	6.70	6.54	16.78	16.62	13.53	13.37	6.76	6.60
Ni										
Total	0.03	0.00	0.00	-0.02	0.07	0.05	0.10	0.07	0.07	0.05
Dissolved	0.04	0.02	0.05	0.03	0.07	0.05	0.13	0.11	0.05	0.03
P										
Total	0.20	-0.02	0.11	-0.11	0.19	-0.03	0.06	-0.16	0.12	-0.10
Dissolved	0.22	0.02	0.19	-0.01	0.12	-0.08	<.0000	0.00	0.26	0.06
Pb										
Total	0.02	0.01	0.30	0.28	0.30	0.29	0.20	0.19	0.35	0.34
Dissolved	0.08	0.08	<.0000	0.00	0.21	0.21	0.19	0.19	0.14	0.14
S										
Total	2.15	1.95	2.09	1.89	31.14	30.94	97.18	96.98	8.80	8.60
Dissolved	1.96	1.78	2.26	2.08	30.86	30.68	94.69	94.51	2.07	1.89
Se										
Total	<.0000	0.00	<.0000	0.00	<.0000	0.00	<.0000	0.00	<.0000	0.00
Dissolved	<.0000	0.00	<.0000	0.00	<.0000	0.00	<.0000	0.00	<.0000	0.00
Si										
Total	0.76	0.76	0.81	0.81	7.18	7.18	7.60	7.60	1.12	1.12
Dissolved	0.88	0.86	1.11	1.09	6.36	6.33	7.16	7.13	0.91	0.88
Sn										
Total	0.04	0.00	0.05	0.01	0.09	0.05	0.01	-0.03	0.03	-0.01
Dissolved	0.07	0.07	0.04	0.04	0.05	0.04	0.07	0.06	0.06	0.05
V										
Total	<.0000	0.00	<.0000	0.00	<.0000	0.00	<.0000	0.00	<.0000	0.00
Dissolved	<.0000	0.00	<.0000	0.00	<.0000	0.00	<.0000	0.00	<.0000	0.00
Zn										
Total	0.24	0.24	0.23	0.23	3.29	3.29	12.64	12.64	3.57	3.57
Dissolved	0.23	0.23	0.24	0.24	2.88	2.88	11.67	11.67	0.17	0.17
CO3		<1		<1		<1		<1		<1
HCO3		<1		<1		8.00		<1		<1
Cl-		9.80		9.70		26.00		20.00		9.00
Nitrate		<0.03		<0.03		<0.03		<0.03		<0.03
Nitrite		<0.1		<0.01		<0.01		<0.01		<0.01
SO4-		3.70		3.70		80.00		290.00		110.00
pH		4.58		4.50		6.15		6.22		6.24
EC		45.50		41.40		OFL		OFL		38.40
Temperature		8.90		9.10		10.20		8.10		8.80
Eh		247.00		260.00		137.00		113.00		182.00
pe		4.42		4.64		2.44		2.03		3.25

Main adit		Mixing Zone		Sed. Trap		Balstrup Drain		Standard
2.74	2.74	1.93	1.93	15.20	15.20	5.28	5.28	<.0000
1.15	1.15	0.63	0.63	13.06	13.06	4.66	4.66	<.0000
<.0000	0.00	<.0000	<.0000	0.04	0.04	<.0000	0.00	<.0000
<.0000	0.00	0.03	0.03	0.11	0.11	0.13	0.13	<.0000
0.22	0.16	0.17	0.11	0.06	-0.01	0.08	0.02	0.07
0.02	-0.02	0.09	0.05	0.10	0.06	<.0000	0.00	0.04
0.02	0.01	0.02	0.02	0.03	0.03	0.02	0.02	0.00
0.01	0.01	0.02	0.02	0.03	0.03	0.02	0.02	<.0000
16.94	16.94	12.83	12.83	12.15	12.15	3.54	3.54	<.0000
15.94	15.94	11.46	11.46	11.07	11.07	3.21	3.21	0.00
0.05	0.05	0.04	0.04	0.18	0.18	0.29	0.29	<.0000
0.05	0.05	0.03	0.03	0.16	0.16	0.27	0.27	<.0000
0.04	0.02	0.03	0.02	0.37	0.35	0.06	0.04	0.02
0.04	0.02	0.04	0.02	0.35	0.33	0.07	0.04	0.02
0.05	0.03	0.04	0.02	<.0000	<.0000	0.05	0.03	0.02
0.05	0.05	0.05	0.04	0.02	0.02	0.03	0.02	0.01
0.05	0.02	0.04	0.01	0.07	0.04	0.04	0.01	0.03
0.05	0.02	0.04	0.01	0.07	0.04	0.06	0.03	0.03
23.93	23.91	16.29	16.27	2.80	2.78	28.73	28.71	0.02
19.82	19.80	13.41	13.39	2.47	2.45	26.13	26.11	0.02
0.43	0.43	0.45	0.45	4.31	4.31	1.27	1.27	<.0000
0.33	0.33	0.30	0.30	4.03	4.03	1.12	1.12	<.0000
9.48	9.48	7.28	7.27	64.53	64.53	6.41	6.41	0.00
8.81	8.81	6.95	6.94	59.35	59.35	6.07	6.07	0.00
2.93	2.93	2.10	2.09	0.90	0.90	3.12	3.12	0.00
2.78	2.78	1.97	1.97	0.82	0.82	2.88	2.87	0.00
0.03	0.03	0.01	0.01	0.05	0.05	0.05	0.05	<.0000
0.02	0.01	0.01	0.00	0.06	0.06	0.05	0.05	0.01
8.27	8.06	8.26	8.05	13.76	13.55	10.85	10.64	0.21
7.87	7.71	7.37	7.22	12.65	12.49	10.00	9.84	0.16
0.06	0.04	0.07	0.05	0.41	0.39	0.14	0.11	0.02
0.03	0.02	0.02	0.00	0.38	0.36	0.10	0.08	0.02
0.13	-0.09	0.22	0.00	0.24	0.02	0.03	-0.18	0.22
0.05	-0.15	0.09	-0.12	0.22	0.01	0.13	-0.07	0.20
0.42	0.41	0.31	0.30	6.20	6.19	0.55	0.54	0.01
0.17	0.17	0.37	0.37	5.67	5.67	0.48	0.48	<.0000
			0.00					
50.63	50.43	38.91	38.71	140.40	140.20	74.72	74.52	0.20
49.07	48.89	37.34	37.16	130.60	130.42	71.42	71.24	0.18
<.0000	0.00	<.0000	0.00	<.0000	0.00	<.0000	0.00	<.0000
<.0000	0.00	<.0000	0.00	<.0000	0.00	<.0000	0.00	<.0000
3.39	3.39	2.67	2.67	5.47	5.47	2.40	2.40	<.0000
3.28	3.25	2.69	2.66	5.27	5.25	2.72	2.69	0.02
0.01	-0.03	0.04	0.00	0.01	-0.03	0.00	-0.04	0.04
0.04	0.03	0.00	0.00	<.0000	0.00	0.04	0.03	0.01
<.0000	0.00	<.0000	0.00	<.0000	0.00	<.0000	0.00	<.0000
<.0000	0.00	<.0000	0.00	<.0000	0.00	<.0000	0.00	<.0000
14.25	14.25	10.47	10.47	40.77	40.77	46.59	46.59	<.0000
13.59	13.59	9.71	9.71	36.00	36.00	42.39	42.39	<.0000
	<1		<1		<1		<1	
	<1		<1		<1		<1	
	10.00		11.00		15.00		8.10	
	<0.03		<0.03		<0.03		<0.03	
	<0.01		<0.01		<0.01		<0.01	
	29.00		100.00		290.00		400.00	
	4.97		5.29		3.29		6.03	
	OFL		181.70		OFL		OFL	
	10.50		9.60		9.00		10.80	
	186.00		201.00		413.00		298.00	
	3.31		3.58		7.38		5.29	

22 Sep

rpm

DRY	Upstream		Background		Adit2		Adit3	
Al								
t	0.37	0.31	0.07	0.00	0.20	0.13	1.20	1.13
d	<.0000	0.00	9.42	9.37	0.16	0.11	0.09	0.05
As								
t	0.06	0.05	<.0000	0.00	<.0000	0.00	0.05	0.04
d	0.49	0.45	0.16	0.13	0.14	0.10	0.04	0.00
B								
t	0.01	0.00	0.01	0.00	0.09	0.08	0.14	0.13
d	0.14	0.13	0.06	0.04	0.11	0.09	0.01	-0.01
Ba								
t	0.01	0.00	0.01	0.00	0.11	0.00	0.04	0.00
d	0.03	-0.01	0.03	-0.01	0.04	0.01	0.01	-0.03
Ca								
t	2.99	2.96	2.88	2.84	18.86	18.82	41.77	41.73
d	43.84	35.40	6.93	-1.52	39.34	30.90	2.89	-5.56
Cd						0.00		
t	0.01	0.00	0.01	-0.01	0.02	0.01	0.02	0.01
d	0.04	0.03	0.22	0.21	0.01	0.00	0.01	0.00
Co								
t	0.03	0.01	0.01	-0.01	0.07	0.05	0.09	0.07
d	0.05	0.03	0.13	0.11	0.09	0.07	0.03	0.00
Cr								
t	0.04	0.00	<.0000	0.00	<.0000	0.00	0.01	0.00
d	0.04	0.00	<.0000	0.00	0.02	0.00	<.0000	0.00
Cu								
t	0.04	0.00	0.07	0.03	0.03	0.00	0.05	0.01
d	0.01	-0.03	0.07	0.03	0.03	-0.01	0.04	0.00
Fe								
t	1.08	0.95	1.31	1.18	26.82	26.69	43.49	43.36
d	46.04	43.20	18.39	15.55	34.46	31.62	1.05	-1.80
K								
t	0.56	0.50	0.54	0.48	1.15	1.09	1.38	1.31
d	0.67	0.18	1.19	0.69	1.28	0.79	0.76	0.27
Mg								
t	2.40	2.38	2.40	2.38	10.17	10.15	32.93	32.91
d	21.24	17.78	18.36	14.90	28.71	25.25	2.39	-1.08
Mn								
t	0.10	0.00	0.13	0.00	9.69	0.00	5.91	0.00
d	7.56	7.15	2.40	1.99	5.47	5.06	0.12	-0.29
Mo								
t	<.0000	0.00	<.0000	0.00	<.0000	0.00	0.02	0.02
d	0.02	0.00	0.11	0.00	0.02	0.00	<.0000	0.00
Na								
t	11.85	11.60	11.38	11.13	17.94	17.69	14.82	14.57
d	10.10	1.05	18.37	9.32	13.75	4.70	11.92	2.87
Ni						0.00		
t	<.0000	0.00	<.0000	0.00	0.07	0.05	0.09	0.07
d	0.05	0.04	0.22	0.22	0.07	0.06	<.0000	0.00
P								
t	<.0000	0.00	0.03	0.00	<.0000	0.00	<.0000	0.00
d	<.0000	0.00	0.12	0.12	<.0000	0.00	0.01	0.00
Pb								
t	0.22	0.03	0.13	-0.06	0.51	0.32	0.13	-0.05
d	0.13	-0.09	4.69	4.47	0.23	0.02	0.21	-0.01
S								
t	9.34	8.60	8.94	8.21	51.23	50.50	164.30	163.57
d	175.80	164.12	130.70	119.02	120.80	109.12	9.25	-2.43
Se								
t	0.04	0.01	0.01	-0.02	<.0000	0.00	<.0000	0.00
d	<.0000	0.00	<.0000	0.00	<.0000	0.00	0.03	0.00
Si								
t	2.91	2.87	2.90	2.85	7.60	7.56	7.34	7.30
d	7.12	5.04	6.17	4.08	6.38	4.30	2.84	0.76
Sn								
t	<.0000	0.00	<.0000	0.00	0.03	0.00	<.0000	0.00
d	0.01	0.01	0.06	0.05	<.0000	0.00	0.01	0.01
V								
t	0.01	-0.01	0.00	-0.02	0.00	-0.02	<.0000	0.00
d	<.0000	0.00	<.0000	0.00	<.0000	0.00	<.0000	0.00
Zn								
t	0.58	0.56	0.59	0.57	2.94	2.92	13.02	13.00
d	24.60	23.86	63.51	62.77	11.87	11.13	0.65	-0.09
CO3	<1	0.00	<1	0.00	<1	0.00	<1	0.00
HCO3	<1	0.00	<1	0.00	6.00	6.00	<1	0.00
Cl-	17.00	16.84	17.00	16.84	26.00	25.84	19.00	18.84
Nitrate	<0.03	0.00	<0.03	0.00	<0.03	0.00	<0.03	0.00
Nitrite	<0.1	0.00	<0.1	0.00	<0.1	0.00	<0.1	0.00
SO4-	12.00	-24.00	13.00	-23.00	80.00	44.00	300.00	264.00
pH		5.46		5.29		6.13		6.39
EC		63.00		62.90		216.00		429.00
Temperature		6.70		6.80		9.70		9.60
Eh		226.00		213.00		116.00		90.00
pe		18.02		18.01		17.83		17.83

Road		MainA		Mixing		Balstrup		Standard
0.28	0.21	2.94	2.87	3.24	3.17	11.20	11.13	0.07
0.58	0.53	0.01	-0.03	<.0000	0.00	<.0000	0.00	0.04
0.13	0.12	0.11	0.10	0.17	0.16	0.41	0.40	0.01
0.03	0.00	0.03	-0.01	0.11	0.08	0.09	0.05	0.03
0.02	0.01	0.16	0.15	0.17	0.16	0.11	0.10	0.01
0.15	0.13	0.03	0.02	0.04	0.02	0.01	-0.01	0.02
0.04	0.00	0.03	0.03	0.04	0.04	0.03	0.03	<.0000
0.03	-0.01	0.10	0.06	0.10	0.06	0.02	-0.02	0.04
8.63	8.59	46.57	46.53	45.59	45.55	7.63	7.59	0.04
44.14	35.70	17.85	9.41	18.67	10.23	2.85	-5.59	8.44
0.01	0.00	0.04	0.03	0.04	0.03	0.25	0.24	0.01
0.03	0.03	0.02	0.02	0.02	0.01	0.01	0.00	0.01
0.02	0.00	0.06	0.04	0.07	0.04	0.14	0.12	0.02
0.06	0.03	0.06	0.03	0.05	0.03	0.04	0.01	0.02
0.02	0.00	0.04	0.04	0.02	0.02	0.04	0.04	<.0000
0.04	0.00	<.0000	0.00	<.0000	0.00	<.0000	0.00	<.0000
0.02	-0.01	0.04	0.00	0.02	-0.02	0.05	0.02	0.04
0.00	-0.04	0.06	0.02	0.04	-0.01	0.04	0.00	0.05
3.18	3.06	54.94	54.81	52.97	52.84	36.09	35.96	0.13
48.98	46.14	8.98	6.14	9.24	6.40	0.94	-1.90	2.84
0.50	0.44	0.63	0.57	0.68	0.62	1.26	1.20	0.06
0.64	0.14	1.12	0.63	1.10	0.61	0.68	0.18	0.49
3.62	3.60	28.07	28.05	27.29	27.27	19.67	19.65	0.02
26.08	22.82	9.70	6.24	9.94	6.48	2.37	-1.09	3.46
0.41	0.00	9.38	9.38	7.92	7.92	2.70	2.70	<.0000
7.72	7.31	6.72	6.31	6.98	6.57	0.12	-0.30	0.41
<.0000	0.00	0.03	0.03	0.03	0.03	0.10	0.00 0.10	0.00
0.07	0.00	0.01	0.00	<.0000	0.00	<.0000	0.00	<.0000
9.49	9.24	10.41	10.16	10.63	10.38	19.44	19.19	0.25
9.77	0.73	16.81	7.76	17.60	8.55	11.52	2.47	9.05
<.0000	0.00	0.06	0.04	0.07	0.05	0.27	0.25	0.02
0.05	0.05	0.01	0.01	0.07	0.07	<.0000	0.00	0.01
0.01	0.00	<.0000	0.00	<.0000	0.00	<.0000	0.00	<.0000
<.0000	0.00	<.0000	0.00	<.0000	0.00	<.0000	0.00	0.01
0.27	0.09	0.33	0.15	0.34	0.16	5.79	5.61	0.18
0.13	-0.08	0.18	-0.03	0.19	-0.02	0.07	-0.15	0.21
10.54	9.81	185.10	184.37	177.70	0.00 176.97	168.60	167.87	0.73
181.80	170.12	33.92	22.24	52.06	40.38	9.18	-2.51	11.68
0.09	0.07	<.0000	0.00	<.0000	0.00	<.0000	0.00	0.02
<.0000	0.00	0.14	0.00	<.0000	0.00	<.0000	0.00	<.0000
1.85	1.81	7.78	7.74	7.73	7.68	6.98	6.94	0.04
7.33	5.25	6.18	4.09	6.32	4.23	3.04	0.95	2.08
0.02	0.00	<.0000	0.00	<.0000	0.00	<.0000	0.00	<.0000
<.0000	0.00	0.01	0.00	<.0000	0.00	<.0000	0.00	0.00
0.02	0.00	<.0000	0.00	0.00	-0.02	0.03	0.01	0.02
<.0000	0.00	<.0000	0.00	0.00	-0.01	0.02	0.01	0.01
0.69	0.67	27.67	27.65	26.80	26.78	76.16	76.14	0.02
25.76	25.02	2.84	2.10	2.73	1.99	0.56	-0.18	0.74
<1	0.00	<1	0.00	<1	0.00	<1	0.00	<1
<1	0.00	7.00	0.00	<1	0.00	<1	0.00	<1
14.00	13.84	13.00	12.84	14.00	13.84	28.00	27.84	0.16
<0.03	0.00	<0.03	0.00	<0.03	0.00	<0.03	0.00	<0.03
<0.1	0.00	<0.1	0.00	<0.1	0.00	<0.1	0.00	<0.1
360.00	324.00	18.00	-18.00	360.00	324.00	530.00	494.00	36.00
	6.42		6.04		5.81		4.50	
	80.10		483.00		461.00		OFL	
	8.20		10.30		9.90		7.50	
	156.00		152.00		86.00		344.00	
	17.92		17.79		17.81		17.97	

Appendix 4:

Mass Loads of Elements in High and Low Flow Conditions.

Appendix 4. Mass Loads of Elements in High and Low Flow Conditions.

Dry Mass Loads				
	Mass Load (t/yr) (mass load*31536000/100000	Shortfall in Mixing Zone Total (T/Y)	Mass Load (t/yr) nass load*31536000/100000	Shortfall in Mixing Zone Dissolved (T/Y)
Al				
5	0.00		0.00	
6	16.39		0.33	
7	5.80	10.59	0.00	0.33
As				
5	0.00		0.00	
6	0.62		0.01	
7	0.31	0.31	0.00	0.01
B				
5	0.00		0.00	
6	0.89		0.02	
7	0.30	0.59	0.00	0.02
Ba				
5	0.00		0.00	
6	0.19		0.00	
7	0.07	0.12	0.00	0.00
Ca				
5	0.00		0.00	
6	259.65		5.61	
7	81.66	177.99	0.00	5.61
Cd				
5	0.00		0.00	
6	0.23		0.00	
7	0.07	0.16	0.00	0.00
Co				
5	0.00		0.00	
6	0.34		0.01	
7	0.12	0.22	0.00	0.01
Cr				
5	0.00		0.00	
6	0.22		0.01	
7	0.04	0.18	0.00	0.01
Cu				
5	0.00		0.00	
6	0.21		0.01	
7	0.03	0.18	0.00	0.01
Fe				
5	0.00		0.00	
6	306.32		6.67	
7	94.88	211.44	0.00	6.67
K				
5	0.00		0.00	
6	3.50		0.07	
7	1.22	2.28	0.00	0.07
Mg				
5	0.00		0.00	
6	156.51		3.39	
7	48.88	107.62	0.00	3.39
Mn				
5	0.00		0.00	
6	52.28		1.20	
7	14.18	38.10	0.00	1.20
Mo				
5	0.00		0.00	
6	0.15		0.00	
7	0.06	0.09	0.00	0.00
Na				
5	0.00		0.00	
6	58.04		1.23	
7	19.04	39.00	0.00	1.23
Ni				
5	0.00		0.00	
6	0.35		0.01	
7	0.13	0.22	0.00	0.01
P				
5	0.00		0.00	
6	0.00		0.00	
7	0.00	0.00	0.00	0.00
Pb				
5	0.00		0.00	
6	1.85		0.04	
7	0.61	1.24	0.00	0.04
S				
5	0.00		0.00	
6	1032.04		22.51	
7	318.30	713.74	0.00	22.51
Se				
5	0.00		0.00	
6	0.00		0.00	
7	0.00	0.00	0.00	0.00
Si				
5	0.00		0.00	
6	43.38		0.93	
7	13.84	29.54	0.00	0.93
Sn				
5	0.00		0.00	
6	0.00		0.00	
7	0.00	0.00	0.00	0.00
V				
5	0.00		0.00	
6	0.00		0.00	
7	0.01	-0.01	0.00	0.00
Zn				
5	0.00		0.00	

6	154.28	106.27	3.35	3.35
7	48.01		0.00	

Wet Mass Loads

Al	Total Mass Load (Tonnes/year	Shortfall in Mixing Zone Total (T/Y)	Dissolved Mass Load (tonnes/year)	Shortfall in Mixing Zone Dissolved (T/Y)
5	3.86		1.19	
6	27.86		11.71	
7	14.82	16.90	4.87	8.03
As				
5	0.00		0.00	
6	0.00		0.00	
7	0.00	0.00	0.21	-0.21
B				
5	0.00		0.04	
6	2.27		0.23	
7	1.34	0.93	0.69	-0.42
Ba				
5	0.06		0.06	
6	0.16		0.08	
7	0.13	0.08	0.12	0.02
Ca				
5	7.58		4.23	
6	172.42		162.24	
7	98.73	81.27	88.19	78.29
Cd				
5	0.11		0.00	
6	0.53		0.49	
7	0.29	0.35	0.26	0.23
Co				
5	0.10		0.09	
6	0.40		0.45	
7	0.26	0.24	0.30	0.24
Cr				
5	0.02		0.06	
6	0.55		0.51	
7	0.29	0.29	0.36	0.21
Cu				
5	0.18		0.15	
6	0.46		0.55	
7	0.27	0.37	0.30	0.39
Fe				
5	8.17		2.13	
6	243.56		201.73	
7	125.35	126.38	103.19	100.66
K				
5	1.63		0.86	
6	4.34		3.34	
7	3.47	2.49	2.32	1.88
Mg				
5	8.33		4.87	
6	96.48		89.70	
7	55.98	48.83	53.46	41.11
Mn				
5	1.13		0.26	
6	29.86		28.27	
7	16.13	14.86	15.14	13.39
Mo				
5	0.02		0.00	
6	0.29		0.20	
7	0.10	0.21	0.06	0.14
Na				
5	25.82		23.91	
6	84.16		80.11	
7	63.58	46.41	56.74	47.29
Ni				
5	0.24		0.18	
6	0.61		0.34	
7	0.55	0.30	0.13	0.39
P				
5	0.43		0.93	
6	1.32		0.54	
7	1.69	0.05	0.67	0.80
Pb				
5	1.23		0.48	
6	4.32		1.76	
7	2.41	3.13	2.84	-0.59
S				
5	31.11		7.33	
6	515.31		499.44	
7	299.42	247.01	287.34	219.43
Se				
5	0.00		0.00	
6	0.00		0.00	
7	0.00	0.00	0.00	0.00
Si				
5	3.98		3.21	
6	34.51		33.36	
7	20.52	17.97	20.68	15.89
Sn				
5	0.10		0.21	
6	0.05		0.38	
7	0.28	-0.12	0.02	0.57
V				
5	0.00		0.00	
6	0.00		0.00	
7	0.00	0.00	0.00	0.00
Zn				
5	12.64		0.61	

6	145.04		138.32	
7	80.57	77.11	74.68	64.25

Appendix 5:

Element Concentrations During Storm Sampling.

Appendix 5. Element Concentrations During Storm Sampling

Al	Total	Dissolved
02.09.00 17:30	1.68	0.47
03.09.00 02:20	1.76	0.45
3:20	1.86	0.52
4:20	1.73	0.54
5:20	1.70	0.53
6:20	1.81	0.35
7:20	1.71	0.60
15:20	1.52	0.50
16:20	1.68	0.46

As	Total	Dissolved
02.09.00 17:30	0.01	0.31
03.09.00 02:20	0.18	0.24
3:20	0.21	0.37
4:20	0.10	0.34
5:20	0.43	0.25
6:20	0.31	0.31
7:20	0.26	0.35
15:20	0.09	0.36
16:20	0.29	0.32

B	Total	Dissolved
02.09.00 17:30	0.04	0.05
03.09.00 02:20	0.13	0.12
3:20	0.11	0.12
4:20	0.04	0.12
5:20	0.13	0.12
6:20	0.13	0.12
7:20	0.13	0.12
15:20	0.01	0.09
16:20	0.11	0.10

Ba	Total	Dissolved
02.09.00 17:30	0.05	0.04
03.09.00 02:20	0.05	0.04
3:20	0.04	0.05
4:20	0.05	0.04
5:20	0.04	0.04
6:20	0.05	0.04
7:20	0.05	0.04
15:20	0.04	0.04
16:20	0.04	0.04

Mn	Total	Dissolved
02.09.00 17:30	8.43	8.30
03.09.00 02:20	8.31	8.34
3:20	8.42	8.42
4:20	8.53	8.34
5:20	8.43	8.47
6:20	8.34	8.39
7:20	8.28	8.36
15:20	7.11	7.01
16:20	7.00	7.09

Mo	Total	Dissolved
02.09.00 17:30	0.08	<.0000
03.09.00 02:20	0.03	0.04
3:20	0.02	0.04
4:20	0.04	0.06
5:20	0.02	0.03
6:20	<.0000	0.03
7:20	0.03	0.03
15:20	0.06	0.04
16:20	0.04	0.03

Na	Total	Dissolved
02.09.00 17:30	8.89	8.95
03.09.00 02:20	8.75	8.78
3:20	8.18	8.26
4:20	8.72	8.72
5:20	8.54	8.19
6:20	8.59	8.68
7:20	8.67	8.15
15:20	8.41	8.20
16:20	8.22	8.69

Ni	Total	Dissolved
02.09.00 17:30	0.06	0.05
03.09.00 02:20	0.07	0.05
3:20	0.05	0.05
4:20	0.05	0.08
5:20	0.06	0.06
6:20	0.05	0.06
7:20	0.05	0.07
15:20	0.05	0.05
16:20	0.04	0.04

Appendix 10:

In Situ Water Measurements of Leach Columns.

Appendix 10. In Situ Water Measurements of Leach Columns.

pH

Date each Column	1	2	3
1N	1.19	3.01	3.01
1D	2.62	4.06	3.2
2N	2.36	2.89	2.69
2D	3.33	3.02	2.8
3N	3.15	2.74	2.62
3D	3.31	2.79	2.7
4N	2.48	2.69	2.59
4D	1.79	2.72	2.6
5N	3.39	3.51	3.46
5D	2.83	3.55	3.5
6N	2.48	3.19	3.28
6D	2.36	3.16	3.26
7N	2.81	3.23	2.45
7D	2.43	3.4	2.38
10N	3.1	4.12	4.11
10D	3.01	4.05	3.98
11N	2.97	3.78	3.68
11D	3.37	3.91	3.9
GN	4.01	4.5	4.64
GD	3.4	4.87	4.46
SN	3.81	3.94	4.11
SD	3.12	4.06	4.03
PN	4.33	4.3	4.21
PD	2.36	4.41	3.23
BN	2.77	4.12	4.2
BD	2.27	3.7	4.35

Eh

Date Leach Column	1	2	3
1N	465	480	514
1D	418	448	429
2N	452	483	490
2D	327	494	469
3N	445	465	477
3D	408	470	466
4N	415	372	475
4D	438	484	479
5N	380	397	420
5D	350	372	414
6N	482	564	555
6D	519	552	563
7N	404	456	501
7D	407	440	473
10N	394	334	415
10D	382	341	421
11N	409	348	402
11D	317	302	347
GN	325	350	464
GD	424	371	428
SN	408	332	455
SD	347	416	444
PN	475	400	425
PD	323	454	507
BN	473	401	460
BD	545	440	450

Temperature

Date each Column	1	2	3
1N	17.4	19	18.6
1D	17.8	19	19.1
2N	17.8	18.2	18.9
2D	17.3	18.5	18.7
3N	17.5	18	19
3D	17.7	17.8	18.7
4N	17.8	17.9	19
4D	17.5	17.6	18.9
5N	17.4	18.2	18.7
5D	17.8	17.6	18.4
6N	17.3	17.9	19.1
6D	17.3	17.6	18.6
7N	17.5	17.8	18.7
7D	17.3	17.5	18.7
10N	17.3	18	19
10D	17.4	17.5	18.5
11N	17.2	18.3	18.7
11D	17.3	18	18.5
GN	17.3	18.4	19.1
GD	17.2	18.3	18.8
SN	17.4	17.9	18.7
SD	17.1	17.7	18.6
PN	17.7	17.8	18.9
PD	17.3	18.2	18.7
BN	15.1	18.1	19.3
BD	15.4	18.4	19.1

Electrical Conductivity

Date Leach Column	1	2	3
1N	2.12	1	0.336
1D	1.833	1.277	0.248
2N	1.375	0.963	
2D	0.718	1.483	0.527
3N	1.22	2.5	0.822
3D	2.113	2.11	0.681
4N	2.563	2.19	0.769
4D	2.61	1.685	0.661
5N	1.842	1.75	0.577
5D	1.842	1.34	0.43
6N	1.751	0.65	0.1477
6D	1.972	0.5	0.265
7N	1.811	1.3	0.401
7D	2.133	0.78	0.265
10N	1.216	0.41	0.117
10D	1.117	0.51	0.0968
11N	1.947	0.87	0.567
11D	1.4	1.49	0.371
GN	0.391	0.42	0.956
GD	0.352	0.13	0.0232
SN	0.681	0.39	0.1216
SD	0.557	0.81	0.329
PN	1.288	1.39	0.364
PD	1.993	0.39	0.248
BN	0.546	0.1661	0.0375
BD	1.411	0.1466	0.0606

Appendix 11:

Ion Concentration Analysis Results for Leach Columns.

Appendix 11. Ion Concentration Analysis Results for Leach Columns.

	1D1	1N1		2D1	2N1		3D1	3N1
Al	35.59	25.22	Al	22.70	30.31	Al	26.28	34.26
As	<.0000	0.02	As	0.35	0.28	As	0.38	<.0000
B	0.10	0.12	B	0.10	0.06	B	0.19	0.17
Ba	0.02	0.08	Ba	0.03	0.02	Ba	0.02	0.01
Ca	3.73	15.85	Ca	5.47	7.79	Ca	20.24	25.97
Cd	0.09	0.14	Cd	1.09	1.00	Cd	1.92	1.70
Co	0.92	0.16	Co	1.41	1.43	Co	0.53	0.63
Cr	<.0000	<.0000	Cr	<.0000	<.0000	Cr	0.09	0.03
Cu	<.0000	0.06	Cu	0.30	0.19	Cu	0.02	0.05
Fe	29.94	36.15	Fe	28.92	13.99	Fe	66.15	55.17
K	27.09	36.11	K	25.36	24.28	K	21.05	23.63
Mg	8.51	27.08	Mg	24.17	22.06	Mg	28.22	34.93
Mn	0.68	2.06	Mn	0.98	1.14	Mn	3.64	4.56
Mo	0.26	0.11	Mo	0.04	0.03	Mo	0.10	0.09
Na	7.96	16.88	Na	2.68	14.59	Na	1.85	13.66
Ni	1.96	0.32	Ni	4.49	4.43	Ni	5.43	6.54
P	<.0000	0.12	P	<.0000	0.04	P	<.0000	<.0000
Pb	7.86	8.31	Pb	5.67	5.80	Pb	4.05	4.14
S	185.10	108.90	S	94.33	112.00	S	177.80	207.30
Se	<.0000	<.0000	Se	<.0000	<.0000	Se	<.0000	<.0000
Si	8.12	21.28	Si	9.09	11.40	Si	12.30	17.00
Sn	<.0000	0.09	Sn	0.12	0.18	Sn	0.09	0.09
V	0.03	0.04	V	<.0000	<.0000	V	<.0000	<.0000
Zn	271.60	102.50	Zn	13.64	16.48	Zn	77.61	86.94
mg/L CaCO3	<1	<1	mg/L CaCO3	<1	<1	mg/L CaCO3	<1	<1
Sulphate	860	590	Sulphate	600	630	Sulphate	840	900

	4D1	4N1		5D1	5N1
Al	10.40	9.03	Al	76.42	81.97
As	0.25	<.0000	As	0.44	0.13
B	0.31	0.33	B	0.45	0.26
Ba	0.02	0.01	Ba	0.02	0.01
Ca	7.87	9.86	Ca	15.87	17.33
Cd	0.60	0.63	Cd	0.10	0.08
Co	0.03	0.05	Co	3.90	4.01
Cr	0.12	0.14	Cr	0.18	0.04
Cu	0.64	0.84	Cu	<.0000	<.0000
Fe	126.70	140.60	Fe	193.50	105.00
K	15.51	15.23	K	29.09	29.63
Mg	13.79	15.42	Mg	18.05	25.74
Mn	3.70	3.58	Mn	2.14	2.10
Mo	0.09	0.12	Mo	0.29	0.29
Na	4.13	13.95	Na	5.74	16.18
Ni	0.08	0.22	Ni	6.91	6.82
P	<.0000	<.0000	P	<.0000	<.0000
Pb	10.09	8.93	Pb	3.92	4.06
S	133.00	140.00	S	341.10	333.70
Se	<.0000	<.0000	Se	<.0000	<.0000
Si	25.45	26.46	Si	9.02	10.61
Sn	0.09	0.13	Sn	0.03	0.17
V	0.02	<.0000	V	0.43	0.25
Zn	87.53	74.90	Zn	393.70	425.00
mg/L CaCO3	<1	<1	mg/L CaCO3	<1	<1
Sulphate	730	800	Sulphate	940	1200

	6D1	6N1
Al	12.93	10.70
As	0.22	<.0000
B	0.03	0.03
Ba	0.02	0.02
Ca	5.97	7.91
Cd	0.61	0.60
Co	0.16	0.07
Cr	<.0000	<.0000
Cu	0.02	0.03
Fe	8.33	4.78
K	10.96	11.11
Mg	10.64	12.70
Mn	1.21	1.41
Mo	0.04	0.03
Na	3.99	15.09
Ni	0.26	0.14
P	0.07	0.16
Pb	10.79	10.67
S	57.40	56.63
Se	<.0000	<.0000
Si	8.62	11.19
Sn	<.0000	0.10
V	0.00	<.0000
Zn	21.09	13.01
mg/L CaCO3	<1	<1
Sulphate	400	940

	7D1	7N1
Al	14.97	20.81
As	0.40	0.09
B	0.12	0.11
Ba	0.02	0.01
Ca	6.24	10.13
Cd	2.27	2.98
Co	0.37	0.43
Cr	<.0000	0.01
Cu	<.0000	<.0000
Fe	38.56	35.06
K	20.74	24.22
Mg	14.81	26.02
Mn	1.29	2.09
Mo	0.26	0.24
Na	4.15	16.92
Ni	0.68	0.80
P	<.0000	0.02
Pb	8.56	8.12
S	146.90	198.10
Se	<.0000	<.0000
Si	7.28	13.33
Sn	<.0000	0.10
V	0.04	0.06
Zn	247.50	318.00
mg/L CaCO3	<1	<1
Sulphate	820	870

	BD1	BN1
Al	6.25	2.22
As	0.21	0.32
B	0.02	0.02
Ba	0.01	0.02
Ca	1.19	2.44
Cd	<.0000	0.00
Co	0.01	0.01
Cr	<.0000	<.0000
Cu	<.0000	<.0000
Fe	3.17	1.04
K	0.61	0.73
Mg	2.32	3.98
Mn	0.08	0.21
Mo	0.01	0.02
Na	0.31	10.10
Ni	0.00	0.04
P	0.08	0.32
Pb	<.0000	0.13
S	0.06	4.89
Se	0.01	<.0000
Si	3.87	4.85
Sn	0.11	0.21
V	<.0000	<.0000
Zn	0.40	1.00
mg/L CaCO3	<1	<1
Sulphate	29	280

	11D1	11N1
Al	10.61	13.00
As	0.26	<.0000
B	0.27	0.11
Ba	<.0000	0.00
Ca	1.20	3.00
Cd	4.40	5.23
Co	1.59	1.40
Cr	0.12	<.0000
Cu	<.0000	0.05
Fe	121.10	36.06
K	0.46	0.97
Mg	3.17	5.78
Mn	2.18	2.56
Mo	0.33	0.37
Na	0.90	11.77
Ni	2.26	2.00
P	<.0000	0.03
Pb	4.45	4.59
S	267.30	286.10
Se	<.0000	<.0000
Si	9.35	11.61
Sn	0.07	0.06
V	<.0000	<.0000
Zn	570.50	595.00
mg/L CaCO3	<1	<1
Sulphate	560	630

	10D1	10N1
Al	5.68	5.02
As	0.19	<.0000
B	0.07	0.08
Ba	<.0000	<.0000
Ca	21.61	33.58
Cd	0.53	0.41
Co	0.04	0.04
Cr	<.0000	<.0000
Cu	<.0000	<.0000
Fe	20.43	22.04
K	0.90	1.16
Mg	8.79	14.81
Mn	8.04	11.81
Mo	0.20	0.23
Na	0.98	11.78
Ni	0.03	0.07
P	0.06	0.11
Pb	9.14	7.19
S	121.00	137.70
Se	<.0000	<.0000
Si	3.66	5.37
Sn	0.09	0.10
V	<.0000	0.05
Zn	226.00	278.40
mg/L CaCO3	<1	<1
Sulphate	1100	1100

Appendix 17: Departmental Rock catalogue.

Catalog#	Field# (25 characters)	Rock Name (25 characters)	Rock description (55 characters)	AMG Northing (16 characters)	AMG Easting (18 characters)	Full Map Title (75 characters)	Map Scale (10 characters)	Position (35 characte	Area 25 characters	State (20 characters)	Country (15 characters)
145690	1	talc	massive talc.	5366600N	357615E	In-house: Comsl	1:3000		123M/47	Tasmania	Australia
145691	2	shale	carbonaceous shale, some graphitic alteration.	5387405N	357604E	In-house: Comsl	1:3000		123M/48	Tasmania	Australia
145692	3	shale	carbonaceous shale, with talc layers.	5366508N	357593E	In-house: Comsl	1:3000		123M/49	Tasmania	Australia
145693	4	talc/silicate	silica rich, talcose cap rock.	5386420N	357603E	In-house: Comsl	1:3000		123M/50	Tasmania	Australia
145694	5	talc	talc	5386660N	357590E	In-house: Comsl	1:3000		123M/51	Tasmania	Australia
145695	6	talc	quartz rich talc.	5360459N	357500E	In-house: Comsl	1:3000		123M/52	Tasmania	Australia
145696	7	talc	talc	5360672N	357582E	In-house: Comsl	1:3000		123M/53	Tasmania	Australia
145697	8	gal., sph., pyr.	interbedded sulphide ores, highly weathered.	5386689N	357657E	In-house: Comsl	1:3000		123M/54	Tasmania	Australia
145698	9	pyr.in talc	highly weathered ore in a ptly. silicified talcose host.	5360250N	357410E	In-house: Comsl	1:3000		123M/55	Tasmania	Australia
145699	10	pyrite	subhedral to euhedral	5360488N	357376E	In-house: Comsl	1:3000		123M/56	Tasmania	Australia
145700	11	gal., sph., pyr.	massive to subhedral	5360400N	357600E	In-house: Comsl	1:3000		123M/57	Tasmania	Australia
145701	12	sph.	massive, interspersed with pyrite and talc.	5360400N	357600E	In-house: Comsl	1:3000		123M/58	Tasmania	Australia
				5360400N	357600E	In-house: Comsl	1:3000		123M/59	Tasmania	Australia

Biostratigraphy (30 characters)	Lithostratigrapl (50 characters)	Supergroup (40 characters)	Group (35 characters)	Subgroup (25 characters)	Formation (30 characters)	Depositional environment ((30 characters)	Preps (25 characters)	Comment (unlimited l	Authors (75 characters)	Year Published (4 characters)	Title (200 characters)	Degree B.SC. (hons)
Late Precambriai	Late Precambrian				Upper Oonah Foma	Turbidite Sequence	R, CR		U. Meskanen	Unpub.	AMD at the Comstock Ag-Pb-Zn Mine	B.SC. (hons)
Late Precambriai	Late Precambrian				Upper Oonah Foma	Turbidite Sequence	R CR		U. Meskanen	Unpub.	AMD at the Comstock Ag-Pb-Zn Mine	B.SC. (hons)
Late Precambriai	Late Precambrian				Upper Oonah Foma	Turbidite Sequence	R, TS, CR		U. Meskanen	Unpub.	AMD at the Comstock Ag-Pb-Zn Mine	B.SC. (hons)
Late Precambriai	Late Precambrian				Upper Oonah Foma	Turbidite Sequence	R, TS, CR		U. Meskanen	Unpub.	AMD at the Comstock Ag-Pb-Zn Mine	B.SC. (hons)
Late Precambriai	Late Precambrian				Upper Oonah Foma	Turbidite Sequence	R, TS, CR		U. Meskanen	Unpub.	AMD at the Comstock Ag-Pb-Zn Mine	B.SC. (hons)
Late Precambriai	Late Precambrian				Upper Oonah Foma	Turbidite Sequence	R, TS, CR		U. Meskanen	Unpub.	AMD at the Comstock Ag-Pb-Zn Mine	B.SC. (hons)
Late Precambriai	Late Precambrian				Upper Oonah Foma	Turbidite Sequence	R, TS, CR		U. Meskanen	Unpub.	AMD at the Comstock Ag-Pb-Zn Mine	B.SC. (hons)
Late Precambriai	Late Precambrian				Upper Oonah Foma	Turbidite Sequence	R, TS, CR		U. Meskanen	Unpub.	AMD at the Comstock Ag-Pb-Zn Mine	B.SC. (hons)
Devonian	Devonian				Upper Oonah Foma	Turbidite Sequence	R, TS, CR		U. Meskanen	Unpub.	AMD at the Comstock Ag-Pb-Zn Mine	B.SC. (hons)
Devonian	Devonian				Upper Oonah Foma	Turbidite Sequence	R, CR		U. Meskanen	Unpub.	AMD at the Comstock Ag-Pb-Zn Mine	B.SC. (hons)
Devonian	Devonian				Upper Oonah Foma	Turbidite Sequence	R CR		U. Meskanen	Unpub.	AMD at the Comstock Ag-Pb-Zn Mine	B.SC. (hons)
Devonian	Devonian				Upper Oonah Foma	Turbidite Sequence	R,CR		U. Meskanen	Unpub.	AMD at the Comstock Ag-Pb-Zn Mine	B.SC. (hons)
Devonian	Devonian				Upper Oonah Foma	Turbidite Sequence	R,CR		U. Meskanen	Unpub.	AMD at the Comstock Ag-Pb-Zn Mine	B.SC. (hons)

Ca		
	Total	Dissolved
02.09.00 17:30	45.81	45.40
03.09.00 02:20	45.04	44.53
3:20	44.91	44.85
4:20	45.39	44.81
5:20	43.89	44.43
6:20	44.78	44.41
7:20	44.90	44.19
15:20	39.52	39.17
16:20	38.44	38.48

Cd		
	Total	Dissolved
02.09.00 17:30	0.02	0.02
03.09.00 02:20	0.02	0.02
3:20	0.02	0.01
4:20	0.03	0.02
5:20	0.02	0.02
6:20	0.02	0.03
7:20	0.02	0.02
15:20	0.02	0.02
16:20	0.01	0.02

Co		
	Total	Dissolved
02.09.00 17:30	0.04	0.04
03.09.00 02:20	0.04	0.05
3:20	0.04	0.05
4:20	0.05	0.04
5:20	0.05	0.03
6:20	0.04	0.04
7:20	0.03	0.04
15:20	0.03	0.04
16:20	0.04	0.04

Cr		
	Total	Dissolved
02.09.00 17:30	0.01	0.01
03.09.00 02:20	0.07	0.06
3:20	0.04	0.06
4:20	0.01	0.06
5:20	0.07	0.06
6:20	0.06	0.05
7:20	0.07	0.04
15:20	<.0000	0.02
16:20	0.04	0.04

P		
	Total	Dissolved
02.09.00 17:30	0.25	0.22
03.09.00 02:20	<.0000	<.0000
3:20	0.15	<.0000
4:20	0.16	<.0000
5:20	0.18	0.12
6:20	<.0000	0.12
7:20	0.13	<.0000
15:20	0.37	0.02
16:20	0.18	<.0000

Pb		
	Total	Dissolved
02.09.00 17:30	0.02	<.0000
03.09.00 02:20	0.11	0.00
3:20	0.17	0.03
4:20	0.16	<.0000
5:20	0.16	0.12
6:20	0.21	0.07
7:20	0.15	0.15
15:20	0.07	0.10
16:20	0.19	0.11

S		
	Total	Dissolved
02.09.00 17:30	96.44	98.56
03.09.00 02:20	100.60	101.80
3:20	100.60	103.20
4:20	97.75	102.30
5:20	100.80	104.00
6:20	101.00	103.70
7:20	99.74	103.30
15:20	83.82	88.24
16:20	86.54	88.64

Se		
	Total	Dissolved
02.09.00 17:30	0.07	<.0000
03.09.00 02:20	<.0000	<.0000
3:20	<.0000	<.0000
4:20	<.0000	<.0000
5:20	<.0000	<.0000
6:20	<.0000	<.0000
7:20	<.0000	<.0000
15:20	<.0000	<.0000
16:20	<.0000	<.0000

Cu		
	Total	Dissolved
02.09.00 17:30	<.0000	0.01
03.09.00 02:20	<.0000	<.0000
3:20	<.0000	<.0000
4:20	0.00	<.0000
5:20	0.02	0.00
6:20	<.0000	<.0000
7:20	<.0000	<.0000
15:20	<.0000	<.0000
16:20	<.0000	<.0000

Si		
	Total	Dissolved
02.09.00 17:30	7.87	7.83
03.09.00 02:20	7.88	7.72
3:20	7.80	7.73
4:20	7.86	7.69
5:20	7.62	7.58
6:20	7.67	7.74
7:20	7.74	7.49
15:20	7.19	6.94
16:20	6.94	6.80

Fe		
	Total	Dissolved
02.09.00 17:30	6.54	16.71
03.09.00 02:20	52.03	49.69
3:20	41.69	49.54
4:20	11.87	49.59
5:20	51.39	48.89
6:20	51.39	48.94
7:20	52.05	48.26
15:20	0.30	40.11
16:20	44.35	40.42

Sn		
	Total	Dissolved
02.09.00 17:30	0.05	0.05
03.09.00 02:20	0.18	<.0000
3:20	0.14	0.09
4:20	0.02	<.0000
5:20	0.01	0.11
6:20	0.15	0.10
7:20	0.12	0.05
15:20	0.07	0.09
16:20	0.04	0.06

K		
	Total	Dissolved
02.09.00 17:30	0.83	0.85
03.09.00 02:20	0.80	0.76
3:20	0.77	0.63
4:20	0.75	0.79
5:20	0.70	0.65
6:20	0.71	0.68
7:20	0.77	0.64
15:20	0.67	0.65
16:20	0.68	0.63

V		
	Total	Dissolved
02.09.00 17:30	<.0000	<.0000
03.09.00 02:20	0.02	0.01
3:20	<.0000	0.01
4:20	0.03	<.0000
5:20	0.01	<.0000
6:20	<.0000	0.02
7:20	<.0000	0.02
15:20	<.0000	0.02
16:20	<.0000	0.02

Mg		
	Total	Dissolved
02.09.00 17:30	28.41	28.63
03.09.00 02:20	28.20	28.58
3:20	23.13	23.23
4:20	28.59	28.56
5:20	28.33	23.20
6:20	28.16	28.46
7:20	28.50	22.78
15:20	20.33	20.24
16:20	20.10	25.37

Zn		
	Total	Dissolved
02.09.00 17:30	25.62	25.30
03.09.00 02:20	25.64	25.42
3:20	25.74	25.72
4:20	26.34	25.58
5:20	25.93	25.72
6:20	25.52	25.63
7:20	25.40	25.39
15:20	21.27	20.94
16:20	21.00	21.11

Appendix 6:

Mass Loading Calculations for Storm Sampling.

At what sampling point?

Appendix 6

Mass Loading Calculations for total and dissolved elements in a storm event.

Al	Total	Water Flow (m3/s)	Mass Load (g/s)	Mass Loading (t/y)	Dissolved	Mass Load (g/s)	Mass Loading (t/y)
02.09.00 17:30	1.68	159.00	267.76	8.44	0.47	74.92	0.24
03.09.00 02:20	1.76	170.90	299.93	9.46	0.45	76.89	0.24
0.14	1.86	151.10	280.44	8.84	0.52	78.07	0.25
0.18	1.73	170.90	295.49	9.32	0.54	92.66	0.29
0.22	1.70	223.00	378.65	11.94	0.53	117.77	0.37
0.26	1.81	126.85	229.85	7.25	0.35	44.55	0.14
0.31	1.71	118.80	203.15	6.41	0.60	71.07	0.22
0.64	1.52	201.35	305.85	9.65	0.50	101.16	0.32
0.68	1.68	201.35	338.67	10.68	0.46	92.86	0.29

As	Total	Water Flow (m3/s)	Mass Load (g/s)	Mass Loading (t/y)	Dissolved	Mass Load (g/s)	Mass Loading (t/y)
02.09.00 17:30	0.01	159.00	1.84	0.06	0.31	48.84	0.15
03.09.00 02:20	0.18	170.90	31.48	0.99	0.24	40.26	0.13
0.14	0.21	151.10	31.93	1.01	0.37	55.88	0.18
0.18	0.10	170.90	16.90	0.53	0.34	57.99	0.18
0.22	0.43	223.00	96.87	3.05	0.25	56.13	0.18
0.26	0.31	126.85	39.10	1.23	0.31	39.60	0.12
0.31	0.26	118.80	31.11	0.98	0.35	41.95	0.13
0.64	0.09	201.35	17.52	0.55	0.36	73.37	0.23
0.68	0.29	201.35	57.79	1.82	0.32	64.43	0.20

B	Total	Water Flow (m3/s)	Mass Load (g/s)	Mass Loading (t/y)	Dissolved	Mass Load (g/s)	Mass Loading (t/y)
02.09.00 17:30	0.04	159.00	7.04	0.22	0.05	8.22	0.03
03.09.00 02:20	0.13	170.90	22.56	0.71	0.12	21.12	0.07
0.14	0.11	151.10	15.88	0.50	0.12	18.63	0.06
0.18	0.04	170.90	7.47	0.24	0.12	20.56	0.06
0.22	0.13	223.00	28.16	0.89	0.12	26.43	0.08
0.26	0.13	126.85	16.36	0.52	0.12	14.98	0.05
0.31	0.13	118.80	15.21	0.48	0.12	13.94	0.04
0.64	0.01	201.35	1.75	0.06	0.09	17.98	0.06
0.68	0.11	201.35	22.61	0.71	0.10	20.30	0.06

Ba	Total	Water Flow (m3/s)	Mass Load (g/s)	Mass Loading (t/y)	Dissolved	Mass Load (g/s)	Mass Loading (t/y)
02.09.00 17:30	0.05	159.00	7.23	0.23	0.04	7.08	0.02
03.09.00 02:20	0.05	170.90	8.05	0.25	0.04	7.57	0.02
0.14	0.04	151.10	5.74	0.18	0.05	7.03	0.02
0.18	0.05	170.90	7.78	0.25	0.04	6.68	0.02
0.22	0.04	223.00	9.63	0.30	0.04	10.01	0.03
0.26	0.05	126.85	5.85	0.18	0.04	5.52	0.02
0.31	0.05	118.80	5.48	0.17	0.04	4.95	0.02
0.64	0.04	201.35	7.05	0.22	0.04	8.88	0.03
0.68	0.04	201.35	7.73	0.24	0.04	7.49	0.02

Ca	Total	Water Flow (m3/s)	Mass Load (g/s)	Mass Loading (t/y)	Dissolved	Mass Load (g/s)	Mass Loading (t/y)
02.09.00 17:30	45.81	159.00	7283.79	229.70	45.40	7218.60	22.78
03.09.00 02:20	45.04	170.90	7697.34	242.74	44.53	7610.18	24.02
0.14	44.91	151.10	6785.90	214.00	44.85	6776.84	21.39
0.18	45.39	170.90	7757.15	244.63	44.81	7658.03	24.17
0.22	43.89	223.00	9787.47	308.66	44.43	9907.89	31.27
0.26	44.78	126.85	5680.34	179.14	44.41	5633.41	17.78
0.31	44.90	118.80	5334.12	168.22	44.19	5249.77	16.57
0.64	39.52	201.35	7957.35	250.94	39.17	7886.88	24.89
0.68	38.44	201.35	7739.89	244.09	38.48	7747.95	24.45

Cd	Total	Water Flow (m3/s)	Mass Load (g/s)	Mass Loading (t/y)	Dissolved	Mass Load (g/s)	Mass Loading (t/y)
02.09.00 17:30	0.02	159.00	2.80	0.09	0.02	3.34	0.01
03.09.00 02:20	0.02	170.90	3.23	0.10	0.02	2.75	0.01
0.14	0.02	151.10	3.67	0.12	0.01	2.09	0.01
0.18	0.03	170.90	4.36	0.14	0.02	3.02	0.01
0.22	0.02	223.00	3.75	0.12	0.02	3.61	0.01
0.26	0.02	126.85	2.27	0.07	0.03	3.26	0.01
0.31	0.02	118.80	1.78	0.06	0.02	2.58	0.01
0.64	0.02	201.35	4.17	0.13	0.02	4.21	0.01
0.68	0.01	201.35	2.64	0.08	0.02	4.29	0.01

Co	Total	Water Flow (m3/s)	Mass Load (g/s)	Mass Loading (t/y)	Dissolved	Mass Load (g/s)	Mass Loading (t/y)
02.09.00 17:30	0.04	159.00	7.12	0.22	0.04	6.73	0.02
03.09.00 02:20	0.04	170.90	7.30	0.23	0.05	8.73	0.03
0.14	0.04	151.10	6.74	0.21	0.05	7.77	0.02
0.18	0.05	170.90	7.91	0.25	0.04	6.53	0.02
0.22	0.05	223.00	10.15	0.32	0.03	7.45	0.02
0.26	0.04	126.85	4.92	0.16	0.04	5.68	0.02
0.31	0.03	118.80	4.11	0.13	0.04	4.94	0.02
0.64	0.03	201.35	5.90	0.19	0.04	8.42	0.03
0.68	0.04	201.35	7.73	0.24	0.04	8.54	0.03

Cr	Total	Water Flow (m3/s)	Mass Load (g/s)	Mass Loading (t/y)	Dissolved	Mass Load (g/s)	Mass Loading (t/y)
02.09.00 17:30	0.01	159.00	1.65	0.05	0.01	1.91	0.01
03.09.00 02:20	0.07	170.90	12.78	0.40	0.06	10.58	0.03
0.14	0.04	151.10	5.94	0.19	0.06	9.08	0.03
0.18	0.01	170.90	2.32	0.07	0.06	9.96	0.03
0.22	0.07	223.00	16.39	0.52	0.06	12.27	0.04
0.26	0.06	126.85	8.12	0.26	0.05	6.65	0.02
0.31	0.07	118.80	7.76	0.24	0.04	4.69	0.01
0.64	<.0000	201.35	0.00	0.00	0.02	4.17	0.01
0.68	0.04	201.35	8.86	0.28	0.04	8.90	0.03

Fe	Total	Water Flow (m3/s)	Mass Load (g/s)	Mass Loading (t/y)	Dissolved	Mass Load (g/s)	Mass Loading (t/y)
02.09.00 17:30	6.54	159.00	1039.70	32.79	16.71	2656.89	8.39
03.09.00 02:20	52.03	170.90	8891.93	280.42	49.69	8492.02	26.80
0.14	41.69	151.10	6299.36	198.66	49.54	7485.49	23.62
0.18	11.87	170.90	2028.58	63.97	49.59	8474.93	26.75
0.22	51.39	223.00	11459.97	361.40	48.89	10902.47	34.41
0.26	51.39	126.85	6518.82	205.58	48.94	6208.04	19.59
0.31	52.05	118.80	6183.54	195.00	48.26	5733.29	18.09
0.64	0.30	201.35	60.55	1.91	40.11	8076.15	25.49
0.68	44.35	201.35	8929.87	281.61	40.42	8138.57	25.69

K	Total	Water Flow (m3/s)	Mass Load (g/s)	Mass Loading (t/y)	Dissolved	Mass Load (g/s)	Mass Loading (t/y)
02.09.00 17:30	0.83	159.00	131.67	4.15	0.85	134.63	0.42
03.09.00 02:20	0.80	170.90	137.44	4.33	0.76	129.32	0.41
0.14	0.77	151.10	116.94	3.69	0.63	94.75	0.30
0.18	0.75	170.90	128.48	4.05	0.79	134.72	0.43
0.22	0.70	223.00	157.15	4.96	0.65	145.26	0.46
0.26	0.71	126.85	90.39	2.85	0.68	86.59	0.27
0.31	0.77	118.80	91.77	2.89	0.64	75.63	0.24
0.64	0.67	201.35	135.69	4.28	0.65	130.23	0.41
0.68	0.68	201.35	137.76	4.34	0.63	127.19	0.40

Mg	Total	Water Flow (m3/s)	Mass Load (g/s)	Mass Loading (t/y)	Dissolved	Mass Load (g/s)	Mass Loading (t/y)
02.09.00 17:30	28.41	159.00	4517.19	142.45	28.63	4552.17	14.37
03.09.00 02:20	28.20	170.90	4819.38	151.98	28.58	4884.32	15.41
0.14	23.13	151.10	3494.94	110.22	23.23	3510.05	11.08
0.18	28.59	170.90	4886.03	154.09	28.56	4880.90	15.40
0.22	28.33	223.00	6317.59	199.23	23.20	5173.60	16.33
0.26	28.16	126.85	3572.10	112.65	28.46	3610.15	11.39
0.31	28.50	118.80	3385.80	106.77	22.78	2706.26	8.54
0.64	20.33	201.35	4093.45	129.09	20.24	4075.32	12.86
0.68	20.10	201.35	4047.14	127.63	25.37	5108.25	16.12

Mn	Total	Water Flow (m3/s)	Mass Load (g/s)	Mass Loading (t/y)	Dissolved	Mass Load (g/s)	Mass Loading (t/y)
02.09.00 17:30	8.43	159.00	1339.89	42.25	8.30	1319.54	4.16
03.09.00 02:20	8.31	170.90	1420.01	44.78	8.34	1424.96	4.50
0.14	8.42	151.10	1272.26	40.12	8.42	1272.72	4.02
0.18	8.53	170.90	1457.26	45.96	8.34	1425.48	4.50
0.22	8.43	223.00	1880.56	59.31	8.47	1888.59	5.96
0.26	8.34	126.85	1058.06	33.37	8.39	1064.65	3.36
0.31	8.28	118.80	984.14	31.04	8.36	992.81	3.13
0.64	7.11	201.35	1432.20	45.17	7.01	1410.66	4.45
0.68	7.00	201.35	1408.85	44.43	7.09	1428.38	4.51

P	Total	Water Flow (m3/s)	Mass Load (g/s)	Mass Loading (t/y)	Dissolved	Mass Load (g/s)	Mass Loading (t/y)
02.09.00 17:30	0.25	159.00	39.11	1.23	0.22	34.53	0.11
03.09.00 02:20	<.0000	170.90	0.00	0.00	<.0000	0.00	0.00
0.14	0.15	151.10	22.29	0.70	<.0000	0.00	0.00
0.18	0.16	170.90	27.10	0.85	<.0000	0.00	0.00
0.22	0.18	223.00	41.21	1.30	0.12	26.51	0.08
0.26	<.0000	126.85	0.00	0.00	0.12	15.84	0.05
0.31	0.13	118.80	15.23	0.48	<.0000	0.00	0.00
0.64	0.37	201.35	74.40	2.35	0.02	3.87	0.01
0.68	0.18	201.35	36.42	1.15	<.0000	0.00	0.00

Pb	Total	Water Flow (m3/s)	Mass Load (g/s)	Mass Loading (t/y)	Dissolved	Mass Load (g/s)	Mass Loading (t/y)
02.09.00 17:30	0.02	159.00	3.02	0.10	<.0000	0.00	0.00
03.09.00 02:20	0.11	170.90	19.23	0.61	0.00	0.80	0.00
0.14	0.17	151.10	26.17	0.83	0.03	5.08	0.02
0.18	0.16	170.90	28.04	0.88	<.0000	0.00	0.00
0.22	0.16	223.00	34.85	1.10	0.12	27.63	0.09
0.26	0.21	126.85	26.11	0.82	0.07	8.52	0.03
0.31	0.15	118.80	17.99	0.57	0.15	17.68	0.06
0.64	0.07	201.35	14.46	0.46	0.10	19.77	0.06
0.68	0.19	201.35	38.88	1.23	0.11	21.77	0.07

S	Total	Water Flow (m3/s)	Mass Load (g/s)	Mass Loading (t/y)	Dissolved	Mass Load (g/s)	Mass Loading (t/y)
02.09.00 17:30	96.44	159.00	15333.96	483.57	98.56	15671.04	49.46
03.09.00 02:20	100.60	170.90	17192.54	542.18	101.80	17397.62	54.91
0.14	100.60	151.10	15200.66	479.37	103.20	15593.52	49.21
0.18	97.75	170.90	16705.48	526.82	102.30	17483.07	55.18
0.22	100.80	223.00	22478.40	708.88	104.00	23192.00	73.19
0.26	101.00	126.85	12811.85	404.03	103.70	13154.35	41.52
0.31	99.74	118.80	11849.11	373.67	103.30	12272.04	38.73
0.64	83.82	201.35	16877.16	532.24	88.24	17767.12	56.07
0.68	86.54	201.35	17424.83	549.51	88.64	17847.66	56.33

Mo	Total	Water Flow (m3/s)	Mass Load (g/s)	Mass Loading (t/y)	Dissolved	Mass Load (g/s)	Mass Loading (t/y)
02.09.00 17:30	0.08	159.00	12.48	0.39	<.0000	0.00	0.00
03.09.00 02:20	0.03	170.90	4.34	0.14	0.04	7.37	0.02
0.14	0.02	151.10	3.38	0.11	0.04	5.41	0.02
0.18	0.04	170.90	6.41	0.20	0.06	9.90	0.03
0.22	0.02	223.00	4.71	0.15	0.03	6.00	0.02
0.26	<.0000	126.85	0.00	0.00	0.03	3.78	0.01
0.31	0.03	118.80	3.46	0.11	0.03	3.60	0.01
0.64	0.06	201.35	11.82	0.37	0.04	7.39	0.02
0.68	0.04	201.35	7.43	0.23	0.03	6.34	0.02

Na	Total	Water Flow (m3/s)	Mass Load (g/s)	Mass Loading (t/y)	Dissolved	Mass Load (g/s)	Mass Loading (t/y)
02.09.00 17:30	8.89	159.00	1413.35	44.57	8.95	1422.57	4.49
03.09.00 02:20	8.75	170.90	1495.55	47.16	8.78	1500.84	4.74
0.14	8.18	151.10	1236.45	38.99	8.26	1248.54	3.94
0.18	8.72	170.90	1489.91	46.99	8.72	1490.42	4.70
0.22	8.54	223.00	1903.97	60.04	8.19	1827.26	5.77
0.26	8.59	126.85	1089.26	34.35	8.68	1100.80	3.47
0.31	8.67	118.80	1029.40	32.46	8.15	968.70	3.06
0.64	8.41	201.35	1693.96	53.42	8.20	1650.06	5.21
0.68	8.22	201.35	1654.49	52.18	8.69	1750.54	5.52

Ni	Total	Water Flow (m3/s)	Mass Load (g/s)	Mass Loading (t/y)	Dissolved	Mass Load (g/s)	Mass Loading (t/y)
02.09.00 17:30	0.06	159.00	9.35	0.29	0.05	8.32	0.03
03.09.00 02:20	0.07	170.90	11.18	0.35	0.05	8.02	0.03
0.14	0.05	151.10	7.84	0.25	0.05	7.25	0.02
0.18	0.05	170.90	8.68	0.27	0.08	12.85	0.04
0.22	0.06	223.00	13.22	0.42	0.06	13.71	0.04
0.26	0.05	126.85	6.49	0.20	0.06	7.36	0.02
0.31	0.05	118.80	6.14	0.19	0.07	8.43	0.03
0.64	0.05	201.35	10.65	0.34	0.05	9.95	0.03
0.68	0.04	201.35	8.68	0.27	0.04	8.44	0.03

Si	Total	Water Flow (m3/s)	Mass Load (g/s)	Mass Loading (t/y)	Dissolved	Mass Load (g/s)	Mass Loading (t/y)
02.09.00 17:30	7.87	159.00	1251.81	39.48	7.83	1245.61	3.93
03.09.00 02:20	7.88	170.90	1346.35	42.46	7.72	1319.18	4.16
0.14	7.80	151.10	1178.13	37.15	7.73	1167.85	3.69
0.18	7.86	170.90	1342.59	42.34	7.69	1314.56	4.15
0.22	7.62	223.00	1700.15	53.62	7.58	1690.56	5.34
0.26	7.67	126.85	973.45	30.70	7.74	981.18	3.10
0.31	7.74	118.80	919.51	29.00	7.49	889.69	2.81
0.64	7.19	201.35	1447.30	45.64	6.94	1398.17	4.41
0.68	6.94	201.35	1396.36	44.04	6.80	1368.37	4.32

Sn	Total	Water Flow (m3/s)	Mass Load (g/s)	Mass Loading (t/y)	Dissolved	Mass Load (g/s)	Mass Loading (t/y)
02.09.00 17:30	0.05	159.00	8.22	0.26	0.05	7.19	0.02
03.09.00 02:20	0.18	170.90	30.35	0.96	<.0000	0.00	0.00
0.14	0.14	151.10	20.67	0.65	0.09	12.96	0.04
0.18	0.02	170.90	3.93	0.12	<.0000	0.00	0.00
0.22	0.01	223.00	1.83	0.06	0.11	25.09	0.08
0.26	0.15	126.85	19.36	0.61	0.10	13.19	0.04
0.31	0.12	118.80	14.81	0.47	0.05	6.50	0.02
0.64	0.07	201.35	13.49	0.43	0.09	17.40	0.05
0.68	0.04	201.35	8.76	0.28	0.06	12.58	0.04

Zn	Total	Water Flow (m3/s)	Mass Load (g/s)	Mass Loading (t/y)	Dissolved	Mass Load (g/s)	Mass Loading (t/y)
02.09.00 17:30	25.62	159.00	4073.58	128.46	25.30	4022.70	12.70
03.09.00 02:20	25.64	170.90	4381.88	138.19	25.42	4344.28	13.71
0.14	25.74	151.10	3889.31	122.65	25.72	3886.29	12.27
0.18	26.34	170.90	4501.51	141.96	25.58	4371.62	13.80
0.22	25.93	223.00	5782.39	182.35	25.72	5735.56	18.10
0.26	25.52	126.85	3237.21	102.09	25.63	3251.17	10.26
0.31	25.40	118.80	3017.52	95.16	25.39	3016.33	9.52
0.64	21.27	201.35	4282.71	135.06	20.94	4216.27	13.31
0.68	21.00	201.35	4228.35	133.35	21.11	4250.50	13.41

SO4	Water Flow (m3/s)	Mass Load (g/s)	Mass Loading (t/y)
02.09.00 17:30	330.00	159.00	52470.00	1654.69
03.09.00 02:20	360.00	170.90	61524.00	1940.22
0.14	380.00	151.10	57418.00	1810.73
0.18	380.00	170.90	64942.00	2048.01
0.22	390.00	223.00	86970.00	2742.69
0.26	400.00	126.85	50740.00	1600.14
0.31	400.00	118.80	47520.00	1498.59
0.64	340.00	201.35	68459.00	2158.92
0.68	330.00	201.35	66445.50	2095.43

Appendix 7:

Geochemical Modelling: Input and Output Data for PHREEQC.

Reading data base.

SOLUTION_MASTER_SPECIES
SOLUTION_SPECIES
PHASES
EXCHANGE_MASTER_SPECIES
EXCHANGE_SPECIES
SURFACE_MASTER_SPECIES
SURFACE_SPECIES
END

Reading input data for simulation 1

TITLE Example 1.dry main adit
SOLUTION 1 dry main adit

units	ppm
pH	6.04
pe	17.79
density	1
temp	10.3
Ca	9.41
Fe	6.14
K	0.63
Mg	6.24
Mn	6.31
Na	7.76
Si	4.09
Zn	2.1
Cl	12.84
S(6)	22.24

SOLUTION_MASTER_SPECIES
SOLUTION_SPECIES
PHASES
END

TITLE

Example 1.dry main adit

Beginning of initial solution calculations.

Initial solution 1 dry main adit

#NAME? composition

Elements	Molality	Moles
Ca	2.37E-04	2.37E-04
Cl	3.54E-04	3.54E-04
Fe	1.06E-04	1.06E-04
K	1.61E-05	1.61E-05
Mg	2.59E-04	2.59E-04
Mn	1.11E-04	1.11E-04
Na	3.38E-04	3.38E-04
S(6)	2.26E-04	2.26E-04
Si	6.81E-05	6.81E-05
Zn	3.24E-05	3.24E-05

#NAME? of solution

pH	=	6.04		
pe	=	17.79		
Activity of	water	=	0.1	
Ionic	strength	=	2.10E-03	
Mass of	water	(kg)	=	1.00E+00
Total	alkalinity	(eq/kg)	=	-6.11E-05
Total	carbon	(mol/kg)	=	0.00E+00
Total	CO2	(mol/kg)	=	0.00E+00
Temperatu	(deg	C)	=	10.3
Electrical	balance	(eq)	=	9.24E-04
Iterations	=	101		
Total	H	=	1.11E+02	
Total	O	=	3.17E+02	

#NAME? of species

	Log Species	Log Molality	Log Activity	Molality	Activity	Gamma
	H+	9.55E-07	9.12E-07	-6.02	-6.04	-0.02
	OH-	3.46E-10	3.29E-10	-9.461	-9.482	-0.022
	H2O	5.55E+01	1.00E-01	-1	-1	0
Ca	2.37E-04					
	Ca+2	2.31E-04	1.90E-04	-3.636	-3.721	-0.085
	CaSO4	5.70E-06	5.70E-06	-5.244	-5.244	0
	CaHSO4+	2.74E-11	2.61E-11	-10.563	-10.584	-0.022
	CaOH+	3.64E-12	3.46E-12	-11.439	-11.461	-0.022
Cl	3.54E-04					
	Cl-	3.54E-04	3.37E-04	-3.451	-3.473	-0.022
	MnCl+	1.23E-07	1.17E-07	-6.911	-6.933	-0.022
	ZnCl+	1.24E-08	1.18E-08	-7.906	-7.928	-0.022
	FeCl+2	1.25E-10	1.03E-10	-9.903	-9.989	-0.086
	ZnOHCl	3.15E-11	3.15E-11	-10.502	-10.502	0
	MnCl2	1.71E-11	1.71E-11	-10.766	-10.766	0
	ZnCl2	3.91E-12	3.91E-12	-11.408	-11.408	0
	FeCl2+	2.65E-13	2.52E-13	-12.577	-12.599	-0.022
	MnCl3-	1.67E-15	1.59E-15	-14.777	-14.799	-0.022
	ZnCl3-	1.41E-15	1.35E-15	-14.849	-14.871	-0.022
	FeCl+	3.19E-16	3.03E-16	-15.496	-15.518	-0.022
	FeCl3	8.47E-18	8.47E-18	-17.072	-17.072	0
	ZnCl4-2	2.45E-19	2.01E-19	-18.611	-18.697	-0.086
Fe(2)	8.12E-13					
	Fe+2	7.97E-13	6.53E-13	-12.099	-12.185	-0.086
	FeSO4	1.52E-14	1.52E-14	-13.818	-13.818	0
	FeCl+	3.19E-16	3.03E-16	-15.496	-15.518	-0.022
	FeOH+	7.50E-18	7.13E-18	-17.125	-17.147	-0.022
	FeHSO4+	9.41E-20	8.95E-20	-19.026	-19.048	-0.022
	Fe(OH)2	1.73E-24	1.74E-24	-23.761	-23.761	0
	Fe(OH)3-	6.38E-30	6.07E-30	-29.195	-29.217	-0.022
Fe(3)	1.06E-04					

Reading data base.

SOLUTION_MASTER_SPECIES
SOLUTION_SPECIES
PHASES
EXCHANGE_MASTER_SPECIES
EXCHANGE_SPECIES
SURFACE_MASTER_SPECIES
SURFACE_SPECIES
END

Reading input data for simulation 1

TITLE Example 1.wet main adit
SOLUTION 1 wet main adit

units	ppm
pH	4.97
pe	3.31
density	1
temp	10.5
Al	1.15
Ca	15.94
Fe	19.8
Mg	8.81
Na	7.71
Mn	2.78
Si	3.25
Zn	13.59
Cl	10
S(6)	5.8
S(-2)	43.09

SOLUTION_MASTER_SPECIES
SOLUTION_SPECIES
PHASES
END

TITLE

Example 1.wet main adit

Beginning of initial solution calculations.

Initial solution 1 wet main adit

#NAME? composition

Elements	Molality	Moles
Al	4.26E-05	4.26E-05
Ca	3.98E-04	3.98E-04
Cl	2.82E-04	2.82E-04
Fe	3.55E-04	3.55E-04
Mg	3.62E-04	3.62E-04
Mn	5.06E-05	5.06E-05
Na	3.35E-04	3.35E-04
S(-2)	1.34E-03	1.34E-03
S(6)	6.04E-05	6.04E-05
Si	5.41E-05	5.41E-05
Zn	2.08E-04	2.08E-04

#NAME? of solution

pH	=	4.97		
pe	=	3.31		
Activity of	water	=	1	
Ionic	strength	=	2.88E-03	
Mass of	water	(kg)	=	1.00E+00
Total	alkalinity	(eq/kg)	=	4.38E-04
Total	carbon	(mol/kg)	=	0.00E+00
Total	CO2	(mol/kg)	=	0.00E+00
Temperatu	(deg	C)	=	10.5
Electrical	balance	(eq)	=	2.37E-03
Iterations	=	8		
Total	H	=	1.11E+02	
Total	O	=	5.55E+01	

#NAME? couples

Redox	couple	pe	Eh	(volts)
S(-2)/S(6)	-0.9927	-0.0559		

#NAME? of species

	Log Species	Log Molality	Log Activity	Molality	Activity	Gamma
	H+	1.13E-05	1.07E-05	-4.947	-4.97	-0.023
	OH-	3.02E-10	2.85E-10	-9.52	-9.545	-0.025
	H2O	5.55E+01	1.00E+00	0	0	0
Al	4.26E-05					
	Al+3	3.11E-05	1.85E-05	-4.508	-4.733	-0.225
	AlOH+2	8.16E-06	6.48E-06	-5.088	-5.188	-0.1
	AlSO4+	2.12E-06	2.00E-06	-5.674	-5.699	-0.025
	Al(OH)2+	1.26E-06	1.19E-06	-5.899	-5.924	-0.025
	Al(OH)3	5.03E-09	5.03E-09	-8.298	-8.298	0
	Al(SO4)2-	2.60E-09	2.48E-09	-8.585	-8.61	-0.025
	Al(OH)4-	8.21E-10	7.75E-10	-9.086	-9.111	-0.025
	AlHSO4+2	2.17E-12	1.72E-12	-11.664	-11.764	-0.1
Ca	3.98E-04					
	Ca+2	3.96E-04	3.16E-04	-3.403	-3.501	-0.098
	CaSO4	2.27E-06	2.27E-06	-5.644	-5.643	0
	CaHSO4+	1.30E-10	1.22E-10	-9.886	-9.913	-0.025
	CaOH+	5.18E-12	4.89E-12	-11.286	-11.311	-0.025
Cl	2.82E-04					
	Cl-	2.82E-04	2.66E-04	-3.55	-3.575	-0.025
	FeCl+	1.07E-07	1.01E-07	-6.973	-6.998	-0.025
	MnCl+	4.59E-08	4.33E-08	-7.338	-7.363	-0.025
	MnCl2	5.03E-12	5.03E-12	-11.298	-11.298	0
	ZnCl+	2.68E-12	2.53E-12	-11.572	-11.597	-0.025

	Fe(OH)2+	9.97E-05	9.49E-05	-4.001	-4.023	-0.022
	FeOH+2	5.73E-08	4.70E-08	-5.242	-5.328	-0.086
	Fe(OH)3	6.83E-07	6.83E-07	-6.166	-6.166	0
	Fe+3	2.58E-08	1.65E-08	-7.589	-7.783	-0.194
	FeSO4+	2.34E-08	2.23E-08	-7.63	-7.652	-0.022
	Fe2(OH)2+	2.49E-09	1.13E-09	-8.604	-8.949	-0.345
	Fe3(OH)4+	3.21E-10	9.29E-11	-9.493	-10.032	-0.539
	FeCl+2	1.25E-10	1.03E-10	-9.903	-9.989	-0.086
	Fe(SO4)2-	8.37E-11	7.97E-11	-10.077	-10.099	-0.022
	Fe(OH)4-	3.86E-11	3.67E-11	-10.414	-10.436	-0.022
	FeCl2+	2.65E-13	2.52E-13	-12.577	-12.599	-0.022
	FeHSO4+2	6.92E-14	5.68E-14	-13.16	-13.246	-0.086
	FeCl3	8.47E-18	8.47E-18	-17.072	-17.072	0
H(0)	0.00E+00					
	H2	0.00E+00	0.00E+00	-50.794	-50.794	0
K	1.61E-05					
	K+	1.61E-05	1.53E-05	-4.792	-4.814	-0.022
	KSO4-	1.50E-08	1.43E-08	-7.824	-7.845	-0.022
Mg	2.59E-04					
	Mg+2	2.53E-04	2.09E-04	-3.597	-3.681	-0.084
	MgSO4	5.70E-06	5.70E-06	-5.244	-5.244	0
	MgOH+	2.16E-11	2.06E-11	-10.666	-10.687	-0.022
Mn(2)	1.06E-04					
	Mn+2	1.04E-04	8.51E-05	-3.984	-4.07	-0.086
	MnSO4	1.96E-06	1.96E-06	-5.709	-5.709	0
	MnCl+	1.23E-07	1.17E-07	-6.911	-6.933	-0.022
	MnOH+	7.15E-11	6.80E-11	-10.146	-10.167	-0.022
	MnCl2	1.71E-11	1.71E-11	-10.766	-10.766	0
	MnCl3-	1.67E-15	1.59E-15	-14.777	-14.799	-0.022
	Mn(OH)3-	1.87E-24	1.78E-24	-23.728	-23.75	-0.022
Mn(3)	2.65E-13					
	Mn+3	2.65E-13	1.70E-13	-12.577	-12.771	-0.194
Mn(6)	2.26E-13					
	MnO4-2	2.26E-13	1.85E-13	-12.646	-12.733	-0.086
Mn(7)	4.83E-06					
	MnO4-	4.83E-06	4.59E-06	-5.316	-5.338	-0.022
Na	3.38E-04					
	Na+	3.38E-04	3.22E-04	-3.471	-3.493	-0.021
	NaSO4-	2.67E-07	2.54E-07	-6.574	-6.596	-0.022
O(0)	2.61E+02					
	O2	1.31E+02	1.31E+02	2.116	2.116	0
S(6)	2.26E-04					
	SO4-2	2.11E-04	1.74E-04	-3.675	-3.761	-0.085
	CaSO4	5.70E-06	5.70E-06	-5.244	-5.244	0
	MgSO4	5.70E-06	5.70E-06	-5.244	-5.244	0
	MnSO4	1.96E-06	1.96E-06	-5.709	-5.709	0
	ZnSO4	9.31E-07	9.32E-07	-6.031	-6.031	0
	NaSO4-	2.67E-07	2.54E-07	-6.574	-6.596	-0.022
	FeSO4+	2.34E-08	2.23E-08	-7.63	-7.652	-0.022
	KSO4-	1.50E-08	1.43E-08	-7.824	-7.845	-0.022
	HSO4-	1.20E-08	1.14E-08	-7.922	-7.943	-0.022
	Zn(SO4)2-2	1.81E-09	1.48E-09	-8.743	-8.83	-0.086
	Fe(SO4)2-	8.37E-11	7.97E-11	-10.077	-10.099	-0.022
	CaHSO4+	2.74E-11	2.61E-11	-10.563	-10.584	-0.022
	FeHSO4+2	6.92E-14	5.68E-14	-13.16	-13.246	-0.086
	FeSO4	1.52E-14	1.52E-14	-13.818	-13.818	0
	FeHSO4+	9.41E-20	8.95E-20	-19.026	-19.048	-0.022
Si	6.81E-05					
	H4SiO4	6.81E-05	6.81E-05	-4.167	-4.167	0
	H3SiO4-	6.58E-09	6.26E-09	-8.182	-8.203	-0.022
	H2SiO4-2	2.00E-16	1.64E-16	-15.698	-15.785	-0.086
Zn	3.24E-05					
	Zn+2	3.15E-05	2.58E-05	-4.502	-4.588	-0.086
	ZnSO4	9.31E-07	9.32E-07	-6.031	-6.031	0
	ZnCl+	1.24E-08	1.18E-08	-7.906	-7.928	-0.022
	Zn(SO4)2-2	1.81E-09	1.48E-09	-8.743	-8.83	-0.086
	ZnOH+	1.01E-09	9.60E-10	-8.996	-9.018	-0.022
	ZnOHCl	3.15E-11	3.15E-11	-10.502	-10.502	0
	ZnCl2	3.91E-12	3.91E-12	-11.408	-11.408	0
	Zn(OH)2	3.90E-12	3.90E-12	-11.409	-11.408	0
	ZnCl3-	1.41E-15	1.35E-15	-14.849	-14.871	-0.022
	Zn(OH)3-	1.42E-18	1.35E-18	-17.847	-17.868	-0.022
	ZnCl4-2	2.45E-19	2.01E-19	-18.611	-18.697	-0.086
	Zn(OH)4-2	2.87E-26	2.35E-26	-25.542	-25.628	-0.086

	ZnOHCl	5.68E-15	5.69E-15	-14.245	-14.245	0
	ZnCl2	6.62E-16	6.63E-16	-15.179	-15.179	0
	MnCl3-	3.91E-16	3.69E-16	-15.408	-15.433	-0.025
	FeCl+2	1.44E-16	1.15E-16	-15.84	-15.94	-0.1
	FeCl2+	2.34E-19	2.21E-19	-18.631	-18.656	-0.025
	ZnCl3-	1.91E-19	1.81E-19	-18.718	-18.743	-0.025
	ZnCl4-2	2.69E-23	2.13E-23	-22.571	-22.671	-0.1
	FeCl3	5.88E-24	5.88E-24	-23.231	-23.231	0
Fe(2)	3.55E-04					
	Fe+2	3.45E-04	2.74E-04	-3.463	-3.563	-0.1
	Fe(HS)2	8.42E-06	8.42E-06	-5.075	-5.075	0
	FeSO4	1.53E-06	1.53E-06	-5.815	-5.814	0
	FeCl+	1.07E-07	1.01E-07	-6.973	-6.998	-0.025
	Fe(HS)3-	5.71E-09	5.39E-09	-8.244	-8.269	-0.025
	FeOH+	2.74E-09	2.59E-09	-8.562	-8.587	-0.025
	FeHSO4+	1.12E-10	1.06E-10	-9.949	-9.974	-0.025
	Fe(OH)2	5.45E-16	5.46E-16	-15.263	-15.263	0
	Fe(OH)3-	1.73E-21	1.63E-21	-20.763	-20.788	-0.025
Fe(3)	1.12E-10					
	Fe(OH)2+	1.04E-10	9.86E-11	-9.981	-10.006	-0.025
	FeOH+2	7.18E-12	5.69E-12	-11.145	-11.245	-0.1
	Fe(OH)3	6.09E-13	6.10E-13	-12.215	-12.215	0
	Fe+3	3.89E-14	2.32E-14	-13.41	-13.635	-0.225
	FeSO4+	7.99E-15	7.54E-15	-14.098	-14.123	-0.025
	FeCl+2	1.44E-16	1.15E-16	-15.84	-15.94	-0.1
	Fe(OH)4-	2.98E-17	2.81E-17	-16.526	-16.551	-0.025
	Fe(SO4)2-	6.85E-18	6.47E-18	-17.164	-17.189	-0.025
	FeHSO4+2	2.84E-19	2.25E-19	-18.547	-18.647	-0.1
	FeCl2+	2.34E-19	2.21E-19	-18.631	-18.656	-0.025
	Fe2(OH)2+4	4.10E-21	1.63E-21	-20.387	-20.787	-0.4
	FeCl3	5.88E-24	5.88E-24	-23.231	-23.231	0
	Fe3(OH)4+5	5.79E-28	1.37E-28	-27.237	-27.862	-0.625
H(0)	4.04E-20					
	H2	2.02E-20	2.02E-20	-19.695	-19.694	0
Mg	3.62E-04					
	Mg+2	3.61E-04	2.88E-04	-3.443	-3.54	-0.097
	MgSO4	1.90E-06	1.90E-06	-5.722	-5.721	0
	MgOH+	2.61E-11	2.47E-11	-10.583	-10.608	-0.025
Mn(2)	5.06E-05					
	Mn+2	5.03E-05	4.00E-05	-4.298	-4.398	-0.1
	MnSO4	2.21E-07	2.21E-07	-6.655	-6.655	0
	MnCl+	4.59E-08	4.33E-08	-7.338	-7.363	-0.025
	MnOH+	2.93E-11	2.77E-11	-10.533	-10.558	-0.025
	MnCl2	5.03E-12	5.03E-12	-11.298	-11.298	0
	MnCl3-	3.91E-16	3.69E-16	-15.408	-15.433	-0.025
	Mn(OH)3-	5.46E-25	5.15E-25	-24.263	-24.288	-0.025
Mn(3)	4.57E-28					
	Mn+3	4.57E-28	2.72E-28	-27.34	-27.565	-0.225
Mn(6)	0.00E+00					
	MnO4-2	0.00E+00	0.00E+00	-75.359	-75.459	-0.1
Mn(7)	0.00E+00					
	MnO4-	0.00E+00	0.00E+00	-82.505	-82.53	-0.025
Na	3.35E-04					
	Na+	3.35E-04	3.17E-04	-3.475	-3.499	-0.025
	NaSO4-	6.35E-08	6.00E-08	-7.197	-7.222	-0.025
O(0)	0.00E+00					
	O2	0.00E+00	0.00E+00	-58.011	-58.011	0
S(-2)	1.34E-03					
	H2S	9.05E-04	9.06E-04	-3.043	-3.043	0
	Zn(HS)2	2.08E-04	2.08E-04	-3.682	-3.682	0
	Fe(HS)2	8.42E-06	8.42E-06	-5.075	-5.075	0
	HS-	6.22E-06	5.88E-06	-5.206	-5.231	-0.025
	Zn(HS)3-	1.87E-08	1.77E-08	-7.728	-7.753	-0.025
	Fe(HS)3-	5.71E-09	5.39E-09	-8.244	-8.269	-0.025
	S6-2	8.79E-11	7.21E-11	-10.056	-10.142	-0.086
	S5-2	7.66E-11	6.25E-11	-10.116	-10.204	-0.089
	S4-2	4.34E-11	3.52E-11	-10.362	-10.453	-0.091
	S-2	2.94E-14	2.33E-14	-13.532	-13.632	-0.1
	S3-2	1.45E-14	1.17E-14	-13.839	-13.933	-0.094
	S2-2	7.59E-16	6.08E-16	-15.12	-15.216	-0.096
S(6)	6.04E-05					
	SO4-2	5.22E-05	4.16E-05	-4.282	-4.381	-0.099
	CaSO4	2.27E-06	2.27E-06	-5.644	-5.643	0
	AlSO4+	2.12E-06	2.00E-06	-5.674	-5.699	-0.025
	MgSO4	1.90E-06	1.90E-06	-5.722	-5.721	0
	FeSO4	1.53E-06	1.53E-06	-5.815	-5.814	0
	MnSO4	2.21E-07	2.21E-07	-6.655	-6.655	0
	NaSO4-	6.35E-08	6.00E-08	-7.197	-7.222	-0.025
	HSO4-	3.42E-08	3.22E-08	-7.467	-7.492	-0.025
	Al(SO4)2-	2.60E-09	2.45E-09	-8.585	-8.61	-0.025
	CaHSO4+	1.30E-10	1.22E-10	-9.888	-9.913	-0.025
	FeHSO4+	1.12E-10	1.06E-10	-9.949	-9.974	-0.025
	ZnSO4	6.00E-11	6.00E-11	-10.222	-10.222	0
	AlHSO4+2	2.17E-12	1.72E-12	-11.664	-11.764	-0.1
	Zn(SO4)2-2	2.88E-14	2.28E-14	-13.541	-13.641	-0.1
	FeSO4+	7.99E-15	7.54E-15	-14.098	-14.123	-0.025
	Fe(SO4)2-	6.85E-18	6.47E-18	-17.164	-17.189	-0.025
	FeHSO4+2	2.84E-19	2.25E-19	-18.547	-18.647	-0.1
Si	5.41E-05					
	H4SiO4	5.41E-05	5.41E-05	-4.267	-4.267	0
	H3SiO4-	4.53E-10	4.27E-10	-9.344	-9.369	-0.025
	H2SiO4-2	1.22E-18	9.69E-19	-17.914	-18.014	-0.1
Zn	2.08E-04					
	Zn(HS)2	2.08E-04	2.08E-04	-3.682	-3.682	0
	Zn(HS)3-	1.87E-08	1.77E-08	-7.728	-7.753	-0.025
	Zn+2	8.71E-09	6.92E-09	-8.06	-8.16	-0.1
	ZnSO4	6.00E-11	6.00E-11	-10.222	-10.222	0
	ZnCl+	2.66E-12	2.53E-12	-11.572	-11.597	-0.025
	ZnOH+	2.36E-13	2.23E-13	-12.627	-12.652	-0.025
	Zn(SO4)2-2	2.88E-14	2.28E-14	-13.541	-13.641	-0.1
	ZnOHCl	5.68E-15	5.69E-15	-14.245	-14.245	0
	Zn(OH)2	7.58E-16	7.58E-16	-15.12	-15.12	0
	ZnCl2	6.62E-16	6.63E-16	-15.179	-15.179	0
	ZnCl3-	1.91E-19	1.81E-19	-18.718	-18.743	-0.025
	Zn(OH)3-	2.37E-22	2.24E-22	-21.625	-21.65	-0.025
	ZnCl4-2	2.69E-23	2.13E-23	-22.571	-22.671	-0.1
	Zn(OH)4-2	4.17E-30	3.31E-30	-29.38	-29.48	-0.1

#NAME? Indices

Phase	SI	log	IAP	log	KT
ZnMetal	-67.32	-40.17	27.16	Zn	
H2(g)	-47.71	-47.66	0.05	H2	
Mn2(SO4)3	-32.6	16.18	48.78	Mn2(SO4)3	
Zn3O(SO4	-31.58	-10.21	21.38	ZnO:2ZnSO4	
Greenalite	-30.46	-9.65	20.81	Fe3Si2O5(OH)4	
Zn5(OH)8C	-28.07	10.43	38.5	Zn5(OH)8Cl2	
Tremolite	-26.88	33.38	60.26	Ca2Mg5Si8O22(OH)2	
Melanterite	-20.54	-22.95	-2.41	FeSO4:7H2O	
Zn4(OH)6S	-20.27	8.13	28.4	Zn4(OH)6SO4	
ZnCl2	-19.23	-11.53	7.69	ZnCl2	
Mirabilite	-18.91	-20.75	-1.84	Na2SO4:10H2O	
Chrysotile	-18.25	15.86	34.11	Mg3Si2O5(OH)4	
Portlandite	-17.62	6.36	23.98	Ca(OH)2	
Forsterite	-17.52	12.63	30.15	Mg2SiO4	
MnCl2:4H2	-17.07	-15.02	2.05	MnCl2:4H2O	
Sepiolite(d'	-13.86	4.8	18.66	Mg2Si3O7.5OH:3H2O	
Goslarite	-13.26	-15.35	-2.09	ZnSO4:7H2O	
Zn2(OH)3C	-12.73	2.47	15.2	Zn2(OH)3Cl	
Blanchite	-12.59	-14.35	-1.76	ZnSO4:6H2O	
Epsomite	-12.19	-14.44	-2.25	MgSO4:7H2O	
Zincosite	-12.09	-8.35	3.74	ZnSO4	
Brucite	-11.47	6.4	17.87	Mg(OH)2	
Sepiolite	-11.37	4.8	16.17	Mg2Si3O7.5OH:3H2O	
MnSO4	-11.09	-7.83	3.26	MnSO4	
Diopside	-10.7	10.42	21.12	CaMgSi2O6	
Talc	-10.63	12.53	23.16	Mg3Si4O10(OH)2	
Thenardite	-10.59	-10.75	-0.16	Na2SO4	
Zn2(OH)2S	-10.36	-2.86	7.5	Zn2(OH)2SO4	
Pyrochroite	-9.19	6.01	15.2	Mn(OH)2	
ZnSO4:H2	-9.18	-9.35	-0.17	ZnSO4:H2O	
Halite	-8.51	-6.97	1.55	NaCl	
Fe3(OH)8	-7.65	39.35	47	Fe3(OH)8	
Zn(OH)2-a	-6.96	5.49	12.45	Zn(OH)2	
Clinoenstat	-6.87	5.23	12.1	MgSiO3	
Zn(OH)2-c	-6.71	5.49	12.2	Zn(OH)2	
Zn(OH)2-b	-6.26	5.49	11.75	Zn(OH)2	
Zn(OH)2-g	-6.22	5.49	11.71	Zn(OH)2	

#NAME? Indices

Phase	SI	log	IAP	log	KT
Mn2(SO4)3	-64.02	-15.32	48.71	Mn2(SO4)3	
O2(g)	-55.12	33.12	88.24	O2	
Tremolite	-49.46	10.74	60.2	Ca2Mg5Si8O22(OH)2	
Zn5(OH)8C	-46.69	-8.19	38.5	Zn5(OH)8Cl2	

Zn(OH)2-e	-6.01	5.49	11.5	Zn(OH)2
Willemite	-5.78	10.82	16.6	Zn2SiO4
Zincite(c)	-5.48	6.49	11.97	ZnO
Gypsum	-4.89	-9.48	-4.59	CaSO4:2H2O
ZnO(a)	-4.82	6.49	11.31	ZnO
JarositeH	-4.38	32.49	36.87	(H3O)Fe3(SO4)2(OH)6
Magadiite	-3.32	-17.62	-14.3	NaSi7O13(OH)3:3H2O
Anhydrite	-3.15	-7.48	-4.34	CaSO4
Jarosite-Na	-0.22	36.04	36.26	NaFe3(SO4)2(OH)6
SiO2(a)	0.67	-2.17	-2.84	SiO2
ZnSiO3	0.7	4.32	3.62	ZnSiO3
Silicagel	1.02	-2.17	-3.19	SiO2
Chalcedon	1.56	-2.17	-3.73	SiO2
Cristobalite	1.63	-2.17	-3.8	SiO2
Quartz	2.04	-2.17	-4.21	SiO2
Fe(OH)3(a	2.45	20.73	18.28	Fe(OH)3
Jarosite-K	2.58	34.72	32.14	KFe3(SO4)2(OH)6
Hausmann	2.83	67.69	64.86	Mn3O4
Jarosite(ss	4.18	34.51	30.33	(K0.77Na0.03H0.2)Fe3(SO4)2(O
Manganite	4.5	29.84	25.34	MnOOH
O2(g)	5.01	93.32	88.31	O2
Bixbyite	7.73	60.68	52.95	Mn2O3
Fe(OH)2.7	7.82	18.17	10.35	Fe(OH)2.7Cl0.3
Goethite	9.21	21.73	12.52	FeOOH
Pyrolusite	9.82	53.67	43.86	MnO2
Bimessite	10.07	53.67	43.6	MnO2
Magnetite	10.91	43.35	32.43	Fe3O4
Nsutite	11.11	53.67	42.56	MnO2
Maghemite	11.29	44.45	33.16	Fe2O3
Hematite	20.51	44.45	23.94	Fe2O3

Zn3O(SO4	-44.64	-23.3	21.34	ZnO:2ZnSO4
ZnMetal	-41.92	-14.78	27.14	Zn
Chlorite7A	-38.02	39.55	77.57	Mg5Al2Si3O10(OH)8
Zn4(OH)6S	-35.6	-7.2	28.4	Zn4(OH)6SO4
Chlorite14A	-34.5	39.55	74.06	Mg5Al2Si3O10(OH)8
Hausmann	-31.62	33.19	64.8	Mn3O4
Bixbyite	-25.27	27.64	52.91	Mn2O3
Chrysotile	-23.42	10.67	34.09	Mg3Si2O5(OH)4
ZnCl2	-23	-15.31	7.68	ZnCl2
Pyrolusite	-21.72	22.1	43.82	MnO2
Forsterite	-21.59	8.53	30.13	Mg2SiO4
Birnessite	-21.5	22.1	43.6	MnO2
JarositeH	-21.49	15.33	36.82	(H3O)Fe3(SO4)2(OH)6
Talc	-21	2.13	23.14	Mg3Si4O10(OH)2
Nsutite	-20.46	22.1	42.56	MnO2
Zn2(OH)3C	-20.19	-4.99	15.2	Zn2(OH)3Cl
Jarosite-Na	-19.42	16.8	36.22	NaFe3(SO4)2(OH)6
Sepiolite(d	-18.66	0	18.66	Mg2Si3O7.5OH:3H2O
Zn2(OH)2S	-18.26	-10.76	7.5	Zn2(OH)2SO4
Portlandite	-17.52	6.44	23.96	Ca(OH)2
Willemite	-17.29	-0.71	16.58	Zn2SiO4
Diopside	-16.8	4.31	21.11	CaMgSi2O6
H2(g)	-16.61	-16.56	0.05	H2
Zincosite	-16.27	-12.54	3.73	ZnSO4
Sepiolite	-16.16	0	16.16	Mg2Si3O7.5OH:3H2O
Prehnite	-16	20.43	36.43	Ca2Al2Si3O10(OH)2
Magadiite	-14.09	-28.39	-14.3	NaSi7O13(OH)3:3H2O
MnCl2:4H2	-13.61	-11.55	2.06	MnCl2:4H2O
ZnSO4:H2O	-12.37	-12.54	-0.17	ZnSO4:H2O
MnSO4	-12.03	-8.78	3.25	MnSO4
Manganite	-11.52	13.82	25.34	MnOOH
Brucite	-11.46	6.4	17.86	Mg(OH)2
Fe3(OH)8	-11.3	35.69	46.99	Fe3(OH)8
Thenardite	-11.22	-11.38	-0.16	Na2SO4
Wairakite	-11.1	9.73	20.83	CaAl2Si4O12:2H2O
Bianchite	-10.78	-12.54	-1.76	ZnSO4:6H2O
Zn(OH)2-a	-10.67	1.78	12.45	Zn(OH)2
Goslarite	-10.46	-12.54	-2.08	ZnSO4:7H2O
Zn(OH)2-c	-10.42	1.78	12.2	Zn(OH)2
Greenalite	-10.21	10.6	20.81	Fe3Si2O5(OH)4
Zincite(c)	-10.18	1.78	11.96	ZnO
Anorthite	-10.11	18.26	28.37	CaAl2Si2O8
Zn(OH)2-b	-9.97	1.78	11.75	Zn(OH)2
Clinoenstat	-9.96	2.13	12.09	MgSiO3
Zn(OH)2-g	-9.93	1.78	11.71	Zn(OH)2
Zn(OH)2-e	-9.72	1.78	11.5	Zn(OH)2
Pyrochroite	-9.66	5.54	15.2	Mn(OH)2
Mirabilite	-9.55	-11.38	-1.83	Na2SO4:10H2O
ZnO(a)	-9.53	1.78	11.31	ZnO
MnS(Greer	-8.68	2.5	11.17	MnS
Halite	-8.62	-7.07	1.55	NaCl
Analcime	-7.76	3.12	10.88	NaAlSi2O6:H2O
Albite	-6.44	-1.15	5.29	NaAlSi3O8
Laumonite	-6.34	9.73	16.07	CaAl2Si4O12:4H2O
ZnSiO3	-6.1	-2.49	3.61	ZnSiO3
Epsomite	-5.68	-7.92	-2.25	MgSO4:7H2O
Melanterite	-5.54	-7.94	-2.4	FeSO4:7H2O
Leonhardit	-4.45	19.46	23.9	Ca2Al4Si8O24:7H2O
Maghemite	-3.84	29.31	33.15	Fe2O3
Fe(OH)3(a	-3.62	14.66	18.27	Fe(OH)3
Anhydrite	-3.55	-7.88	-4.34	CaSO4
Gypsum	-3.29	-7.88	-4.59	CaSO4:2H2O
H2S(g)	-2.22	-3.04	-0.83	H2S
Halloysite	-2.17	11.82	13.99	Al2Si2O5(OH)4
Al(OH)3(a)	-1.62	10.18	11.79	Al(OH)3
SiO2(a)	-1.43	-4.27	-2.84	SiO2
Silicagel	-1.09	-4.27	-3.18	SiO2
Jurbanite	-0.91	-4.14	-3.23	AlOHSO4
Chalcedon	-0.54	-4.27	-3.73	SiO2
Cristobalite	-0.47	-4.27	-3.79	SiO2
Montmorill	-0.19	9.12	9.31	Ca0.165Al2.33Si3.67O10(OH)2
Quartz	-0.06	-4.27	-4.2	SiO2
FeS(ppt)	0.09	3.33	3.24	FeS
Boehmite	0.54	10.18	9.64	AlOOH
ZnS(a)	0.77	-1.26	-2.03	ZnS
Mackinawit	0.82	3.33	2.51	FeS
Gibbsite	1.21	10.18	8.96	Al(OH)3
Wurtzite	1.45	-1.26	-2.71	ZnS
Fe(OH)2.7	1.75	12.09	10.34	Fe(OH)2.7Cl0.3
Goethite	2.14	14.66	12.51	FeOOH
Diaspore	2.37	10.18	7.8	AlOOH
Kaolinite	3.08	11.82	8.76	Al2Si2O5(OH)4
Pyrophyllite	3.09	3.29	0.2	Al2Si4O10(OH)2
Magnetite	3.3	35.69	32.39	Fe3O4
Sphalerite	3.51	-1.26	-4.77	ZnS
Basaluminit	3.69	26.39	22.7	Al4(OH)10SO4
Hematite	5.4	29.31	23.91	Fe2O3
Sulfur	8.31	13.52	5.21	S
Greigite	13.16	23.52	10.36	Fe3S4
Pyrite	21.44	16.85	-4.59	FeS2

End of simulation.

Reading input data for simulation 2

End of run.

Reading data base.

SOLUTION_MASTER_SPECIES
SOLUTION_SPECIES
PHASES
EXCHANGE_MASTER_SPECIES
EXCHANGE_SPECIES
SURFACE_MASTER_SPECIES
SURFACE_SPECIES
END

Reading input data for simulation 1

TITLE Example 1.dry mix
SOLUTION 1 dry mix
units ppm
pH 5.81
pe 17.79
density 1
temp 10.3
Ca 10.23
Fe 6.4
Mg 6.48
Mn 6.57
K 0.61
Na 1.05
Si 4.23
Zn 1.99
Cl 13.84
S(6) 102.204
SOLUTION_MASTER_SPECIES
SOLUTION_SPECIES
PHASES
END

TITLE

Example 1.dry mix

Beginning of initial solution calculations.

Initial solution 1 dry mix
#NAME? composition

Elements	Molality	Moles
Ca	2.55E-04	2.55E-04
Cl	3.90E-04	3.90E-04
Fe	1.41E-04	1.41E-04
K	1.56E-05	1.56E-05
Mg	2.67E-04	2.67E-04
Mn	1.20E-04	1.20E-04
Na	4.57E-05	4.57E-05
S(6)	1.06E-03	1.06E-03
Si	7.04E-05	7.04E-05
Zn	3.05E-05	3.05E-05

#NAME? of solution

pH	=	5.81			
pe	=	17.79			
Activity	of	water	=	0.188	
Ionic	strength	=	3.52E-03		
Mass	of	water	(kg)	=	1.00E+00
Total	alkalinity	(eq/kg)	=	-8.23E-06	
Total	carbon	(mol/kg)	=	0.00E+00	
Total	CO2	(mol/kg)	=	0.00E+00	
Temperatu	(deg	C)	=	10.3	
Electrical	balance	(eq)	=	-9.66E-04	
Iterations	=	101			
Total	H	=	1.11E+02		
Total	O	=	1.66E+02		

#NAME? of species

	Log Species	Log Molality	Log Activity	Molality	Activity	Gamma
	H+	1.64E-06	1.55E-06	-5.785	-5.81	-0.025
	OH-	3.88E-10	3.65E-10	-9.411	-9.438	-0.027
	H2O	5.55E+01	1.88E-01	-0.728	-0.726	0
Ca	2.55E-04					
	Ca+2	2.31E-04	1.80E-04	-3.637	-3.744	-0.107
	CaSO4	2.43E-05	2.44E-05	-4.614	-4.613	0
	CaHSO4+	2.02E-10	1.89E-10	-9.696	-9.723	-0.027
	CaOH+	3.87E-12	3.63E-12	-11.413	-11.44	-0.027
Cl	3.90E-04					
	Cl-	3.90E-04	3.66E-04	-3.409	-3.436	-0.028
	MnCl+	1.36E-07	1.27E-07	-6.868	-6.895	-0.027
	ZnCl+	1.11E-08	1.05E-08	-7.953	-7.981	-0.027
	FeCl+2	1.55E-10	1.20E-10	-9.811	-9.921	-0.11
	ZnOHCl	3.08E-11	3.09E-11	-10.511	-10.511	0
	MnCl2	2.03E-11	2.04E-11	-10.692	-10.691	0
	ZnCl2	3.76E-12	3.77E-12	-11.425	-11.424	0
	FeCl2+	3.41E-13	3.20E-13	-12.467	-12.494	-0.027
	MnCl3-	2.19E-15	2.05E-15	-14.66	-14.688	-0.027
	ZnCl3-	1.50E-15	1.41E-15	-14.823	-14.851	-0.027
	FeCl+	3.78E-16	3.55E-16	-15.423	-15.45	-0.027
	FeCl3	1.17E-17	1.17E-17	-16.931	-16.931	0

Reading data base.

SOLUTION_MASTER_SPECIES
SOLUTION_SPECIES
PHASES
EXCHANGE_MASTER_SPECIES
EXCHANGE_SPECIES
SURFACE_MASTER_SPECIES
SURFACE_SPECIES
END

Reading input data for simulation 1

TITLE Example 1.wet mix
SOLUTION 1 wet mix
units ppm
pH 5.29
pe 3.58
density 1
temp 9.6
Al 0.63
Ca 11.46
Fe 13.39
Mg 6.94
Mn 1.97
Na 7.22
Si 2.66
Zn 9.71
Cl 11
S(6) 33.4
SOLUTION_MASTER_SPECIES
SOLUTION_SPECIES
PHASES
END

TITLE

Example 1.wet mix

Beginning of initial solution calculations.

Initial solution 1 wet mix
#NAME? composition

Elements	Molality	Moles
Al	2.34E-05	2.34E-05
Ca	2.86E-04	2.86E-04
Cl	3.10E-04	3.10E-04
Fe	2.40E-04	2.40E-04
Mg	2.86E-04	2.86E-04
Mn	3.59E-05	3.59E-05
Na	3.14E-04	3.14E-04
S(6)	3.48E-04	3.48E-04
Si	4.43E-05	4.43E-05
Zn	1.49E-04	1.49E-04

#NAME? of solution

pH	=	5.29			
pe	=	3.58			
Activity	of	water	=	1	
Ionic	strength	=	2.93E-03		
Mass	of	water	(kg)	=	1.00E+00
Total	alkalinity	(eq/kg)	=	3.77E-06	
Total	carbon	(mol/kg)	=	0.00E+00	
Total	CO2	(mol/kg)	=	0.00E+00	
Temperatu	(deg	C)	=	9.6	
Electrical	balance	(eq)	=	1.37E-03	
Iterations	=	4			
Total	H	=	1.11E+02		
Total	O	=	5.55E+01		

#NAME? of species

	Log Species	Log Molality	Log Activity	Molality	Activity	Gamma
	H+	5.41E-06	5.13E-06	-5.267	-5.29	-0.023
	OH-	5.83E-10	5.50E-10	-9.234	-9.259	-0.025
	H2O	5.55E+01	1.00E+00	0	0	0
Al	2.34E-05					
	Al+3	1.13E-05	6.70E-06	-4.948	-5.174	-0.227
	AlOH+2	5.80E-06	4.60E-06	-5.236	-5.337	-0.101
	AlSO4+	4.51E-06	4.26E-06	-5.346	-5.371	-0.025
	Al(OH)2+	1.70E-06	1.61E-06	-5.769	-5.794	-0.025
	Al(SO4)2-	3.29E-08	3.10E-08	-7.483	-7.509	-0.025
	Al(OH)3	1.31E-08	1.31E-08	-7.883	-7.883	0
	Al(OH)4-	4.45E-09	4.19E-09	-8.352	-8.377	-0.025
	AlHSO4+2	2.20E-12	1.75E-12	-11.657	-11.758	-0.101
Ca	2.86E-04					
	Ca+2	2.77E-04	2.20E-04	-3.558	-3.657	-0.099
	CaSO4	9.37E-06	9.38E-06	-5.028	-5.028	0
	CaHSO4+	2.54E-10	2.40E-10	-9.595	-9.62	-0.025
	CaOH+	7.56E-12	7.13E-12	-11.122	-11.147	-0.025
Cl	3.10E-04					
	Cl-	3.10E-04	2.93E-04	-3.508	-3.534	-0.025
	FeCl+	7.93E-08	7.48E-08	-7.101	-7.126	-0.025

	ZnCl4-2	2.95E-19	2.29E-19	-18.531	-18.64	-0.11
	9.78E-13					
	Fe+2	9.04E-13	7.02E-13	-12.044	-12.154	-0.11
	FeSO4	7.35E-14	7.36E-14	-13.133	-13.133	0
	FeCl+	3.78E-16	3.55E-16	-15.423	-15.45	-0.027
	FeOH+	9.04E-18	8.48E-18	-17.044	-17.072	-0.027
	FeHSO4+	7.84E-19	7.36E-19	-18.106	-18.133	-0.027
	Fe(OH)2	2.28E-24	2.28E-24	-23.642	-23.642	0
	Fe(OH)3-	9.42E-30	8.84E-30	-29.026	-29.054	-0.027
	1.41E-04					
	Fe(OH)2+	1.33E-04	1.25E-04	-3.876	-3.904	-0.027
	FeOH+2	7.19E-06	5.58E-06	-5.143	-5.253	-0.11
	Fe(OH)3	9.94E-07	9.94E-07	-6.003	-6.002	0
	FeSO4+	1.15E-07	1.08E-07	-6.94	-6.967	-0.027
	Fe+3	3.13E-08	1.77E-08	-7.505	-7.752	-0.247
	Fe2(OH)2+	4.37E-09	1.59E-09	-8.36	-8.799	-0.439
	Fe(SO4)2-	1.85E-09	1.74E-09	-8.732	-8.76	-0.027
	Fe3(OH)4+	8.38E-10	1.73E-10	-9.077	-9.763	-0.686
	FeCl+2	1.55E-10	1.20E-10	-9.811	-9.921	-0.11
	Fe(OH)4-	6.30E-11	5.91E-11	-10.201	-10.228	-0.027
	FeHSO4+2	6.01E-13	4.67E-13	-12.221	-12.331	-0.11
	FeCl2+	3.41E-13	3.20E-13	-12.467	-12.494	-0.027
	FeCl3	1.17E-17	1.17E-17	-16.931	-16.931	0
	0.00E+00					
	H2	0.00E+00	0.00E+00	-50.334	-50.334	0
	1.56E-05					
	K+	1.55E-05	1.46E-05	-4.809	-4.836	-0.028
	KSO4-	6.52E-08	6.12E-08	-7.186	-7.213	-0.027
	2.67E-04					
	Mg+2	2.43E-04	1.90E-04	-3.614	-3.72	-0.106
	MgSO4	2.34E-05	2.34E-05	-4.63	-4.63	0
	MgOH+	2.21E-11	2.08E-11	-10.655	-10.683	-0.027
	1.19E-04					
	Mn+2	1.10E-04	8.54E-05	-3.959	-4.069	-0.11
	MnSO4	8.83E-06	8.84E-06	-5.054	-5.054	0
	MnCl+	1.36E-07	1.27E-07	-6.868	-6.895	-0.027
	MnOH+	8.04E-11	7.55E-11	-10.095	-10.122	-0.027
	MnCl2	2.03E-11	2.04E-11	-10.692	-10.691	0
	MnCl3-	2.19E-15	2.05E-15	-14.66	-14.688	-0.027
	Mn(OH)3-	2.57E-24	2.42E-24	-23.589	-23.617	-0.027
	3.00E-13					
	Mn+3	3.00E-13	1.70E-13	-12.523	-12.77	-0.247
	4.31E-14					
	MnO4-2	4.31E-14	3.35E-14	-13.366	-13.476	-0.11
	8.85E-07					
	MnO4-	8.85E-07	8.30E-07	-6.053	-6.081	-0.027
	4.57E-05					
	Na+	4.55E-05	4.28E-05	-4.342	-4.369	-0.027
	NaSO4-	1.62E-07	1.52E-07	-6.791	-6.818	-0.027
	1.11E+02					
	O2	5.54E+01	5.55E+01	1.744	1.744	0
	1.06E-03					
	SO4-2	1.00E-03	7.82E-04	-2.998	-3.107	-0.108
	CaSO4	2.43E-05	2.44E-05	-4.614	-4.613	0
	MgSO4	2.34E-05	2.34E-05	-4.63	-4.63	0
	MnSO4	8.83E-06	8.84E-06	-5.054	-5.054	0
	ZnSO4	3.41E-06	3.41E-06	-5.467	-5.467	0
	NaSO4-	1.62E-07	1.52E-07	-6.791	-6.818	-0.027
	FeSO4+	1.15E-07	1.08E-07	-6.94	-6.967	-0.027
	HSO4-	9.30E-08	8.73E-08	-7.032	-7.059	-0.027
	KSO4-	6.52E-08	6.12E-08	-7.186	-7.213	-0.027
	Zn(SO4)2-2	3.15E-08	2.45E-08	-7.502	-7.612	-0.11
	Fe(SO4)2-	1.85E-09	1.74E-09	-8.732	-8.76	-0.027
	CaHSO4+	2.02E-10	1.89E-10	-9.696	-9.723	-0.027
	FeHSO4+2	6.01E-13	4.67E-13	-12.221	-12.331	-0.11
	FeSO4	7.35E-14	7.36E-14	-13.133	-13.133	0
	FeHSO4+	7.84E-19	7.36E-19	-18.106	-18.133	-0.027
	7.04E-05					
	H4SiO4	7.04E-05	7.05E-05	-4.152	-4.152	0
	H3SiO4-	4.07E-09	3.82E-09	-8.391	-8.418	-0.027
	H2SiO4-2	7.59E-17	5.89E-17	-16.12	-16.23	-0.11
	3.05E-05					
	Zn+2	2.70E-05	2.10E-05	-4.569	-4.678	-0.11
	ZnSO4	3.41E-06	3.41E-06	-5.467	-5.467	0
	Zn(SO4)2-2	3.15E-08	2.45E-08	-7.502	-7.612	-0.11
	ZnCl+	1.11E-08	1.05E-08	-7.953	-7.981	-0.027
	ZnOH+	9.20E-10	8.63E-10	-9.036	-9.064	-0.027
	ZnOHCl	3.08E-11	3.09E-11	-10.511	-10.511	0
	Zn(OH)2	3.88E-12	3.89E-12	-11.411	-11.41	0
	ZnCl2	3.76E-12	3.77E-12	-11.425	-11.424	0
	ZnCl3-	1.50E-15	1.41E-15	-14.823	-14.851	-0.027
	Zn(OH)3-	1.59E-18	1.49E-18	-17.799	-17.826	-0.027
	ZnCl4-2	2.95E-19	2.29E-19	-18.531	-18.64	-0.11
	Zn(OH)4-2	3.69E-26	2.87E-26	-25.433	-25.542	-0.11

#NAME? indices

Phase	SI	log	IAP	log	KT
ZnMetal	-67.41	-40.26	27.16	Zn	
H2(g)	-47.25	-47.2	0.05	H2	
Tremolite	-32.41	27.84	60.26	Ca2Mg5Si8O22(OH)2	
Greenalite	-31.44	-10.63	20.81	Fe3Si2O5(OH)4	
Zn3O(SO4	-30.73	-9.35	21.38	ZnO:2ZnSO4	
Mn2(SO4)3	-30.63	18.12	48.76	Mn2(SO4)3	
Zn5(OH)8C	-28.09	10.41	38.5	Zn5(OH)8Cl2	
Zn4(OH)6S	-19.72	8.68	28.4	Zn4(OH)6SO4	
Chrysotile	-19.45	14.67	34.11	Mg3Si2O5(OH)4	
ZnCl2	-19.25	-11.55	7.69	ZnCl2	
Forsterite	-18.51	11.65	30.15	Mg2SiO4	
Melanterite	-17.94	-20.34	-2.41	FeSO4:7H2O	
Portlandite	-17.55	6.42	23.98	Ca(OH)2	
Mirabilite	-17.27	-19.1	-1.84	Na2SO4:10H2O	
MnCl2:4H2	-15.89	-13.85	2.05	MnCl2:4H2O	
Sepiolite(d	-14.95	3.71	18.66	Mg2Si3O7.5OH:3H2O	

	ZnCl+	4.61E-08	4.35E-08	-7.336	-7.361	-0.025
	MnCl+	3.50E-08	3.30E-08	-7.456	-7.481	-0.025
	ZnOHCl	2.14E-10	2.14E-10	-9.671	-9.67	0
	ZnCl2	1.25E-11	1.25E-11	-10.904	-10.903	0
	MnCl2	4.21E-12	4.22E-12	-11.375	-11.375	0
	ZnCl3-	3.94E-15	3.72E-15	-14.404	-14.43	-0.025
	MnCl3-	3.60E-16	3.40E-16	-15.444	-15.469	-0.025
	FeCl+2	1.84E-16	1.46E-16	-15.735	-15.836	-0.101
	ZnCl4-2	6.05E-19	4.80E-19	-18.219	-18.319	-0.101
	FeCl2+	3.38E-19	3.19E-19	-18.471	-18.496	-0.025
	FeCl3	9.32E-24	9.33E-24	-23.03	-23.03	0
Fe(2)	2.40E-04					
	Fe+2	2.34E-04	1.85E-04	-3.631	-3.732	-0.101
	FeSO4	6.07E-06	6.08E-06	-5.217	-5.216	0
	FeCl+	7.93E-08	7.48E-08	-7.101	-7.126	-0.025
	FeOH+	3.60E-09	3.40E-09	-8.444	-8.469	-0.025
	FeHSO4+	2.14E-10	2.02E-10	-9.67	-9.696	-0.025
	Fe(OH)2	1.37E-15	1.37E-15	-14.863	-14.863	0
	Fe(OH)3-	8.98E-21	8.48E-21	-20.047	-20.072	-0.025
Fe(3)	5.17E-10					
	Fe(OH)2+	4.94E-10	4.66E-10	-9.306	-9.331	-0.025
	FeOH+2	1.69E-11	1.34E-11	-10.773	-10.874	-0.101
	Fe(OH)3	5.77E-12	5.77E-12	-11.239	-11.239	0
	FeSO4+	5.56E-14	5.25E-14	-13.255	-13.28	-0.025
	Fe+3	4.66E-14	2.76E-14	-13.332	-13.559	-0.227
	Fe(OH)4-	5.66E-16	5.34E-16	-15.247	-15.272	-0.025
	Fe(SO4)2-	2.84E-16	2.68E-16	-15.547	-15.573	-0.025
	FeCl+2	1.84E-16	1.46E-16	-15.735	-15.836	-0.101
	FeHSO4+2	9.52E-19	7.55E-19	-18.021	-18.122	-0.101
	FeCl2+	3.38E-19	3.19E-19	-18.471	-18.496	-0.025
	Fe2(OH)2+	2.38E-20	9.41E-21	-19.623	-20.026	-0.403
	FeCl3	9.32E-24	9.33E-24	-23.03	-23.03	0
	Fe3(OH)4+	1.75E-26	4.10E-27	-25.757	-26.387	-0.629
H(0)	2.68E-21					
	H2	1.34E-21	1.34E-21	-20.874	-20.873	0
Mg	2.86E-04					
	Mg+2	2.77E-04	2.21E-04	-3.557	-3.655	-0.098
	MgSO4	8.46E-06	8.47E-06	-5.072	-5.072	0
	MgOH+	3.83E-11	3.61E-11	-10.417	-10.442	-0.025
Mn(2)	3.59E-05					
	Mn+2	3.49E-05	2.77E-05	-4.457	-4.558	-0.101
	MnSO4	8.96E-07	8.97E-07	-6.047	-6.047	0
	MnCl+	3.50E-08	3.30E-08	-7.456	-7.481	-0.025
	MnOH+	3.92E-11	3.70E-11	-10.407	-10.432	-0.025
	MnCl2	4.21E-12	4.22E-12	-11.375	-11.375	0
	MnCl3-	3.60E-16	3.40E-16	-15.444	-15.469	-0.025
	Mn(OH)3-	3.45E-24	3.25E-24	-23.462	-23.488	-0.025
Mn(3)	5.12E-28					
	Mn+3	5.12E-28	3.04E-28	-27.291	-27.517	-0.227
Mn(6)	0.00E+00					
	MnO4-2	0.00E+00	0.00E+00	-72.246	-72.347	-0.101
Mn(7)	0.00E+00					
	MnO4-	0.00E+00	0.00E+00	-79.187	-79.213	-0.025
Na	3.14E-04					
	Na+	3.14E-04	2.96E-04	-3.503	-3.528	-0.025
	NaSO4-	3.52E-07	3.32E-07	-6.453	-6.478	-0.025
O(0)	0.00E+00					
	O2	0.00E+00	0.00E+00	-55.981	-55.981	0
S(6)	3.48E-04					
	SO4-2	3.12E-04	2.48E-04	-3.506	-3.605	-0.099
	CaSO4	9.37E-06	9.38E-06	-5.028	-5.028	0
	MgSO4	8.46E-06	8.47E-06	-5.072	-5.072	0
	FeSO4	6.07E-06	6.08E-06	-5.217	-5.216	0
	ZnSO4	5.81E-06	5.81E-06	-5.236	-5.236	0
	AlSO4+	4.51E-06	4.26E-06	-5.346	-5.371	-0.025
	MnSO4	8.96E-07	8.97E-07	-6.047	-6.047	0
	NaSO4-	3.52E-07	3.32E-07	-6.453	-6.478	-0.025
	HSO4-	9.59E-08	9.05E-08	-7.018	-7.043	-0.025
	Al(SO4)2-	3.29E-08	3.10E-08	-7.483	-7.509	-0.025
	Zn(SO4)2-2	1.68E-08	1.33E-08	-7.776	-7.877	-0.101
	CaHSO4+	2.54E-10	2.40E-10	-9.595	-9.62	-0.025
	FeHSO4+	2.14E-10	2.02E-10	-9.67	-9.696	-0.025
	AlHSO4+2	2.20E-12	1.75E-12	-11.657	-11.758	-0.101
	FeSO4+	5.56E-14	5.25E-14	-13.255	-13.28	-0.025
	Fe(SO4)2-	2.84E-16	2.68E-16	-15.547	-15.573	-0.025
	FeHSO4+2	9.52E-19	7.55E-19	-18.021	-18.122	-0.101
SI	4.43E-05					
	H4SiO4	4.43E-05	4.43E-05	-4.354	-4.354	0
	H3SiO4-	7.45E-10	7.03E-10	-9.128	-9.153	-0.025
	H2SiO4-2	3.92E-18	3.11E-18	-17.407	-17.508	-0.101
Zn	1.49E-04					
	Zn+2	1.43E-04	1.13E-04	-3.846	-3.946	-0.101
	ZnSO4	5.81E-06	5.81E-06	-5.236	-5.236	0
	ZnCl+	4.61E-08	4.35E-08	-7.336	-7.361	-0.025
	Zn(SO4)2-2	1.68E-08	1.33E-08	-7.776	-7.877	-0.101
	ZnOH+	7.48E-09	7.06E-09	-8.126	-8.151	-0.025
	ZnOHCl	2.14E-10	2.14E-10	-9.671	-9.67	0
	Zn(OH)2	5.41E-11	5.42E-11	-10.267	-10.266	0
	ZnCl2	1.25E-11	1.25E-11	-10.904	-10.903	0
	ZnCl3-	3.94E-15	3.72E-15	-14.404	-14.43	-0.025
	Zn(OH)3-	3.54E-17	3.34E-17	-16.451	-16.476	-0.025
	ZnCl4-2	6.05E-19	4.80E-19	-18.219	-18.319	-0.101
	Zn(OH)4-2	1.30E-24	1.03E-24	-23.886	-23.986	-0.101

#NAME? indices

Phase	SI	log	IAP	log	KT
Mn2(SO4)3	-61.7	-12.77	48.93	Mn2(SO4)3	
O2(g)	-53.09	35.48	88.57	O2	
Tremolite	-46.8	13.64	60.44	Ca2Mg5Si8O22(OH)2	
ZnMetal	-38.33	-11.11	27.23	Zn	
Chlorite7A	-35	42.95	77.95	Mg5Al2Si3O10(OH)8	
Chlorite14A	-31.47	42.95	74.43	Mg5Al2Si3O10(OH)8	
Zn3O(SO4	-29.96	-8.47	21.5	ZnO:2ZnSO4	

Talc	-13.17	9.99	23.16	Mg3Si4O10(OH)2
Zn2(OH)3C	-12.74	2.46	15.2	Zn2(OH)3Cl
Sepiolite	-12.46	3.71	16.17	Mg2Si3O7.5OH:3H2O
Diopside	-12.2	8.92	21.12	CaMgSi2O6
Thenardite	-11.69	-11.84	-0.16	Na2SO4
Zincosite	-11.52	-7.79	3.74	ZnSO4
Brucite	-11.42	6.45	17.87	Mg(OH)2
Goslarite	-10.78	-12.87	-2.09	ZnSO4:7H2O
MnSO4	-10.43	-7.18	3.26	MnSO4
Bianchite	-10.38	-12.14	-1.76	ZnSO4:6H2O
Zn2(OH)2S	-9.8	-2.3	7.5	Zn2(OH)2SO4
Epsomite	-9.66	-11.91	-2.25	MgSO4:7H2O
Halite	-9.35	-7.81	1.55	NaCl
Pyrochroite	-9.1	6.1	15.2	Mn(OH)2
ZnSO4:H2(	-8.35	-8.51	-0.17	ZnSO4:H2O
Clinoenstat	-7.63	4.47	12.1	MgSiO3
Fe3(OH)8	-7.21	39.79	47	Fe3(OH)8
Zn(OH)2-a	-6.96	5.49	12.45	Zn(OH)2
Willemite	-6.87	9.73	16.6	Zn2SiO4
Magadiite	-6.79	-21.09	-14.3	NaSi7O13(OH)3:3H2O
Zn(OH)2-c	-6.71	5.49	12.2	Zn(OH)2
Zn(OH)2-b	-6.26	5.49	11.75	Zn(OH)2
Zn(OH)2-g	-6.22	5.49	11.71	Zn(OH)2
Zn(OH)2-e	-6.01	5.49	11.5	Zn(OH)2
Zincite(c)	-5.76	6.22	11.97	ZnO
ZnO(a)	-5.09	6.22	11.31	ZnO
Gypsum	-3.71	-8.3	-4.59	CaSO4:2H2O
Anhydrite	-2.52	-6.85	-4.34	CaSO4
JarositeH	-2.21	34.66	36.87	(H3O)Fe3(SO4)2(OH)6
ZnSiO3	-0.11	3.52	3.62	ZnSiO3
SiO2(a)	0.14	-2.7	-2.84	SiO2
Silicagel	0.49	-2.7	-3.19	SiO2
Jarosite-Na	0.57	36.83	36.26	NaFe3(SO4)2(OH)6
Chalcedon	1.03	-2.7	-3.73	SiO2
Cristobalite	1.1	-2.7	-3.8	SiO2
Quartz	1.51	-2.7	-4.21	SiO2
Hausmann	2.09	66.95	64.86	Mn3O4
Fe(OH)3(a	2.61	20.89	18.28	Fe(OH)3
Jarosite-K	4.22	36.36	32.14	KFe3(SO4)2(OH)6
Manganite	4.36	29.7	25.34	MnOOH
O2(g)	4.63	92.95	88.31	O2
Jarosite(ss	5.85	36.18	30.33	(K0.77Na0.03H0.2)Fe3(SO4)2(OH)6
Bixbyite	7.17	60.12	52.95	Mn2O3
Fe(OH)2.7(	7.98	18.33	10.35	Fe(OH)2.7Cl0.3
Goethite	9.09	21.61	12.52	FeOOH
Pyrolusite	9.44	53.3	43.86	MnO2
Birnessite	9.7	53.3	43.6	MnO2
Magnetite	10.26	42.69	32.43	Fe3O4
Nsutite	10.74	53.3	42.56	MnO2
Maghemite	10.79	43.95	33.16	Fe2O3
Hematite	20.01	43.95	23.94	Fe2O3

Hausmann	-29.24	35.81	65.05	Mn3O4
Bixbyite	-23.29	29.78	53.08	Mn2O3
Zn5(OH)8C	-22.98	15.52	38.5	Zn5(OH)8Cl2
Chrysotile	-22.14	12.07	34.21	Mg3Si2O5(OH)4
Forsterite	-20.75	9.5	30.25	Mg2SiO4
Pyrolusite	-20.22	23.76	43.98	MnO2
Talc	-19.89	3.36	23.25	Mg3Si4O10(OH)2
Birnessite	-19.84	23.76	43.6	MnO2
Nsutite	-18.8	23.76	42.56	MnO2
ZnCl2	-18.74	-11.01	7.73	ZnCl2
JarositeH	-18.25	18.78	37.03	(H3O)Fe3(SO4)2(OH)6
Sepiolite(d	-17.87	0.79	18.66	Mg2Si3O7.5OH:3H2O
H2(g)	-17.79	-17.74	0.05	H2
Portlandite	-17.11	6.92	24.04	Ca(OH)2
Zn4(OH)6S	-16.05	12.35	28.4	Zn4(OH)6SO4
Diopside	-16.04	5.14	21.19	CaMgSi2O6
Jarosite-Na	-15.84	20.54	36.38	NaFe3(SO4)2(OH)6
Sepiolite	-15.4	0.79	16.19	Mg2Si3O7.5OH:3H2O
Prehnite	-14.44	22.18	36.62	Ca2Al2Si3O10(OH)2
Magadiite	-14.41	-28.71	-14.3	NaSi7O13(OH)3:3H2O
MnCl2:4H2	-13.64	-11.63	2.02	MnCl2:4H2O
MnSO4	-11.45	-8.16	3.29	MnSO4
Zincosite	-11.33	-7.55	3.78	ZnSO4
Brucite	-11	6.92	17.92	Mg(OH)2
Zn2(OH)3C	-10.76	4.44	15.2	Zn2(OH)3Cl
Thenardite	-10.51	-10.66	-0.16	Na2SO4
Manganite	-10.45	14.89	25.34	MnOOH
Wairakite	-10.07	10.9	20.97	CaAl2Si4O12:2H2O
Clinoenstat	-9.57	2.57	12.14	MgSiO3
Pyrochroite	-9.18	6.02	15.2	Mn(OH)2
Greenalite	-8.97	11.84	20.81	Fe3Si2O5(OH)4
Anorthite	-8.94	19.61	28.55	CaAl2Si2O8
Mirabilite	-8.79	-10.66	-1.87	Na2SO4:10H2O
Fe3(OH)8	-8.75	38.28	47.03	Fe3(OH)8
Halite	-8.61	-7.06	1.55	NaCl
Zn2(OH)2S	-8.42	-0.92	7.5	Zn2(OH)2SO4
Willemite	-7.75	8.91	16.66	Zn2SiO4
ZnSO4:H2(	-7.41	-7.55	-0.15	ZnSO4:H2O
Analcime	-7.19	3.75	10.94	NaAlSi2O6:H2O
Albite	-5.93	-0.6	5.33	NaAlSi3O8
Zn(OH)2-a	-5.82	6.63	12.45	Zn(OH)2
Bianchite	-5.79	-7.55	-1.76	ZnSO4:6H2O
Zn(OH)2-c	-5.57	6.63	12.2	Zn(OH)2
Goslarite	-5.46	-7.55	-2.09	ZnSO4:7H2O
Zincite(c)	-5.38	6.63	12.01	ZnO
Laumontite	-5.28	10.9	16.18	CaAl2Si4O12:4H2O
Zn(OH)2-b	-5.12	6.63	11.75	Zn(OH)2
Zn(OH)2-g	-5.08	6.63	11.71	Zn(OH)2
Epsomite	-5.01	-7.26	-2.25	MgSO4:7H2O
Melanterite	-4.92	-7.34	-2.42	FeSO4:7H2O
Zn(OH)2-e	-4.87	6.63	11.5	Zn(OH)2
ZnO(a)	-4.68	6.63	11.31	ZnO
Anhydrite	-2.93	-7.26	-4.34	CaSO4
Gypsum	-2.67	-7.26	-4.59	CaSO4:2H2O
Fe(OH)3(a	-2.58	15.72	18.3	Fe(OH)3
Leonhardit	-2.3	21.8	24.1	Ca2Al4Si8O24:7H2O
Maghemite	-1.76	31.44	33.2	Fe2O3
SiO2(a)	-1.51	-4.35	-2.85	SiO2
Halloysite	-1.41	12.68	14.09	Al2Si2O5(OH)4
ZnSiO3	-1.38	2.28	3.66	ZnSiO3
Al(OH)3(a)	-1.16	10.7	11.86	Al(OH)3
Silicagel	-1.16	-4.35	-3.2	SiO2
Chalcedon	-0.81	-4.35	-3.74	SiO2
Cristobalite	-0.55	-4.35	-3.81	SiO2
Jurbanite	-0.28	-3.49	-3.23	AlOHSO4
Quartz	-0.13	-4.35	-4.22	SiO2
Montmorill	0.68	10.09	9.41	Ca0.165Al2.33Si3.67O10(OH)2
Boehmite	0.99	10.7	9.71	AlOOH
Gibbsite	1.68	10.7	9.02	Al(OH)3
Fe(OH)2.7(	2.7	13.07	10.37	Fe(OH)2.7Cl0.3
Diaspore	2.83	10.7	7.86	AlOOH
Goethite	3.17	15.72	12.54	FeOOH
Pyrophyllite	3.57	3.98	0.41	Al2Si4O10(OH)2
Kaolinite	3.84	12.68	8.84	Al2Si2O5(OH)4
Magnetite	5.72	38.28	32.56	Fe3O4
Basalumini	5.9	28.6	22.7	Al4(OH)10SO4
Hematite	7.4	31.44	24.04	Fe2O3

End of simulation.

Reading input data for simulation 2

End of run.

```
data base.

SOLUTION_MASTER_SPECIES
SOLUTION_SPECIES
PHASES
EXCHANGE_MASTER_SPECIES
EXCHANGE_SPECIES
SURFACE_MASTER_SPECIES
SURFACE_SPECIES
END

input data for simulation 1

TITLE Example 1.wet background
SOLUTION 1 wet background
units ppm
pH 4.5
pe 4.64
density 1
temp 9.1
Mg 0.82
Na 6.54
Ca 412.3
Cl 9.7
S(6) 1.273
S(-2) 0.5
SOLUTION_MASTER_SPECIES
SOLUTION_SPECIES
PHASES
END

Example 1.wet background

ning of initial solution calculations.

l solution 1 wet background

ME? composition

Elements Molality Moles

Ca 1.03E-02 1.03E-02
Cl 2.74E-04 2.74E-04
Mg 3.37E-05 3.37E-05
Na 2.85E-04 2.85E-04
S(-2) 1.56E-05 1.56E-05
S(6) 1.33E-05 1.33E-05

AME? of solution

pH = 4.5
pe = 4.64
Activity of water = 1
Ionic strength = 2.10E-02
Mass of water (kg) = 1.00E+00
Total alkalinity (eq/kg) = -3.55E-05
Total carbon (mol/kg) = 0.00E+00
Total CO2 (mol/kg) = 0.00E+00
Temperatu (deg C) = 9.1
Electrical balance (eq) = 2.07E-02
Iterations = 4
Total H = 1.11E+02
Total O = 5.55E+01

#NAME? couples

Redox couple pe Eh (volts)

S(-2)/S(6) -0.2706 -0.0152

#NAME? of species

Log Log Log
Species Molality Activity Molality Activity Gamma

H+ 3.55E-05 3.16E-05 -4.449 -4.5 -0.051
OH- 9.80E-11 8.54E-11 -10.009 -10.069 -0.06
H2O 5.55E+01 1.00E+00 0 0 0
Ca 1.03E-02
Ca+2 1.03E-02 6.06E-03 -1.988 -2.218 -0.23
CaSO4 4.96E-06 4.98E-06 -5.305 -5.303 0.002
CaHSO4+ 8.97E-10 7.82E-10 -9.047 -9.107 -0.06
CaOH+ 3.65E-11 3.18E-11 -10.438 -10.498 -0.06
Cl 2.74E-04
Cl- 2.74E-04 2.38E-04 -3.563 -3.624 -0.062
H(0) 7.70E-22
H2 3.85E-22 3.87E-22 -21.415 -21.413 0.002
Mg 3.37E-05
Mg+2 3.37E-05 2.01E-05 -4.472 -4.697 -0.225
MgSO4 1.47E-08 1.47E-08 -7.834 -7.832 0.002
MgOH+ 5.81E-13 5.06E-13 -12.236 -12.296 -0.06
Na 2.85E-04
Na+ 2.85E-04 2.48E-04 -3.546 -3.605 -0.059
NaSO4- 6.19E-09 5.40E-09 -8.208 -8.268 -0.06
O(0) 0.00E+00
O2 0.00E+00 0.00E+00 -55.086 -55.086 0.002
S(-2) 1.56E-05
```

```
Reading data base.

SOLUTION_MASTER_SPECIES
SOLUTION_SPECIES
PHASES
EXCHANGE_MASTER_SPECIES
EXCHANGE_SPECIES
SURFACE_MASTER_SPECIES
SURFACE_SPECIES
END

Reading input data for simulation 1

TITLE Example 1.Dry background
SOLUTION 1 dry background
units ppm
pH 5.29
pe 18.01
density 1
temp 6.8
Al 9.37
Fe 15.55
K 0.69
Mg 14.9
Mn 1.99
Na 9.32
Pb 4.47
Si 4.08
Zn 62.77
Cl 16.84
S(-2) 119.02
SOLUTION_MASTER_SPECIES
SOLUTION_SPECIES
PHASES
END

TITLE

Example 1.Dry background

Beginning of initial solution calculations.

Initial solution 1 dry background

#NAME? composition

Elements Molality Moles

Al 3.47E-04 3.47E-04
Cl 4.75E-04 4.75E-04
Fe 2.79E-04 2.79E-04
K 1.77E-05 1.77E-05
Mg 6.13E-04 6.13E-04
Mn 3.62E-05 3.62E-05
Na 4.06E-04 4.06E-04
Pb 2.16E-05 2.16E-05
S(-2) 3.71E-03 3.71E-03
Si 6.79E-05 6.79E-05
Zn 9.61E-04 9.61E-04

#NAME? of solution

pH = 5.29
pe = 18.01
Activity of water = 0.927
Ionic strength = 3.18E-03
Mass of water (kg) = 1.00E+00
Total alkalinity (eq/kg) = 2.10E-03
Total carbon (mol/kg) = 0.00E+00
Total CO2 (mol/kg) = 0.00E+00
Temperatu (deg C) = 6.8
Electrical balance (eq) = 2.43E-03
Iterations = 14
Total H = 1.11E+02
Total O = 6.41E+01

#NAME? of species

Log Log Log
Species Molality Activity Molality Activity Gamma

H+ 5.42E-06 5.13E-06 -5.266 -5.29 -0.024
OH- 4.20E-10 3.96E-10 -9.376 -9.402 -0.026
H2O 5.55E+01 9.27E-01 -0.033 -0.033 0
Al 3.47E-04
Al+3 2.37E-04 1.38E-04 -3.626 -3.86 -0.234
AlOH+2 9.20E-05 7.24E-05 -4.036 -4.14 -0.104
Al(OH)2+ 1.85E-05 1.74E-05 -4.734 -4.76 -0.026
Al(OH)3 1.01E-07 1.01E-07 -6.995 -6.994 0
Al(OH)4- 3.17E-08 2.99E-08 -7.499 -7.525 -0.026
Cl 4.75E-04
Cl- 4.75E-04 4.47E-04 -3.323 -3.349 -0.026
MnCl+ 5.51E-08 5.19E-08 -7.259 -7.285 -0.026
FeCl+2 2.16E-10 1.70E-10 -9.665 -9.769 -0.104
MnCl2 1.01E-11 1.01E-11 -10.995 -10.995 0
ZnCl+ 1.47E-12 1.39E-12 -11.832 -11.858 -0.026
FeCl2+ 6.68E-13 6.29E-13 -12.175 -12.201 -0.026
PbCl+ 3.32E-13 3.13E-13 -12.478 -12.504 -0.026
ZnOHCl 7.24E-15 7.24E-15 -14.14 -14.14 0
```

H2S	1.56E-05	1.56E-05	-4.808	-4.806	0.002
HS-	3.73E-08	3.25E-08	-7.428	-7.488	-0.06
S6-2	2.02E-13	1.35E-13	-12.695	-12.869	-0.174
S5-2	1.65E-13	1.08E-13	-12.783	-12.967	-0.184
S4-2	9.52E-14	6.07E-14	-13.021	-13.217	-0.196
S-2	6.83E-17	3.93E-17	-16.166	-16.405	-0.239
S3-2	3.24E-17	2.00E-17	-16.49	-16.699	-0.209
S2-2	1.72E-18	1.03E-18	-17.766	-17.986	-0.221
S(6)	1.33E-05				
SO4-2	8.27E-06	4.82E-06	-5.083	-5.317	-0.234
CaSO4	4.96E-06	4.98E-06	-5.305	-5.303	0.002
MgSO4	1.47E-08	1.47E-08	-7.834	-7.832	0.002
HSO4-	1.23E-08	1.07E-08	-7.909	-7.969	-0.06
NaSO4-	6.19E-09	5.40E-09	-8.208	-8.268	-0.06
CaHSO4+	8.97E-10	7.82E-10	-9.047	-9.107	-0.06

#NAME? indices----------

Phase	SI	log	IAP	log	KT
O2(g)	-52.2	36.56	88.76	O2	
H2(g)	-18.34	-18.28	0.06	H2	
Portlandite	-17.3	6.78	24.08	Ca(OH)2	
Brucite	-13.66	4.3	17.96	Mg(OH)2	
Thenardite	-12.37	-12.53	-0.16	Na2SO4	
Mirabilite	-10.63	-12.53	-1.9	Na2SO4:10H2O	
Halite	-8.77	-7.23	1.54	NaCl	
Epsomite	-7.76	-10.01	-2.26	MgSO4:7H2O	
H2S(g)	-4	-4.81	-0.81	H2S	
Anhydrite	-3.2	-7.53	-4.34	CaSO4	
Gypsum	-2.94	-7.53	-4.59	CaSO4:2H2O	
Sulfur	8.23	13.47	5.25	S	

End of simulation.

Reading input data for simulation 2

End of run.

MnCl3-	1.32E-15	1.25E-15	-14.878	-14.904	-0.026
ZnCl2	6.00E-16	6.00E-16	-15.222	-15.222	0
FeCl+	4.52E-16	4.26E-16	-15.345	-15.371	-0.026
PbCl2	3.18E-16	3.19E-16	-15.497	-15.497	0
FeCl3	2.81E-17	2.81E-17	-16.551	-16.551	0
ZnCl3-	2.85E-19	2.68E-19	-18.546	-18.572	-0.026
PbCl3-	1.07E-19	1.00E-19	-18.972	-18.998	-0.026
ZnCl4-2	6.55E-23	5.15E-23	-22.184	-22.288	-0.104
PbCl4-2	2.35E-23	1.85E-23	-22.628	-22.732	-0.104
Fe(2)	1.13E-12				
Fe+2	8.77E-13	6.90E-13	-12.057	-12.161	-0.104
Fe(HS)2	2.51E-13	2.51E-13	-12.601	-12.601	0
Fe(HS)3-	5.85E-16	5.51E-16	-15.233	-15.259	-0.026
FeCl+	4.52E-16	4.26E-16	-15.345	-15.371	-0.026
FeOH+	9.84E-18	9.27E-18	-17.007	-17.033	-0.026
Fe(OH)2	2.64E-24	2.64E-24	-23.578	-23.578	0
Fe(OH)3-	1.56E-29	1.47E-29	-28.807	-28.833	-0.026
Fe(3)	2.79E-04				
Fe(OH)2+	2.65E-04	2.50E-04	-3.577	-3.603	-0.026
FeOH+2	1.11E-05	8.69E-06	-4.957	-5.061	-0.104
Fe(OH)3	2.50E-06	2.50E-06	-5.603	-5.603	0
Fe+3	4.00E-08	2.33E-08	-7.398	-7.632	-0.234
Fe2(OH)2+4	1.18E-08	4.53E-09	-7.928	-8.344	-0.416
Fe3(OH)4+5	6.31E-09	1.41E-09	-8.2	-8.85	-0.65
FeCl+2	2.16E-10	1.70E-10	-9.665	-9.769	-0.104
Fe(OH)4-	2.01E-10	1.89E-10	-9.698	-9.724	-0.026
FeCl2+	6.68E-13	6.29E-13	-12.175	-12.201	-0.026
FeCl3	2.81E-17	2.81E-17	-16.551	-16.551	0
H(0)	0.00E+00				
H2	0.00E+00	0.00E+00	-49.73	-49.73	0
K	1.77E-05				
K+	1.77E-05	1.66E-05	-4.753	-4.779	-0.026
Mg	6.13E-04				
Mg+2	6.13E-04	4.86E-04	-3.213	-3.314	-0.101
MgOH+	5.88E-11	5.54E-11	-10.23	-10.256	-0.026
Mn(2)	3.62E-05				
Mn+2	3.62E-05	2.85E-05	-4.442	-4.546	-0.104
MnCl+	5.51E-08	5.19E-08	-7.259	-7.285	-0.026
MnOH+	2.89E-11	2.73E-11	-10.539	-10.565	-0.026
MnCl2	1.01E-11	1.01E-11	-10.995	-10.995	0
MnCl3-	1.32E-15	1.25E-15	-14.878	-14.904	-0.026
Mn(OH)3-	2.83E-24	2.67E-24	-23.548	-23.574	-0.026
Mn(3)	9.10E-14				
Mn+3	9.10E-14	5.31E-14	-13.041	-13.275	-0.234
Mn(6)	1.58E-16				
MnO4-2	1.58E-16	1.24E-16	-15.802	-15.906	-0.104
Mn(7)	3.01E-09				
MnO4-	3.01E-09	2.84E-09	-8.521	-8.547	-0.026
Na	4.06E-04				
Na+	4.06E-04	3.82E-04	-3.392	-3.418	-0.026
O(0)	8.55E+00				
O2	4.28E+00	4.28E+00	0.631	0.631	0
Pb	2.16E-05				
Pb(HS)2	2.16E-05	2.16E-05	-4.666	-4.666	0
Pb(HS)3-	9.23E-09	8.70E-09	-8.035	-8.061	-0.026
Pb+2	3.61E-11	2.84E-11	-10.442	-10.546	-0.104
PbCl+	3.32E-13	3.13E-13	-12.478	-12.504	-0.026
PbOH+	1.06E-13	1.00E-13	-12.973	-12.999	-0.026
PbCl2	3.18E-16	3.19E-16	-15.497	-15.497	0
Pb(OH)2	7.04E-18	7.05E-18	-17.152	-17.152	0
PbCl3-	1.07E-19	1.00E-19	-18.972	-18.998	-0.026
Pb2OH+3	1.09E-22	6.38E-23	-21.961	-22.195	-0.234
PbCl4-2	2.35E-23	1.85E-23	-22.628	-22.732	-0.104
Pb(OH)3-	1.55E-23	1.46E-23	-22.809	-22.835	-0.026
Pb(OH)4-2	7.70E-30	6.06E-30	-29.113	-29.217	-0.104
Pb3(OH)4+2	2.25E-36	1.77E-36	-35.649	-35.753	-0.104
S(-2)	3.71E-03				
H2S	1.73E-03	1.73E-03	-2.763	-2.762	0
Zn(HS)2	9.60E-04	9.61E-04	-3.018	-3.017	0
Pb(HS)2	2.16E-05	2.16E-05	-4.666	-4.666	0
HS-	2.14E-05	2.02E-05	-4.669	-4.695	-0.026
Zn(HS)3-	2.98E-07	2.81E-07	-6.526	-6.552	-0.026
Pb(HS)3-	9.23E-09	8.70E-09	-8.035	-8.061	-0.026
S6-2	6.36E-10	5.18E-10	-9.197	-9.286	-0.089
S5-2	4.45E-10	3.61E-10	-9.351	-9.443	-0.092
S4-2	2.50E-10	2.01E-10	-9.601	-9.696	-0.095
Fe(HS)2	2.51E-13	2.51E-13	-12.601	-12.601	0
S-2	1.60E-13	1.26E-13	-12.795	-12.899	-0.104
S3-2	8.23E-14	6.57E-14	-13.085	-13.182	-0.098
S2-2	4.21E-15	3.34E-15	-14.376	-14.476	-0.1
Fe(HS)3-	5.85E-16	5.51E-16	-15.233	-15.259	-0.026
Si	6.79E-05				
H4SiO4	6.79E-05	6.80E-05	-4.168	-4.168	0
H3SiO4-	1.01E-09	9.55E-10	-8.994	-9.02	-0.026
H2SiO4-2	4.29E-18	3.38E-18	-17.367	-17.471	-0.104
Zn	9.61E-04				
Zn(HS)2	9.60E-04	9.61E-04	-3.018	-3.017	0
Zn(HS)3-	2.98E-07	2.81E-07	-6.526	-6.552	-0.026
Zn+2	3.44E-09	2.71E-09	-8.464	-8.568	-0.104
ZnCl+	1.47E-12	1.39E-12	-11.832	-11.858	-0.026
ZnOH+	1.31E-13	1.23E-13	-12.883	-12.909	-0.026
ZnOHCl	7.24E-15	7.24E-15	-14.14	-14.14	0
Zn(OH)2	1.11E-15	1.11E-15	-14.954	-14.953	0
ZnCl2	6.00E-16	6.00E-16	-15.222	-15.222	0
ZnCl3-	2.85E-19	2.68E-19	-18.546	-18.572	-0.026
Zn(OH)3-	6.76E-22	6.37E-22	-21.17	-21.196	-0.026
ZnCl4-2	6.55E-23	5.15E-23	-22.184	-22.288	-0.104
Zn(OH)4-2	2.32E-29	1.82E-29	-28.635	-28.739	-0.104

#NAME? indices----------

Phase	SI	log	IAP	log	KT
ZnMetal	-72.1	-44.59	27.51	Zn	
PbMetal	-50.82	-46.57	4.25	Pb	

H2(g)	-46.66	-46.6	0.06	H2
Zn5(OH)8C	-45.98	-7.48	38.5	Zn5(OH)8Cl2
Greenalite	-33.92	-13.11	20.81	Fe3Si2O5(OH)4
Minium	-32.02	46.57	78.59	Pb3O4
Chlorite7A	-31.5	47.65	79.15	Mg5Al2Si3O10(OH)8
Annite	-28.75	-4.73	24.03	KFe3AlSi3O10(OH)2
Chlorite14A	-27.95	47.65	75.6	Mg5Al2Si3O10(OH)8
Pb2O(OH)2	-26.23	-0.03	26.2	PbO:Pb(OH)2
Pb2SiO4	-25.1	-4.1	21	Pb2SiO4
Phlogopite	-23.5	21.82	45.32	KMg3AlSi3O10(OH)2
ZnCl2	-23.13	-15.27	7.86	ZnCl2
Chrysotile	-21.17	13.43	34.6	Mg3Si2O5(OH)4
Forsterite	-20.26	10.37	30.62	Mg2SiO4
Zn2(OH)3C	-19.91	-4.71	15.2	Zn2(OH)3Cl
Talc	-18.35	5.26	23.61	Mg3Si4O10(OH)2
Pb2(OH)3C	-17.46	-8.67	8.79	Pb2(OH)3Cl
Willemite	-17.06	-0.14	16.92	Zn2SiO4
Sepiolite(d)	-16.61	2.05	18.66	Mg2Si3O7.5OH:3H2O
Pb2O3	-14.47	46.57	61.04	Pb2O3
Sepiolite	-14.22	2.05	16.27	Mg2Si3O7.5OH:3H2O
Massicot	-13.71	0	13.71	PbO
Litharge	-13.5	0	13.5	PbO
MnCl2:4H2	-13.26	-11.38	1.88	MnCl2:4H2O
PbO:0.3H2	-12.99	-0.01	12.98	PbO:0.33H2O
Magadiite	-12.71	-27.01	-14.3	NaSi7O13(OH)3:3H2O
Cotunnite	-12.21	-17.25	-5.04	PbCl2
PbSiO3	-11.86	-4.1	7.76	PbSiO3
Brucite	-10.93	7.2	18.13	Mg(OH)2
Zn(OH)2-a	-10.5	1.95	12.45	Zn(OH)2
Zn(OH)2-c	-10.25	1.95	12.2	Zn(OH)2
Zincite(c)	-10.2	1.98	12.18	ZnO
Zn(OH)2-b	-9.8	1.95	11.75	Zn(OH)2
Zn(OH)2-g	-9.76	1.95	11.71	Zn(OH)2
Zn(OH)2-e	-9.55	1.95	11.5	Zn(OH)2
ZnO(a)	-9.33	1.98	11.31	ZnO
Laurionite	-9.26	-8.64	0.62	PbOHCl
Pyrochroite	-9.23	5.97	15.2	Mn(OH)2
Clinoenstat	-9.17	3.13	12.3	MgSiO3
Pb(OH)2	-8.85	-0.03	8.82	Pb(OH)2
Halite	-8.31	-6.77	1.54	NaCl
MnS(Greer	-8.03	3.27	11.3	MnS
FeS(ppt)	-7.65	-4.34	3.31	FeS
Mackinawit	-6.92	-4.34	2.57	FeS
Plattnerite	-6.1	46.57	52.67	PbO2
ZnSiO3	-5.92	-2.12	3.8	ZnSiO3
Fe3(OH)8	-5.59	41.59	47.18	Fe3(OH)8
Analcime	-5.55	5.58	11.13	NaAlSi2O6:H2O
Phillipsite	-4.02	0.8	4.82	Na0.5K0.5AlSi3O8:H2O
Albite	-3.95	1.51	5.46	NaAlSi3O8
Adularia	-2.5	0.15	2.65	KAlSi3O8
H2S(g)	-1.98	-2.76	-0.78	H2S
Hausmann	-1.25	64.57	65.83	Mn3O4
SiO2(a)	-1.23	-4.1	-2.87	SiO2
Silicagel	-0.87	-4.1	-3.23	SiO2
Chalcedon	-0.33	-4.1	-3.78	SiO2
Cristobalite	-0.25	-4.1	-3.85	SiO2
Al(OH)3(a)	0.15	11.91	12.06	Al(OH)3
Quartz	0.16	-4.1	-4.27	SiO2
Halloysite	1.25	15.65	14.4	Al2Si2O5(OH)4
ZnS(a)	1.25	-0.75	-2	ZnS
Illite	1.3	15.23	13.92	K0.6Mg0.25Al2.3Si3.5O10(OH)2
Montmorillk	1.55	12.61	11.06	(HNaK)0.14Mg0.45Fe0.33Al1.47Si3.82O10(OH)2
Wurtzite	1.95	-0.75	-2.7	ZnS
Boehmite	2.02	11.94	9.93	AlOOH
Gibbsite	2.72	11.91	9.2	Al(OH)3
Montmorillk	3.04	10.13	7.09	(HNaK)0.09Mg0.29Fe0.24Al1.57Si3.93O10(OH)2
Fe(OH)3(a	3.25	21.62	18.37	Fe(OH)3
O2(g)	3.5	93.13	89.63	O2
Galena	3.75	-2.73	-6.48	PbS
Diaspore	3.89	11.94	8.06	AlOOH
Manganite	3.93	29.27	25.34	MnOOH
Sphalerite	4.04	-0.75	-4.79	ZnS
Beidellite	4.05	13.44	9.39	(NaKMg0.5)0.11Al2.33Si3.67O10(OH)2
Bixbyite	4.98	58.57	53.59	Mn2O3
Pyrophyllite	6.41	7.48	1.07	Al2Si4O10(OH)2
Kaolinite	6.54	15.65	9.12	Al2Si2O5(OH)4
Pyrolusite	8.09	52.57	44.48	MnO2
Kmica	8.51	24.04	15.53	KAl3Si3O10(OH)2
Fe(OH)2.7C	8.8	19.04	10.44	Fe(OH)2.7Cl0.3
Magnetite	8.62	41.73	33.1	Fe3O4
Birnessite	8.97	52.57	43.6	MnO2
Goethite	9.01	21.65	12.65	FeOOH
Maghemite	9.99	43.34	33.35	Fe2O3
Nsutite	10	52.57	42.56	MnO2
Hematite	18.91	43.34	24.42	Fe2O3
Greigite	19.99	30.81	10.82	Fe3S4
Sulfur	38.52	43.84	5.31	S
Pyrite	44.07	39.49	-4.57	FeS2

End of simulation.

Reading input data for simulation 2

End of run.

Reading data base.

SOLUTION_MASTER_SPECIES
SOLUTION_SPECIES
PHASES
EXCHANGE_MASTER_SPECIES
EXCHANGE_SPECIES
SURFACE_MASTER_SPECIES
SURFACE_SPECIES
END

Reading input data for simulation 1

TITLE	Example	1.--Wet	Upstream
SOLUTION	1	wet	upstream
units	ppm		
pH	4.58		
pe	4.42		
density	1		
temp	8.9		
Fe	0.58		
Mg	0.9		
Na	7.18		
Cl	9.8		
Si	0.76		
S(6)	1.23		

SOLUTION_MASTER_SPECIES
SOLUTION_SPECIES
PHASES
END

TITLE

Example 1.--Wet Upstream

Beginning of initial solution calculations.

Initial solution 1 wet upstream

#NAME? composition

Elements	Molality	Moles
Cl	2.76E-04	2.76E-04
Fe	1.04E-05	1.04E-05
Mg	3.70E-05	3.70E-05
Na	3.12E-04	3.12E-04
S(6)	1.28E-05	1.28E-05
Si	1.27E-05	1.27E-05

#NAME? of solution

pH	=	4.58			
pe	=	4.42			
Activity	of	water	=	1	
Ionic	strength	=	4.28E-04		
Mass	of	water	(kg)	=	1.00E+00
Total	alkalinity	(eq/kg)	=	-2.69E-05	
Total	carbon	(mol/kg)	=	0.00E+00	
Total	CO2	(mol/kg)	=	0.00E+00	
Temperatur	(deg	C)	=	8.9	
Electrical	balance	(eq)	=	1.32E-04	
Iterations	=	3			
Total	H	=	1.11E+02		
Total	O	=	5.55E+01		

#NAME? of species

	Log Species	Log Molality	Log Activity	Molality	Activity	Gamma
	H+	2.69E-05	2.63E-05	-4.57	-4.58	-0.01
	OH-	1.03E-10	1.01E-10	-9.987	-9.997	-0.01
	H2O	5.55E+01	1.00E+00	0	0	0
Cl	2.76E-04					
	Cl-	2.76E-04	2.70E-04	-3.558	-3.568	-0.01
	FeCl+	3.61E-09	3.52E-09	-8.443	-8.453	-0.01
	FeCl+2	4.87E-17	4.44E-17	-16.312	-16.352	-0.04
	FeCl2+	9.41E-20	9.20E-20	-19.026	-19.036	-0.01
	FeCl3	2.48E-24	2.48E-24	-23.605	-23.605	0
Fe(2)	1.04E-05					
	Fe+2	1.04E-05	9.45E-06	-4.984	-5.024	-0.04
	FeSO4	1.43E-08	1.43E-08	-7.846	-7.846	0
	FeCl+	3.61E-09	3.52E-09	-8.443	-8.453	-0.01
	FeOH+	3.26E-11	3.19E-11	-10.487	-10.497	-0.01
	FeHSO4+	2.49E-12	2.43E-12	-11.605	-11.615	-0.01
	Fe(OH)2	2.35E-18	2.35E-18	-17.63	-17.63	0
	Fe(OH)3-	2.87E-24	2.80E-24	-23.542	-23.552	-0.01
Fe(3)	6.64E-12					
	Fe(OH)2+	5.69E-12	5.56E-12	-11.245	-11.255	-0.01
	FeOH+2	9.24E-13	8.42E-13	-12.034	-12.075	-0.04
	Fe(OH)3	1.30E-14	1.30E-14	-13.887	-13.887	0
	Fe+3	1.15E-14	9.35E-15	-13.939	-14.029	-0.09
	FeSO4+	8.33E-16	8.14E-16	-15.079	-15.089	-0.01
	FeCl+2	4.87E-17	4.44E-17	-16.312	-16.352	-0.04
	Fe(OH)4-	2.32E-19	2.27E-19	-18.634	-18.644	-0.01
	Fe(SO4)2-	1.98E-19	1.93E-19	-18.705	-18.715	-0.01
	FeCl2+	9.41E-20	9.20E-20	-19.026	-19.036	-0.01
	FeHSO4+2	6.61E-20	6.03E-20	-19.18	-19.22	-0.04

Reading data base.

SOLUTION_MASTER_SPECIES
SOLUTION_SPECIES
PHASES
EXCHANGE_MASTER_SPECIES
EXCHANGE_SPECIES
SURFACE_MASTER_SPECIES
SURFACE_SPECIES
END

Reading input data for simulation 1

TITLE	Example	1.dry	upstream
SOLUTION	1	dry	upstream
units	ppm		
pH	5.46		
pe	18.02		
density	1		
temp	8.7		
Ca	35.4		
Fe	43.2		
Mg	17.78		
Mn	7.15		
Na	1.05		
Si	5.04		
Zn	23.86		
Cl	16.84		
S(6)	8.016		
S(-2)	156.104		

SOLUTION_MASTER_SPECIES
SOLUTION_SPECIES
PHASES
END

TITLE

Example 1.dry upstream

Beginning of initial solution calculations.

Initial solution 1 dry upstream

#NAME? composition

Elements	Molality	Moles
Ca	8.84E-04	8.84E-04
Cl	4.75E-04	4.75E-04
Fe	7.74E-04	7.74E-04
Mg	7.32E-04	7.32E-04
Mn	1.30E-04	1.30E-04
Na	4.57E-05	4.57E-05
S(-2)	4.87E-03	4.87E-03
S(6)	8.35E-05	8.35E-05
Si	8.39E-05	8.39E-05
Zn	3.65E-04	3.65E-04

#NAME? of solution

pH	=	5.46			
pe	=	18.02			
Activity	of	water	=	0.763	
Ionic	strength	=	4.34E-03		
Mass	of	water	(kg)	=	1.00E+00
Total	alkalinity	(eq/kg)	=	7.84E-04	
Total	carbon	(mol/kg)	=	0.00E+00	
Total	CO2	(mol/kg)	=	0.00E+00	
Temperatur	(deg	C)	=	8.7	
Electrical	balance	(eq)	=	3.61E-03	
Iterations	=	43			
Total	H	=	1.11E+02		
Total	O	=	8.34E+01		

#NAME? couples

Redox	couple	pe	Eh	(volts)
S(-2)/S(6)	-1.5273	-0.0848		

#NAME? of species

	Log Species	Log Molality	Log Activity	Molality	Activity	Gamma
	H+	3.69E-06	3.47E-06	-5.433	-5.46	-0.027
	OH-	5.12E-10	4.78E-10	-9.291	-9.321	-0.03
	H2O	5.55E+01	7.63E-01	-0.117	-0.117	0
Ca	8.84E-04					
	Ca+2	8.77E-04	8.70E-04	-3.057	-3.174	-0.117
	CaSO4	6.13E-06	6.13E-06	-5.213	-5.212	0
	CaHSO4+	1.11E-10	1.04E-10	-9.955	-9.985	-0.03
	CaOH+	2.62E-11	2.45E-11	-10.582	-10.612	-0.03
Cl	4.75E-04					
	Cl-	4.75E-04	4.43E-04	-3.323	-3.354	-0.03
	MnCl+	1.90E-07	1.77E-07	-6.722	-6.752	-0.03
	FeCl+2	4.18E-10	3.17E-10	-9.379	-9.499	-0.12
	MnCl2	3.42E-11	3.42E-11	-10.467	-10.466	0
	FeCl2+	1.25E-12	1.16E-12	-11.904	-11.934	-0.03

Fe2(OH)2+	5.58E-23	3.86E-23	-22.253	-22.414	-0.16
FeCl3	2.48E-24	2.48E-24	-23.605	-23.605	0
Fe3(OH)4+	3.84E-31	2.15E-31	-30.416	-30.667	-0.251
1.47E-21					
H2	7.37E-22	7.37E-22	-21.132	-21.132	0
3.70E-05					
Mg+2	3.70E-05	3.37E-05	-4.432	-4.472	-0.04
MgSO4	5.91E-08	5.91E-08	-7.229	-7.229	0
MgOH+	1.03E-12	1.00E-12	-11.989	-11.999	-0.01
3.12E-04					
Na+	3.12E-04	3.05E-04	-3.505	-3.515	-0.01
NaSO4-	1.63E-08	1.59E-08	-7.789	-7.799	-0.01
0.00E+00					
O2	0.00E+00	0.00E+00	-55.72	-55.72	0
1.28E-05					
SO4-2	1.27E-05	1.16E-05	-4.896	-4.936	-0.04
MgSO4	5.91E-08	5.91E-08	-7.229	-7.229	0
HSO4-	2.19E-08	2.14E-08	-7.66	-7.67	-0.01
NaSO4-	1.63E-08	1.59E-08	-7.789	-7.799	-0.01
FeSO4	1.43E-08	1.43E-08	-7.846	-7.846	0
FeHSO4+	2.49E-12	2.43E-12	-11.605	-11.615	-0.01
FeSO4+	8.33E-16	8.14E-16	-15.079	-15.089	-0.01
Fe(SO4)2-	1.98E-19	1.93E-19	-18.705	-18.715	-0.01
FeHSO4+2	6.61E-20	6.03E-20	-19.18	-19.22	-0.04
1.27E-05					
H4SiO4	1.27E-05	1.27E-05	-4.898	-4.898	0
H3SiO4-	3.89E-11	3.80E-11	-10.41	-10.42	-0.01
H2SiO4-2	3.40E-20	3.10E-20	-19.469	-19.509	-0.04

E? indices----------

Phase	SI	log	IAP	log	KT
O2(g)	-52.84	36	88.84	O2	
Chrysotile	-30.04	4.27	34.31	Mg3Si2O5(OH)4	
Talc	-28.87	-5.53	23.34	Mg3Si4O10(OH)2	
JarositeH	-25.98	11.21	37.19	(H3O)Fe3(SO4)2(OH)6	
Forsterite	-25.86	4.48	30.34	Mg2SiO4	
Jarosite-Na	-24.23	12.28	36.51	NaFe3(SO4)2(OH)6	
Sepiolite(d)	-23.98	-5.32	18.66	Mg2Si3O7.5OH:3H2O	
Sepiolite	-21.53	-5.32	16.21	Mg2Si3O7.5OH:3H2O	
Magadiite	-18.92	-33.22	-14.3	NaSi7O13(OH)3:3H2O	
Greenalite	-18.2	2.61	20.81	Fe3Si2O5(OH)4	
H2(g)	-18.06	-18	0.06	H2	
Fe3(OH)8	-16.67	30.41	47.07	Fe3(OH)8	
Brucite	-13.29	4.69	17.97	Mg(OH)2	
Clinoenstati	-12.39	-0.21	12.18	MgSiO3	
Thenardite	-11.81	-11.97	-0.16	Na2SO4	
Mirabilite	-10.06	-11.97	-1.91	Na2SO4:10H2O	
Halite	-8.63	-7.08	1.54	NaCl	
Melanterite	-7.53	-9.96	-2.43	FeSO4:7H2O	
Epsomite	-7.15	-9.41	-2.26	MgSO4:7H2O	
Maghemite	-6.96	26.27	33.24	Fe2O3	
Fe(OH)3(a)	-5.18	13.14	18.32	Fe(OH)3	
Magnetite	-2.29	30.41	32.7	Fe3O4	
SiO2(a)	-2.05	-4.9	-2.85	SiO2	
Silicagel	-1.69	-4.9	-3.2	SiO2	
Chalcedony	-1.15	-4.9	-3.75	SiO2	
Cristobalite	-1.08	-4.9	-3.82	SiO2	
Quartz	-0.67	-4.9	-4.23	SiO2	
Fe(OH)2.7C	0.31	10.69	10.39	Fe(OH)2.7Cl0.3	
Goethite	0.57	13.14	12.57	FeOOH	
Hematite	2.14	26.27	24.13	Fe2O3	

End of simulation.

Reading input data for simulation 2

End of run.

	ZnCl+	4.62E-14	4.31E-14	-13.335	-13.365	-0.03
	MnCl3-	4.47E-15	4.17E-15	-14.35	-14.38	-0.03
	FeCl+	8.38E-16	7.82E-16	-15.077	-15.107	-0.03
	ZnOHCl	2.76E-16	2.76E-16	-15.56	-15.559	0
	FeCl3	5.15E-17	5.15E-17	-16.289	-16.288	0
	ZnCl2	1.85E-17	1.85E-17	-16.733	-16.733	0
	ZnCl3-	8.76E-21	8.18E-21	-20.057	-20.087	-0.03
	ZnCl4-2	2.05E-24	1.56E-24	-23.688	-23.808	-0.12
Fe(2)	7.33E-12					
	Fe(HS)2	5.58E-12	5.59E-12	-11.253	-11.253	0
	Fe+2	1.69E-12	1.28E-12	-11.773	-11.893	-0.12
	Fe(HS)3-	4.57E-14	4.26E-14	-13.34	-13.37	-0.03
	FeSO4	8.76E-15	8.77E-15	-14.057	-14.057	0
	FeCl+	8.38E-16	7.82E-16	-15.077	-15.107	-0.03
	FeOH+	2.22E-17	2.07E-17	-16.653	-16.683	-0.03
	FeHSO4+	2.12E-19	1.98E-19	-18.674	-18.704	-0.03
	Fe(OH)2	7.12E-24	7.13E-24	-23.148	-23.147	0
	Fe(OH)3-	5.16E-29	4.81E-29	-28.288	-28.318	-0.03
Fe(3)	7.74E-04					
	Fe(OH)2+	7.39E-04	6.89E-04	-3.132	-3.162	-0.03
	FeOH+2	2.61E-05	1.98E-05	-4.583	-4.703	-0.12
	Fe(OH)3	8.35E-06	8.36E-06	-5.079	-5.078	0
	Fe3(OH)4+5	1.16E-07	2.06E-08	-6.936	-7.686	-0.751
	Fe+3	8.19E-08	4.40E-08	-7.087	-7.357	-0.27
	Fe2(OH)2+4	7.15E-08	2.37E-08	-7.146	-7.626	-0.48
	FeSO4+	1.85E-08	1.72E-08	-7.734	-7.764	-0.03
	Fe(OH)4-	8.21E-10	7.66E-10	-9.086	-9.116	-0.03
	FeCl+2	4.18E-10	3.17E-10	-9.379	-9.499	-0.12
	Fe(SO4)2-	2.06E-11	1.92E-11	-10.686	-10.716	-0.03
	FeCl2+	1.25E-12	1.16E-12	-11.904	-11.934	-0.03
	FeHSO4+2	2.25E-13	1.71E-13	-12.648	-12.768	-0.12
	FeCl3	5.15E-17	5.15E-17	-16.289	-16.288	0
H(0)	0.00E+00					
	H2	0.00E+00	0.00E+00	-50.09	-50.09	0
Mg	7.32E-04					
	Mg+2	7.27E-04	5.57E-04	-3.138	-3.254	-0.116
	MgSO4	4.34E-06	4.35E-06	-5.362	-5.362	0
	MgOH+	8.20E-11	7.65E-11	-10.086	-10.116	-0.03
Mn(2)	1.30E-04					
	Mn+2	1.29E-04	9.80E-05	-3.889	-4.009	-0.12
	MnSO4	6.61E-07	6.62E-07	-6.18	-6.179	0
	MnCl+	1.90E-07	1.77E-07	-6.722	-6.752	-0.03
	MnOH+	1.21E-10	1.13E-10	-9.916	-9.946	-0.03
	MnCl2	3.42E-11	3.42E-11	-10.467	-10.466	0
	MnCl3-	4.47E-15	4.17E-15	-14.35	-14.38	-0.03
	Mn(OH)3-	1.77E-23	1.66E-23	-22.751	-22.781	-0.03
Mn(3)	3.43E-13					
	Mn+3	3.43E-13	1.84E-13	-12.465	-12.735	-0.27
Mn(6)	5.90E-15					
	MnO4-2	5.90E-15	4.48E-15	-14.229	-14.349	-0.12
Mn(7)	1.10E-07					
	MnO4-	1.10E-07	1.03E-07	-6.958	-6.988	-0.03
Na	4.57E-05					
	Na+	4.57E-05	4.27E-05	-4.34	-4.37	-0.03
	NaSO4-	1.12E-08	1.04E-08	-7.953	-7.983	-0.03
O(0)	2.79E+01					
	O2	1.39E+01	1.39E+01	1.144	1.144	0
S(-2)	4.87E-03					
	H2S	4.06E-03	4.07E-03	-2.391	-2.391	0
	Zn(HS)2	3.65E-04	3.65E-04	-3.438	-3.438	0
	HS-	7.50E-05	7.00E-05	-4.125	-4.155	-0.03
	Zn(HS)3-	3.96E-07	3.70E-07	-6.402	-6.432	-0.03
	S6-2	3.35E-09	2.66E-09	-8.475	-8.576	-0.101
	S5-2	2.34E-09	1.84E-09	-8.632	-8.736	-0.104
	S4-2	1.32E-09	1.03E-09	-8.881	-8.989	-0.108
	Fe(HS)2	5.58E-12	5.59E-12	-11.253	-11.253	0
	S-2	8.46E-13	6.42E-13	-12.073	-12.193	-0.12
	S3-2	4.33E-13	3.35E-13	-12.364	-12.475	-0.112
	Fe(HS)3-	4.57E-14	4.26E-14	-13.34	-13.37	-0.03
	S2-2	2.22E-14	1.70E-14	-13.654	-13.769	-0.115
S(6)	8.35E-05					
	SO4-2	7.23E-05	5.51E-05	-4.141	-4.259	-0.118
	CaSO4	6.13E-06	6.13E-06	-5.213	-5.212	0
	MgSO4	4.34E-06	4.35E-06	-5.362	-5.362	0
	MnSO4	6.61E-07	6.62E-07	-6.18	-6.179	0
	FeSO4+	1.85E-08	1.72E-08	-7.734	-7.764	-0.03
	HSO4-	1.38E-08	1.29E-08	-7.861	-7.891	-0.03
	NaSO4-	1.12E-08	1.04E-08	-7.953	-7.983	-0.03
	CaHSO4+	1.11E-10	1.04E-10	-9.955	-9.985	-0.03
	Fe(SO4)2-	2.06E-11	1.92E-11	-10.686	-10.716	-0.03
	ZnSO4	9.49E-13	9.50E-13	-12.023	-12.022	0
	FeHSO4+2	2.25E-13	1.71E-13	-12.648	-12.768	-0.12
	FeSO4	8.76E-15	8.77E-15	-14.057	-14.057	0
	Zn(SO4)2-2	6.51E-16	4.94E-16	-15.186	-15.306	-0.12
	FeHSO4+	2.12E-19	1.98E-19	-18.674	-18.704	-0.03
Si	8.39E-05					
	H4SiO4	8.39E-05	8.40E-05	-4.076	-4.076	0
	H3SiO4-	1.86E-09	1.74E-09	-8.73	-8.76	-0.03
	H2SiO4-2	1.19E-17	9.02E-18	-16.925	-17.045	-0.12
Zn	3.65E-04					
	Zn(HS)2	3.65E-04	3.65E-04	-3.438	-3.438	0
	Zn(HS)3-	3.96E-07	3.70E-07	-6.402	-6.432	-0.03
	Zn+2	1.13E-10	8.55E-11	-9.948	-10.068	-0.12
	ZnSO4	9.49E-13	9.50E-13	-12.023	-12.022	0
	ZnCl+	4.62E-14	4.31E-14	-13.335	-13.365	-0.03
	ZnOH+	5.04E-15	4.70E-15	-14.298	-14.328	-0.03
	Zn(SO4)2-2	6.51E-16	4.94E-16	-15.186	-15.306	-0.12
	ZnOHCl	2.76E-16	2.76E-16	-15.56	-15.559	0
	Zn(OH)2	5.21E-17	5.21E-17	-16.283	-16.283	0
	ZnCl2	1.85E-17	1.85E-17	-16.733	-16.733	0
	ZnCl3-	8.76E-21	8.18E-21	-20.057	-20.087	-0.03
	Zn(OH)3-	3.89E-23	3.63E-23	-22.41	-22.44	-0.03
	ZnCl4-2	2.05E-24	1.56E-24	-23.688	-23.808	-0.12
	Zn(OH)4-2	1.67E-30	1.27E-30	-29.778	-29.898	-0.12

#NAME? indices----------

Phase	SI	log	IAP	log KT
ZnMetal	-73.63	-46.11	27.52	Zn
Zn5(OH)8Cl	-52.81	-14.31	38.5	Zn5(OH)8Cl2
Zn3O(SO4)	-49.91	-27.92	21.99	ZnO:2ZnSO4
H2(g)	-47.02	-46.96	0.06	H2
Zn4(OH)6S	-40.88	-12.48	28.4	Zn4(OH)6SO4
Tremolite	-39.06	22.15	61.22	Ca2Mg5Si8O22(OH)2
Mn2(SO4)3	-34.41	15.25	49.65	Mn2(SO4)3
Greenalite	-32	-11.19	20.81	Fe3Si2O5(OH)4
ZnCl2	-24.64	-16.78	7.87	ZnCl2
Zn2(OH)3Cl	-22.66	-7.46	15.2	Zn2(OH)3Cl
Zn2(OH)2S	-21.21	-13.71	7.5	Zn2(OH)2SO4
Chrysotile	-19.88	14.73	34.61	Mg3Si2O5(OH)4
Forsterite	-19.38	11.26	30.63	Mg2SiO4
Willemite	-19.3	-2.37	16.93	Zn2SiO4
Zincosite	-18.26	-14.33	3.93	ZnSO4
Portlandite	-16.77	7.51	24.29	Ca(OH)2
Talc	-16.46	7.16	23.62	Mg3Si4O10(OH)2
Sepiolite(d)	-15.5	3.16	18.66	Mg2Si3O7.5OH:3H2O
Melanterite	-14.51	-16.97	-2.46	FeSO4:7H2O
ZnSO4:H2O	-14.38	-14.44	-0.06	ZnSO4:H2O
Diopside	-13.95	7.49	21.44	CaMgSi2O6
Bianchite	-13.27	-15.03	-1.76	ZnSO4:6H2O
Sepiolite	-13.11	3.16	16.27	Mg2Si3O7.5OH:3H2O
MnCl2:4H2	-13.06	-11.19	1.88	MnCl2:4H2O
Goslarite	-13.03	-15.15	-2.12	ZnSO4:7H2O
Thenardite	-12.85	-13	-0.15	Na2SO4
Mirabilite	-12.15	-14.17	-2.02	Na2SO4:10H2O
Magadiite	-12.08	-26.38	-14.3	NaSi7O13(OH)3:3H2O
Zn(OH)2-a	-11.83	0.62	12.45	Zn(OH)2
MnSO4	-11.68	-8.27	3.41	MnSO4
Zn(OH)2-c	-11.58	0.62	12.2	Zn(OH)2
Zincite(c)	-11.45	0.73	12.19	ZnO
Zn(OH)2-b	-11.13	0.62	11.75	Zn(OH)2
Zn(OH)2-g	-11.09	0.62	11.71	Zn(OH)2
Zn(OH)2-e	-10.88	0.62	11.5	Zn(OH)2
Brucite	-10.71	7.43	18.14	Mg(OH)2
ZnO(a)	-10.58	0.73	11.31	ZnO
Halite	-9.26	-7.72	1.54	NaCl
Clinoenstati	-8.6	3.71	12.3	MgSiO3
Pyrochroite	-8.52	6.68	15.2	Mn(OH)2
ZnSiO3	-6.91	-3.11	3.81	ZnSiO3
MnS(Green	-6.78	4.52	11.3	MnS
FeS(ppt)	-6.67	-3.36	3.31	FeS
Epsomite	-6.06	-8.34	-2.28	MgSO4:7H2O
Mackinawite	-5.94	-3.36	2.58	FeS
Fe3(OH)8	-4.09	43.1	47.19	Fe3(OH)8
Anhydrite	-3.09	-7.43	-4.34	CaSO4
Gypsum	-3.07	-7.67	-4.6	CaSO4:2H2O
H2S(g)	-1.61	-2.39	-0.78	H2S
JarositeH	-1.36	36.34	37.71	(H3O)Fe3(SO4)2(OH)6
SiO2(a)	-0.97	-3.84	-2.87	SiO2
Silicagel	-0.61	-3.84	-3.23	SiO2
Chalcedony	-0.06	-3.84	-3.78	SiO2
Cristobalite	0.01	-3.84	-3.85	SiO2
Quartz	0.43	-3.84	-4.27	SiO2
ZnS(a)	0.47	-1.54	-2	ZnS
Jarosite-Na	0.64	37.55	36.91	NaFe3(SO4)2(OH)6
Wurtzite	1.16	-1.54	-2.7	ZnS
Hausmannit	1.37	67.22	65.85	Mn3O4
Sphalerite	3.25	-1.54	-4.79	ZnS
Fe(OH)3(a)	3.78	22.15	18.37	Fe(OH)3
O2(g)	4.02	93.69	89.67	O2
Manganite	4.82	30.16	25.34	MnOOH
Bixbyite	6.82	60.43	53.61	Mn2O3
Fe(OH)2.7C	9.1	19.55	10.44	Fe(OH)2.7Cl0.3
Pyrolusite	9.14	53.64	44.5	MnO2
Goethite	9.62	22.27	12.65	FeOOH
Birnessite	10.04	53.64	43.6	MnO2
Magnetite	10.45	43.57	33.12	Fe3O4
Nsutite	11.07	53.64	42.56	MnO2
Maghemite	11.31	44.66	33.35	Fe2O3
Hematite	20.22	44.66	24.44	Fe2O3
Greigite	23.65	34.48	10.83	Fe3S4
Sulfur	39.25	44.57	5.32	S
Pyrite	45.78	41.21	-4.57	FeS2

End of simulation.

Reading input data for simulation 2

End of run.

```
-----------
Reading data base.
-----------

        SOLUTION_MASTER_SPECIES
        SOLUTION_SPECIES
        PHASES
        EXCHANGE_MASTER_SPECIES
        EXCHANGE_SPECIES
        SURFACE_MASTER_SPECIES
        SURFACE_SPECIES
        END
-------------------------
Reading input data for simulation 1
-------------------------

        TITLE Example 1.dry road
        SOLUTION 1 dry road
        units ppm
        pH 6.42
        pe 17.92
        density 1
        temp 8.2
        Al 0.53
        Ca 35.7
        Fe 46.14
        Mg 22.62
        Mn 7.31
        Na 0.73
        Si 5.25
        Zn 25.02
        Cl 13.84
        S(6) 108.216
        S(-2) 61.905
        SOLUTION_MASTER_SPECIES
        SOLUTION_SPECIES
        PHASES
        END
-----
TITLE
-----

        Example 1.dry road

-------------------------
Beginning of initial solution calculations.
-------------------------

Initial solution 1 dry road

#NAME? composition----------

        Elements Molality Moles

        Al 5.22E-06 5.22E-06
        Ca 8.23E-04 8.23E-04
        Cl 1.41E-04 1.41E-04
        Fe 1.84E-04 1.84E-04
        Mg 8.67E-04 8.67E-04
        Mn 2.94E-05 2.94E-05
        Na 3.40E-05 3.40E-05
        S(-2) 1.14E-03 1.14E-03
        S(6) 4.17E-04 4.17E-04
        Si 8.73E-05 8.73E-05
        Zn 3.41E-04 3.41E-04

#NAME? of solution----------

        pH = 6.42
        pe = 17.92
        Activity of water = 0.1
        Ionic strength = 8.12E-03
        Mass of water (kg) = 1.00E+00
        Total alkalinity (eq/kg) = 7.53E-04
        Total carbon (mol/kg) = 0.00E+00
        Total CO2 (mol/kg) = 0.00E+00
        Temperatu (deg C) = 8.2
        Electrical balance (eq) = 2.54E-03
        Iterations = 101
        Total H = 1.11E+02
        Total O = 2.06E+03

#NAME? couples----------
```

```
-----------
Reading data base.
-----------

        SOLUTION_MASTER_SPECIES
        SOLUTION_SPECIES
        PHASES
        EXCHANGE_MASTER_SPECIES
        EXCHANGE_SPECIES
        SURFACE_MASTER_SPECIES
        SURFACE_SPECIES
        END
-------------------------
Reading input data for simulation 1
-------------------------

        TITLE Example 1.wet road drain
        SOLUTION 1 wet road drain
        units ppm
        pH 6.24
        pe 3.25
        density 1
        temp 8.8
        Ca 1.2
        Fe 0.58
        Mg 1.37
        Na 6.6
        Si 0.88
        Cl 9
        S(6) 36.7
        SOLUTION_MASTER_SPECIES
        SOLUTION_SPECIES
        PHASES
        END
-----
TITLE
-----

        Example 1.wet road drain

-------------------------
Beginning of initial solution calculations.
-------------------------

Initial solution 1 wet road drain

#NAME? composition----------

        Elements Molality Moles

        Ca 2.99E-05 2.99E-05
        Cl 2.54E-04 2.54E-04
        Fe 1.04E-05 1.04E-05
        Mg 5.64E-05 5.64E-05
        Na 2.87E-04 2.87E-04
        S(6) 3.82E-04 3.82E-04
        Si 1.47E-05 1.47E-05

#NAME? of solution----------

        pH = 6.24
        pe = 3.25
        Activity of water = 1
        Ionic strength = 1.21E-03
        Mass of water (kg) = 1.00E+00
        Total alkalinity (eq/kg) = -6.02E-07
        Total carbon (mol/kg) = 0.00E+00
        Total CO2 (mol/kg) = 0.00E+00
        Temperatu (deg C) = 8.8
        Electrical balance (eq) = -5.37E-04
        Iterations = 4
        Total H = 1.11E+02
        Total O = 5.55E+01

#NAME? of species----------

        Log Log Log
        Species Molality Activity Molality Activity Gamma

        H+ 5.97E-07 5.75E-07 -6.224 -6.24 -0.016
        OH- 4.74E-09 4.57E-09 -8.324 -8.34 -0.017
        H2O 5.55E+01 1.00E+00 0 0 0
Ca 2.99E-05
        Ca+2 2.86E-05 2.46E-05 -4.544 -4.609 -0.065
        CaSO4 1.36E-06 1.36E-06 -5.867 -5.867 0
```

	Redox	couple	pe	Eh	(volts)	
	S(-2)/S(6)	-2.1087	-0.1177			

#NAME? of species----------

	Log Species	Log Molality	Log Activity	Molality	Activity	Gamma
	H+	4.13E-07	3.80E-07	-6.385	-6.42	-0.035
	OH-	7.18E-10	6.55E-10	-9.144	-9.184	-0.04
	H2O	5.55E+01	1.00E-01	-1	-1	0
Al	5.22E-06					
	Al+3	2.60E-06	1.14E-06	-5.585	-5.944	-0.359
	AlOH+2	1.33E-06	9.56E-07	-5.86	-6.02	-0.16
	AlSO4+	8.05E-07	7.35E-07	-6.094	-6.134	-0.04
	Al(OH)2+	4.26E-07	3.88E-07	-6.371	-6.411	-0.04
	Al(SO4)2-	6.04E-09	5.51E-09	-8.219	-8.259	-0.04
	Al(OH)3	3.75E-09	3.75E-09	-8.427	-8.426	0.001
	Al(OH)4-	1.77E-09	1.61E-09	-8.752	-8.792	-0.04
	AlHSO4+2	3.21E-14	2.22E-14	-13.494	-13.653	-0.16
Ca	8.23E-04					
	Ca+2	7.98E-04	5.59E-04	-3.098	-3.253	-0.155
	CaSO4	2.43E-05	2.43E-05	-4.615	-4.614	0.001
	CaHSO4+	4.99E-11	4.56E-11	-10.302	-10.342	-0.04
	CaOH+	2.67E-11	2.44E-11	-10.573	-10.613	-0.04
Cl	1.41E-04					
	Cl-	1.41E-04	1.29E-04	-3.85	-3.89	-0.041
	MnCl+	5.76E-10	5.25E-10	-9.24	-9.28	-0.04
	FeCl+2	1.94E-11	1.34E-11	-10.712	-10.872	-0.16
	MnCl2	2.95E-14	2.95E-14	-13.531	-13.53	0.001
	ZnCl+	1.62E-14	1.48E-14	-13.789	-13.829	-0.04
	FeCl2+	1.49E-14	1.36E-14	-13.827	-13.867	-0.04
	ZnOHCl	1.05E-16	1.05E-16	-15.979	-15.978	0.001
	FeCl+	3.95E-17	3.61E-17	-16.403	-16.443	-0.04
	ZnCl2	1.86E-18	1.86E-18	-17.731	-17.731	0.001
	MnCl3-	1.15E-18	1.05E-18	-17.94	-17.98	-0.04
	FeCl3	1.75E-19	1.75E-19	-18.758	-18.757	0.001
	ZnCl3-	2.65E-22	2.42E-22	-21.577	-21.617	-0.04
	ZnCl4-2	1.96E-26	1.35E-26	-25.709	-25.868	-0.16
Fe(2)	1.06E-12					
	Fe(HS)2	7.56E-13	7.57E-13	-12.122	-12.121	0.001
	Fe+2	2.93E-13	2.03E-13	-12.533	-12.693	-0.16
	FeSO4	6.70E-15	6.71E-15	-14.174	-14.173	0.001
	Fe(HS)3-	5.85E-15	5.33E-15	-14.233	-14.273	-0.04
	FeCl+	3.95E-17	3.61E-17	-16.403	-16.443	-0.04
	FeOH+	4.89E-18	4.46E-18	-17.311	-17.351	-0.04
	FeHSO4+	1.81E-20	1.65E-20	-19.742	-19.782	-0.04
	Fe(OH)2	2.12E-24	2.12E-24	-23.674	-23.673	0.001
	Fe(OH)3-	1.91E-29	1.74E-29	-28.719	-28.759	-0.04
Fe(3)	1.84E-04					
	Fe(OH)2+	1.76E-04	1.60E-04	-3.755	-3.795	-0.04
	FeOH+2	5.22E-06	3.62E-06	-5.282	-5.442	-0.16
	Fe(OH)3	2.50E-06	2.50E-06	-5.603	-5.602	0.001
	Fe+3	1.39E-08	6.07E-09	-7.857	-8.217	-0.359
	FeSO4+	1.27E-08	1.16E-08	-7.897	-7.937	-0.04
	Fe2(OH)2+4	3.20E-09	7.35E-10	-8.496	-9.134	-0.638
	Fe3(OH)4+5	1.27E-09	1.27E-10	-8.898	-9.896	-0.998
	Fe(OH)4-	3.22E-10	2.93E-10	-9.493	-9.533	-0.04
	Fe(SO4)2-	6.66E-11	6.08E-11	-10.176	-10.216	-0.04
	FeCl+2	1.94E-11	1.34E-11	-10.712	-10.872	-0.16
	FeHSO4+2	1.80E-14	1.24E-14	-13.746	-13.905	-0.16
	FeCl2+	1.49E-14	1.36E-14	-13.827	-13.867	-0.04
	FeCl3	1.75E-19	1.75E-19	-18.758	-18.757	0.001
H(0)	0.00E+00					
	H2	0.00E+00	0.00E+00	-51.812	-51.812	0.001
Mg	8.67E-04					
	Mg+2	8.44E-04	5.94E-04	-3.074	-3.226	-0.153
	MgSO4	2.26E-05	2.27E-05	-4.645	-4.645	0.001
	MgOH+	1.25E-10	1.14E-10	-9.905	-9.944	-0.04
Mn(2)	1.48E-06					
	Mn+2	1.45E-06	1.00E-06	-5.84	-6	-0.16
	MnSO4	3.26E-08	3.26E-08	-7.487	-7.486	0.001
	MnCl+	5.76E-10	5.25E-10	-9.24	-9.28	-0.04
	MnOH+	1.74E-12	1.59E-12	-11.76	-11.8	-0.04
	MnCl2	2.95E-14	2.95E-14	-13.531	-13.53	0.001
	MnCl3-	1.15E-18	1.05E-18	-17.94	-17.98	-0.04
	Mn(OH)3-	3.16E-25	2.89E-25	-24.5	-24.54	-0.04
Mn(3)	4.37E-15					
	Mn+3	4.37E-15	1.91E-15	-14.36	-14.719	-0.359
Mn(6)	1.56E-12					
	MnO4-2	1.56E-12	1.08E-12	-11.806	-11.966	-0.16
Mn(7)	2.79E-05					
	MnO4-	2.79E-05	2.55E-05	-4.554	-4.594	-0.04
	CaOH+	7.37E-12	7.09E-12	-11.133	-11.149	-0.017
	CaHSO4+	4.02E-12	3.87E-12	-11.396	-11.413	-0.017
Cl	2.54E-04					
	Cl-	2.54E-04	2.44E-04	-3.595	-3.612	-0.017
	FeCl+	3.01E-09	2.90E-09	-8.521	-8.538	-0.017
	FeCl+2	2.85E-18	2.45E-18	-17.545	-17.611	-0.066
	FeCl2+	4.78E-21	4.60E-21	-20.321	-20.337	-0.017
	FeCl3	1.12E-25	1.12E-25	-24.949	-24.949	0
Fe(2)	1.04E-05					
	Fe+2	1.00E-05	8.60E-06	-4.999	-5.065	-0.066
	FeSO4	3.63E-07	3.63E-07	-6.44	-6.44	0
	FeCl+	3.01E-09	2.90E-09	-8.521	-8.538	-0.017
	FeOH+	1.37E-09	1.31E-09	-8.865	-8.881	-0.017
	FeHSO4+	1.41E-12	1.35E-12	-11.852	-11.869	-0.017
	Fe(OH)2	4.38E-15	4.38E-15	-14.359	-14.359	0
	Fe(OH)3-	2.48E-19	2.39E-19	-18.605	-18.622	-0.017
Fe(3)	8.07E-10					
	Fe(OH)2+	7.30E-10	7.03E-10	-9.137	-9.153	-0.017
	Fe(OH)3	7.45E-11	7.45E-11	-10.128	-10.128	0
	FeOH+2	2.72E-12	2.34E-12	-11.565	-11.631	-0.066
	Fe(OH)4-	6.17E-14	5.93E-14	-13.21	-13.227	-0.017
	FeSO4+	1.45E-15	1.39E-15	-14.84	-14.856	-0.017
	Fe+3	8.05E-16	5.71E-16	-15.094	-15.243	-0.149
	Fe(SO4)2-	9.61E-18	9.25E-18	-17.017	-17.034	-0.017
	FeCl+2	2.85E-18	2.45E-18	-17.545	-17.611	-0.066
	FeCl2+	4.78E-21	4.60E-21	-20.321	-20.337	-0.017
	FeHSO4+2	2.63E-21	2.26E-21	-20.58	-20.647	-0.066
	Fe2(OH)2+4	5.50E-22	2.99E-22	-21.26	-21.525	-0.265
	FeCl3	1.12E-25	1.12E-25	-24.949	-24.949	0
	Fe3(OH)4+5	5.53E-28	2.13E-28	-27.258	-27.672	-0.414
H(0)	1.54E-22					
	H2	7.72E-23	7.72E-23	-22.112	-22.112	0
Mg	5.64E-05					
	Mg+2	5.41E-05	4.66E-05	-4.267	-4.332	-0.065
	MgSO4	2.28E-06	2.28E-06	-5.642	-5.642	0
	MgOH+	6.50E-11	6.25E-11	-10.187	-10.204	-0.017
Na	2.87E-04					
	Na+	2.87E-04	2.76E-04	-3.543	-3.559	-0.016
	NaSO4-	4.19E-07	4.03E-07	-6.378	-6.395	-0.017
O(0)	0.00E+00					
	O2	0.00E+00	0.00E+00	-53.797	-53.797	0
S(6)	3.82E-04					
	SO4-2	3.78E-04	3.25E-04	-3.423	-3.489	-0.066
	MgSO4	2.28E-06	2.28E-06	-5.642	-5.642	0
	CaSO4	1.36E-06	1.36E-06	-5.867	-5.867	0
	NaSO4-	4.19E-07	4.03E-07	-6.378	-6.395	-0.017
	FeSO4	3.63E-07	3.63E-07	-6.44	-6.44	0
	HSO4-	1.36E-08	1.31E-08	-7.867	-7.883	-0.017
	CaHSO4+	4.02E-12	3.87E-12	-11.396	-11.413	-0.017
	FeHSO4+	1.41E-12	1.35E-12	-11.852	-11.869	-0.017
	FeSO4+	1.45E-15	1.39E-15	-14.84	-14.856	-0.017
	Fe(SO4)2-	9.61E-18	9.25E-18	-17.017	-17.034	-0.017
	FeHSO4+2	2.63E-21	2.26E-21	-20.58	-20.647	-0.066
Si	1.47E-05					
	H4SiO4	1.46E-05	1.47E-05	-4.834	-4.834	0
	H3SiO4-	2.08E-09	2.00E-09	-8.682	-8.698	-0.017
	H2SiO4-2	8.62E-17	7.40E-17	-16.064	-16.131	-0.066

#NAME? indices----------

Phase	SI	log	IAP	log	KT
O2(g)	-50.91	37.96	88.87	O2	
Tremolite	-42.85	17.81	60.65	Ca2Mg5Si8O22(OH)2	
Chrysotile	-19.54	14.78	34.32	Mg3Si2O5(OH)4	
H2(g)	-19.04	-18.98	0.06	H2	
Forsterite	-18.89	11.46	30.35	Mg2SiO4	
JarositeH	-18.44	18.78	37.22	(H3O)Fe3(SO4)2(OH)6	
Talc	-18.24	5.11	23.35	Mg3Si4O10(OH)2	
Sepiolite(d	-16.87	1.79	18.66	Mg2Si3O7.5OH:3H2O	
Magadiite	-16.86	-31.16	-14.3	NaSi7O13(OH)3:3H2O	
Portlandite	-16.23	7.87	24.11	Ca(OH)2	
Jarosite-Na	-15.07	21.46	36.53	NaFe3(SO4)2(OH)6	
Diopside	-14.91	6.35	21.26	CaMgSi2O6	
Sepiolite	-14.42	1.79	16.21	Mg2Si3O7.5OH:3H2O	
Thenardite	-10.45	-10.61	-0.15	Na2SO4	
Brucite	-9.83	8.15	17.98	Mg(OH)2	
Clinoenstat	-8.87	3.31	12.19	MgSiO3	
Halite	-8.71	-7.17	1.54	NaCl	
Mirabilite	-8.69	-10.61	-1.91	Na2SO4:10H2O	
Greenalite	-8.23	12.58	20.81	Fe3Si2O5(OH)4	
Melanterite	-6.13	-8.55	-2.43	FeSO4:7H2O	
Fe3(OH)8	-5.85	41.22	47.08	Fe3(OH)8	
Epsomite	-5.56	-7.82	-2.26	MgSO4:7H2O	
Anhydrite	-3.76	-8.1	-4.34	CaSO4	

Na	3.40E-05					
	Na+	3.40E-05	3.10E-05	-4.469	-4.508	-0.039
	NaSO4-	3.92E-08	3.58E-08	-7.407	-7.446	-0.04
O(0)	2.00E+03					
	O2	1.00E+03	1.00E+03	3.38	3.381	0.001
S(-2)	1.14E-03					
	H2S	3.87E-04	3.88E-04	-3.412	-3.412	0.001
	Zn(HS)2	3.41E-04	3.42E-04	-3.467	-3.466	0.001
	HS-	7.09E-05	6.47E-05	-4.149	-4.189	-0.04
	Zn(HS)3-	3.50E-07	3.20E-07	-6.456	-6.496	-0.04
	S6-2	3.00E-08	2.24E-08	-7.523	-7.65	-0.127
	S5-2	2.30E-08	1.69E-08	-7.639	-7.771	-0.133
	S4-2	1.31E-08	9.49E-09	-7.884	-8.023	-0.139
	S-2	8.77E-12	6.07E-12	-11.057	-11.217	-0.16
	S3-2	4.35E-12	3.12E-12	-11.361	-11.506	-0.145
	Fe(HS)2	7.56E-13	7.57E-13	-12.122	-12.121	0.001
	S2-2	2.26E-13	1.60E-13	-12.645	-12.796	-0.151
	Fe(HS)3-	5.85E-15	5.33E-15	-14.233	-14.273	-0.04
S(6)	4.17E-04					
	SO4-2	3.69E-04	2.58E-04	-3.433	-3.589	-0.157
	CaSO4	2.43E-05	2.43E-05	-4.615	-4.614	0.001
	MgSO4	2.26E-05	2.27E-05	-4.645	-4.645	0.001
	AlSO4+	8.05E-07	7.35E-07	-6.094	-6.134	-0.04
	NaSO4-	3.92E-08	3.58E-08	-7.407	-7.446	-0.04
	MnSO4	3.26E-08	3.26E-08	-7.487	-7.486	0.001
	FeSO4+	1.27E-08	1.16E-08	-7.897	-7.937	-0.04
	HSO4-	7.43E-09	6.78E-09	-8.129	-8.169	-0.04
	Al(SO4)2-	6.04E-09	5.51E-09	-8.219	-8.259	-0.04
	Fe(SO4)2-	6.66E-11	6.08E-11	-10.176	-10.216	-0.04
	CaHSO4+	4.99E-11	4.56E-11	-10.302	-10.342	-0.04
	ZnSO4	4.92E-12	4.93E-12	-11.308	-11.307	0.001
	AlHSO4+2	3.21E-14	2.22E-14	-13.494	-13.653	-0.16
	FeHSO4+2	1.80E-14	1.24E-14	-13.746	-13.905	-0.16
	Zn(SO4)2-2	1.71E-14	1.18E-14	-13.767	-13.927	-0.16
	FeSO4	6.70E-15	6.71E-15	-14.174	-14.173	0.001
	FeHSO4+	1.81E-20	1.65E-20	-19.742	-19.782	-0.04
Si	8.73E-05					
	H4SiO4	8.73E-05	8.74E-05	-4.059	-4.058	0.001
	H3SiO4-	1.93E-08	1.76E-08	-7.714	-7.754	-0.04
	H2SiO4-2	1.36E-15	9.41E-16	-14.867	-15.027	-0.16
Zn	3.41E-04					
	Zn(HS)2	3.41E-04	3.42E-04	-3.467	-3.466	0.001
	Zn(HS)3-	3.50E-07	3.20E-07	-6.456	-6.496	-0.04
	Zn+2	1.35E-10	9.37E-11	-9.869	-10.028	-0.16
	ZnSO4	4.92E-12	4.93E-12	-11.308	-11.307	0.001
	Zn(SO4)2-2	1.71E-14	1.18E-14	-13.767	-13.927	-0.16
	ZnCl+	1.62E-14	1.48E-14	-13.789	-13.829	-0.04
	ZnOH+	7.67E-15	7.00E-15	-14.115	-14.155	-0.04
	ZnOHCl	1.05E-16	1.05E-16	-15.979	-15.978	0.001
	Zn(OH)2	8.14E-17	8.16E-17	-16.089	-16.088	0.001
	ZnCl2	1.86E-18	1.86E-18	-17.731	-17.731	0.001
	ZnCl3-	2.65E-22	2.42E-22	-21.577	-21.617	-0.04
	Zn(OH)3-	7.44E-23	6.79E-23	-22.128	-22.168	-0.04
	ZnCl4-2	1.96E-26	1.35E-26	-25.709	-25.868	-0.16
	Zn(OH)4-2	4.09E-30	2.83E-30	-29.389	-29.548	-0.16

#NAME? indices----------

Phase	SI	log	IAP	log	KT
ZnMetal	-73.24	-45.87	27.37	Zn	
Zn5(OH)8C	-53.06	-14.56	38.5	Zn5(OH)8Cl2	
H2(g)	-48.74	-48.68	0.06	H2	
Zn3O(SO4	-47.16	-25.42	21.73	ZnO:2ZnSO4	
Zn4(OH)6S	-39.58	-11.18	28.4	Zn4(OH)6SO4	
Mn2(SO4)3	-36.2	13.07	49.28	Mn2(SO4)3	
Greenalite	-29.49	-8.68	20.81	Fe3Si2O5(OH)4	
ZnCl2	-25.6	-17.81	7.8	ZnCl2	
Zn2(OH)3C	-22.89	-7.69	15.2	Zn2(OH)3Cl	
Chlorite7A	-22.02	56.52	78.55	Mg5Al2Si3O10(OH)8	
Melanterite	-20.85	-23.28	-2.44	FeSO4:7H2O	
Mirabilite	-20.66	-22.61	-1.95	Na2SO4:10H2O	
Zn2(OH)2S	-20.31	-12.81	7.5	Zn2(OH)2SO4	
MnCl2:4H2	-19.73	-17.78	1.95	MnCl2:4H2O	
Goslarite	-18.51	-20.62	-2.1	ZnSO4:7H2O	
Chlorite14A	-18.49	56.52	75.01	Mg5Al2Si3O10(OH)8	
Tremolite	-18.04	42.78	60.81	Ca2Mg5Si8O22(OH)2	
Bianchite	-17.86	-19.62	-1.76	ZnSO4:6H2O	
Zincosite	-17.47	-13.62	3.85	ZnSO4	
Portlandite	-16.57	7.59	24.16	Ca(OH)2	
Forsterite	-15.26	15.17	30.43	Mg2SiO4	
Willemite	-15.23	1.56	16.79	Zn2SiO4	
Chrysotile	-14.68	19.72	34.4	Mg3Si2O5(OH)4	
ZnSO4:H2I	-14.51	-14.62	-0.1	ZnSO4:H2O	
MnSO4	-12.94	-9.59	3.35	MnSO4	
Gypsum	-3.5	-8.1	-4.59	CaSO4:2H2O	
SiO2(a)	-1.98	-4.83	-2.85	SiO2	
Silicagel	-1.63	-4.83	-3.2	SiO2	
Fe(OH)3(a	-1.41	16.9	18.32	Fe(OH)3	
Chalcedon	-1.08	-4.83	-3.75	SiO2	
Cristobalite	-1.02	-4.83	-3.82	SiO2	
Quartz	-0.6	-4.83	-4.23	SiO2	
Maghemite	0.57	33.81	33.24	Fe2O3	
Fe(OH)2.7(	3.56	13.95	10.39	Fe(OH)2.7Cl0.3	
Goethite	4.33	16.9	12.57	FeOOH	
Magnetite	8.51	41.22	32.72	Fe3O4	
Hematite	9.66	33.81	24.15	Fe2O3	

End of simulation.

Reading input data for simulation 2

End of run.

Thenardite	-12.45	-12.61	-0.15	Na2SO4
Zn(OH)2-a	-11.64	0.81	12.45	Zn(OH)2
Epsomite	-11.55	-13.82	-2.26	MgSO4:7H2O
Zn(OH)2-c	-11.39	0.81	12.2	Zn(OH)2
Sepiolite(d	-11.11	7.55	18.66	Mg2Si3O7.5OH:3H2O
Zn(OH)2-b	-10.94	0.81	11.75	Zn(OH)2
Zn(OH)2-g	-10.9	0.81	11.71	Zn(OH)2
Zn(OH)2-e	-10.69	0.81	11.5	Zn(OH)2
Brucite	-10.41	7.61	18.03	Mg(OH)2
Pyrochroite	-10.36	4.84	15.2	Mn(OH)2
Zincite(c)	-10.29	1.81	12.1	ZnO
Halite	-9.94	-8.4	1.54	NaCl
ZnO(a)	-9.5	1.81	11.31	ZnO
Sepiolite	-8.68	7.55	16.23	Mg2Si3O7.5OH:3H2O
Diopside	-8.23	13.08	21.31	CaMgSi2O6
MnS(Greer	-7.82	3.43	11.25	MnS
Talc	-6.82	16.61	23.43	Mg3Si4O10(OH)2
FeS(ppt)	-6.55	-3.26	3.28	FeS
Fe3(OH)8	-5.99	41.12	47.11	Fe3(OH)8
Mackinawit	-5.81	-3.26	2.55	FeS
Clinoenstat	-5.66	6.56	12.22	MgSiO3
Gypsum	-4.25	-8.84	-4.59	CaSO4:2H2O
ZnSiO3	-3.98	-0.25	3.73	ZnSiO3
JarositeH	-3.75	33.6	37.35	(H3O)Fe3(SO4)2(OH)6
Prehnite	-3.27	33.63	36.91	Ca2Al2Si3O10(OH)2
Magadiite	-3.2	-17.5	-14.3	NaSi7O13(OH)3:3H2O
Analcime	-2.92	8.11	11.03	NaAlSi2O6:H2O
H2S(g)	-2.61	-3.41	-0.8	H2S
Anhydrite	-2.5	-6.84	-4.34	CaSO4
Al(OH)3(a)	-1.64	10.32	11.96	Al(OH)3
Jurbanite	-0.88	-4.11	-3.23	AlOHSO4
Anorthite	-0.73	28.1	28.83	CaAl2Si2O8
Hausmann	-0.23	65.2	65.43	Mn3O4
Jarosite-Na	-0.12	36.51	36.63	NaFe3(SO4)2(OH)6
Wairakite	0.78	21.99	21.2	CaAl2Si4O12:2H2O
SiO2(a)	0.8	-2.06	-2.86	SiO2
Silicagel	1.15	-2.06	-3.21	SiO2
Gibbsite	1.21	10.32	9.11	Al(OH)3
ZnS(a)	1.42	-0.6	-2.02	ZnS
Boehmite	1.5	11.32	9.82	AlOOH
Albite	1.66	7.05	5.39	NaAlSi3O8
Chalcedon	1.7	-2.06	-3.76	SiO2
Cristobalite	1.77	-2.06	-3.83	SiO2
Wurtzite	2.11	-0.6	-2.71	ZnS
Quartz	2.18	-2.06	-4.24	SiO2
Fe(OH)3(a	3.15	21.49	18.33	Fe(OH)3
Halloysite	3.27	17.51	14.25	Al2Si2O5(OH)4
Diaspore	3.36	11.32	7.96	AlOOH
Laumontite	3.62	19.99	16.36	CaAl2Si4O12:4H2O
Manganite	3.84	29.18	25.34	MnOOH
Basalumini	4.13	26.83	22.7	Al4(OH)10SO4
Sphalerite	4.18	-0.6	-4.78	ZnS
Bixbyite	6.03	59.36	53.33	Mn2O3
O2(g)	6.26	95.36	89.1	O2
Fe(OH)2.7	8.29	18.69	10.4	Fe(OH)2.7Cl0.3
Kaolinite	8.53	17.51	8.98	Al2Si2O5(OH)4
Pyrolusite	9.29	53.52	44.23	MnO2
Goethite	9.89	22.49	12.6	FeOOH
Birnessite	9.92	53.52	43.6	MnO2
Montmorill	10.83	20.39	9.57	Ca0.165Al2.33Si3.67O10(OH)2
Nsutite	10.96	53.52	42.56	MnO2
Magnetite	12.29	45.12	32.83	Fe3O4
Maghemite	12.7	45.97	33.27	Fe2O3
Pyrophyllit	13.66	14.4	0.74	Al2Si4O10(OH)2
Leonhardit	16.56	40.97	24.41	Ca2Al4Si8O24:7H2O
Hematite	21.74	45.97	24.23	Fe2O3
Greigite	24.83	35.48	10.64	Fe3S4
Sulfur	40	45.27	5.27	S
Pyrite	46.58	42	-4.58	FeS2

Appendix 8:

Assumptions and Limitations of Acid-Base Accounting.

Appendix 8

Assumptions and limitations of Acid Base Accounting.

The interpretation of acid-base accounting results relies on assumptions that can impact the relevance and reliability of experiment results. The assumptions mainly concern geochemical weathering reactions, the implications of whole rock mineralogy and reaction stoichiometry. The predominate assumptions and limitations of ABA experiments are discussed with reference to implications for the Comstock samples, and on-site AMD.

NAPP tests determine the difference between the total amount of acid potentially producible (MPA) and the total potential acid neutralising capability (ANC) of a sample. The difference between these values is the net acid producing potential, as shown below (Equation 3):

NAPP? $\mathbf{MPA = MPA - ANC}$

(Equation 3)

Total sulphur is used to determine total potential acidity, based on the assumption that all sulphur in the rock will react and form sulfuric acid. Conventionally, acid production is expressed as calcite units (kg $CaCO_3$/ton), according to reactions for pyrite oxidation (Equation 4), and acid consumption by calcium carbonate (Equation 5; MEND Report, 1991);

$$\mathbf{FeS_2 + 15/4O_2 + 7/2H_2O \rightarrow Fe(OH)_3 + 2SO^{2-}{}_4 + 4H^+}$$

(Equation 5-4)

and;

$$\mathbf{CaCO_3 + 2H^+ \rightarrow Ca^{2+} + CO_2 + H_2O}$$

(Equation 5-5)

Theoretically then, 1 mole of sulphur is equivalent to 1 mole of $CaCO_3$ (MEND Report, 1991). Weight for weight, 1g of S is neutralised by 3.125g of calcite, thus total S obtained experimentally is multiplied by 31.25 to give a Maximum Potential Acidity (MPA) in kg $CaCO_3$/t of rock (MEND Report, 1991). This assumption is problematic

because in real situations acid neutralisation occurs by the following reaction when water is above pH 4.5 (Equation 5-6; Rose & Cravotta, 1999):

$$CaCO_3 + H^+ \rightarrow Ca^{2+} + HCO^-_3$$

(Equation 5-6)

In this situation the conversion factor for total sulphur to kg $CaCO_3$ would be 62.5 (MEND Report, 1991). Laboratory tests of both methods have concluded that, although both neutralisation reactions occur in nature, the factor of 31.25 produces results that most accurately predict net alkalinity in a range of situations (Brady *et al.*, 1994).

Whole rock analysis measures sulphur in all forms including; sulphide, sulphate and organic sulphur (Kania, 1999). Only sulphide sulfur (particularly pyrite) produces AMD, (MEND Report, 1991). Sulphate sulphur does not produce acid (because S is already in its reduced form), but can be important if associated with iron because oxidation of Fe^{2+} releases H^+ ions (MEND Report, 1991). However, partially weathered sulphates may dissolve and release contaminants, consequently their presence should be included in MPA calculations (Kania, 1999). It has been determined that total sulphur calculations are generally the most reliable, reproducible and predictive of all methods used to calculate MPA (Kania, 1999; MEND Report, 1998).

MPA is also formulated around the assumption that the only source of acidity is from weathering of sulphide minerals, particularly pyrite (MEND Project, 1998). The weathering of other sulphide minerals also has the potential to generate AMD, for example, pyrrhotite and marcasite. Fe^{3+} hydrolysis will theoretically produce H^+ ions, as will the weathering of some other minerals (e.g. iron silicates), although the proportion of acid produced in this way is much lower than from reactive sulphides. Theoretical ratios for the amount of acid buffered by a mineral differ widely; for example, the oxidation of pyrrhotite (Equation 7) has a different relationship between sulphur and calcite than in pyrite oxidation (MEND Report, 1998);

$$Fe_{1-x}S + 3(3-x)/4O_2 + (5-3x)/2H_2O \rightarrow (1-x)Fe(OH)_3 + SO_4^{2-} + 2H^+$$

(Equation 7)

The MEND Project (1.16.1c) proposed that if sulphide oxidation occurred in a closed system, CO_2 would not be exsolved and carbonic acid would increase the acidity of the solution. In situations such as in waste rock piles, this assumption would require consideration during data interpretation. Consequently, this needs to be considered in lieu of the fact that the samples represent the potential composition of waste rock piles at Comstock.

The "fizz" test can be used as an initial estimate of neutralisation potential because no fizz indicates that no alkalinity can be contributed to drainage waters (Kania, 1999). The test was formulated around an assumption that all neutralising capacity occurs as calcite. The "fizz" of other neutralising minerals, such as dolomite and siderite, are less pronounced in test conditions and more vigorous in different circumstances (i.e. hot acid; Kania, 1999). A subjective test, it determines experimental conditions (NaOH concentrations and amounts) and results, thus affecting the reliability and reproducibility of the rest of the experiment. This may impact the interpretations of these experiments because most neutralisation will be from aluminosilicates. Such minerals do not react vigorously with acid, thus their neutralising ability may have been somewhat underestimated, which may have affected the reliability of the NAPP test results.

Paste pH is analysed to determine the number of free H^+ ions released when a sample is mixed with distilled water (Kania, 1999). Results are only indicative of immediate oxidation reactions, whereas AMD is a time dependant phenomenon, consequently this experiment reveals little about the ability of a sample to produce acid over a long time. Another factor that inhibits the applicability of paste pH results is its inherent unreliability. Paste pH will indicate an unweathered, high sulphur sample has a neutral pH whereas a slightly weathered, low sulphur sample gives anomolously low pH results (Kania, 1999).

Tests of net acid generation are designed to support basic NAPP assessments of AMD potential. H_2O_2 is added to each sample in order to oxidise all reactive sulphides. The following back-titration quantifies the amount of acid produced minus the neutralising effects of any buffering minerals. NAG pH is used to determine the amount of H^+ ions released by total oxidation (using H_2O_2) of a pulverised sample. This provides an estimate of the total acidity expected from a sample after complete oxidation has taken

place; NAG pH does not constrain reactivity or lag times, that would be expected in natural conditions.

NAG tests provide a quantitative reinforcement to results obtained in initial NAPP tests. Instead of separately assessing the MPA and ANC, the test measures the net amount of acid produced or buffered by the sample, thus reinforcing separate experimental results.

Appendix 9:

XRF Results.

Appendix 9. XRF Results

FINAL SUMMARY											
%											
Ident	7	3	4	5	6	1	11	9	8	10	12
	sandstone/siltstone	carbonaceous shale	siliceous cap rock	talc	unknown	unknown	galena	crushing	south Comstock	pyrite	sphalerite
SiO2	65.3	57.77	49.64	49.28	67.13	79.74	2.37	25.85	7.46	4.27	4.10
TiO2	0.01	0.62	<0.01	<0.01	0.01	0.01	0.12	0.02	0.03	0.04	0.01
Al2O3	0.25	16.07	0.03	1.52	0.38	0.32	<0.02	<0.02	1.52	0.82	0.10
Fe2O3	1.56	6.99	4.21	2.39	2.08	1.3	2.77	21.97	12.92	58.43	16.02
MnO	0	0.06	1.14	0.14	0.01	0.07	0.19	0.25	0.22	0.06	0.84
MgO	26.83	1.52	16.87	22.02	21.82	14.15	<0.05	1.64	0.16	0.37	0.10
CaO	<0.01	0.10	6.40	<0.01	<0.01	0.02	0.03	0.07	<0.01	0.08	<0.01
Na2O	not available										
K2O	<0.01	5.16	0.02	0.03	0.01	0.02	0.03	<0.01	0.04	0.18	0.03
P2O5	0.01	0.1	<0.01	0.14	<0.01	<0.01	0.07	0.03	0.03	0.06	0.02
S	0.04	5.27	0.52	1.78	0.04	0.55	17.61	26.37	28.86	49.32	33.10
Cu	<0.01	<0.01	<0.01	<0.01	0.01	<0.01	0.01	<0.01	0.02	<0.01	0.06
Pb	<0.02	0.02	0.21	0.22	0.08	0.07	69.83	15.98	1.42	0.55	2.49
Zn	0.02	0.06	0.11	1.9	<0.01	0.12	8.19	11.96	47.47	0.98	45.82
As	<0.02	<0.02	<0.02	<0.02	<0.02	<0.02	<0.02	0.06	0.02	0.08	0.03
Loss	4.84	11.14	21.39	21.63	7.89	4.13	3.28	16.24	17.14	31.62	18.32
(1000degrees C)											
							galena ?		sphalerite ?	pyrite?	